Parkinson's Disease Prognosis using Diffusion Tensor Imaging Features Fusion

Pronostic de la maladie de Parkinson basé sur la fusion des caractéristiques d'Images par Résonance Magnétique de Diffusion

Teză destinată obţinerii
titlului ştiinţific de doctor inginer
la
Universitatea "Politehnica" din Timişoara
în domeniul "Ştiinţa Calculatoarelor"
de către

Roxana Oana TEODORESCU

Conducător ştiinţific:	prof.univ.dr.ing. Vladimir Ioan CRETU (UPT)
	prof.univ.dr.ing. Daniel RACOCEANU (UFC)
Referenţi ştiinţifici:	prof.univ.dr.ing. Noureddine ZERHOUNI (UFC)
	prof.univ.dr.ing. Sergiu NEDEVSCHI (UTC)
	prof.univ.dr.ing. Nicolae ROBU (UPT)

Ziua susţinerii tezei: 22 Ocombrie 2010

Seriile Teze de doctorat ale UPT sunt:

1. Automatică
2. Chimie
3. Energetică
4. Ingineria Chimică
5. Inginerie Civilă
6. Inginerie Electrică
7. Inginerie Electronică şi Telecomunicaţii
8. Inginerie Industrială
9. Inginerie Mecanică
10. Ştiinţa Calculatoarelor
11. Ştiinţa şi Ingineria Materialelor

Universitatea „Politehnica” din Timişoara a iniţiat seriile de mai sus în scopul diseminării expertizei, cunoştinţelor şi rezultatelor cercetărilor întreprinse în cadrul şcolii doctorale a universităţii. Seriile conţin, potrivit H.B.Ex.S Nr. 14 / 14.07.2006, tezele de doctorat susţinute în universitate începând cu 1 octombrie 2006.

România, 300159 Timişoara, Bd. Republicii 9,
tel. 0256 403823, fax. 0256 403221
e-mail: editura@edipol.upt.ro

Acknowledgments

The work presented in the thesis has been the result of a collaboration with Dr. MD Ling-Ling Chan and her team from Singapore General Hospital (SGH). We would like to express our gratitude for all the brain anatomy and diagnostic radiology lessons and the images, as well as for her work for gathering the database and make it available for us.

At the beginning, we have collaborated with Dr. MD Karl Olof Lövblad from the Universities Hospitals of Geneva and we thank him for his time and his patience.
The research stages made in Singapore from 2007 until 2009 have been useful in the research and by the help of IPAL[1], NUS[2] and UPT[3] all this work was possible. This stages have been supported by CNRS[4] and the CNCSIS[5] scholarship TD[6] 46/2008 from the Romanian government.

Roxana Oana Teodorescu Timișoara, October 2010

[1] Image and Pervassive Access Lab - http://www.ipal.i2r.a-star.edu.sg/
[2] National University of Singapore – http://www.nus.edu.sg/
[3] „Politehnica" University of Timisoara – http://www.cs.upt.ro/
[4] Centre National de la Recherche Scientifique (French National Research Centre) – http://www.cnrs.fr/
[5] CNCSIS – http://www.cncsis.ro/

[6] TD – Young PhD students scholarship

Teodorescu, Roxana Oana

Parkinson's Disease Prognosis using Diffusion Tensor Imaging Features Fusion – *Pronostic de la Maladie de Parkinson basé sur la fusion des caractéristiques d'Images par Résonance Magnétique de Diffusion*

Teze de doctorat ale UPT, Seria 10, Nr. 30, Editura Politehnica, 2010, pagini, 41 figuri, 11 tabele.

ISSN: 1842-7707

ISBN: 978-606-554-158-0

Keywords: Medical Image Processing, Medical Image Analysis, Automatic VOI detection, Parkinson's Disease, PD Detection, Prognosis

Abstract: Our research focuses in finding original solutions in software engineering for medical image processing and analysis using MRI images, with applications in Parkinson's Disease prognosis. We propose new image processing algorithms, independent on the patient variability, for detecting specific anatomical structures as volumes of interest. Our system is fusing information extracted from different medical image types. A rigid registration with automatic detection of the geometrical parameters, allows a fusion phase, by eliminating the volume variability. The analysis is possible by tracking the neuromotor fibers, even in the gray matter, and defining new metrics for the extracted fibers. The whole approach is automatic. Detecting the specific geometrical 3D features in each volume overcomes the inter-patient variability.

We study Parkinson's Disease (PD) using an automatic approach based on an intuitive specialized atlas. A total of 143 subjects, among who 68 patients diagnosed clinically with PD and 75 control cases, underwent DTI imaging. The EPIs have lower resolution but provide essential anisotropy information for the fiber tracking process. The two volumes of interest (VOI) represented by the Substantia Nigra (SN) and the Putamen are detected by our original algorithms on the EPI and FA respectively. We use the VOIs for a geometry-based rigid registration, before fusing the anatomical detail detected on FA image for the Putamen volume with the EPI.

After a 3D fibers growing, we compute the fiber density (FD) and the fiber volume (FV). Furthermore, we compare patients based on the extracted fibers and evaluate them according to Hoehn&Yahr (H&Y) scale. The determined fibers, evaluated with our own metrics, represent the source for the analysis module. This element uses the extracted features and using an Adaptive Network-based Fuzzy Inference System (ANFIS) adapted for our needs, performs PD diagnosis and prognosis.

This work introduces the method used for automatic volume detection and evaluates the fiber growing method on these volumes. Our approach is important from the clinical standpoint, providing a new tool for the neurologists to evaluate and predict PD evolution. From the technological point of view, the fusion approach deals with the tensor based information (EPI) and the extraction of the anatomical detail (FA and EPI).

PDFibAtl@s represents a platform built for clinical Prove of Concept for Parkinson's Disease prognosis, including the image analysis technology proposed here, the artificial intelligence tools and the medical knowledge. We introduce a new approach for VOI detection, image segmentation and image analysis levels.

Teodorescu, Roxana Oana

Pronostic de la Maladie de Parkinson basé sur la fusion des caractéristiques d'Images par Résonance Magnétique de Diffusion

Mots clès : Traitement d'Images Médicales, Analyse d'Images Médicales, Détection automatique des VOI, Diagnostic, Pronostic, Maladie de Parkinson

Résumé : Notre étude concerne un système automatique de détection et de pronostic d'évolution de la maladie de Parkinson. L'étude est basée sur le traitement et l'analyse des images IRM (Imagerie par Résonance Magnétique). Nous proposons des algorithmes de détection des volumes d'intérêt du cerveau, relevant pour le diagnostic de la maladie de Parkinson. Cette nouvelle approche élimine la variation inter-patients. Une fusion de données au niveau des volumes d'intérêt est présentée, en utilisant un récalage basé sur la géométrie du cerveau. Cette fusion permet l'application d'un algorithme de détection des fibres motrices du cerveau.

Notre étude est basée sur une cohorte de 143 sujets : 68 patients avec la maladie de Parkinson et 75 cas de contrôle. En utilisant les images EPI (écho-planar) nous procédons à la détection des volumes de mésencéphale, la formation anatomique qui contient la substantia nigra, celle qui produit la dopamine, un des principaux neurotransmetteurs qui détermine la maladie de Parkinson. L'autre volume d'intérêt est le Putamen, une formation anatomique cérébrale traversée par les fibres motrices.

Ce volume d'intérêt est déterminé sur l'image FA (Anisotropie Fractionnelle) qui est après alignée avec l'image EPI et un recalage entre les deux volumes permet l'utilisation des volumes pour limiter l'algorithme de croissance des fibres qui résident au niveau du mésencéphale et passent par le Putamen. En analysent les fibres extraites, nous intégrons la connaissance médicale pour mettre en place une stratégie de pronostic en utilisant des techniques neuro-floues (Adaptive Network-based Fuzzy Inference System - ANFIS). L'évaluation de notre système se fait en prenant en compte l'échelle de Hoehn & Yahr, utilisée habituellement par les cliniciens pour estimer la sévérité de la maladie de Parkinson.

Notre étude présente un intérêt à la fois technologique et médical. Du point de vue technologique (imagerie et aide a la décision), l'algorithme de détection des volumes ainsi que l'algorithme d'analyse et d'aide au diagnostic / pronostic, représentent des nouvelles approches dans ce domaine. Du point de vue médical, ce système représente un moyen pour les neurologistes de vérifier leur diagnostic/pronostic (seconde opinion). Un prototype, intitulé PDFibAtl@s a été construit pour mettre en œuvre, illustrer et valider cliniquement nos algorithmes, sous la forme d'un atlas IRM spécialisé dans la maladie de Parkinson.

Contents

List of Figures

List of Tables

Chapter 1

Introduction

Contents

As currently diagnosis on Parkinson's Disease (PD) is based exclusively on cognitive testing, an alternative method taking into account the image specification can reveal additional information and augment the prognosis rate. Our work offers the possibility to include an alternative source of information on the diagnosis process and additionally extends the utilization of the features extracted for prognosis functionality. Presently, there are no systems that estimate the severity of Parkinson's disease. Our approach performs this task, together with the placing of the patient on a severity scale used for cognitive test in order to have a common ground with the usual clinical a posteriori method.

Our aim is thus to use medical imaging, in particular DTI imaging, as a bio-marker for PD diagnosis and prognosis. This approach offers a measurable value of the severity of the disease and including in the diagnosis process the image features as well. But to reach this purpose we must study the modality in which the medical image can offer assistance for PD and the features that can be extracted from the images. The medical studies provide these features, specific for PD, and our research resides at not just verifying the medical suppositions, but also in finding a correlation between the image extracted ones and the severity of the disease. That is because even if the medical theories are correct and proven, the medical images could not always be able to provide with

the needed accuracy at the anatomical level for the needed features and even in this case, the elements need to be extracted from the images.

Pursuing this purpose, our work introduces new image processing and analysis methods for medical image information extraction from specific features, relevant for PD. It also develops segmentation and registration techniques with disease specific analysis rules, thus giving the user a quantification of the disease at the image level. Managing the information specific to medical imaging is achieved in our methods by using mathematical morphology and algorithms for automatic segmentation based on medical knowledge. These methods are integrated at the image interpretation level and 3D volumes of interest are extracted. By co-registering the extracted 3D volumes for a fiber growth modified algorithm, new features are introduced. Defining new metrics for these features permits an evaluation of the disease. Introducing specific artificial intelligence approaches using rule-based classification and fuzzy logic allow us to perform this analysis.

We perform an initial study on the specific characteristics of the medical images currently used by the medical doctors, as well as technical details of the different protocol procedures that apply on PD. We briefly present the Digital Imaging and Communications in Medicine (DICOM) standard, since it is used at large scale in most of the hospitals and also compliant with the database applied to this study. The Analyze standard for medical images is presented as well, as we use it in the processing stage for intermediate storing of processed images. We perform a deeper study on the Magnetic Resonance Images (MRI) images, with detailed presentation of the Diffusion Tensor Images (DTI) protocol. The image quality is very important, as it influences the performances of the processing algorithms and determines the pre-processing steps used to eliminate the noise and artefacts. This is the reason for evaluating the quality of the images in our database. Only after this evaluation can we identify the problems at the processing level, what these images are able to provide, and envision a competent approach for using them by creating new algorithms at the image level. The medical images were employed to determine the fractional anisotropy (FA) and the apparent diffusion coefficient level in order to determine the relevance of these indicator relative to PD.

According to our medical expert, the skull influenced too much the value of the FA on the computed images. This is the reason for removing the skull at the preprocessing step on our approach. Furthermore, although we can obtain the FA image from the ecoplanar images (EPI) by computation, for our system, the medical doctors provide directly this type of images from the scanner, eliminating an additional step at the processing level. The scanner provides the fractional anisotropy images by taking into account the diffusion at the *voxel* level together with the ecoplanar image (EPI) acquisition. All our work is performed at the 3D level, using as basic information the voxel value. A voxel is a pixel in the volumetric space, defined more accurately in 2.1.2. Concurrent systems existing in the state of the art are tested on our database and the results compared with our own approach.

This study provides specific characteristics of the images allowing us to better exploit the features. Thus, specific metrics for PD in the DTI images are introduced to evaluate to provide a numerical value attached to these features : the fibre density (FD), the fiber density relative to the volume of interest (FD_{rel}) and the fiber density at the 3D level (FD_{3D}).

We retrieve the 3D volume image of the brain from the image level, treat the volume

by examining the interesting areas, extract the motor fibers and compute their density and relative volume.

In the first phase of the processing, we detect the volume of interest as being the source of the dopamine, where the neural fibers from the motor tract are growing. These are the main indicators, together with the cognitive tests, for the installation of the disease on a subject. A global study of the brain is performed on specific areas of the brain and used to analyze the medical images and to make a correlation between the disease and the image characteristics. Our system detects the relevant features for PD. Based on these features, we develop a diagnosis and a prognosis system. Following the presented principles, we developed a prototype - entitled PDFibAtl@s - to accomplish a diagnosis analysis based on 3D image processing, as a Proof of Concept (POC) of the new methods at the image and analysis level.

1.1 Motivation. Purpose. Idea

Parkinson's disease affects a population that has, on average, 61 years, even if it begins around 40 years [PD 2009]. From this point of view, the continuous aging of the population, combined with the actual late detection (impossibility to reverse or stabilize the PD evolution) justifies strong concerns for a prediction system. By the time the disease is detected, the patient has already lost 80-90% of the dopamine cells [Today 2009], those that represent one of the main neurotransmitters. The treatments are less effective after the disease develops. Thus, a prognosis of this disease could diminish the effect of the PD or even reverse it. Analyzing the current diagnostic procedure, our idea aims at augmenting the trust of the diagnosis by adding the image in the process of detection of the disease and making the detection possible at an early stage as well (prognosis).

For introducing and using the medical image in prognosis of PD as bio-marker, there are three main steps in the research demarche:

- Determining and finding the bio-markers at the anatomical level from the medical point of view - stating the PD diagnosis at the anatomical level and defining the medical theories behind our approach

- Determining the feasibility and the applicability of the medical theories at the image level: proving that the bio-markers from the medical theories are indeed found at the image level and that they can be used for PD evaluation

- Finding and developing methods to extract the features from the images and analyse them.

For the first two steps our neuro-radiologist collaborator from the Singapore General Hospital (SGH) provided us with the medical knowledge, as well as the image database for the entire study. The standard rating on the severity used currently for PD provided the ground truth for validating the tests.

1.1.1 Current diagnosis for Parkinson's Disease

Currently, PD's diagnostic procedure relies on cognitive testing of the patients. According to their cognitive testing scores the patients are placed on a predefined scale: Unified Parkinson Rating Scale or H&Y. This manner of diagnosis does not take into account the information provided by the images. Performing an analysis of the images and finding an association between the effect of the disease represented by image specific indicators, we can integrate this perspective in the diagnose decision as well. Following this new procedure presents the advantage of compounding the cognitive aspects with the anatomical and even physiological ones. Our medical team provided us with the H&Y scale for all the patients as a ground truth for the relation between the parameters computed and the PD severity.

According to the study performed by our collaborators neuroradiologists [Chan 2007], there is a match between the dopamine level in the Substantia Nigra and the Parkinson's disease evolution [Atasoy 2004]. The study takes into account the manually detected area where the Substantia Nigra(SN) is supposed to be anatomically placed. This segmented area is further studied to determine the correlation between the PD patients and the dopamine level in this area. A correlation has been found indeed, but to make the difference for diagnoses purposes, this correlation is not enough and unreliable. David Vaillancourt, assistant professor at UIC has scanned the part of the brain called Substantia Nigra on Parkinson's patients using DTI images and has discovered that the number of dopaminergic neurons in certain areas of this region is 50% less [Vaillancourt 2009]. His study includes 28 subjects from which half have symptoms of early Parkinson's disease and another half do not have these symptoms.

A study performed to show the relationship between cerebral morphology and the expression of dopamine receptors conducted on 45 healthy patients, reveals that on grey matter images, there is a direct correlation at the SN level. This study [Woodward 2009] uses T_1 weighted structural MRI images. Using Voxel-based morphometry (VBM) the authors create grey matter volumes and density images and correlate these images with Biological Parametric toolbox. Voxel-wise normalization also revealed that the grey matter volume and SN are correlated. On the brain fiber tracts the dopamine should flow from the back of the brain (posterior area) toward the front (anterior area) and from the top of the head towards the basis of the brain. In [Lehericyr 2004] a manual detection of the regions of interest in the basal ganglia area has been operated and some differences are observed. One of the main effects of Parkinson is represented by the lost of mobility, perceived as a trembling effect on the patients. In order to quantify this impact, we study the motor tracts in order to determine if there is a direct link to the loss of dopamine and the degeneration of the neural fibers of this tract. A statistical analysis of the number of fibers and their density is able to reveal a relationship between the fibers and the PD severity.

1.1.2 Thesis Objectives

After defining the medical background on the PD and the actual procedure used for PD detection, the theoretical hypothesis and anatomical elements relevant to PD are stated so that they can be determined in the images. These represent the state of the art for using the

image as a bio-marker.

Developing methods based on an Adaptive Neural Fuzzy Inference System (ANFIS) modified represents the final aim of the thesis. The features employed in the prognosis system are extracted from several medical image modalities, fused by developing a geometrical registration method. For the feature extraction, we develop specific volume segmentation methods, completed by pre-processing methods that determine geometrical features. The features extracted at the image level are volumes of interest (VOI) that are further used by a tractography method in order to extract the fibers from the neuro-motor tract.

In order to identify the right bundle of fibers from the motor tract, we choose the seed and the target volumes of interest such that all the fibers that do not cross the two VOIs at the same time can be eliminated. As the dopamine is produced in the Substantia Nigra volume, the starting point (seed) for these fibers is represented by the midbrain, containing this specific anatomical region. Then, using a global deterministic tractography, we choose the Putamen volume as the second volume (target) for the selected fibers.

As shown in figure 1.1 there are several levels where the information is manipulated:

- Image level
- Feature level
- Knowledge Level

Our prototype - PDFibAtl@s - implements the methods described in this thesis and takes the images from the medical station, by processing and analyzing them and finally by extracting the significant features and quantifying them. The first level of information, the *image level*, deals with the medical image standard files and extracts the primary information from it, making the difference between the image and the protocol elements. At the *feature level*, a preprocessing step is needed on the image file from the medical standard. The information retrieved by feature extraction encapsulates medical knowledge as well. When developing the algorithms for the analysis step, we introduce new measures for the specific features extracted. Having as input the quantization of the features by using these measures we develop the algorithms at the *knowledge level* that perform diagnosis and prognosis evaluation. The knowledge from the medical domain provided by radiologists, acquired when defining the specific problems related to PD detection, determine the technical challenges in the anatomical details and the images used.

The fact that each brain structure is different from one patient to the other (e.g the placement of the Putamen with regard to the center of mass of the brain and/or the size of it) represents a challenge from the specificity point of view. A brain image has a different aspect, just like the portrait photo differs from one person to another. This is the reason why determining a certain anatomical aspect from a brain image is similar to determining the nose position or the mouth in a portraits database.

Detecting an anatomical volume automatically on a medical image can be compared with the same challenge on a 3D image of a person. While there are several algorithms that can provide the position of the eyes and/or the mouth - face recognition specific algorithms-, we cannot say the same things for the brain images. Atlases for the brain have the same meaning

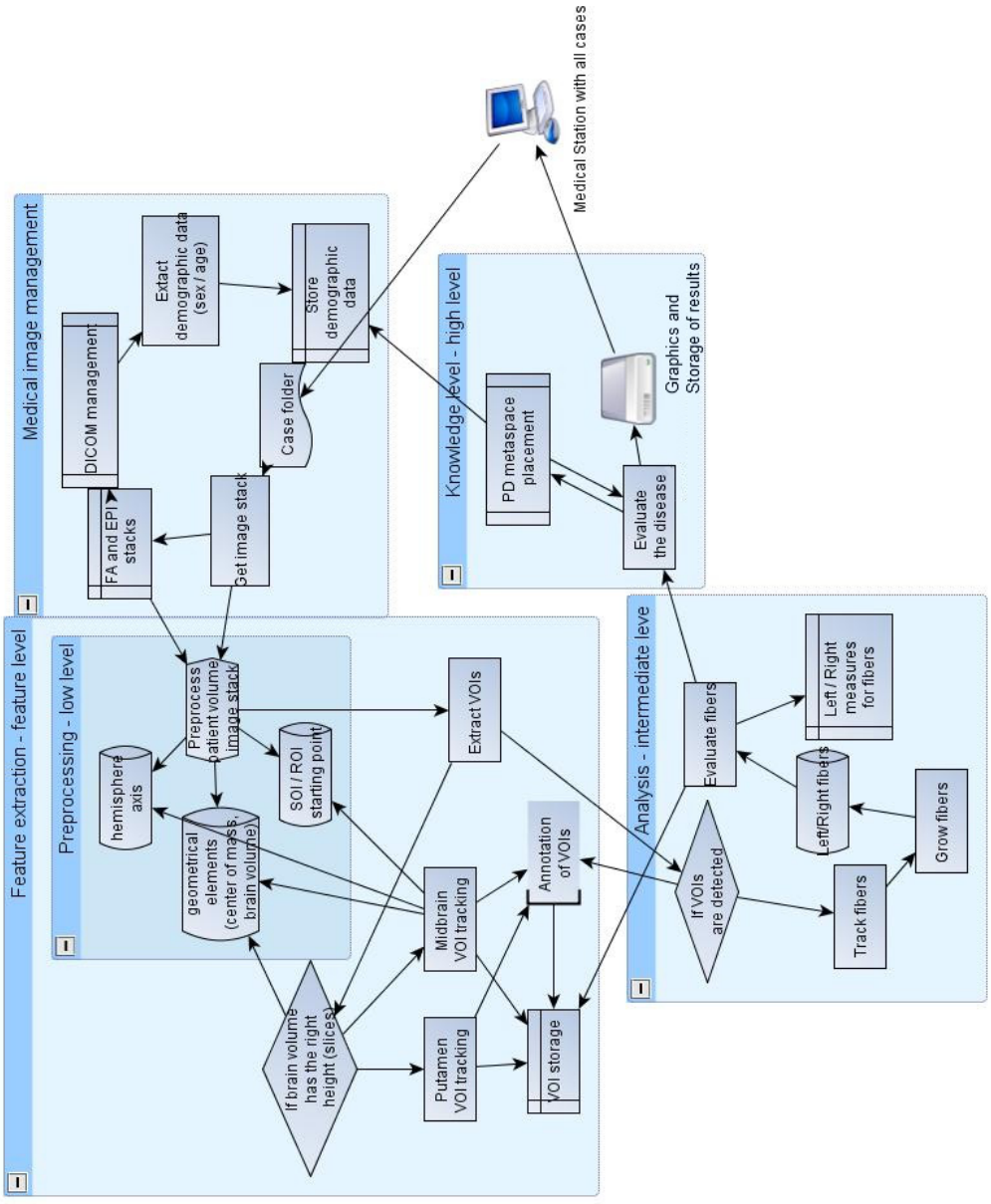

Figure 1.1: Thesis methods and data in workflow - PDFibAtl@s

as image patterns applied for portraits. On the portraits all the anatomical elements are known, but not the same things are applicable for the brain images - there are formations that can be placed in different positions with respect to the center of mass of the image or of the brain; different sizes with regard to the other elements inside the same brain. This is the reason why an atlas applied like a pattern or a mask on a brain will not necessarily give a correct result when detecting a specific anatomical element. A specialized algorithm for detecting an anatomical volume inside a brain that does not rely on the specificity of an image is much needed at this point. This kind of algorithm must have robustness and be exact as well on determining the needed elements. Technically, this represents a challenge and relies on finding undeviating points in the anatomy of the brain, as well as relative positions for the searched areas.

There are special limitations regarding the medical images resolution and specificity for such an algorithm. One of the main tasks is to find the appropriate slice in which to look for the volume of interest. Each slice contains different information and we rely on volumetric information when choosing the slice of interest for each of the segmentation algorithms. The position of each patient in the image is different, as is the size and shape of the head, and this aspect determines volumes of the brain taken lower or higher on a patient (starting from the nose level or from the eyes level) or for the same number of slices the whole brain or only a part of it (for smaller skulls the whole brain can be scanned, whereas for bigger ones, only a percentage of it, even if the scanning starts at the same level). This aspect determines an evaluation of the volume content in the image stack provided. This evaluation relative to the center of mass of the brain determines the position on the stack of images for the midbrain. The position of the Putamen is determined relative to the midbrain.

The Putamen is not symmetrically placed on the left and right side of the middle axis that separates the hemispheres, neither at the same relative position with regard to the center of mass of the brain. This is one of the challenges together with the fact that the right side Putamen can have a different shape and size from the left side and be placed higher or lower than the other one. Tough finding the midline that delimits the two hemispheres of the brain is another bid as it must be determined. The two hemispheres are not symmetrical and the line is not necessarily perpendicular on the horizontal axis of the image. The need to determine this axis with no connection to the specificity of the patient determines also a need for an automatic overall approach to determine it.

The specific algorithms that detect the volumes of interest take into account the voxel intensity and are defined and presented in Chapter 3.

Registration represents another major objective of this study, as the T_1/T_2 images have high resolution, but the intensity of the pixels does not permit an accurate limitation for the detection algorithm, applied on the FA image. This provides an accurate result but needs to be registered with the EPI image for further use in the fiber growth algorithm. Although the geometrical rigid registration algorithm by itself does not represent a new approach, the detection of the parameters for applying this algorithm does. We make the detection for the algorithm by using specific geometrical parameters, such as the middle hemisphere axis, determined by an original approach as well.

The final aim in determining the diagnosis is represented by the limitation of the grown

fibers and finding the appropriate image interpretation algorithm in order to be able to use the extracted information not only as a diagnosis value, but also for prognosis purpose. The algorithm does not make any difference between the tensors at the fiber level, their anatomical placement and the tract that they belong to. We only need the motor tract for PD and we are using the detected volumes to select the fibers that pass through both volumes of interest so that we are analyzing just the needed tract.

1.1.3 Proposed Approach

We need to automatically detect from the Echo-Planar Images (EPI), using the DICOM standard as an input and reading the header file, the slice where the midbrain area is located and the Substantia Nigra resides. Substantia Nigra represents the area of the brain where the dopamine is produced. This area is not anatomically defined in the specialized atlases and does not have clear boundaries for a detection approach. This is the reason why we identify the midbrain area, as it surely contains the Substantia Nigra. The Putamen area is not well defined on the EPI images, or in the T_2 images, but the FA images have a clear boundary of it. We try using the FA images to locate and extract the specified volume of interest. Mathematical morphology will be used for preprocessing the DICOM images and the 3D stack can be constructed and aligned.

Working with 3D images, the medical theories provided two volumes of interest for PD represented by the midbrain (2 slices), as apparently 80% of the Substantia Nigra can be found in a 4 mm slice [Chan 2007], and the Putamen by using several slices each time (3 slices). We start the tracking process from the midbrain toward the Putamen, but as one of the volumes is identified on another image type, image registration is required. This processing step is based on the brain geometry and uses automatic detection of landmarks. The fibers selected by the program are then statistically analyzed using the T-Test. We examine the correlation between the coefficients determined on the fibers and the evolution of the disease integrating the extracted features on an image interpretation model.

1.2 General presentation of our scientific demarche

As the medical theories hold *the motor tract responsable for the trembling effect manifested on the PD patients*, this particular tract could be indicative of the disease installation and/or evolution. The fibers constituting the motor tract are usually determined in the EPI images.

Another medical theory sustains that *the lack of dopamine*, produced by the SN, is the cause of the deterioration of the motor tract, and thus the cause of tremblement in PD patients. This theory imposes the SN area as one of the volumes of interest. As this area at the image level is not well defined, the midbrain containing the SN represents the volume of interest that should be extracted at the image level.

Analyzing the images taken form PD patients graded on the H&Y scale we grow the fibers from the motor tract and study the relation between the situation of the fibers and the rated values. After this analysis, as the identification of the volumes of interest should

be automatic and adaptive for each case, replacing the standard atlas approach by using an automatic dedicated adaptive atlas for PD regions. Making a variation function to show the PD evolution, based on the fibers coefficients,and furthermore extrapolating this function, we can determine the values of the coefficients for the early PD cases. This extrapolation factor gives a prognosis value that can be used and tested on the early PD cases.

The approach taken at the processing level for image segmentation includes a new automatic detection algorithm for the midbrain area together with a geometric approach for detecting the Putamen as a basis for an automated PD specific atlas of the brain. We refer the proposed segmentation as an atlas because it is based on the relative position of the anatomical regions at the brain level and it is capable to identify the specific volumes inside it. We modify an existing algorithm for fiber growth by limiting the fibers using the automatically detected volumes.

The metrics introduced as support for evaluating the value at the fiber level are computed separately for each hemisphere of the brain as the disease impact is distinct on each side [Chan 2007]. These metrics at the fiber level - the three levels of fiber density - relative to the whole brain (FD), relative to the volume of interest (FD_{rel}) and to the 3D representation (FD_{3D}) - together with the relative position of the midbrain on the brain volume (P_{slice}) evaluated at the image level, represents our own metrics. The methods at each level of information work together as a system, integrated as the prototype PDFibAtl@s, and not as independent modules, but provide all the numerical values extracted at each level for further analysis.

1.3 Thesis structure

Starting from the whole brain analysis, we move onward by determining the neural fibers from the motor tract and PDFibAtl@s design. The interpretation step and the analysis algorithm performing the prognosis part represent the final part of the thesis. The image analysis and the specificity of the medical image standard used are presented in chapter 2.1. After a general view on the standard medial images, an overview of the specific head imaging types and their characteristics is given in chapter 2.1.2. We need to refer to the specific protocol used for our database as well (see section 2.3.2), as it influences the modality in which we conceive the algorithms for the processing. An overview of the existing systems in the head image processing using DTI images, in section 2.5.1, helps us identifying the existing problems and placing our system among the others. The specific parameters used to acquire the images are presented in next chapter at section 3.1. A preprocessing step with the image acquisition and information analysis is detailed next in 3.3. These methods determine the position of the center of gravity for the brain, eliminating the skull and the artefacts. Also the axis limiting the two hemispheres is determined by a methods described in the same chapter. All the elements determined by these methods provide the parameters for the automatic methods for segmentation and registration presented next.

The methods developed for the volume segmentation and registration are provided in chapter 4, together with a modified version of an algorithm of tractography. We developed

individual algorithms for the midbrain volume and the Putamen volumes - on the left and right side. The Putamen is detected on a different type of image so registration is needed. The method for registration using the geometrical elements extracted by the pre-processing methods is presented in 4.4. The modified tractography method is presented in 4.6.

Emphasizing the applicability of the new developed methods and the importance of their applicability is presented the following chapter 5, with the diagnosis method and the new introduced prognosis mechanism as well. For the new introduced algorithms we need a way to evaluate them and the results and this step is presented by the chapter 6. An overview of the new methods with the scientific perspectives and conclusions are presented in chapter 7.

1.4 Conclusion

The purpose of our work is to detect and predict the evolution of the PD. We implement several algorithms for detection and segmentation of the volumes of interest and registration in order to integrate a fusion of information from the two types of modalities involved: EPI and FA. From the detected volumes of interest we grow the fibers and using their density we analyze the effects of the disease by implementing an image interpretation step used for prognosis.

At the theoretical level, we attempt a manual testing on a limited amount of patients to confirm the hypothesis basing our research. At this level, additional problems arose from the preliminary testing.

Considering the medical needs we have several problems to solve from the technical point of view:

- Automatic detection of volumes of interest
- Fusion of image information
- Medical image registration
- Fiber tractography using the detected volumes of interest
- Determining the coefficients to evaluate the conditions of the fibers - defining metrics
- Introducing a function that uses the extracted features in a correlation with the H&Y scale for prognosis

To reach these goals we need also to solve issues related to:

- Efficient algorithms for DICOM header management and
- Medical image preprocessing at the mathematical morphology level as well.

These are the main contribution developed in this thesis and illustrated at the end by an open-source prototype: PDFibAtl@s, able to be used by all the research community and easy integrable in the ImageJ environment. From the clinical point of view, translational researches are necessary by next to go from the Proof of Concept to the Proof of Value (POV).

Chapter 2

Imaging modalities for Parkinson's Disease Diagnosis

Contents

MEDICAL IMAGING INCLUDES THE TECHNIQUES USED TO ACQUIRE IMAGES from the human body using specialized techniques and machines. These types of images provide information that can define human anatomy in 3D providing volume information. Our interest at the image level resides at the anatomical level as we need to establish which medical image contains the medical data useful for our research and which can be better processed to evaluate and extract this particular data data. Also, the need for the motor tract as a

marker for PD extracted from the image, determines using a dedicated image technique for this purpose.

The fact that in medical images the human body provides views acquired in-vivo, while the patient is alive, breathing, all the internal organs are functioning, the heart is oscillating as well as the lungs, so that all these movements make the final image full of artifacts. These movements, combined with the fact that the acquisition time for the image is long, leads to blurred images. Another specificity of the medical data is the complex information contained in each medical image, as there are several tissues overlapping, together with bone fragments and liquids as blood. These kind of problems are rarely encountered in non-medical images and aspects like larger pixels combined with lower resolution provide low fidelity for the image acquired [Sonka 2009]. As the surfaces of the anatomical details varies from one subject to another, we need an algorithm to determine major differences from non-medical images and to define the requirements for special handling.

These are problems specific to medical images and they need specialized algorithms and handling. The purpose of medical imaging - developing a specific approach for visualization, processing and analysis - intersects with our own vision on using the medical images as biomarker.

An overview of the main medical imaging methods used for head images is presented in this chapter, with higher emphasis on the ones we are using. The characteristics of those types of medical images provide specific features used for diagnosis purpose. Those characteristics provide the motivation for using a specific type of medical images. The feature extraction process represents the area where our new methods are developed thus an overview on the existing methods and sets of algorithms is needed. We test the existing algorithms using our own cohort to evaluate our algorithms and to place our methods among the existing ones.

2.1 Imaging Modalities

Working with medical image processing provides supplementary specific information on each image, but medical standards include more information in a file than just the usual general standard image. There are several medical imaging standards, providing, together with the medical image, some basic information about the patient and the protocol used to acquire the medical image.

We further define the medical image standards used for our imaging modalities, their specificities and the way we use them for processing further on. Also specific imaging techniques attached to the imaging modalities are analyzed.

2.1.1 DICOM standard

Digital Imaging and Communications in Medicine (DICOM) is a standard used for managing medical imaging. This standard has its own file format definition as well as a network communications protocol [NEMA 2008].

From the technical point of view, the relevance of the system resides in the automatic detection of the volumes of interest and the management of the medical images, as well as the fiber growth algorithm. For the medical image processing we deal with the DICOM format. This specific medical image format consists of a header file and the image information encapsulated in the same DICOM file.

The header file contains the patient information, as well as the angulation and the type of the image. We are parsing the images from a folder reading the patient identification number (patient id) and the image type. Once we know the type of image that we need for processing (EPI / FA), we read the slice number and the direction of diffusion for making the volume for the patient that we are dealing with. All this preliminary steps are performed using imageJ [1] toolbox in Java.

The DICOM file format contains a header and the image data. The header file contains information about the patient and the technique used for acquiring the image, as well as some characteristics. Another file format used for medical imaging is called Analyze, but in this case for each instance of a medical file two files are created: one containing the header information (*.hdr file) and the other containing the image data (*.img) file. The DICOM file format has the advantage of compressing the files in order to reduce the image size [University 2008][NEMA 2008]. In the case of neuroimagery, we need to transform these files into Analyze format, in order to be able to perform a normalization on the images using Statistical Parameter Mapping (SPM) . Also the Analyze standard offers separately the image information and the hearer and occupies less space.

The DICOM header is contained in the first 794 bits of the digital image. This header contains the image characteristics, as well as image information about the parameters of the scan. In this file we have the elements 0002:0010 encapsulating the information about the structure of the image data described by the 'Transfer Syntax Unique Identification'. The image characteristics are stored for some color images (e.g. RGB) on 3-samples per pixel (one each for red, green and blue) and the monochrome images store on only one sample per image. For each image there are 8-bits (256 levels) stored or 16-bits per sample (65,536 levels), even if some scanners save data in 12-bit or 32-bit resolution. A RGB image that stores 3 samples per pixel at 8-bits per can potentially describe 16 million colors (256 cubed) [NEMA 2008].

These characteristics determine the format of the DICOM header, providing the physical characteristics of the images and the contextual information regarding the patients, used in our case for statistical purpose.

Digital image processing is concerned with working with programs that manage the digital images in order to modify their characteristics. The methods implemented in this area take as input images and provide the same number of images as output. The *Image Analysis* is concerned with extracting information linked to the context of the image, but not to alter the image, as it is the case with the digital image processing domain [Burger 2008]. In this case the methods developed take as input images, but the output can be only one image or numerical data. Our system also deals with the *Computer Vision* domain, as it will interpret the medical images together and understand the diagnoses at the end. These three domains

[1] imageJ -http://rsbweb.nih.gov/ij/

are the ones in which our work is placed.

For each image type we are trying to extract common features, as well as specific elements that are better presented in that type of image. This is the reason why for each image we have different techniques applied for preprocessing and for the analysis. In the preprocessing step we are using a Java program that contains imageJ features and is able to extract and store the information from the DICOM headers into the MySQL tables. The *imageJ software* is a platform for digital image processing and analysis, able to deal with several types of medical images.

2.1.2 Medical Images used in PD

In the medical standard, there can be several imaging types included in the image files (*.img file). These standards represent the actual visual information displayed when we want to see one of the images (e.g. MRI, ultrasound, X-ray image, tomography). When we refer to a certain *imaging type*, we actually mean the technique used (e.g. DTI, fMRI) to capture the image appertaining to a specific imaging modality (e.g. MRI). *Medical Images* are digital

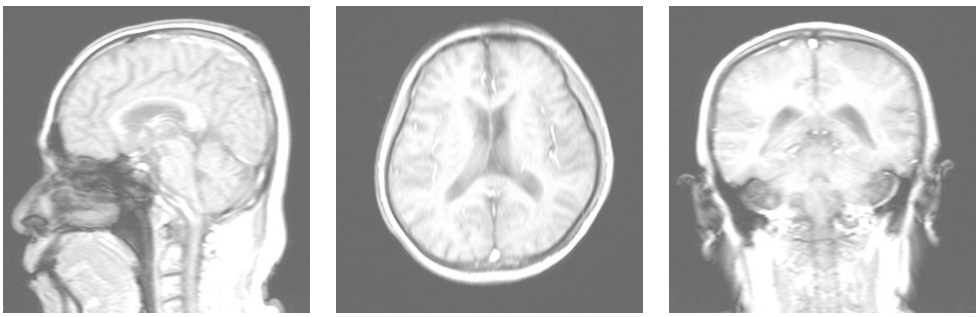

(a) Sagital slice (b) Axial slice (c) Coronal slice

Figure 2.1: Head MRI slice views

representation of aspects on human anatomy - body parts, tissues, organs - by using advanced techniques and processes that allow visualization inside the body for clinical purpose [Dictionary 2010]. Depending on the imaging angulation, there are several sectional views that provide human body images: axial view, sagital view and coronal view (see Fig. 2.1). The 2D images (ex. Fig. 2.6) that represent consecutive sectional views constitute a 3D image, a volume (ex. Fig. 3.4). In our study, we are working with medical image sequences or slices - consecutive sectional views (see Fig. 2.2) - stored in a medical standard format, together with the acquisition protocol and information regarding the patient and the clinic where the acquisition/diagnosis is performed. If at 2D level we are working with pixels when representing digital images as numeric format, at the volume level we are using *voxels*. A voxel does not posses its position encoded, it is relative to the other voxels, but they represent the empty and occupied space in a volume. They possess sizes that make possible volume

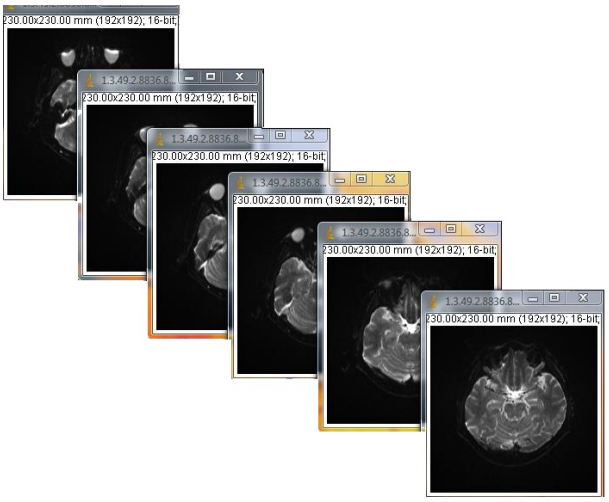

Figure 2.2: Example of consecutive axial views - slices of a stack

estimation. The voxel can be defined as a three dimensional pixel, a volumetric pixel. For a correct 3D representation of the sequence of 2D acquired images, an alignment between the consecutive image slices is needed, in order to obtain smooth and continuous anatomical details.

For the head images, we analyze by next the CT and MRI imaging modalities, as they are the most used for neuroimaging.

Computer Tomography (CT) Images are obtained using a tomograph, which produces an X-ray beam that parses the 3D volume of the body in a process known as windowing. The digital image obtained for the head images does not have the detail that we need for brain analysis in PD.

Magnetic Resonance Images (MRI) are used in radiology for the detailed visualization of the internal structure of the human body. The contrast offered by these types of images is enough to make the difference between the soft tissues inside the body, especially in neurology. This is the reason why our study focuses on this type of images. There are several types of MRI scans that differ according to the protocol parameters, the techniques used at the modality level and the purpose.

T_1 **weighted** use a gradient echo (GRE) sequence with short echo time (T_E) and short repetition time (T_R)

T_2 **weighted** use a spin echo(SE) sequence with long T_E and long T_R

Specialized MRI scans are based on more complex techniques for acquisition of images, depending on the application area:

- Diffusion MRI represents the diffusion of water molecules at the tissue level - is able to acquire several types of imaging types : diffusion weighted imaging (DWI), echo planar imaging (EPI)
- Fluid attenuated inversion recovery (FLAIR) is based on the inversion-recovery pulse sequence that has null signal from fluids
- Functional MRI (fMRI) is able to measure signal changes that represent neural activity in the brain

There are other types of MRI sequences, as well as other specialized MRI scans that combine techniques in order to obtain better images. At this moment each of the MRI sequence has been developed for a certain type of application, for a certain part of the body and specific to a disease. The DTI is used in the study of the brain as it offers the possibility to examine areas of the brain at the axon level. The water molecules in the biological tissues have special comportment.

2.1.3 Using DTI specificity

Naturally the water molecules do not have a regular movement, but at the tissue level, the diffusion of these molecules can be anisotropic. Due to the fact that the axon of a neuron does not usually cross a myelin membrane, the water molecule will be diffused along the neural fiber. We use this propriety and by analyzing the diffusion in different directions, we are able to detect the main neural fibers by tractography. The study of the fibers, as presented in Chapter 1 represents one of the main challenges.

2.1.3.1 DTI sequences characteristics

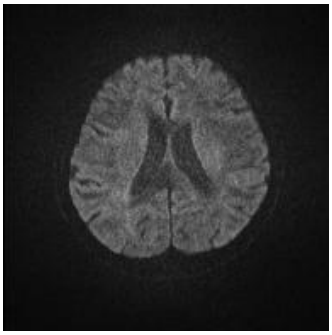

Figure 2.3: Echo planar axial 2D image example

Our medical partners offered us the possibility to study several DTI scans before making a decision on the one that our system would work on. The fact that each DTI scan has different purpose, supply us with different characteristics that can be combined and can complement each other for a more accurate analysis.

The Echo Planar (EPI) sequence represent a volume image in each diffusion direction. These DTI images have been generated using a value of B0=800 and 13 directions (12 directions + image with no diffusion) of scanning as specified in table 3.1. The image acquired with no diffusion is used for computing the ADC value and it is used as a reference image for this purpose. The *B value* is used for

changing the level of sensibility for diffusion - diffusion weighting value (e.g. standard value for adults is 1000 and for children is 500) [Rorden 2008].

The diffusivity is computed in one direction at the time for all the directions in which the diffusion was produced (different gradients). DTI images use tensors for expressing the direction of the diffusion. The tensor has three directions that generate eigenvectors and eigenvalues. If we are working with more directions then the image, features are better emphasized, but in this manner, we can induce noise more easily among the features and the trust degree in the extracted data is diminished [Curran 2005].

We will apply an algorithm that uses functions from the SPM and VBM for computing the anisotropy and diffusivity values : FA and ADC. The FA gives us the value of the water diffusivity and in this manner makes the difference between tissues. The ADC represents the directionality of the diffusion and it reveals the fiber orientation in the brain. These values are computed for each stack image that has been segmented into GM , WM and CSF. We will have a value for each tissue segment on the 27 images. For characterizing the entire volume (see figure 3.4) of the brain, we compute the average values of these functions on all the images.

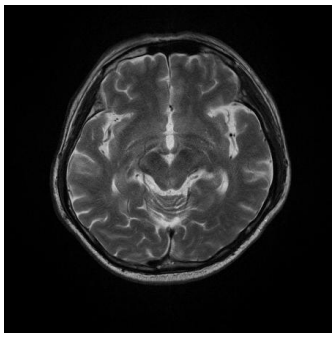

Figure 2.4: Axial 2D FLAIR slice image example

Analysis and processing for FLAIR is usually used to suppress the CSF in multiple sclerosis (MS) analysis. In this case of DTI images we only perform the tissue segmentation and spatial normalization with the Statistical Parameter Mapping (SPM5) and the Voxel Based Morphometry tool(VBM5) on a stack of images constituted by all the 19 images acquired (see Fig. 2.4). The resulted images constitute a single volume image. Afterwards, the diffusivity functions are applied on each processed image and a mean value is computed for all the images that represent the same tissue, for characterizing the whole brain. For this type of images we are performing a segmentation process as explained in subsection 2.1.3.1 using SPM5. The gray matter (GM) and white matter (WM) segmented are used then to create a volume value. At this level we perform the analysis using VBM5 and we compute the FA and ADC value as well. An angular correlation is used at this point in order to overcome the different values of the diffusion and to achieve similar image brightness for all slices. Even with additional optimization on the obtained images, the final result does not provide the same quality as the one generated directly by the scanner.

T_2 DTI overlay and T_1 imaging sequences have a high level of detail and are usually used by the neurologists in the diagnosis process. The acquisition process in this case is the same one used for the AX FLAIR images. When collecting the data from the scanner, turning the gradients to their maximum value generates a more accurate image but it can introduce eddy currents as well. These currents manifest as distortions in the image acquired by the scanner [Rorden 2008]. Computing of the FA value must take into account the motion effect induced

by these currents and in order to overcome the effect, an eddy currents correction function is used.

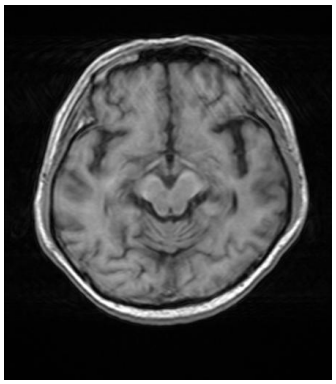

Figure 2.5: T_2 axial slice image example

As the DTI images are characterized by their water diffusion anisotropy in the tissues and by combining the data from the images taken in several directions (the ones generated by the tensor values) we can compute the FA and ADC, as well as construct neural fibers [Chetelat 2005]. We are computing the anisotropy values for these types of images. After eddy-currents correction a correct segmentation is possible on T_1 and T_2 images (e.g. fig.2.5).

2.1.3.2 Motivation for using this type of images

There are three main steps for managing the medical images from our database. The provided images in DICOM format are pre-processed using spatial normalization [Ashburner 2000] and robust smoothness [Kiebel 1999] implemented in statistical parameter mapping(SPM). After this step, the resulted data is segmented using the fMRI module implementing the Tairarchi atlas. The resulted white matter(WM) map is further used for the computation of FA and ADC values that replace the actual voxel values, providing new images.

The DICOM images and header information are stored into a MySQL database along with a list of features ordered according to the patient identification number. Each patient has all the imaging types associated with it and the additional specific information. Data specific to each image is stored as well (e.g. image size, type etc). During this pre-processing stage, images representing the same slice from the brain, but taken with different tensor values, are placed on a stack. Each image is also preprocessed using the Anisotropic diffusion filter in order to obtain a better boundary for the anatomical elements. A contour plotter function implemented in imageJ is used to extract the brain from the background image by using the pixel value. In this manner, we obtain areas with certain geometrical values stored at the level of each image as well. Generally in MRI images, the uniformity of the slices (see figure 2.6) in a stack is not the same - the positioning of the brain inside the image shifts. Thus, extracting the brain in this manner is not suitable due to the misalignment during the volume reconstruction. Another reason is the fact that the intensity of the voxels that represent the head and brain do not have always the same exact value for intensity - *inter-patient variability*. This is the reason why we store this information, momentarily for statistical comparison only and we do not perform the segmentation with this function. Even with the additional algorithms including spatial normalization and Bayesian coefficients for maintaining the deformation ration at the anatomical level, the final images are low resolution. After the atlas-based segmentation into gray matter (GM), white matter(WM) and cerebro-spinal fluid (CSF), we store these images. The stacks generated at this level are then transformed into Analyze format for a better management.

The programs using SPM and VBM run under Matlab 7.0. These toolboxes provide us

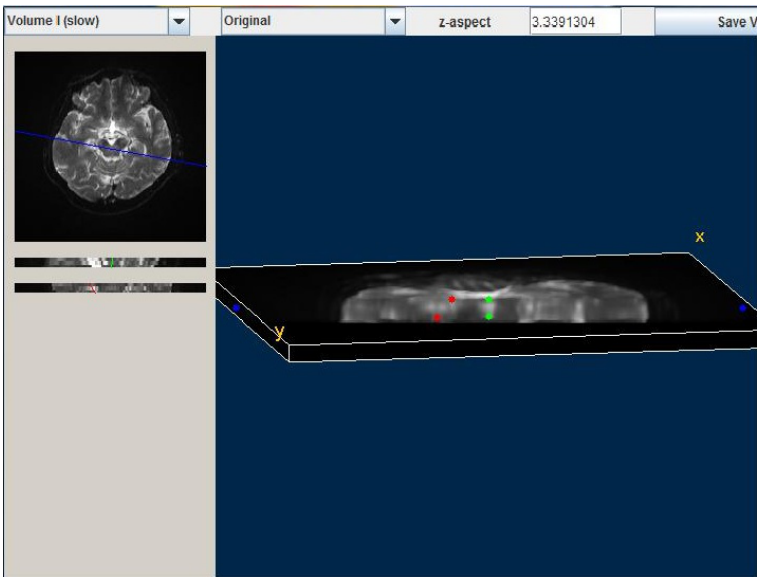

Figure 2.6: Slice view in 3D - voxel level

with the segmented images. The script that computes the FA and ADC takes these images and, using the B0 value and a threshold of 50 for the diffusion values, computes the diffusion tensors values.

The diffusion FA (equation 2.2) and ADC (equation 2.1) values are computed at the image level and the mean value at the stack level. The value that characterizes the image is the mean value from all the values of the stack. The functions that compute the FA and the ADC values are created in Matlab by Craig Jones [Jones 2008] and use the FA/ADC equations from 2.2 and 2.1. The values computed for FA take into account the λ value that represents the eigenvalues determined from the diffusion tensor vectors [Facon 2005]. This value is expressed using the ADC value from equation 2.1.

$$f_{ADC} = \frac{\lambda_x + \lambda_y + \lambda_z}{3} = \lambda \tag{2.1}$$

where $\lambda_x, \lambda_y and \lambda_z$ represent the eigenvalues computed from the x, y and z tensors on these directions.

$$f_{FA} = \sqrt{\frac{3}{2}} \sqrt{\frac{(\lambda_x - \lambda)^2 + (\lambda_y - \lambda)^2 + (\lambda_x - \lambda)^2}{({\lambda_x}^2 + {\lambda_y}^2 + {\lambda_z}^2)}} \tag{2.2}$$

The formulas of these parameters represent standards from the points of view of the diffusion. By computing the value of each of these parameters at the voxel level, we obtain the FA and ADC sequences (Fig. 3.5). These new sequences developed using either directly the pixel/voxel information or from the scanner, represent the value of anisotropy and the diffu-

sivity on a certain patient. The information provided at the image level is low-level and we are extracting it for further use together with medical knowledge in diagnosis and prognosis.

This chapter presents the specific medical imaging techniques used for the head images with emphasis on the techniques used for our database and their characteristics. CT images and MRI are mostly used when performing a head related scanning. As the specific elements of CT recommend this technique for other head injuries (see 2.1.2) rather than the neuro-degenerative diseases, we are studding the MRI. We are starting our analysis by first following the most used techniques in MRI imaging and especially in DTI images (as stated in 2.1.3).

Most of the medical doctors, when analyzing a patient, they first turn to T_1 and T_2 images to see if there are any abnormalities. These MRI techniques have good anatomical details, which represents an important criterion for using them. Also, when analyzing a patient, comparative MRI stack images are opened in parallel because each of them offers a different type of detail for the diagnosis. When the medical doctor detects an abnormality, he inspects the specific imaging MRI that offers information about the disease he might be suspecting. For neuro-degenerative diseases, the medical doctors usually analyze the DTI image. The DTI image technique is an MRI type of image where the diffusion of the water molecules is used to follow the neural impulse through the brain tissues. Following the water molecules in several directions we have the impulse propagation in those directions. The more directions we are following, more complex the image of the neural fibers that conduct the neural impulse is. By trying to fuse the medical knowledge and offer the visual possibility of checking the accuracy of the fusion, we are offering the medical doctors the possibility to analyze one type of image with the features from the others as well.

Afterwards, we follow the approach taken by the medical doctor when analyzing the MRI images also emphasizing the elements needed by the specialists to determine the neuro-degenerative suspicion based exclusively on the image analysis. Several systems that achieve this have been tested using the same imaging technique chosen for our approach.

2.2 Segmentation Techniques with applicability on DTIs

The aim of segmenting images is to classify sections of pixels based on their intensities making regions of pixels with the same intensities and/or similar intensity. These regions have a certain homogeneity that is defined based on a scale or on the fractal features. They can also be defined by their boundaries or their interior. When defined by their boundaries, a contour-based approach tests by whether each pixel appertains or not to the specified contour. For the second case of definition for the regions, based on the interior, there are several features that help this definition: compactness, projections, moments, texture and co-occurrence matrix [Sonka 2009].

Analyzing the co-occurrence matrix we can define a histogram so that the features defined for the morphological features are applicable for classification of the pixels. In this case we can use the energy as a direct measure of homogeneity and the entropy as an inverse measure of it. Using the maximum probability and the contrast as a measure of local image variation the texture can be classified. Also the correlation can be used to differentiate among regions

of pixels at the histogram level.

When talking about classification many approaches can be taken, but it all depends on the final goal of the process: for a pathologist, a classification might be needed to distinguish between sizes of cells, when for a radiologist, is more useful to know if the textures in certain regions are similar, such that the choice of features used for classification can be made. These features are entered on a classifier and produce the class decision. For a robust classification, knowledge of the medical area can be used, but only if this data is available. In this case, we can define a parametric classifier [Bankman 2009].

We can use the discriminatory power of the features for classification, but we need classifier-independent feature analysis(CIFA). Feature analysis for classification usually treats the discriminatory power from the classifier point of view - classifier oriented - by choosing the classifier and then the classes are determined by running the classifier with the selected features. The accuracy of the classification represents, in this case, the discriminatory level of the used feature. When choosing a data-oriented approach, the features are ranked using inter-class specificity. CIFA is specific to diagnosis problems as its purpose is to optimize the classification performance. This is possible by performing a feature analysis based on the structure of the features extracted, determining thresholds based on the discriminatory power of the features and using these thresholds for a more accurate classification.

Computing the relative feature importance (RFI) offers the possibility to rank the features according to their importance and to include, at the same time, the medical knowledge in the ranking process as a diagnosis criterion for classification. The algorithm proposed in [Sonka 2009], estimates the separation between classes using each new feature. In this case, the weighted absolute weight size (WAWS) defines the limits between classes using eigenvectors and eigenvalues. For estimation on the RFI, in order to choose a distance metric, accurate KNN is usually used. Also, a weighting factor after estimation of these features can be attached so that the features lead towards a correct diagnosis.

Intra-patient variability can change the segmentation results and RFI is able to remove this factor. Knowledge-based segmentation takes into account the features, their spatial constraints and the anatomical elements. For a low-level segmentation the spatial constraints are included in the algorithm, with the ROI specificity set as boundaries. For segmentation with active contours, fuzzy logic is applied for a high-level segmentation. In this case, for more accuracy in active contours for internal and external constrained forces additional knowledge is introduced. For the same purpose - more accuracy for edges and regions - some rules can be introduced, rules based on the medical knowledge, the intensity or the spatial structure values. Uncertainty can be taken into account not only with fuzzy logic, but also by modeling and classifying the anatomical variability, with multiple subject analysis and evaluation of spatial distribution in normal anatomy.

2.3 Medical Image Registration overview

When talking about registration, a distinction and definition of the terms is needed. A clear distinction between fusion, warping and registration must be made. Transforming one image

so that it matches another one represents the process of registration. According to [Tretter 1995] it is meant to find an optimal geometrical transformation between two homologous images. The demands with respect to similarity and what is suitable for each matching determines the registration approach.
Integration defines the case where useful data from separate images are complementary put together.
Using elastic deformation to fit an image onto an existing one defines the warping process. The local warping adapts the shape of a certain anatomical feature to an individualized atlas. This process is constituted by the feature specification followed by the warp generation.

The morphing process uses warping to turn one image into another using cross-fading (cross-dissolving). This technique introduces distortions in one image coming from the other image.

For registering two images, the suitable spatial transformation must be found so that from two images that are not aligned, we have the template images (transformed, moving image) mapped into the reference image (fixed image). The movement of the template can induce artifacts due to variation of different objects. A similarity measure is used to evaluate the difference between the two images - the distance between the template and the reference must reach a minimum estate. The transformation process is the one that "moves" the image to match the template.
The MedINRIA module that preforms the registration, called "Image Fusion" as it uses two initial images as input for the module and the result is the target image obtained by moving and/or changing the initial target image. This module provides several methods for registration: manual, diffeomorphic, affine etc. The process of fusion can be integration or a warping in this case. This is fusion defined at the image level. In our approach we fuse information feature, at the second level using registration as a tool for fusion. In our case, the registration only helps for the fusion performing an alignment between two images.

The algorithms for registration can be classified in many manners, depending on the parameters on the two images, the way they are detected and the way the images are transformed based on the similarity measures used.

2.3.1 Registration algorithms

In the registration algorithms, there are several main steps to be done: choosing the fixed image and the transformed one, choosing the landmarks, evaluation of the differences between the two images and the transformation of the moving image. Depending on the way these steps are performed, the registration algorithms can be evaluated. Taking one at the time these steps we have several classifications:

- Landmarks: Landmark-based (Finite Element Method (FEM) registration) vs. non-parametric registration(Fluid registration, Elastic registration)
- Differences: Geometry-based (affine registration, BSpline based registrations: NURBS) vs. Intensity-based (Standard Intensity Based Registration (SIB))

- Transformation: Rigid (Affine registration, Iconic registration) vs. Non-Rigid(Fluid registration, Diffeomorphic registration)

The limits between all these categories are not well defined, as there are registrations that can be included in two or all the three categories, as they use one of the elements from each category. We are now presented the characteristics of several main registration methods with the elements that include them in a specific category.

Based on the landmarks and the way they are chosen, the *landmark-based registration* is performed, when using hard landmarks (prospective) or soft landmarks (retrospective) with respect to the imaging process. If an image is evaluated based on the mass distribution there can be applied a principal axes transform (PAT). If the appropriate distance is used for similarity evaluation, the registration can be improved. There are several ways to choose the appropriate distance: based on the intensity, on the correlation or on mutual information. All these cases define an optimal linear registration.

The *non-parametric image registration* techniques are based on force computation to solve the difference until the two images converge. The elastic registration is justified by the deformation of a body or the tissue. Tensors are used to limit the boundaries for the shape matching. The fluid registration compared with the elastic registration uses the basic fluid mechanics for regularization. These techniques are not recommended for hand and brain images registration, as these tissues do not deform following the mechanics included in these techniques.

For a finite difference approximation in the partial difference equation a gradient-based regularization defines a diffusion registration. Starting from this approach, Thirion in 1995 [Tharin 2007] [Vaillancourt 2009] defined a performing non-rigid registration based on "demons"-diffusion functions. The main idea in this approach is the placement of each demon in the image domain. The "demons" are functions that decide the movement of particles on the template image so that the disparity is minimal. This approach is recommended on large dimensional image data, but measuring smoothness by oscillation of gradients and the fact that it does not represent the actual physical image characteristics are drawbacks.

If the fluid and diffusion registration depend on pre-registered checkpoints in the image domain, the curvature registration does not need that. This type of registration does not depend on the initial points and data, but it changes the shape of the image elements.

Another registration method that uses deformation is the *Finite Element Method (FEM)*, included in the ITK library. This method is based on BSplines and computed the displacement between the images evaluated on a grid. This grid defines a mesh that can be considered adaptive, uniform or even anatomy-based. Using physical transformation (Triangular, hexahedral, tetrahedral, etc) the moving image is deformed to the model. This approach is linked to the specifications given for the geometry and the behavior of the elements, as well as the boundary conditions.

From the non-rigid image algorithms the iconic feature based registration represents the intersection between the geometrical and the standard intensity based registration. The Standard Intensity Based (SIB) registration use the intensity similarities to quantify the quality of the registration. The Iconic Feature Based (IFB) registration uses the geometric approach

for distance evaluation for corresponding features, however the correspondence is based on the pixel intensities [Thomopoulos 1994]. Free From Deformation (FFD) method proposed in [Parker 2004] is based on the idea of deformation of the solid with B-Spline basis or NURBS (Non Uniform Rational B-Spline), but it is computationally large and sometimes insufficient deformed.

The main *problems in registration* are encountered at the beginning, when analyzing the data that the registration is meant to align. The mono and the multi-modality determine different approach on the distance measures, as well as on the transformation techniques. The same elements differ also when talking about intra or inter-patient registration where patient variability determines transformation. Depending on the content of the medical image, limitations are introduced for transformation and to determine a rigid versus non-rigid approach.

A transformation that includes translation, rotation, scaling and other affine transforms represents a linear transformation and does not affect the image information. This transformation defines an *affine registration*. When using the local affine transformation guided by a global affine transformation with mutual information and anatomical mask, the *piecewise affine registration* is performed. Completing this approach by using mutual information generated by mutual information-based thin-plate spline defines a *piecewise affine initialized spline-based registration*. The landmark and intensity based registration methods are part of the non-rigid category of algorithms. A combined method that combines the landmark-based method with the thin-plate spline uses both landmarks and intensity information to estimate the transformations.

Feature-based registration or geometric registration extracts the feature points and, computing the displacement between these points, is able to fit a transformation with or without regularization. The *intensity-based registration* prepares the transformation for optimization of the similarity by directly minimizing its value. The voxel-based methods change the image gray level without prior segmentation. The dispersion in the distribution of the image gray values is evaluated by the *entropy*.

All the registration algorithms follow a few main steps:

Feature Detection choosing the boundaries, the contour lines and intersections; distinctive objects spread on the image; common to the two images; not sensitive to image deformation

Feature Matching correspondence points between features; similarity measures are used combined with spatial relationship among features;

Transform Model Estimation estimates the alignment of the two images; differences between images have to be removed by registration;

Image Transformation mapping functions and transformations with interpolation techniques; the trade-off between the accuracy of the interpolation and the computational complexity

Specific to medical domain an *anatomy equivalence class (AEC)* can be introduced for representing the anatomical equivalence, individualized on patients and useful in estimation of distance and the actual transformation process. This manifold of elements defined as pairs *[transformation, residual]* is able to eliminate confounding data and produce an optimal registration strategy based on the individual anatomy. This approach needs a template and specificity features for each patient for evaluation [Bankman 2009].

Another specific medical feature is defined by the computational anatomy, a parameter that characterizes anatomical differences between the registered images.

2.3.2 Registration Methods

When presenting the modalities used on the evaluated systems for the registration, we are considering the fact that the tests are done using our own images, the checkpoints for us are represented by the fornix and the AC/PC line - the slice that contains that specific axis. We test the registration modalities for intra-patient registration, the images taken at the same time, but different type of images (EPI B0 and FA, T_2 with EPI B0). For volumetric deficits on Alzheimer diagnosis *Jacobians* are used. For a brain development follow-up diffusivity is recommended as approach because it characterizes fractional anisotropy. In our case we will test the diffusivity approach, as FA is important and we are working with this type of image, but also a geometric approach can be useful as we are having intra-patient registration. Using a tissue density map (TDM) a distribution of the anatomical tissues can be achieved. On the second step of the registration process mutual information must be found in the two images. This step enhances the mutual information in the two images without a priority model.

The Diffeomorphic Demon registration (Image Fusion module from MedINRIA) was tested on the T_2 and EPI images, but the information was mixed for the resulting image, in this case we have lost the accuracy of T_2 image as it was compromised by adding noise from the low level image. We could not use the registered image for ROI detection. For some patients the resulting image was ambiguous and the anatomical detail was not good enough even for manual ROI detection.

Another registration possibility with this module is represented by the manual registration algorithm, when the checkpoints are manually detected. This algorithm was unable to determine when to flip the image and the angulations for this procedure. For some patients it performed well, for others it did not, depending on the accuracy and the position of the checkpoints. In the manual approach, the subjectivity of the human input affects the performance.

An atlas based registration is tested on the EPI images using SPM5. The images are mapped on an atlas and depending on the position of the main anatomical structures with regard to the ones in the atlas, the transformation is applied. The problem for our images was the final result as the images were folded on the results and we could not use them further. This registration method includes an anti-folding method, K-fold cross-validation but this method is conceived for the fMRI images, not DTIs.

Complementary to deformation based morphometry (DBM) and tensor based morphometry (TBM), the Voxel Based Morphometry method is tested. In DBM the group difference is established using local deformation, whereas in TBM the tensor information provides the local displacement. In VBM the differences in the local concentration of volume, depending on the tissue type detected at the voxel level, determine the registration landmarks. Completing this method with a voxel-wise statistical analysis for exact determination of the landmarks, offers a better accuracy for this method. The warping transformation represents the final step providing the transformed image.

Another registration method based on regions of interest used as landmarks is provided by the 3D Slicer. This approach is similar with the manual approach as the used chooses manually the corresponding regions and landmarks in these regions. This technique is strongly linked on the checkpoints and the accuracy of the evaluation for these checkpoints. The system offered results only for a few patients, as it was not able to complete the process for most of the volumes provided.

2.3.3 Applicabilities of Registration on our database

We are using this technique as the first one or the VOI is determined on the EPI B0 image and the second one is extracted from the FA image. We need to perform registration in order to map the extracted VOI from the FA image on the EPI.

For our database we need a rigid body registration as we are performing intra-patient registration. Also, the evaluation for the transformation should be determined automatically using geometrical elements to eliminate inter-patient variability from the algorithm. A rigid-body transformation completes the registration that we need.

The mapped VOI is used in the tracking algorithms for choosing the fibers.

2.4 Tractography elements and algorithms

The tracking algorithms are used to evaluate the water diffusion represented by the tensor information in the EPI images and, following the angulations, to reconstruct the neural fibers. These algorithms are defined for WM fiber tracking, where all the fibers run in the same direction. Although this is not the case for us, as we are working in the GM, we evaluate the algorithms on our images.

There are two main approaches on the tractography using DTI images: deterministic and probabilistic. The deterministic approach connects neighbor voxels starting form an initial set of points until the angulation or the FA values reach the threshold values. Probabilistic tractography considers uncertainty of the fiber orientation and uses probabilistic density function to determine the fibers. Using DTIs both methods are able to track the fibers and the fiber density even if there is fiber disruption and reductions, but each method has drawbacks. For a deterministic approach the initial points need to be known and there is certain sensitivity in the estimation of the principal direction of diffusion. The probabilistic

a p p r o a c h needs more computational time due to the probability functions, but its results are better on partial regions. At the voxel level, determining the next step when tracking the fibers, the approaches can be classified in local and global. L o c a l t r a c t o g r a p h y uses a seed voxel or a ROI as starting point for initialization of the fibers. This tracking takes small steps determining at each time the direction of the fiber. For determining this direction when using the deterministic approach only one possible direction is provided as next step, whereas on the probabilistic approach there are several possibilities for the next step. The downside when using the local tractography is the fact that there is no target region defined and extracting a specific bundle of interest in these conditions is challenging. The other approach of following the tracts is by setting up the source seed voxel or ROI and a similar one for the target. Using the deterministic method for choosing the direction of diffusion provides only one possible path and the probabilistic method provides more paths again, depending on the probability distributions. The global tractography is constrained to a specific connection and symmetry between the source and the target [Yendiki 2010].

Based on these approaches new methods of tractography have developed, taking into account other parameters when tracking the neural fibers. Descoteaux et al. in [Descoteaux 2007] use the sharp fiber orientation distribution function (ODF) for a reconstruction from Q-Ball Imaging. This type of imaging uses probability distributions instead of tensors combined with tomography used in high angular resolution diffusion imaging (HARDI) approach. Fillard et al. [Fillard 2009] propose the use of spins with potential energy to trace the fibers on global tractography - the spin glass tractography method (SGT).

Our approach already has the initial volumes of interest representing a global approach as it aims on detecting just the fibers starting at the midbrain VOI and reaching the Putamen VOI: the strationigral tract. We try to achieve this aim using our own images with several systems that perform tractography.

Taking all the fibers determined on the entire brain is time and computational power consuming. This is the main reason why the local probabilistic Slicer tracking module could not complete the estimation of the fibers on our images. It also did not offer the possibility to choose just a bundle from all the fibers or to insert an ROI before tracking.

The DTI tracker from MedINRIA system performs fiber tracking for all the brain and, inserting a VOI, it can extract just the bundle that passes through that specific region/volume. Also the direction of the fibers could not be chosen.

We tested the second order Runge-Kutta method for tracking using the Diffusion Toolkit from TrackVis [2], which is a probabilistic method as it offers for each voxel multiple diffusion directions. We tested this method on our images and applied a global tractography by defining the ROIs manually in TrackVis. The tractography generates, like the DTI Tracker (MedINRIA), all the fibers, but the choice of the bundle of interest can be achieved by using two or more regions of interest (see fig. 2.7). Even if this is a fast method and very close to what we need as final result from the tractography, the generated fibers include also noise. Another global probabilistic tractography is proposed by FreeSurfer [3]: TRActs Constrained by UnderLying Anatomy (TRACULA). The preliminary testing before release on this method uses 60 gradient

[2] TrackVis - `http://www.trackvis.org/`-last accessed on July 2010

[3] FreeSurfer - `http://surfer.nmr.mgh.harvard.edu/`-last accessed on July 2010

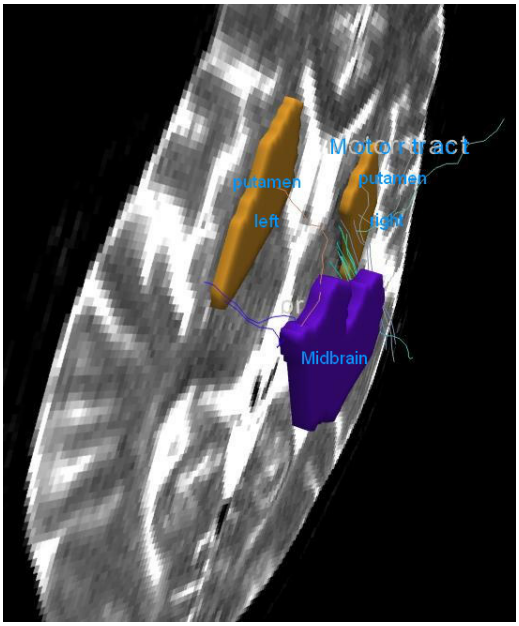

Figure 2.7: The motor tract detected on TrackVis

directions and DWI images of 2x2x2 mm or T_1 images of 1x1x1 mm [Yendiki 2010]. We did not test this software as it has not been released yet.

SPM and VBM do not offer tractography as an application and, considering the long time needed just for ROI extraction, we eliminated this system from the testing batch.

2.5 Algorithms and their applicability on our database

For our fibers, we need an algorithm that economizes time at the growing step by evaluating just the tensors from a defined VOI and starts the growing towards the other determined VOI. We will grow, in this manner, just the fibers that are interesting for us and we will validate only those that reach the second VOI.

2.5.1 Software using DTI images

There are systems using DTI images for analysis and processing, offering different features and data for the user. To present the capabilities of these systems we test them against our own also by using our database, we have a way of evaluating the new prototype PDFibAtl@s by comparing the results obtained with the other systems. All the systems presented are freeware and are dedicated to the medical image processing for DTI images. Other systems

have been tested, but the images either did not provide any result or have managed to close during processing or even stop the machine while processing the data. The systems presented provided the best results for our images. The systems are tested from several perspectives:

- Management of DTI images (12 diffusion directions)
- Registration capabilities
- Tracking algorithms using one or two regions of interest
- Segmentation procedures

First, we evaluate the results on our images for all these perspectives, with validation from the neurologist. Afterwards, we analyze the algorithms used for achieving the tasks. Next we present the systems and then we compare them from the perspectives presented above.

MedINRIA[4] represents a French project by INRIA laboratory in Sophia Antipolis and provides a series of applications for medical image processing and visualization. As provided by the Asclepios site the main interest points provided by this software are the Log Euclidian metrics - metric for tensor estimation, HARDI - high angular resolution diffusion imaging, fiber tracking, block matching, diffeomorphic demons- defined in registration and DT-RefinD-registration technique. This project is structured in independent modules, implementing different algorithms, that offer just specific features when needed: the DTI Track module or the tensor viewer module. The system is implemented using ITK[5] for image processing and VTK[6]. As we are working with DTI images, the DTI tracker was one of the tested modules, together with the Image Fusion module, the one providing several methods for image registration.

3D Slicer, provided by the MIT AI Lab with the Surgical Planning Lab at Birmingham and Women's Hospital, as presented on the home page[7], the software application represents a collection of algorithms and applications dedicated to medical imaging. The application provides not only a 3D image viewer for DTI images, but also tracking algorithms, as well as registration ones. The Slicer provides also an atlas for segmentation of the brain, specialized for DTI images(Fig. 2.8). The system is developed in Visual C, using visualization libraries and advanced computing algorithms like VMTK (vascular modeling toolkit).

Matlab based systems (SPM and VBM) - Statistical Parametric Mapping (SPM)- is a plug - in software that extends statistical processes dedicated to the functional imaging data. The software package performs analysis of brain imaging data sequences[8]. This plug-in software is designed for the Matlab environment. The version of SPM5 accepts DTI images for processing and provides alignment and preprocessing using the fMRI dedicated module.

[4]MedINRIA - `http://www-sop.inria.fr/asclepios/software/MedINRIA/` - last accessed on May 2010
[5]ITK - imaging toolkit `http://www.itk.org` -last accessed on May 2010
[6]VTK - visualization toolkit `http://www.wxwidgets.org` - last accessed on May 2010
[7]Slicer - `http://www.slicer.org/` - last accessed on May 2010
[8]SPM site -`http://www.fil.ion.ucl.ac.uk/spm/` - last accessed on May 2010

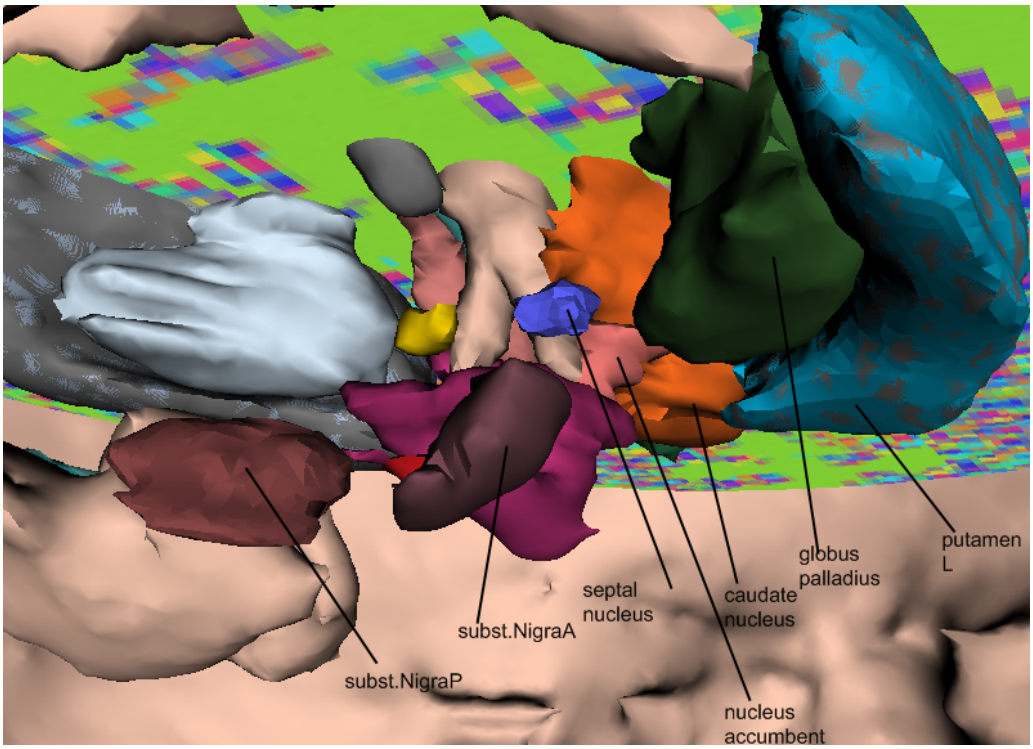

Figure 2.8: Result image when using the 3D Slicer Atlas

Voxel Based Morphometry (VBM)[9] represents another module that can be integrated in Matlab with SPM, as a plug-in in SPM5. This module is able to make segmentation in WM and GM based on voxel-wise comparison.

The TrackVis[10] with the dedicated Diffusion Tracking module uses linear least- squares fitting method and offers Q-Ball/Hardi reconstruction [Wang 2007]. It uses standard FACT for fiber tracking, but we test the Runge-Kutta method as we are using a similar method in our approach. The difference between the results obtained with this approach and our method consists in the obtained fibers that include also noisy elements, specific to the probabilistic global approach. This methods are implemented in C and the visual elements as well as the image processing is created using the VTK library. The Diffusion tracking module performs the image processing taking the DICOM standard images and delivers the computed fiber tracts. The TrackVis module offers visualization for the fibers and the possibility to segment the images and extract bundles of interest from the computed tracts.

[9]Voxel based morphometry (VBM) -http://en.wikipedia.org/wiki/Voxel-based_morphometry - last accessed on May 2010

[10]Diffuion toolkit -dtk - http://www.trackvis.org/dtk/

2.5.2 Classification and segmentation

There are several ways to manage tissue classification to determine detection of anatomical structures or organ limitations. One way used for head images is represented by the brain atlas, a pattern that can be applied on any brain to determine the position of anatomical structures inside the brain. There are several brain patterns used in segmentation algorithms. The inconvenience of this approach is represented by the fact that these algorithms do not take into account the patient variability as it has to provide an atlas for all the demographic type of patients (Asians, Europeans, African). Also a registration between the atlas and the image is needed for a correct detection.

For the other approach the intuitive way is used for detecting the main tissue types: bone (skull), WM, GM, CSF. This technique analyzes the pixel intensities and is able to determine the similar pixels that constitute the same type of tissue. This technique is dependent on the image quality and the threshold set by the user to make the difference between tissue types, managing the sensitivity in this way. Computing the entropy values and setting up a threshold for the main tissue type we are classifying, this algorithm parses the images and places the pixels according to the threshold and entropy values. In this case, the sensitivity represents the main challenge.

The systems that we are testing have different approach on the segmentation algorithms. MedINRIA provides a way of manual definition for the regions of interest, as this is the most accurate way of segmentation. The same accuracy using the manual approach is provided also by the TrackVis module. 3D Slicer and SPM provide atlas-based approaches, but 3D Slicer does not manage to finish the computation for our images and the SPM results are blurry and not accurate.

2.5.3 Segmentation based on atlas

The brain atlases describe a representation of the brain, with anatomical elements and their spatial relationships, the proportionality between these structures and used in registration, warping strategies and annotation systems. There are specialized atlases of the brain image, but there are limitations on the demographic parameters and the imaging types used. One of the most used atlases is the Talairarchi Brain Atlas, integrated in several systems (SPM is using this atlas). There are also deformable brain atlases where the anatomic variability is managed by spatial normalization schemes. The drawback of these atlases is represented by the fact that not all the brain structures can be captured and molded by these algorithms. When talking about brain, the variability is manifested on every metric.

We use the atlas approach on these images for reconstruction of the brain image in 3D and analysis of the basically diffusion characteristics: the *Fractional Anisotropy (FA)* and the *Apparent Diffusion Coefficient (ADC)*. In the case of an equality on all directions for the value of the FA, a low anisotropy is revealed and if its value is produced high in certain directions, a high anisotropy is present. The movement of the water protons and their diffusivity at the voxel level is determined by the ADC value.

The Java program that uses imageJ, after identifying the image being processed as an

EPI DTI image, searches the images that are taken on the same step and contain different gradient levels. Once we have all 12 slices that represent the same image for different diffusion values - values specified in table 3.1 - we generate a stack from these images. The stack is then processed and analyzed in Matlab using SPM and VBM algorithms.

Statistical Parameter Mapping (SPM) is an academic software toolkit used for analyzing functional imaging data in image processing and analysis [Guillaume 2008]. In our work, we use several functions provided by SPM. We use Segmentation features in order to perform bias correction and spatial normalization within the same time as segmentation. In combination with VBM5 (see paragraph 2.5.3), which performs region-wise volumetric comparisons among several subjects, SPM5 requires images that have been spatially normalized. For revealing the physiological elements we need the images to be segmented into different tissue classes. The smoothing process offers us a clearer image which we need prior to performing statistical tests [Friston 2000].

Voxel Based Morphometry (VBM) is used in our system in the image processing stage. We use VBM5 in our work as it completes itself very well with SPM5 toolbox and extends its capabilities. It can use previous segmentation for further analysis [Gaser 2008] and performs a voxel comparison for tissue concentration. Its disadvantage is the susceptibly to registration and segmentation errors and its sensitivity to image characteristics. The image must be preprocessed before VBM5 is applied, as it does not work with any type of image. This preprocessing is done in our case using SPM5. We are using the functions from the brain extraction process for our images and for normalizing GM and WM. With VBM, registering the brain to a template and smoothing the result by applying an average value for each voxel, between itself and its neighbors, overcome the differences between brain anatomies.

The maps from these segmentation algorithms (SPM combined with VBM) provide the results presented in 3.2.1 and they represent a preliminary testing technique applied on our database to evaluate the usefulness of each tissue type. We applied the values computed with equation 2.2 and 2.1 in order to obtain 3.5(a) respectively 3.5(b).

2.6 Conclusion

The medical imaging standard provides not only the image information, but also the *demographic parameters* for statistical study and knowledge-based analysis. We call *"demographic parameters"* the specific parameters to each patient: age, sex and brain volume. The image protocol from the header image contains also the necessary elements for the *3D volume reconstruction* using the 2D sequences. Though when searching or extracting a certain anatomical structure from a 3D volume, the 2D slice containing that particular structure must be found first. This is a challenge as the human bodies are different therefore the volumetric elements differ and the positioning of the patients in the scanner is different as well.

When performing the medical image analysis we are confronted also with *inter-patient variability*, as each patient has different dimensions for the same anatomical structure, as well

as the placement on a general basis, relative to a model perspective. There is also the *intra -patient variability* due to the different imaging techniques that reveal in different manners the same anatomical detail. Overcoming these variations represents a big challenge for the entire medical image processing systems.

MRI sequences have the clarity for the anatomical detail, but also the diffusion value for the neural fiber determination. The MRI sequences have different features that combined become complementary and have greater value together - fusion applicability.

The specificity of the medical images must be taken into account when processing head images, as well as patient variability. The systems tested are specific for the head images processing and allow DTI images to be analyzed.

These systems, together with the associated algorithms, offer a view on the selection criteria for the suited algorithms, interpretations of image features and their applicability on the diagnosis.

Analyzing the medical images, we will use the EPI further for processing and analysis as they offer the tensors for the tractography method. Due to the low resolution, the anatomical detail of these images does not recommend them for segmentation. This is the reason why we use the FA images provided in our database, as they contain the anisotropy and the diffusion, emphasizing the Putamen area. The method chosen for segmentation is based on the voxel entropy, in order to avoid the folding or misplacement caused by an atlas approach.

After testing several registration methods, an automatic approach based on parameters, using the brain geometry. This is a rigid registration that takes landmarks representing specific geometrical parameters and uses affine transformation.

For the tractography we use a deterministic global approach, detecting the fibers that are part of the segmented midbrain area and validating only those that reach the Putamen area. We have tested the probabilistic global approach using the Diffusion Toolkit (TrackVis) and the result included noise. Also the metrics provided by the statistical module for the bundle of interest had a very high value for the number of tracks.

We tested all these methods using our own database in order to include the specificities provided by the acquisition protocol at the image level. This protocol and its importance are presented in the next chapter.

Chapter 3

Database and pre-processing algorithms for PD Prognosis

Contents

THERE ARE SEVERAL ASPECTS WE MUST TAKE INTO ACCOUNT when defining the algorithms for the implementation of PDFibAtl@s. As the images represent the input, their quality influences the overall results and the approach used for the algorithms.

Given the images provided by our medical partners, we further consider several technical facts related to the specificity of the medical images. In order to have the best results on the detection and analysis performed on the images, the quality of these images has to compel with the needs of our algorithms: good resolution and anatomical detail. Another important aspect is represented by the patient identity factor that interferes with our analysis: each patient has a specific anatomy and the slice of interest for different patients is not the same one. As the volume of the brain is not similar for all the patients and as the anatomical detail differs among the cases, the automatic detection of specific areas should be based on the

x	y	z
1.000000	0.414250	-0.414250
1.000000	-0.414250	-0.414250
1.000000	-0.414250	0.414250
1.000000	0.414250	0.414250
0.414250	0.414250	1.000000
0.414250	1.000000	0.414250
0.414250	1.000000	-0.414250
0.414250	0.414250	-1.000000
0.414250	-0.414250	-1.000000
0.414250	-1.000000	-0.414250
0.414250	-1.000000	0.414250
0.414250	-0.414250	1.000000

Table 3.1: Gradient Values used in our protocol for diffusion images

geometrical display of the brain anatomy. In addition, a correlation between the patient's age and sex must be taken into account since we should exclude the atrophy and other geriatric specific elements, as well as differences in the volume of the brain due to sex differentiation.

We will extend in this chapter the analysis at the image level by presenting the protocol for the DTI images that we are using and the specifications for each type appertaining to the DTI imaging method. These characteristics determine the selection of the imaging types used in our study. The pre-processing steps performed on the images are presented in this chapter as well, as they are the result of the specificities of the imaging types further used in our methods.

3.1 Database characteristics - Diffusion Tensor Images

We are presenting the medical image characteristics specific for the DTI images emphasizing on the images that we are using and the specific characteristics of these images.

A number of 68 patients diagnosed clinically with PD and 75 control cases underwent DTI imaging (TR/TE 4300/90; 12 directions; 4 averages; 4/0 mm sections; 1.2 x 1.2 mm in-plane resolution) after giving informed consent. This represents, as far as we know, one of the biggest cohort of PD patients implicated in a study. The heterogeneity of the patients - Asians, Eurasians and Europeans - can also be used to characterize a general trend for PD prognosis. For this type of DTI images, we have 351 images (e.g. Fig. 2.3) that represent slices of 4mm of brain structures taken in 13 directions at each step (one step represents a position on the vertical brain axes). In this case, we have 27 images that constitute a 3D brain image - contain all the possible position in order to show a complete image of the brain in 3D format.

From the database patients we have chosen a cohort of 22 patients and 25 control cases,

correlated as age and sex, for preliminary testing and development of the pre-processing methods. As shown in Figure 3.1, the characteristics of the images taken into account for

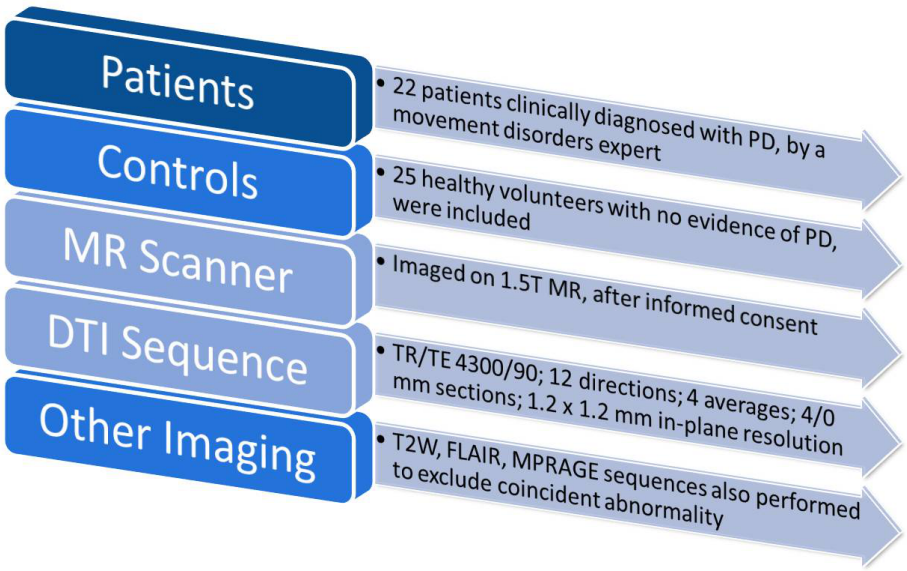

Figure 3.1: Input database

the study present some limitations for certain patients. From this point of view, the image stacks taken for the volume analysis can be placed higher or lower on the body of the subject; hence we have some incomplete studies. The image resolution does not permit an automatic detection in some of the cases as it is not able to detect a significant difference in the contours of certain anatomical regions.

Working with the DTI technique, we rely on the fact that water diffusion is highly anisotropic in white matter (WM) and the reason for that is that the water molecules were restricted in the axons. The DTI images that we are using were taken with a Siemens Avanto 1.5T(B=800, 12 diffusion directions).
All the images are in DICOM format. This format is specific to the medical images, containing the header file and the image encapsulated in the "dcm" (DICOM) file. In the header, all the information regarding the patient is contained together with the technical information regarding the parameters for the acquisition. Reading this file, we are able to establish the order of the slices and create the volume image using the same type of DTI. There are several types of DTI images that differ among them by the fact that the coil that takes the images is differently placed and/or the diffusion is performed in several specific directions.

3.1.0.1 Echo-planar images(EPI)

From the DTI images the EPIs (Fig. 3.2) are among the ones with the lowest resolution. The advantage of this type of DTI is that they contain the tensor information as matrixes, giving the actual orientation of the water flow defining the brain fibers. The diffusion directions have each, as result, one volume of images. In this way, we use for each volume 351 EPI images with 12 diffusion direction, one without diffusion and 27 slices. This is the reason why the tensor computation, which takes the 12 directions into account, has a good accuracy coming from many images.

The tensors are obtained as a result of water diffusion on the neuronal fibers and they are stored as matrix with diffusion directions. This information can give the direction of diffusion, as well as the anisotropy values stored as tensor values. To make use of this information, we limit the value of the anisotropy for noise elimination. The tensors are computed using the diffusion directions and the B0 image as ground truth. Represented as directional-related indices, the tensors offer information regarding the angle between the current location of a fiber and the possible evolution of the same fiber. This angle is limited in our case at 60 degrees minimum, to avoid the noise.

Managing the information coming from the EPI This type of image is not appropriate for the anatomy extraction and analysis, but the tensor and anisotropy values stored represent the bottom line of fiber reconstruction, as well as the source for other images. We perform the entire image preprocessing on the EPIs, as they provide the tensor for the fibers as well. A preprocessing step for these images represents a contrast enhancement of 0.5% for a better detection of the skull and the volumes of interest.

We perform the skull removal process next for detecting the center of mass only on the brain. The contour of the brain can be extracted next for detecting the starting point for the inter-hemisphere axis. The removal of the skull is needed because the results have shown influences of the voxels that are not brain tissue on the anisotropy analysis. We perform the removal task on this type of images because they contain the anisotropy values and the tensors that are used further in the detection of the fibers. They must be uninfluenced by any voxel intensity other than the brain tissue.

3.1.0.2 FA and ADC specific features used

Fractional anisotropy images result from the computation of the anisotropy level for each voxel on the EPI images (Fig. 3.3). They contain not only the anisotropy values, but also the color code for it. This type of image represents the diffusion direction inside the fibers. Because of that, the Putamen area is well defined as the motor tract reaches it and stands out as contour with high anatomical detail, therefore we use it in the automatic detection of this volume of interest.

After a registration of the obtained volume of interest extracted from this image we can use it together with the tensors from the EPI to limit the fibers that we take into account. At

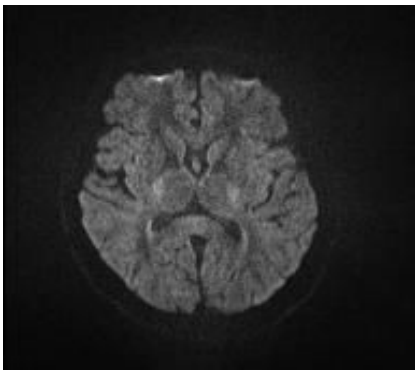

Figure 3.2: Axial slice of an EPI

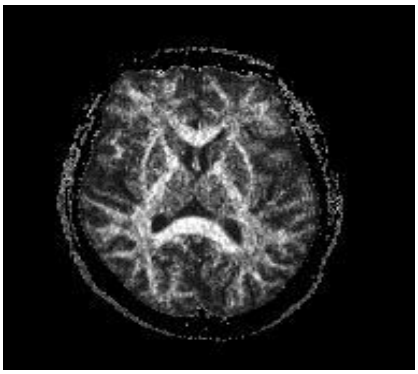

Figure 3.3: Axial slice of a FA image

this point, there is an exchange of information from one image type to another, by information fusion.

3.2 Preparing the image for processing

Due to the complex structure of the medical image encoding manner for the DICOM format we need to take the useful information from the header file. During the processing and analysis steps we only make use of the image by itself, without the additional information. This is the reason why we transform the image from the DICOM format to Analyze and store it as stacks of images that represent an entire brain volume for each patient sorted according to the imaging modality.

The Analyze format is similar to the DICOM one, except that the header file and the image file are stored separately. Also, the header file does not contain as much information as the DICOM one: it does not have any information regarding the acquisition method and parameters (e.g. angulation for the acquisition plane, the series type for the image, the slice number, the diffusion direction). When placing the images on a stack, the alignment between the slices is highly needed. This gives us a clean volume image providing a clean contour for the anatomical volumes.

For the axial plane, the images that we have in our database are taken in AC/PC plane - Anterior Commissure/Posterior Commissure. This axis is significant from the anatomical point of view and it is used by the radiologist because it is distinguishable in all the MRI images. The sagittal plane and the coronal one are not used by our approach.

We evaluate the possibility to apply certain methods onto our database by conducting preliminary testing with the systems presented in the previous chapter. In this section, we present the evaluation and performances together with the applicability of these methods included in other systems. This approach also emphasized the importance of our system in

comparison with other systems, as well as the efficiency of the new algorithms compared with the existing ones.

We first test the FA and ADC values on the whole image, without segmentation, to see if there are any significant differences between the patients and the control cases or among different patients. Then, we evaluate the same parameters on the midbrain area, where the dopamine is produced, so that relevant differences can be discovered among patients and fiber orientation can be discovered for the tracking algorithm.

3.2.1 Preparing the images for 3D handling

Having a small cohort from our database for working with (21 patients and 25 control cases), we are taking the Parkinson patients and for each of them we have four modalities for the image processing step. In this case the amount of images is enough for performing a well-documented study. Depending on the image modality the quality of the images varies.

For measuring the quality of the images we look for images that have a high degree of clarity and accuracy for revealing the anatomical details. Also the fact that we are dealing with medical images, DTIs, we have black and white images, with grey levels. As the images represent slices of 4 mm, the grey level is different from one slice to another due to the fact that the patient can move slightly - when breathing and/or trembling - the resulted image is most of the time blurry.
To overcome this effect, we apply the spatial normalization and inter-slice alignment for constructing the 3D image.

The segmentation is evaluated by assessing the result of the segmentation, the segments - the GM, WM and CSF- the volume obtained by putting all the resulted segments together - the stripped brain, without the skull area. At the image analysis, we are currently working with two parameters: FA and ADC. The obtained values must be close to the value of 1 [Chan 2007]. For our images, we obtain an anisotropy average of 0.56 for each slice image and 0.52 average for the whole brain on the GM images. For the CSF images we have a lower value, as expected, and for WM slightly lower values than for the GM.

For augmenting these values, we change the processing procedure and the preprocessing as well. These results depend on the image processing but also on the diffusion values and the tensor directions. When performed on more diffusion directions, we obtain higher stacks and better the accuracy as well.

For evaluating the analysis step, we are using the H&Y scale (see annex C) where the Parkinson patients are annotated on a scale from 1 to 5, according to the severity of the disease. We are trying to achieve the same classification using the FA and ADC values like the one in the H&Y scale, making the difference between the affected cases and the healthy ones by computing the values for the parameters on the patients as well as on the control images. Also, the different severity of the disease like in the H&Y scale can be determined by the functions that analyze the images.

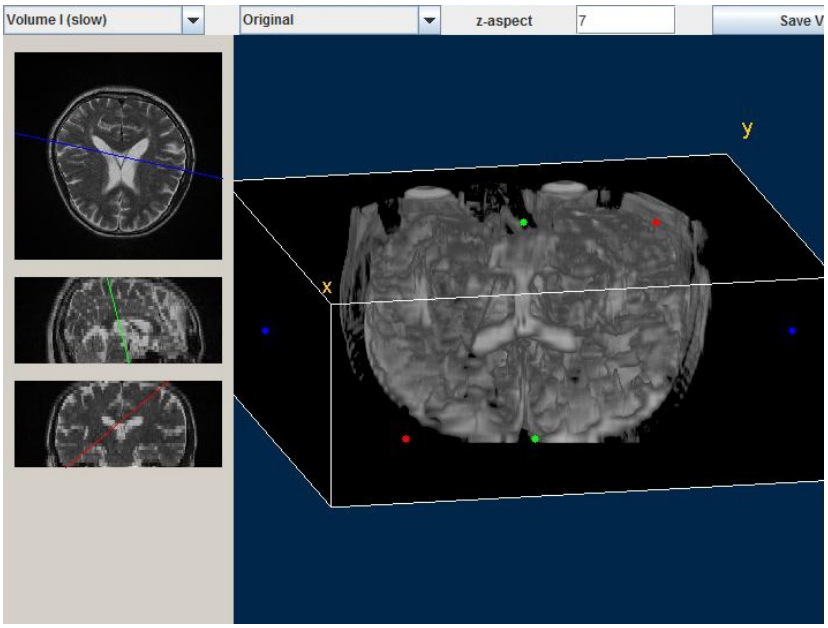

Figure 3.4: 3D Image Stack generated with imageJ

3.2.1.1 FA and ADC computation

An optimization for the brain images is represented by the normalization of the image to a standard space by matching the grey matter to a reference one and eliminating, in this manner, the scalp [Friston 2000]. This process generates grey matter (GM), white matter (WM) and cerebral spinal fluid (CSF)-see Fig. 3.7. In figure 3.6 we have the requirements from VBM functions before processing with this tool [Yaasa 2004]. These requirements are attained by using SPM functions. Performing normalization for an image in the warping process, disturbances introduce some differences. Modulation is used for compensating these differences. By performing modulation the amount of grey matter is preserved in the normalized image. (E.g when a lobe has half the volume of the image in the template, then during normalization the volume could be doubled, but the voxels will be affected in this case because their number will be doubled). Using the modulation process the coordinates in the normalized image will be restored to their original values by using the deformation field values [Friston 2000]. For the normalization process, we can use one or more template images. The algorithm minimizes the sum of squares difference between the image and the templates. The first step creates a match between the images of the head with the skull. The next step performs a matching between the brains and registers the result. The registration step uses a Bayesian framework that searches for the solution that maximizes the a-posteriori probability [Friston 2000]. At this point, in the SPM segmentation algorithm, the deformations are estimated for the modulation

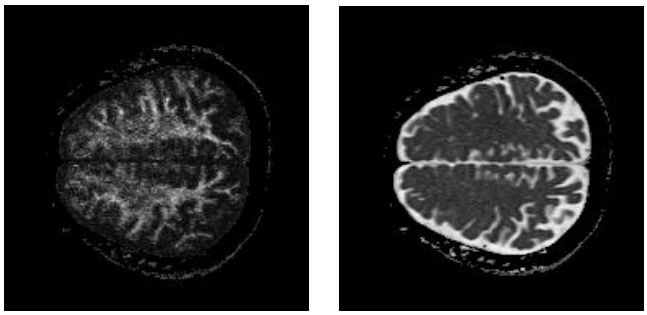

(a) FA image (b) ADC image generated

Figure 3.5: FA 3.5(a) and ADC 3.5(b) example of images

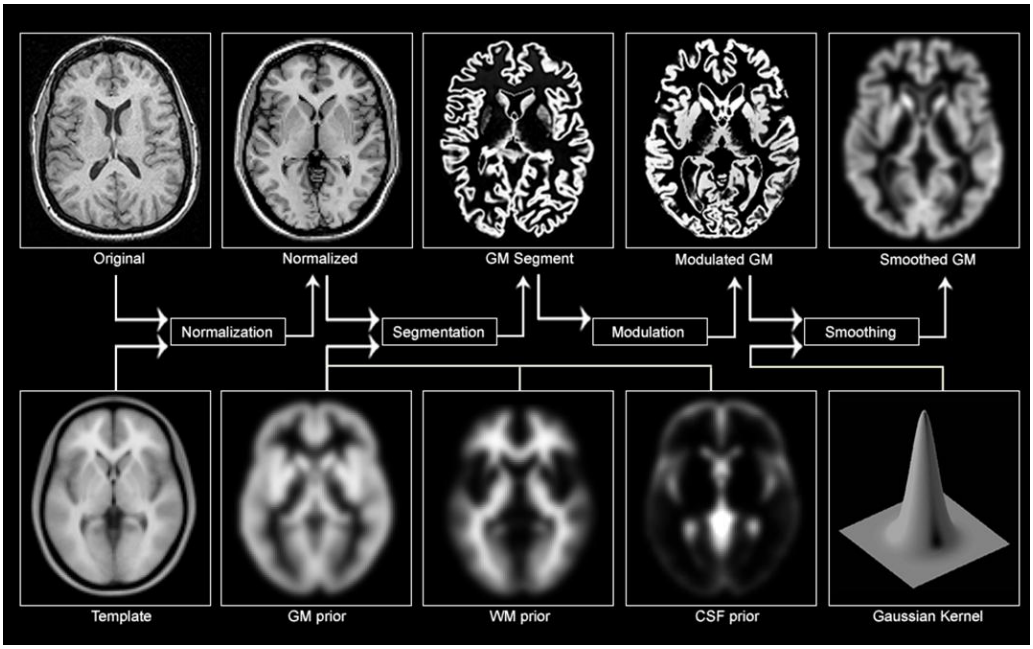

Figure 3.6: VBM Preprocessing requirements [Yaasa 2004]

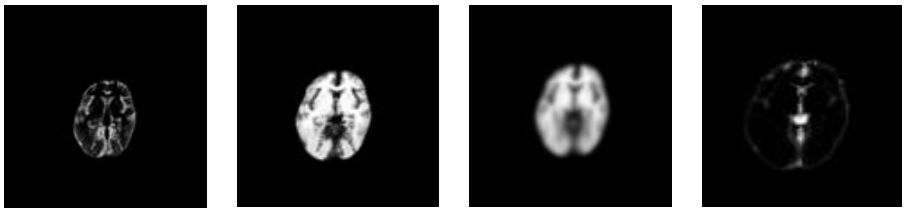

(a) GM (b) WM (c) WM smoothed (d) CSF

Figure 3.7: Images Processed:GM, WM, Smoothed WM and CSF

part.

The registering process for the tissue probability maps and the processed image uses a minimization of the sum of the two terms -the two images. This process is performed by the warping function. For this function, the portability of the data and the parameters are used. We obtain a smoother deformation. The cutoff value included in computing the warp function depends on the point of view of our image. Having a smaller value for the cutoff allows more detailed deformations to be modeled, but the processing time is longer[Friston 2000].

We use a smoothing function from the SPM in order to eliminate the noise or deformations acquired during the processing part. This function performs the smoothing with the Gaussian kernel. This system provides also pathology detection with deformation-based morphometry integrated with pattern theoretic approaches - deformation maps of the variations in normal anatomies based on continuum mechanics [Thomopoulos 1994].

By processing these types of images, we extract specific information from the brain images. At this point we are able to extract the white matter (WM), gray matter (GM) and cerebral spinal fluid (CSF) from all the types of images used. The images containing WM and the smooth modulated images with WM are then used for FA and ADC computation (Fig. 3.5). FA is a useful measure in the DTI images as it reveals the connectivity at the brain level. Again, for all types of images the values are taken and for each patient an average is computed for expressing the values at the volume level. The values used for the images in figure 3.5 are computed using the equations 2.2 and 2.1 on each slice of the volume. The mean value obtained from all the slices for the FA and ADC represents the values that we are studying.

3.2.1.2 Analysis

When processing the images, several parameters are set for the SPM function to generate the maps [Yushkenvich 2008] [Fillard 2002]. We choose the Eastern Asian brain maps for the segmentation phase. This choice was the closest for the population included in our database, but it is restrictive nevertheless. Also regarding the bias regularization, we use the heavy threshold for this purpose, as it eliminates the surrounding noise. These features are then used to characterize each patient from the three perspectives.

3.2.2 Midbrain study - manual approach

We are moving the FA image so that it perfectly overlaps the EPI B0 image of the same patient. As presented in 2.3, there are several main steps to follow when registering two images.

3.2.2.1 Preliminary testing

Our preliminary work is based on the determination of the first region of interest - volume of interest where a study is performed on the FA images considering the color-coding specific for this type of images. The colors for this type of image represent the direction of diffusion into the fiber tracts:

- Red color pixels - for anisotropy orientated from Left to Right (LR);
- Green color pixels - for orientation in Anterior - Posterior directionality (AP);
- Blue color pixels - for orientation in Up - Down directionality (UD);

We analyze the green channel to see if the fibers running in the AP direction are similar for the patients or are degraded depending on the PD level. The easiest way to analyze the green channel is to generate the histogram for this area. The histogram represents the number of pixels that have a certain intensity: $N(b_i)$

$$P(b_i) = \frac{N(b_i)}{N} \tag{3.1}$$

where N represents the total number of pixels.

Based on the fact that the motor tract, according to the brain pathology, follows the anterior -posterior direction, we perform a color analysis on the volume of the midbrain extracted, in order to see whether the fibers starting from this area oriented in AP direction have a correlation with the H&Y scale.

Figure 3.8 represents the main steps in the analysis of the green channel. We make the detection of the midbrain area and compose the volume of interest on the EPI image and then place the determined volume on the FA image for the green channel extraction, performing an alignment between the two image types. Once we split the volume obtained from the FA image on the three channels and take the green one, we perform the histogram and extract the values for the range of interest. This range is chosen in a way that we can exclude the noise and we place it in between 10 and 100. These values are then correlated using PASW 18.0 (Predictive Analytic SoftWare, formerly SPSS- Statistical Package for the Social Sciences) tool with the H&Y values. An analysis of the methods used for correlation, as well as the testing procedure used is presented in chapter 7.

After this study, we continue with the fibers growing, to examine their density and the relation at a higher granularity level with the disease.

This analysis offers the opportunity to see if the PD and the correlation between the disease and the level of green affect fibers starting from the midbrain area, where the dopamine is

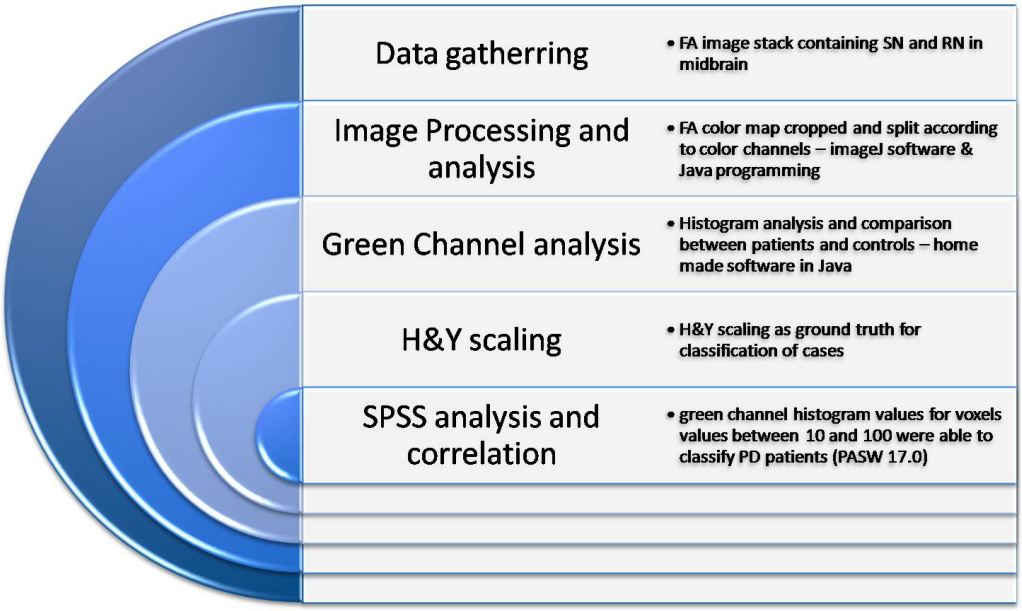

Figure 3.8: Green channel analysis

produced. This level of green represents the anisotropy level as well and this particular area is the one that is correlated with PD, as the motor tract represents most of the fibers going in AP direction. In this case the anisotropy level, if correlated with the H&Y scale represents an indicator of the disease at the midbrain level. Therefore, we are able to determine that the starting point for the fibers we want to grow is relevant for our study.

3.3 Pre-processing algorithms

These algorithms came as a natural need after the pre-testing results. There are several systems that offer the possibilities for performing the processing we needed. Before defining our algorithms we have tested the images on other systems, to evaluate afterwards our own algorithms performances. The need for our new algorithms came due to the images characteristics presented in section 3.1 combined with patient variability. All these methods are performed on the entire image slice, all the slices in the volume stack and represent a global approach.

As the FA values estimated on the whole volume proved to be indecisive as a PD feature, the medical doctor suggested that removing the skull could offer better results, with less residual elements, eliminating the bone tissue. This is the reason why we performed the skull removal process. Together with the bone tissue, the noise surrounding the head images must be eliminated as it represents noise. Next, preparing for the feature extraction algorithms we needed landmarks applicable to all patients that can guide our algorithms without any interference from the patient variability. These elements, together with the hemisphere detection algorithms, set up the elements for the automatic detection of the location where to apply

the feature extraction algorithms.

3.3.1 Skull removal

As the systems considered in section 2.5.1 provided algorithms that performed the skull removal as well, we have tested these algorithms first and then developed our own. The systems are tested using our own images with the characteristics specified in section 3.1 and we are using EPIs, as they are the ones providing the elements for the fiber growth. We need these algorithms for the FA images to eliminate the problem presented in section 3.2.1. We use the atlas-based skull removal method offered by SPM and the one based on the pixel entropy (MedINRIA) because the method based on the atlas offered by Slicer is too slow on our images.

Using the atlas based approach (SPM) , the segmentation detects the skull, as the tissue surrounding the brain. With this approach due to the EPI image quality, some of the other types of tissue were removed or not correctly identified due to patient variability.

The algorithm based on the voxel intensity (MedINRIA)[Fillard 2007] is affected by the the exterior elements and noise and its sensitivity did not provide good results for our database. This is the reason why the exterior noise had to be removed - not to affect the other processing algorithms.

Our own algorithm was applied on the EPI image and it uses KMeans classification for the tissue to detect the bone tissue. This algorithm is implemented in java and was available as a plug-in in imageJ[1]. Actually the FA image containing the anisotropy provides the intensity for the skull voxels similar to the one representing the GM. This is the reason for the noise at the FA computation. We used for our purpose a four class evaluation to distinguish between the bone tissue and the GM, WM and the CSF. The algorithm was not sensitive to the exterior noise as we have applied a noise removal filter provided by the same library. In this way all the elements outside the skull perimeter was considered as noise and eliminated.

At his point the brain tissue represents the only information in the image. Estimation, analysis and processing on these images offer correct results on the brain tissue state.

3.3.2 Retrieving the geometrical elements

Having only the brain as information in the whole volume representation, offers us the possibility to sets landmarks based on the whole volume estimation so that we can eliminate at least a part of the patient variability. This is the reason why we retrieve, using an imageJ plug-in algorithm -object counter[2], the brain center of mass at the volume level and we are able to perform the same feature extraction at the slice level. This landmark is able to offer

[1]KMeans in imageJ: `http://ij-plugins.sourceforge.net/plugins/clustering/index.html` - last accessed on June 2010

[2]imageJ plug-in Object Counter : `http://rsbweb.nih.gov/ij/plugins/track/objects.html` - last accessed on June 2010

us an alignment for all the patients based on their volume, a central axis placement through the aligned volume. Next, we needed a manner in which to find the limit the left and right side of the brain and in thus have another landmark for the patient alignment.

3.3.3 Hemisphere detection

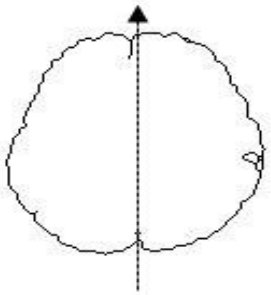

Figure 3.9: Brain edges detected for variability function evaluation

This detection is further needed for patient alignment at the volume level to provide, together with the center of mass, a plan that passes through the center of the brain, making the distinction between the two hemispheres. For this detection we determine the outer boundary of the brain (Fig. 3.9). We analyze this boundary as a variation function determining the maximum inflexion point on the function corresponding to the occipital sinuses at the base of the Occipital Bone of the skull.

This point together with the center of mass of the brain determines a sagital plane between the two hemispheres. Also, used on an image with the center of mass from that image provides a horizontal axis indicating the orientation of the brain in the image. This will be used for registration.

3.3.4 Importance of the performed pre-tests

The whole image testing evaluates the FA and ADC values on the whole volume of the entire image. The mean value on each patient does not offer an average to distinguish between the PD and the control patients, therefore we need further study. The medical doctor suggested that the bone tissue might be affecting the overall FA/ADC values and changes the meaning of the testing. The FA and ADC images obtained computing these values reveal a good image of the dopamine paths of interest. The Putamen is better defined in the FA image level and a more insightful study on this area is possible on this type of image.

From the study of the green channel the AP positioning of the fibers reveal a pattern that follows the disease severity that makes us think that the dopamine flows in this direction. Studying the flow at the midbrain level, where the dopamine is produced and using the FA values from the image, a fiber disposition that follows this direction coded as green on the image, makes the distinction between the fibers that we need for study and the tracking direction to make the distinction on these fibers.

The preliminary testing algorithms validate the medical theoretical hypothesis and offer as well the measure of the image dependability. In this manner the images provide the solution of the following algorithms developed for PDFibAtl@s. By extracting the same features at the pre-testing level and at a higher granularity level, we are able to evaluate the performance of our algorithms on the feature extracted. The green channel analysis is done based on a similar variation on the histogram for the volume of interest on this channel, indicating that

the fibers all follow in AP direction and that there is a correlation between the anisotropic green channel and the H&Y values. Furthermore the fibers that start from that area and grow towards the Putamen have an even stronger correlation with the PD evolution scale.

We will use the image without skull, as apparently it interferes as shown in the whole image processing step. Also, the hemisphere distinction provides a good limitation for the processing and tracking algorithms. PD is more obvious in the left side of the brain, therefore an analysis on this side should be more relevant.

3.4 Conclusion

The H&Y scale represents our system of reference in analyzing the results and elements indicative of the PD. This scale stands for the diseases degree, 1 being the mildest and 5 the most severe. Unfortunately, for several patients there is no clear classification (1.5 or 2.5 on H&Y scale) and for those cases our system would be a confirmation for placing the patients on the 1 or 2 classes for sure, but at this point, our system might put these patients on either of the classes with no mistakes.

The preprocessing step performed on these images represents a system able to gather specific DICOM images and place them on a volume stack. The mild processing for the EPI and FA images is meant to enhance the success of the automatic detection of the volumes of interest and prepare the images for that purpose.

Performing the testing on the entire image we have a global view of the features that the image offers and the possible applications on the image. Also, it is able to give us a starting point for the analysis of our algorithms as it shows the image importance regarding the features. From the whole image study, a more concentrated study on an anatomical region of interest offers a better image of our diagnosis.

Studying the fiber positioning and the link with the FA value offers the image of the fibers that are the most used by the dopamine and the way they are placed at the volume level. Performing the image analysis on the colored FA image on a specific anatomical volume of interest, we are provided with the orientation of the fibers used by the dopamine flow in that anatomical region.

The pre-processing algorithms used prepare the image for the processing step, offering the preliminary geometrical elements, as well as a clear distinction for the two hemispheres for feature extraction and analysis purpose.

Chapter 4

Image Processing Methods

Contents

After presenting the types of images that we are using and the way that we intend to handle the images, in this chapter, we focus on the image processing, locating the volumes of interest(VOI) and their extraction methods. Prior to these objectives, let us enhance the challenge that we are taking in at this point.

After a view on the systems able to process the images from our database in chapter 2 and a closer look on the image characteristics in chapter 3 we are now presenting our algorithms dedicated to the segmentation, registration and tractography. Our methods are meant to eliminate the inter-patient variability and the demographic characteristics using a

fully automatic approach. We present an overview of the main methods and the problems that these methods aim to solve.

4.1 Overview on the system

Testing several systems dealing with specific treatment of DTI images, we construct our approach based on the clinical needs, as well as on the results obtained from other systems. First, by testing other systems with our own images (section 2.5.1), we evaluate the possibilities that we have of using our images and the flows that these images have. At the same time, we evaluate existing algorithms and their effects on our images by analyzing the results these images provide using our database. From figure 4.1, we define the main processes that our information undergoes from the image level to the knowledge level. We start using EPI images, where we extract the midbrain area first. The FA are used for automatic Putamen detection and, registering these images on the EPI, place the detected volumes at the right position on the EPI images. Once these volumes of interest are placed, the algorithm for fiber growth is applied on the EPIs and the fibers extracted are analyzed, together with the detected volumes of interest. Another part is represented by the diagnosis step followed by prognosis. These steps are described in Chapter 5 together with the algorithms implemented. At this stage we are presenting the image processing algorithms, the features analysis being the subject of the next chapter.

We first analyze the flows of our images, the needs of the medical filed meeting the results acquired by the algorithms implemented in other systems and presented in section 2.5.1.

4.1.1 Comparison with other type of images and correlation with current diagnoses system

For the use of the Fusion Image module (MedINRIA system) that performs the manual, automatic affine registration and the diffeomorphic registration, each patient must first be processed using the DICOM dedicated image handler, Image Viewer. This module provides the image format needed by the Fusion Image module. There is no inconvenience except when having a large database. The fact that the registration does not perform with the accuracy needed on our images for enabling us the correct fibers represents the major drawback at the registration level. Also the fact that we cannot limit using two volumes of interest for the chosen fibers, makes us regard another option altogether. Even though, because of technical reasons, manual registration would be optimum for our case, we cannot use the DTI track module that performs the global tractography using Log-Euclidian metrics on a deterministic approach (MedINRIA) because it would mean choosing only one volume of interest, which cannot separate only the bundle of interest.

The probabilistic global approach on tractography is implemented in Diffusion Toolkit (TrackVis). This approach offers several methods for computing the propagation of the diffusion: FACT, second order Runge Kutta, Interpolated Streamline and Tensorline. We are testing the second order Runge Kutta, as it is the closest on our approach. Using a previous

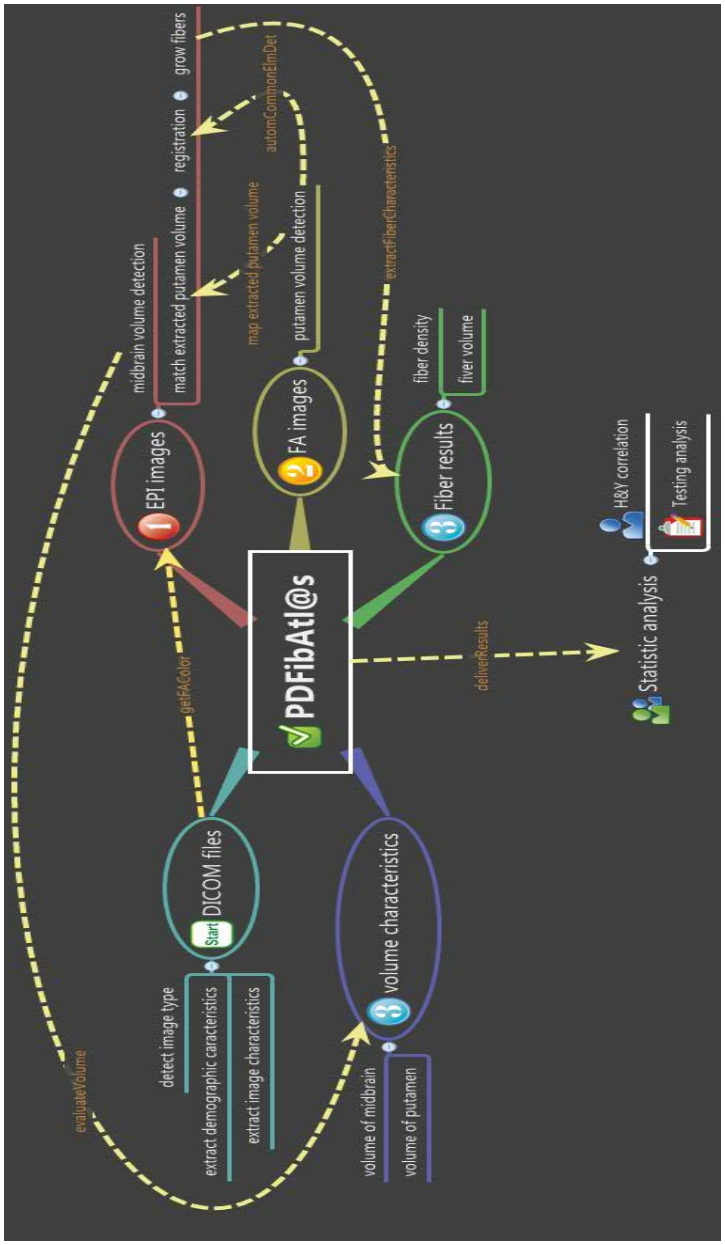

Figure 4.1: Tasks and Processes in PDFibAtl@s

mask for the volumes of interest does not perform well on our data, but the possibility of limiting the computed fibers using a manual ROI or even two VOIs provides the needed bundle of interest. The drawback is the fact that this approach needs to compute all the fibers and limit them afterwards. We do not need all the fibers and this time-consuming process can be avoided with the mask volume. This possibility exists in the Diffusion Toolkit, but our mask volumes could not be read either by the Diffusion Toolkit or the TrackVis module. This aspect constrained us to perform the manual segmentation. With the manually VOIs the results on the fibers were either null or noisy.

Testing Slicer 3D we are offered with the possibility to choose two volumes of interest for limiting the fibers. The registration for the images is done manually by choosing interest points. This time, the system is unable to complete the fibers due to the great number of images loaded corresponding of the directions of diffusion. This make the algorithm stopping before complete computation of the fibers (section 2.4).

Typically, the brain atlases are used for taking the volumes of interest into account. This is not accurate due to the fact that we have a brain database from Singapore that contains not only Caucasians, but also Asians, so that a mapping with the brain has small chances of being correct. Testing Statistical Parametric Mapping algorithms (Maltlab SPM toolbox) we obtain results only on the entire brain analysis and due to the image quality, the skull extraction cannot be properly performed and thus, we have interferences with the results on the anisotropy. A specific atlas that contains automatically detected anatomical volumes represents a tool that can be applied to any type of patient.

At this point, we choose a specialized library that provides us with the elementary image processing elements: medical image reading and writing, basic filters and plug-ins, enables us to use algorithms already implemented and to begin our processing at a higher level of data management. Indeed *imageJ*[1] is a useful open source Java based library conceived for medical image processing and analysis that offers the possibility to develop a Java application that can be used for testing further in this library as a plug-in. It also has the advantage that developers using this library are continuously updating it by offering their contribution as plug-ins. The entire functionality is contained in *ij.jar* for easy integration in a program, as well as for developer testing. In this manner the newest algorithms can be tested with the available images and further development can be made more quickly. Besides, it offers the possibility to test several approaches before deciding on a certain algorithm or approach by directly analyzing the results. This allows us economize effort and time, in this way we used elements from the library together with our own code.
Another reason to use this library is its portability. We wish PDFibAtl@s to be used at any medical station for integration with the systems currently working on these stations. It offers the possibility of using libraries already developed as VTK[2], as a plug-in with several algorithms.

[1] ImageJ website -`http://rsb.info.nih.gov/ij/` - last accessed on June 2010
[2] ij-VTK -`http://ij-plugins.sourceforge.net/ij-vtk/index.html` - last accessed on June 2010

4.1.2 Proposed approach on image processing

From our preliminary studies, we have seen that the *motor fibers* are relevant for the progression of PD. By building a specific Parkinson's Disease atlas, we intent to segment, visualize and quantify VOI characteristics, together with the motor fiber tracts. Substantia Nigra (SN) and the Putamen represent the two extracted VOI, as they represent the origin and the target of the dopamine flow inside the tract, from where we extract the bundle of interest. For these VOIs to be accurately used on the same image, as they are extracted from different image types, we need an intra-patient registration due to the characteristics of the image protocols. Geometrical characteristics of each patient are the landmarks for this geometry-based registration [Zitova 2003], used to align the volumes for FA and EPI. The registration provides a common space for the diffusion tensors -provided by the EPI- and the anatomical elements extracted from the FA, due to the anisotropy flow that makes the contours of the Putamen more visible than other image type. The registered volumes are fused, by acquiring the anatomical part from the FA and applying the aligned mask on the EPI images. This inter-image information fusion enhances the anatomical importance from the color image (FA), taking also into account the anisotropy level provided. On the registered volume of interest on the EPI, we perform fiber growth between the two volumes of interest and we extract the fiber density (FD) and the fiber volume (FV). At this point, our approach differs from other fusion techniques, since we are fusing the images at the information level, using the registration for spatial alignment on the brain volume. We do not rely on prior atlases created for structural MRI and no manual intervention is needed in the process [Lehericyr 2004] [Vaillancourt 2009]. Also, we do not perform prior segmentation on white matter (WM) and grey matter (GM) or use any maps for alignment and registration purposes [Deisseroth 2009] [Woodward 2009].

From the fusion point of view, we have two ways of information fusion: from EPI to FA and on the opposite way as well. We must first take into account the specific characteristics of each image type. The FA image represents the fractional anisotropy on the dopamine flow inside the whole brain, color coding on this image indicating the direction of diffusion as presented in section 2.

EPI volumes contain the tensor matrices that provide the direction of the fibers for the fiber growth algorithm. From this standpoint, the color analysis approach is better on FA image and for the fiber growth we must consider the EPIs. However, on the FA image, the detection of the midbrain area is not possible since the algorithm takes a part of the Cerebro-Spinal Fluid (CSF) as well, and this interferes with our further analysis. Hence, we must work on the midbrain detection on the EPIs. On the other hand, there are problems with detecting the Putamen area even on the T_1/T_2 images because of unclear boundaries between this area and the surrounding ones. On the FA image, due to the dopamine enhanced by color-coding we are able to make a distinct limitation of the Putamen. We use both regions of interest for each step of the analysis part, together with the obtained new parameters at the fiber level.

4.1.3 Main tasks that meet PD diagnosis challenges

Before detecting the volume of interest, we must perform several steps for image preprocessing. This is due to the low resolution of the EPI and the problems presented at the beginning of the chapter and emphasized during the system testing: brain size differences, anatomical difference based on particularities specific to each individual, as well as elements of brain atrophy related to aging process.

The preprocessing part has to overcome the **low resolution** of the EPI, as well as the **demographic characteristics** of the patients (age and sex differences). In our study, we surmount the sex differences by computing the volume of each brain, as there is a difference between female and male volume of the brain, based on smaller skull usually recorded for women.

For detecting the elements related to the volume of interest, we consider the relative position of anatomical elements to a fix point. We have chosen this point to be the center of mass of the brain (X_c, Y_c, Z_c). In order to determine this point, we need to consider the brain, without the skull. Another problem that we have to surmount is the human interference in the segmentation algorithms. The segmentation algorithm methods perform the detection inside the axial slices. In order to start the algorithms at the right place on the right slice, the position of this slice must be determined first. This position represents the placement of the axial plane (O_x and O_y axis inside the volume) relative to the coronal(O_x and O_z axis of the volume) and the sagital (O_y and O_z axis of the volume) planes, on the O_z axis of the brain volume. This aspect provided us with the right placement of the algorithm at the slice level - the **placement at the volume level**. We need to find the anatomical region inside the axial image for which we need the volume definition - **placement inside the slice**, with identification of the right place for the volume detection.

From the segmentation point of view, solutions like the one proposed by SPM that performs the entire head segmentation are not applicable, as we need only our volume of interest, not a certain type of tissue. Due to the **patient variability**, we need robust VOI segmentation algorithms.

As one of the volumes is detected using an image stack (FA stack) different from the stack where we later use it (EPI stack),registration is needed. The problems with registration reside at the **landmark level** and influence the accuracy of this process. With no interference from the user, we perform a geometry based intra-patient registration with the geometrical landmarks automatically detected at the preprocessing level.

For the **bundle of interest** choice we use the two VOIs to limit the tracking starting from the midbrain area by selecting just those that reach the Putamen : deterministic global tractography. At this point, we compute measures based on the density of the fibers in the entire volume of the brain or in the volume of interest.

$$FD = \frac{F_{Nr}}{Vol_{Brain}};\ FD_{rel} = \frac{F_{Nr}}{Vol_{VOI}} \tag{4.1}$$

where FD represents the fiber density computed as the number of fibers - F_{Nr} - in the volume of the entire brain - Vol_{Brain} and FD_{rel} represents the fiber density relative to the volume of interest- Vol_{VOI}. We try to overcome the age difference as well, by taking the

mean age on the testing batch, as close as possible between the PD patients and the control cases. Computing the fiber volume and the brain volume an analysis is possible to detect the geriatric effects on the brain and on the neural fibers al well.

$$FV = F_{Nr} * V_{height} * V_{width} * V_{depth} * F_{leng} \tag{4.2}$$

where FV represents the fiber volume computed as the product of fiber number (F_{Nr}), fiber length (F_{leng}) - constant as the fibers must pass through both regions of interest and the voxel dimensions: $V_{width}, V_{height}, V_{depth}$. According to the medical manifestation of the disease, the fiber density and volume should be diminished for the PD patients, compared with the control cases. The degradation of the fibers should also be correlated with the severity of the disease specified by the H&Y scale. Before reaching the evaluation and diagnosis part for our algorithm, we present our work at the processing level, where we extract the basic image features.

4.2 Image Initialization

There are several steps to be followed in transforming the information from the visual level into cognitive quantitative information. The preprocessing level prepares the image for the algorithms that extract specific information concealing the anatomy and pathology of the subject. These preliminary algorithms eliminate the noise and provide specific landmarks and features used for feature extraction.

When we are talking about image processing, we refer to transforming an image *f* in another image *g*. The first and most used technique is to apply a specific operator ϑ so that:

$$g = \vartheta(f) \text{ [Sonka 2009]} \tag{4.3}$$

In this case, the operator is meant to perform a specific task but preserve the image information. These operators are part of *mathematical morphology* and are usually used for the preprocessing step of the image systems to remove noise, artifact, to enhance certain aspects as the contours. The image operator ϑ must satisfy two properties: distributivity and translation invariance. These properties guarantee the preservation of the initial image attributes. The distributivity means that the effect of the operator on the combined image can be deduced from the individual image and the translation invariant offers the same result on a translated image as it does on the original one [Sonka 2009].

Mathematical morphology is used for image processing and analysis as it offers the possibility to represent any translation invariant operator between complete lattices using elementary morphological operators. We are using the morphological operators at the preprocessing step of our approach. We perform image reconstruction by extracting desirable parts from the image, together with some marking algorithms.

For our system, we need several elements of image preprocessing for a good image quality, before processing. This is prevailed with morphological operators, together with segmentation algorithms and de-noises filters. Our main concerns are linked to the movement artifacts from

our images that must be eliminated for a proper analysis. Due to early study and analysis, the bone tissue constituting the skull needs to be eliminated for a better further processing (section 3.3). At the processing level, another important matter that must be solved is preparing the parameters for our own algorithms, so that the processing algorithms can accomplish the optimal detection of the VOIs : slice detection at the volume level and adaptive anatomical detection at the image level.

4.2.1 Volume management and slice detection

At the volume level, for the slice detection, we use the determined center of mass with the imageJ plug-in by Fabrice Cordelires and Jonathan Jackson called *Object Counter* [3]. This plug-in detects the 3D objects from image stacks and provides their volume, surface, the center of mass and the center of intensity. We use the volume provided for demographic parameter elimination and the center of mass for an inter-patient alignment.

Detecting the slice of interest starting from the center of mass of the brain is done by taking into account the placement of the anatomical regions that we consider as volumes of interest. For the midbrain, on a first attempt, we consider the slice of interest 8 mm lower than the center of mass and for the Putamen area 2 slices higher than the center of mass, thus 8 mm higher than the slice containing the center of mass as well. Due to this manner of placing the slice of interest according to the center of mass, there are several patients that do not perform well. These are the patients that, in the volume acquired in our images, do not have the entire brain and the content is shifted towards the neck more than the brain. In this way, the patients do not have all the slices containing all the upper part of the brain (e.g.the hand commissure- often used as a landmark in alignment and/or registration).

This approach was not very helpful due to the fact that each patient is positioned differently on the image stack - some of the patients are higher on the image, others are lower positioned. The center of mass in this case is relative to the object inside the image, which can contain the entire brain or just a part of it. For the cases with smaller brain volume, the slices could contain the entire brain, the others cannot. In order to establish the position and the content of the brain volume, we select the first and the last slice and extract the volume of the objects from these slices. We establish levels for defining the position of the midbrain relative to the determined center of mass of the brain.

$$P_{slice} = \frac{Vol_{Zslice}}{Vol_{Fslice}} * \frac{100}{ST} \tag{4.4}$$

where Vol_{Zslice} and Vol_{Fslice} represent the volumes of the objects in the slice with the determined center of mass, respectively the first slice on the stack; ST is the slice thickness (4 mm) and the values place the midbrain with relative to the determined center of mass with:

- Slice 0 if P_{slice}<60
- Slice 1 if 60<P_{slice}<70

[3]Object Counter -http://rsbweb.nih.gov/ij/plugins/track/objects.html - last accessed on June 2010

- Slice 2 if 70<P_{slice}<85
- Slice 3 if 85<P_{slice}<100

These threshold values represent the statistical established studies with regard to the midbrain position and its placement relative to the percentage determined value. If the stack is not correct - if it does not contain the minimum slices for the midbrain and the Putamen detection - we transmit an error value for the slice of interest (-1). Once this position is determined, the Putamen algorithm starts with two slices above the midbrain slice - one slice is with the midbrain, and the second one has to contain the AC/PC line. We adjust the Putamen slice if the detected volume is too small (20 pixels) or if it is placed too near to the midline. If this is the case, it means that the brain is bigger and we find the Putamen one slice above the one we have placed the algorithm.

4.2.2 Finding the starting point for anatomical segmentation

Once we have the slice of interest detected for each of the volumes used on the tractography, we need algorithms that determine the placement in the image slice of the anatomical region that we are segmenting. Knowing the location of the regions based on the brain physiology, we design specific algorithms for each volume in order to determine the stating point for the active detection algorithm.

The extraction of the volumes of interest is possible only on the images that provide a clear boundary for the anatomical regions that represent our volumes of interest. The algorithms for extraction must be placed at the right anatomical area in the 3D image volume, for this detection to be as accurate as possible. The automatic detection is possible only after the starting point for the active volume is set. The difficulty in this case lies in finding, in the slice of interest, the right region for the active volume growth.

Detection for the starting point of the volume of interest in the **midbrain area** is done similar to the detection of the slice of interest and it is combined with the division in hemispheres of the brain. We need the hemispheres separately on account of the study of Dr. Chan [Chan 2007] which states that there are different stages of development of PD in the left side of the brain and the right side. Usually the left side of the brain has more fibers grown in between the two chosen volumes of interest. The actual algorithm that makes the division into hemispheres for the brain takes the contour of the brain in the slice of interest. Based on the inflexion point with the maximal value we mark this point as a part of the medial line and together with the center of mass detected in the slice of interest the two points represent the medial limit in between the two hemispheres of the brain (fig. 3.9). This limit is used when we detect the volumes of interest, as we want the algorithm to consider only the needed hemisphere. The algorithm for finding the midbrain starts from the center of mass of the volume inside the slice of interest and following the inter-hemispherial axis searches for a gray matter region placed next to this point or above it.

Detecting the starting point for the **Putamen detection algorithm** is different from the one used for the midbrain, as the Putamen is not placed on the inter-hemispherial axis and does not have a geometrically detectable point or standard distance -patient variability is

present here. We are working on the FA image as it contains the anisotropy that follows the dopamine flow and makes the Putamen more distinguishable than on the other type of images. Our algorithm is also based on the placement of the two areas relatively to the center of mass of the image as well. As this is a more complex matter there are several steps performed for achieving an adequate positioning inside the image and eliminating the inter-patient variability:

- Classification of images (SOI) based on the head shape
- Segmentation on tissue type based on the voxel intensity
- Validation of the Putamen region based on the placement with reference to the center of mass

The first step represents a rough categorization of the head based on the sex variance, as well as on the subject provenance (e.g the shape of eurasians is different of those of Europeans and Afro-Americans). We detect three main classes based on the position of the center of mass with regard to the middle of the image. The second step is meant to distinguish the anatomical areas and make easier the search for the Putamen. This segmentation is performed using the KMeans[4] plug-in based on [Jain 1988]. We establish the number of clusters based on the tissue types the image now contains and the tolerance is left at the default value together with the randomization seed. The image containing all these clusters represents the map for the algorithm that established the volume of interest. Based on this image and the medical knowledge our algorithm starts at the center of mass and follows the hemisphere axis. Depending on the category established at the first step the algorithm chooses the proper level for hemisphere exploration on the left and the right side. Passing two tissue types and reaching the CSF area we then reach the Putamen. At this point, the volume tracking algorithm can be applied.

4.3 Volume Segmentation Algorithms - Active volume segmentation

The process of active volume determination is placed at the slice level and the stack level at the same time. At the slice level, after determining the starting point for the active tracking algorithm on the SOI, we move on to the growing step of the volume determination. We are thus performing a segmentation using the active contour algorithm and setting the threshold for it as voxels appertaining on the other classes rather than the one we are exploring. At this point the algorithms differ much depending on the anatomical region we want to extract, as well as on the hemisphere we are exploring. Nevertheless, after this exploration is finished, we apply this approach on the next slice and in this way we extract volumes by making a stack of the extracted ROIs.

[4] IJ Plugins: Clustering `http://ij-plugins.sourceforge.net/plugins/clustering/index.html` - last accessed on June 2010

The segmentation process is part of the mathematical morphology as well, as it labels areas in an image according to their intensities. The watershed-based segmentation, applied on overlapping and non-overlapping particles represents one of the reference algorithms together with the gray-based algorithm. For our imaging types we have a complex color image, we use KMeans based segmentation again and work on the map image stack, this time for the EPIs in the midbrain detection. Like in the rule-based segmentation, we have a priori knowledge describing how the object is placed in the image, helping to recognize it and segment it correctly [Bankman 2009]. Also, using spatial adjacency of the anatomical structures and completing it with the medical knowledge, we store the tissue types next to the volumes of interest, as in most "normal" brains, the relative position of the anatomical structures shifts only when a tumor is present. This is not the case for our patients, therefore the anatomical structures have the same adjacency (e.g. for all the patients the "left lateral ventricle" is *left of* the "left caudate nucleus" [Kretschmann 2003]).

Regions are typically identified on their internal homogeneity, however the size of the shape is important when defining the homogeneity and fractal features can provide additional information from this perspective. The shape of an object can be defined by the boundary of the region (c o n t o u r - b a s e d) or by the interior (r e g i o n - b a s e d)[Sonka 2009]. As we are using this volumes on the tractography, we need the entire region detected.

When extracting a region or a volume, there are techniques based on initial parameters and those that perform segmentation without initial setting. For the nonparametric feature extraction technique, we need a separation between different types of pixel intensities, where each feature has its own potential for separation. For that purpose the separation need to be measured and a discriminator identified for the class separation.

Considering a generalization on the active volume-tracking algorithm, there are several main steps to be followed:

- Seed placement inside the ROI
- Considering new points for the ROI extension
- Comparison with the voxels in the ROI and threshold elements
- Validation of the considered voxel as part of the ROI

These steps are further adapted and refined to fit our image resolution and the anatomical shapes at the same time. In the algorithm for **detecting the volume of interest in the midbrain area**, we have two steps for detection: the definition and detection of the region of interest and the volume detection. For the region of interest, we use a snake-based algorithm applied on a segmented image with KMeans in imageJ. We segment the EPI stack in imageJ for which we intent to make the difference between the Cerebro Spinal Fluid (CSF) surrounding the midbrain and the area we want to detect. As in the image we have white matter (WM) tissue, gray matter (GM) tissue and CSF, elements due to the image low quality, together with noise and artifacts, a classification algorithm based on the intensity of the pixels is needed. We use these types of tissues and elements as classes for the KMeans algorithm, obtaining a map. On the gray matter class obtained we perform the snake-based algorithm that has

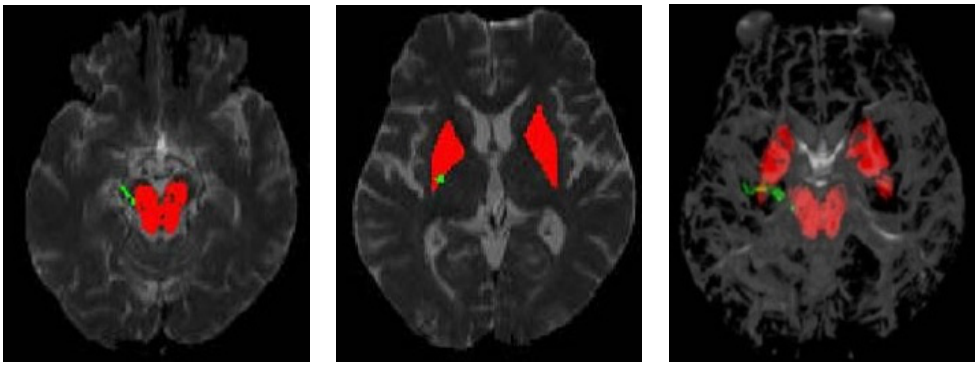

(a) EPI with detected midbrain and fibers

(b) EPI with detected Putamen and fibers

(c) 3D image of fibers detected passing through VOIs

Figure 4.2: EPI with detected VOIs in 4.2(a), 4.2(b) and 4.2(c) with 3D fibers on an example

the starting point as the center of mass in the slice of interest and depending on the side of the brain that we want to explore, our algorithm selects each pixel and compares it with the anterior pixel. This exploration step ends when there is a difference between the new pixel and the previous one or we step on the midline of the brain. After finishing the algorithm on one slice we explore the slice above in similar manner. As we know from the study presented in [Starr 2009], almost 80% of the SN is found in one slice (4 mm) thus we want to make sure that in our volume of interest this anatomical region is contained and for this purpose, we take the two slices that most probably contain the midbrain.

In figure 4.2(a) appears the detected volume of the midbrain for both sides of the brain hemispheres and the fibers projected on the EPI. In figure 4.2(b), after detecting volume of interest on the FA images and registering it on the EPI for both sides, we use it for choosing the fibers. On the image 4.2(c), we have a 3D view of the fibers passing through the detected volumes of interest. The algorithm for detecting and growing the fibers is the one presented in [Westin 2002]. This algorithm is made for the WM fibers that are grown in the same direction, unlike the ones in the GM. The VOI containing SN is GM tissue hence we must adapt our algorithm for our purpose, to have better fibers and clearer result. **For the Putamen volume detection**, we take into account the shape of this specific anatomical region and we construct a totally different algorithm, that must overcome several obstacles: the placement of the Putamen that is not necessarily at the same level in both sides, the size of it differs very much from one hemisphere to the other, as well as its shape. As the FA image offers a better contour of the Putamen than the other type of images due to the dopamine flow, we perform the detection on this type of image.

The Putamen shape on the slice of interest - the slice above the one containing the AC/PC line- is triangular, whereas the slice above this one is more quadrilateral. This is the reason why if we want a high accuracy, we have two kinds of algorithms for the Putamen tracing. One of these algorithms starts from a triangle placed at the seed place. This triangle moves its vertices only on the class of voxels appertaining to the ones from the seed. It stops when

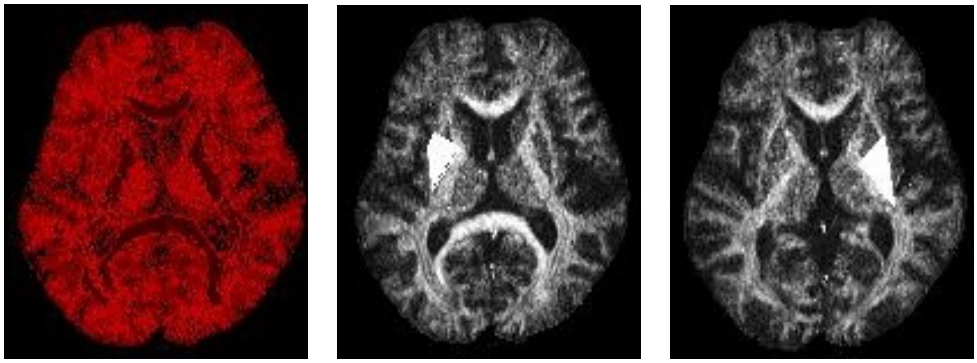

(a) FA image clustered

(b) FA image with detected Putamen on the left side

(c) FA image with detected Putamen on the right side

Figure 4.3: FA image with Putamen detected[Sabau 2010]

reaching another class (3-5 consecutive voxels different from the ones constituting the VOI). The same manner of operating is applied for the other approach, except the fact that it starts from a quadrilateral shape, moving at each step four vertices. We adjust the obtained shape by comparing the left and right limits and the level of the VOIs on the two hemispheres.

As shown in the flowchart from figure 4.4, after the positioning at the volume level in the slice of interest, described in section 4.2.1, the algorithm has to determine the relative position of the head inside the image. Depending on that position, we choose the starting point for the active volume detection. Once the starting point positioned, we choose the suitable algorithm for the shape extraction. We apply the triangular shape growing for the right side and the quadrilateral one for the left side and the upper slices in the volume determination. These algorithms divide the starting point into three respectively four points (fig. 6.4). The three-point algorithm follows the triangular shape of the Putamen, which is more obvious on the slice with the AC/PC line. The choice was made by statistically determining the difference between the two algorithms and the manually segmented images that represents the ideal segmentation shape.

Both algorithms consider the extension of the region of interest by taking each pixel next to the ones that represent the initial points in the clustering area. If the pixel appertains to the cluster of the initial points, it becomes one of the shape defining points - the edge of the triangle for the three points segmentation algorithm, or the edge of the quadrilateral for the four points segmentation algorithm. The active volume determination finishes when other clusters are encountered.

The determined area is placed with respect to the one determined on the other hemisphere. When the positioning of the two determined area is finished, the algorithm is repeated for the upper slice for the volume determination. The regions thus determined are transformed in mask images that are further transformed according to the parameters determined in the registration algorithms.

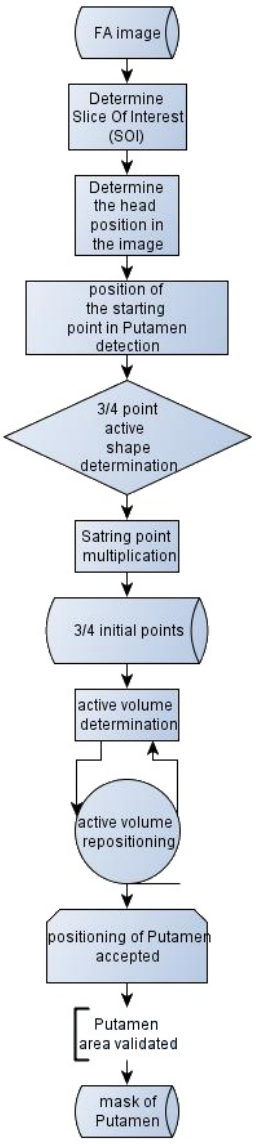

Figure 4.4: Putamen detection on the FA image

As the two volumes of interest are detected using different stacks of images and for further processing we need both detected volumes on the EPI, we perform a registration between FA and EPI and we transform the volume stack with the Putamen mask image.

4.4 VOI Registration

When talking about registration, we refer to matching or bringing the modalities to spatial alignment by finding the optimal geometrical transformation between corresponding image data. The challenges for performing the registration reside in finding the best landmarks in both image types, finding a suitable spatial transformation and, for our type of images, preserving the tensor direction. In our case, we perform intra-subject registration, as we match images appertaining to the same subject. Our registration is a rigid one, as it contains only translations and rotations, affine transformation, and it is fully automatic. Also, due to the fact that we are using homologous features that are mapped using geometrical distances, our registration is a geometrical-based one.

For the midbrain area we use the EPI, as it is clear enough for this purpose, even if the resolution for this type of image is poor. We cannot do the same thing for the Putamen area and even on the high-resolution images like T_1 and T_2 the contour of this anatomical region are not well detected by the algorithms. In this case, we use the FA image and take advantage of the anisotropy difference presented in this type of image as intensity difference. This makes possible detection on the FA image of the Putamen. However, when we use the detected Putamen we want to do that on the EPI image and we need to know that the extracted volume is on the right place.

4.4.1 Automatic detection of checkpoints

For this purpose we verify the placement of the volume of interest relative to the center of mass of the brain, as well as the external limits of this volume related to the same point. In order to determine the directionality of the image we use the symmetry axis and its orientation. It gives us the angle with the horizontal and vertical image axes for the rotation and the displacement parameters. All the transformations are performed

on the mask image extracted from the FA stack, keeping the EPI as model.

Analyzing the technique we used we can say that we perform an iconic registration [Cachier 2003] because we use on one hand the geometrical relations and placement of the center of mass and the external limits, but on the other hand we use the anisotropy values for defining the volume that we register. As we are not using that information directly for the transformation of the image, our registration is more geometrical [Gholinpour 2007] [Maintz 2000].

$$\begin{bmatrix} x' & y' & z' & 1 \end{bmatrix} = \begin{bmatrix} cos\theta_x & sin\theta_x & 0 & d_x \\ -sin\theta_y & cos\theta_y & 0 & d_y \\ 0 & 0 & 1 & d_z \\ 0 & 0 & 0 & 1 \end{bmatrix} \begin{bmatrix} x \\ y \\ z \\ 1 \end{bmatrix} \tag{4.5}$$

4.4.2 Transformation of the image

Representing the transformation applied on the FA image in equation 4.5 we represent the rotation, translation and skewness. The rotation angle for the transformation is computed by taking into account the symmetry axis determined for delimitation of the two brain hemispheres. The θ_x value is the angle between the axis and the O_x axis of the image and the θ_y is the angle between the same axis and the O_y of the image. We compute this angle for each image type and the difference between these angles represents the values for the transformation.

$$sin\alpha_x = \frac{SP_y}{I_1 SP} \tag{4.6}$$

$$sin\alpha_y = \frac{SP_x}{I_2 SP} \tag{4.7}$$

where SP is the starting point of the hemisphere axis given by the inflexion point (occipital sinuses at the base of the Occipital Bone of the skull) placed on the lower part of the brain (posterior area of the brain) and the SP_x and SP_y are the projections of the SP point on the O_x respectively O_y axis; I_1 is the intersection between the axis and O_x and I_2 is the intersection between the axis and O_y.

We compute the α angle for the FA image and the β angle for the EPI image. The θ angle is the difference between α and β and we use it for the rotation. The translation valued from the transformation matrix from equation 4.5 (d_x, d_y and d_z) represents the difference between the centers of mass in the two types of images. Another aspect of the transformation is represented by the axis orientation. The difference between the orientations of the axis determines us to flip the transformed image. This orientation is determined by the placement of the starting point (SP) and the center of mass on the image axes. Different orientation of the axis determines a flipping of the image in horizontal and/or vertical plane.

Because the FA images are generated on the AC/PC plane as well as the EPIs, there could not be any skewness problems or resizing aspects, thus we are concentrating our registration efforts on the translation and the rotation aspects. As the FA images have different orientations we need to be sure that the volume of interest is correctly placed on the model image.

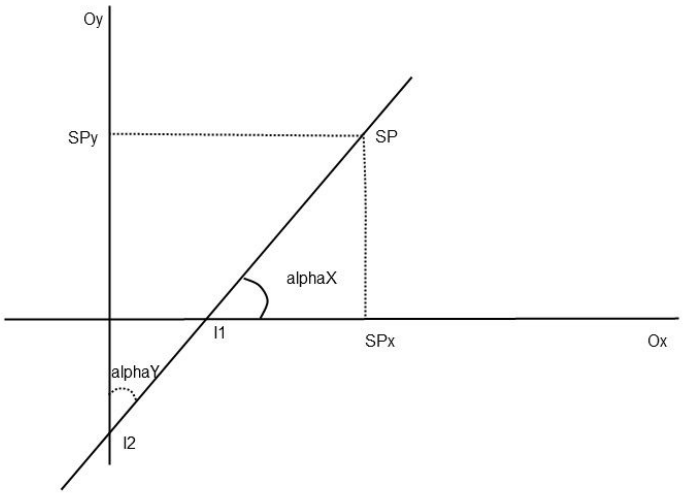

Figure 4.5: Geometrical view of the registration parameters

4.5 Feature Fusion

Fusing two images refers to the process of morphing them or warping them, at the image level. Both these techniques represent registration methods used and alter one of the images by incorporating the information from the other image. In this case, we are talking about fusion from another point of view, as we do not want to change the image, we put together information extracted from the image with different meaning.

The mean diffusivity represents the knowledge encapsulated in the diffusion tensors from the EPI images. It reveals the displacement of the molecules together with the overall presence of obstacles represented by brain anatomical structures. The degree of anisotropy is the expression of the molecular displacement in space and together with the orientation in space of the anatomical structures is found in the FA images. For an accurate determination of the fiber tract trajectories, we need all these information. The tensors from the EPIs cannot be moved, as they represent a huge amount of data, having values for each voxel. Looking at the FA level, the anisotropy guides and helps detecting the Putamen with accuracy in segmentation and helps us decide on the volume of interest needed for the fiber growing algorithm. This justifies extracting the information from the FA level and infusing it into the fiber tracking.

Putting together information from different sources enhances common characteristics and adds the specific elements from each source. In our case, we fuse by putting together the displacement of the molecules and the anatomical regions, with the space displacement from the EPI respectively the FA images. We fuse the information in by taking the detected mask for the Putamen from the FA image and placing it with the tensor information in the EPI. We fuse the two images without blending them [Zitova 2003] or warping them [Gholinpour 2007], just

taking the needed information from one image and inserting it into the other one by using the registration [Maintz 2000] [Wirijadi 2001]. In this manner, after the images are segmented in the means explained in section 4.3 the information from the FA image is registered to the EPI and used further for extraction and validation purposes. The information about the diffusion reveals the trajectories of the neural fibers and this information at the tissue level is stored on the architecture of each voxel of the EPI. This is the reason why, for the tracking algorithm, there are several important steps to be followed.

4.6 Tractography

The initial method introduced by Basser [Basser 2000] takes into account the diffusivity directions and the values of the tensors and Le Bihan [Le Bihan 2001] takes into account the anisotropy characteristics at the tissue level for a better detection of the fibers. We choose this approach because it represents a fundamental way of tracking the fibers, which we can further develop and modify according to out needs. Our approach is a g l o b a l d e t e r m i n i s t i c t r a c t o g r a p h y as it uses the neighbor voxels in tracking the fibers, providing the seeds as the volume of interest and using the thresholds of 0.1 for the FA value and 0.6 for the angulations. It is a local method as it determines just a specific set of fibers, by selecting from these, the bundle of interest.

Before developing the modality to detect and to select the neural fibers, a definition for this concept is necessary from the medical point of view. From the anatomical point of view, the gray matter(GM) is the dendrites of the neuron and the white matter (WM) is the axon of the neuron. Neural fibers represent the linkage between the axon of a neuron with the dendrite of another neuron. The anisotropy enhances the neural flow passing through the axons. The effect of diffusion on the MRI signal is attenuated (A) depending on the tissue type encountered by the water molecules.

$$A = exp(-bD) \text{ [Le Bihan 2001]} \tag{4.8}$$

It all depends on the diffusion coefficient b and the tensor D that characterizes the mobility on each direction of the water molecules [Basser 2000].

$$\underline{D} = \begin{bmatrix} D_{xx} & D_{xy} & D_{xz} \\ D_{yx} & D_{yy} & D_{yz} \\ D_{zx} & D_{zy} & D_{zz} \end{bmatrix} \text{ [Le Bihan 2001]} \tag{4.9}$$

A, the attenuation, represents the effect of diffusion depending on the tensors and the b coefficient as shown in equation 4.8 and can be expressed as in equation 4.10.

$$A = exp(-\sum_{i=x,y,z} \sum_{j=x,y,z} \underline{b}_{ij}\underline{D}_{ij}) \text{ [Le Bihan 2001]} \tag{4.10}$$

For the DTI images, we must first estimate the values for D_{ij} using multiple linear registration on equation 4.10 and the diffusion tensor computation for the degree of anisotropy from each

voxel. This process followed by the determination of the main direction of the diffusivity of each voxel completes preparation of the information of the diffusion value of each voxel. Once this step completed, the trace of the fibers can be studied. For this purpose the diffusion is represented as ellipsoids at 3D level. The tracking based on the diffusion tensor values is computed using equation 4.11.

$$Tr(\underline{D}) = D_{xx} + D_{yy} + D_{zz} \text{ [Basser 2000]} \tag{4.11}$$

For estimation of the fiber trajectories on the 3D space curve, the Feret equation describes it and, with a tangent vector associated with the tangent eigenvalue, an estimation of the tensor is achieved.

$$t(s) = \varepsilon_1(r(s)) \text{ [Basser 2000]} \tag{4.12}$$

where $t(s)$ is the trajectory of the curve s determined by the arc $r(s)$ and represented by the normalized eigenvector ε_1 associated with the tangent eigenvalue. Finding a solution for $r(s)$ can be achieved by using the Euler method, the Runge Kutta or the Gear's method. Gear's method is preferred in [Basser 2000] and we follow the same approach.

Taking this approach we are determining the fibers passing trough the midbrain area, the first volume of interest, and arriving to the Putamen volume on both sides of the brain hemispheres. The approach used by our system is presented as data flow in figure 4.6.

The midbrain area, where the SN resides, is a gray matter volume. The process of growing the fibers starting from the EPI means actually taking the tensor information and, based on the anisotropy value, choosing the starting point of the fibers. In the white matter area, the placement of the fibers is more obvious because the axons represent this area and the neural flow is very intense. That is the reason why it is very challenging to make the fiber recognition and to grow them starting from the midbrain area, where the predominance of the tissue is the GM. At first, we implement a classical fiber growth algorithm based on the white matter (WM) area in order to compare our algorithm on the same set of images with an existing one and to verify the position of the fibers in the volumes of interest.

For our system, we consider the approach presented by Basser in [Basser 2000] and for the tensors approach we use the approach proposed by Bihan in [Le Bihan 2001]. In the Basser approach, the algorithm is based on the Fernet equation for the description of the evolution of a fiber tract. This approach is specific to white matter, as the axons are the white matter. The midbrain area is gray matter. Growing fibers from the gray matter is a challenge since the number of axons in this area is much less than in the white matter and the fibers are not as well aligned as the ones in the white matter. We apply this algorithm in order to see if there are relevant fibers that we can grow between the two VOIs (Fig. 4.2(c)). We use these VOIs to choose the bundle of interest and separate the fibers that we need from the ones that are not part of the motor tract. Although we grow all the fibers from the midbrain, we validate only the ones starting from the midbrain area that also reach the Putamen area. Fibers too small, with anisotropy higher than 0.1, or those that do not go towards the Putamen area, whit angulation that exceeds 0.6 degrees, are not validated. The threshold values are the same used in [Basser 2000] [Le Bihan 2001] [Karagulle Kenedi 2007]. In this manner, with the second region of interest, taking a global tractography approach, we have an element that validates the grown fibers, without needing the SN clearly defined.

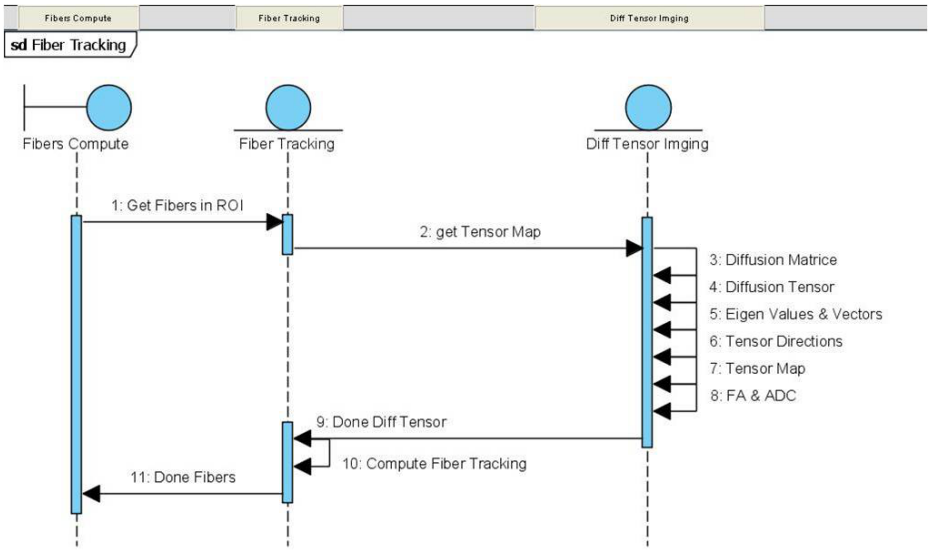

Figure 4.6: Algorithm used for fiber tracking

4.7 Conclusion

The technical challenges taken by our approach in using the medical image as bio-marker are presented in this chapter at the algorithm level. These methods are adapted for medical images in general and the workflow is specific to our purpose, on our approach.

At this point, we are able to automatically detect the volumes of interest by selecting the slice of interest where we are exploring the anatomical regions. Automatically determining the limit between the two hemisphere allows us to make a differentiate analysis for each side of brain. We need this possibility as the PD condition has different level on each side of the brain for the same patient. That is the purpose for separating the left and right side of the brain for the tractography algorithm.

The registration combined with the fusion factor is specific for our imaging types, as well as for the related anatomy. This is based on the geometry registration enhanced by the brain anatomy elements.

As presented in figure 4.7, we define new methods at each informational level to transfer data from the image level to the knowledge level by extracting the features needed for our analysis. This figure represents the workflow in PDFibAtl@s, integrating the methods presented in chapter 3 and 4. For each level of processing, we emphasize the original methods and the results after each step. The figure represents the information hierarchy, starting with the DICOM standard and finishing at the evaluated value for PD. In the next chapter, the methods for diagnosis and prognosis are presented.

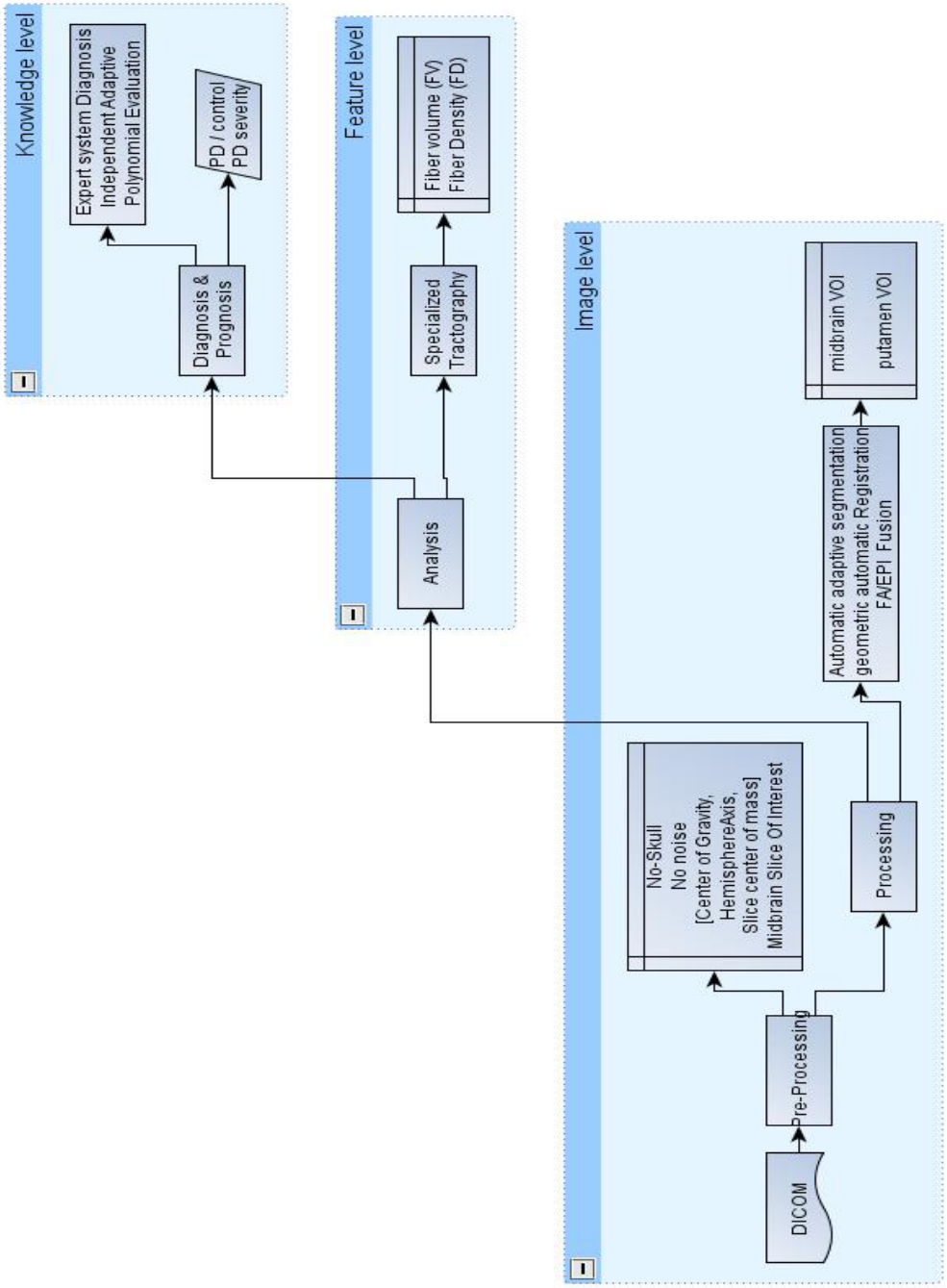

Figure 4.7: Our new methods in the PDFibAtl@s workflow

Chapter 5

Diagnosis and Prognosis Algorithms

Contents

FEATURES EXTRACTION REPRESENTS AN IMPORTANT STEP in medical image processing and analysis. Mixing the anatomy knowledge with the conditions taken at the pathology level, the extracted image features can be interpreted in the context of diagnosis and prognosis. The overall system becomes than a Computer Aided Diagnosis (CAD). In our approach, as in the prototype elaborated from it, managing the features extracted from the image level to the diagnosis and prognosis level is achieved.

Just like the neural network that we are tracing by fiber tracking connects the neurons, a neural network structure constructed as a graph can be used to define concepts or classify features. Using similarity, as well as medical knowledge to define rules can be another way to classify and determine the place of a concept. Passing different levels of abstraction aims at bridging the semantic gap. At this point in our system, already having the features extracted, for the analysis phase, we need to bridge this semantic gap for medical knowledge inclusion and interpretation, for diagnosis and prognosis purpose.

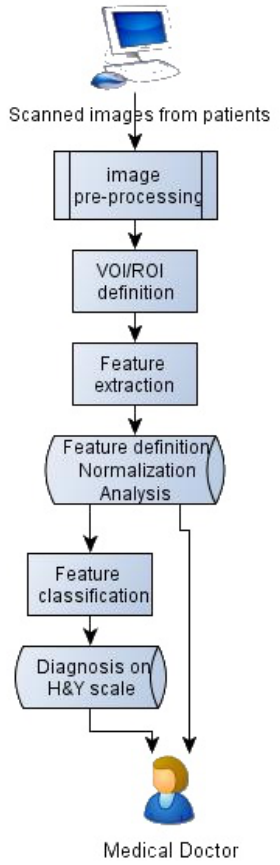

Figure 5.1: Computer Aided Diagnosis System

In this chapter, we present the use of fuzzy logic to make the transfer of information from the extracted and processed features of the motor fibers to the PD diagnosis. Several aspects need to be considered therefore at the diagnosis level:

- The difference between the control patients and the PD cases
- The differences among PD patients with different disease ratings

Pushing this analysis at the next level, we analyze the variation of the fiber parameters in correlation with the disease level. Diagnosis aims at making specific identification of a problem - a disease [Bankman 2009], whereas prognosis follows the problem evolution to reveal the early cases, reaching towards the source of the problem. While diagnosis is concentrated on the whole picture at a given time/snap - the raw images features analysis, the prognosis requires more granularity and reaches on to the detail, as it discovers and correlates the variation of the parameters for early diagnosis purposes.

5.1 Computer Aided Diagnosis (CAD)

The results obtained at the image processing stage that are further analyzed using the tractography provide the input data for this module. The correlation tests performed at each stage informed us that statistically there is a link between the features variation and the severity of the disease, but studying the diagnosis criterions and their applicability helps us to integrate the medical knowledge at the rule level. We analyze the H&Y scale, and since there is a correlation between the features extracted and this scale, we transform the statistical correlation by implementing the rules of the polynomial function. This link is made visible by attaching a variation function onto the features so that the evaluation of the function provides the disease degree (in section 5.2). Following the function, estimating the value of the features for cases that are uncertain could reveal the early cases.

At this stage, our system uses the extracted features for diagnosis. As presented in figure 5.1, there are several stages when defining a Computer Aided Diagnosis (CAD) system. In our case, the first stages with image pre-processing and feature extraction have already been treated in chapter 4 and we need the clustering phase at this stage, with the pre-normalization of the extracted features, to provide diagnosis. Different combination of features gives different classification performances and for a robust classification, fewer parameters are recommended

[Sonka 2009]. As clinically PD is manifested more visible on the left side of the brain, the features extracted on this side will have a higher trust degree in our CAD.

Jain et al. [Jain 1997] have a large categorization for feature selection as deterministic methods - stepwise feature selection, stochastic methods - genetic algorithm feature section, optimal methods - exhaustive search of all possible feature combination. The *stepwise feature selection* is based on successive inclusion of features in the classification algorithm. Each new feature should improve the classification result. In our case, we have only the fibers and the VOIs and we include the fibers first in the classification process and then the volumes for a more refined selection. *Genetic algorithms* are based on the idea of evolution in nature. The solution for these algorithms must be a string and there must be a fitness function for correspondence between the input string and the output one. This variant of classification is not applicable for our case, as we have no strings. The classifiers that usually apply in image based CAD are *pattern classifiers*. The initial image is processed and features that represent the pattern are extracted and fed to the classifier that returns the proper decision class.
When using a classifier, a training stage defines the known classes. The linear discriminant analysis and the classification trees can also be applied to medical image analysis. The *linear discriminant analysis* makes the difference between two classes using a linear decision boundary [Sonka 2009]. This approach is not applicable to our data set. The *artificial neural networks (ANN)* work like the linear discriminants, but they use nonlinear approach. It highlights the underlying density functions of the classes without assuming any rigid form of limitation. For using this approach we must first determine the densities and their attached functions. Another approach on the classifiers part is the *Bayes decision rule* or Bayes optimal discriminant function. It incorporates a priori information into the determination of the classifier parameters for an optimal discriminant function that follows the Bayes function. A *Rule based system* of detection also includes the medical information. The result is not represented by a decision variable in this case. The *Multi objective genetic algorithms (MOGA)* addresses the difficulties of the optimized rule-based schemes by maximizing or minimizing the n component of an objective vector function - optimization of the Receiver Operating Characteristic (ROC) curve.

As presented in section 2, PD diagnosis is achieved by cognitive testing. The score obtained by the patients for this standard tests place them on a severity scale of the disease: UPRS (Unified Parkinson Rating Scale) or H&Y (Hohen & Yahr). Our system extracts the features and by estimating them is able to provide a diagnosis on the same scale. For the database provided by Singapore General Hospital (see specification in section 3.1) the H&Y values for each patient is provided, as a ground truth. This ground truth is not always exact, as it is placed on a scale from 1 to 5, but for certain cases, when the neurologists were not absolutely sure of the disease severity, there are ".5" values (e.g. 1.5 when the disease does not have certain cognitive aspects that most of the 2 degree patients have).

We need a decision-based method to analyze the features and give an exact placement of the case on the PD scale. We can take into account rule-based systems, as they include predicates with medical knowledge. Considering fuzzy logic, we can capture the behavior of the system. Statistical methods include all possibilities for the features, but the selection of a decision threshold is very challenging and subject to sensitivity.

Working with non-probabilistic uncertainties, fuzzy sets, determines an approach based

on fuzzy models. A fuzzy inference system, or fuzzy model, can adapt itself using numerical data. A fuzzy inference system has learning capability and using this aspect the link between the fuzzy controllers and the methodologies for neural networks is possible using the *Adaptive Network-Based Fuzzy Inference Systems (ANFIS)*. These networks have the overall input-output behavior influenced by a set of parameters. These parameters define functions that determine *adaptive nodes* at the network level. Applying the learning techniques from the neural networks to the fuzzy sets allows us to determine an ANFIS structure. For us the fuzzy sets represent the values extracted at the tractography level. These sets are defined in intervals and determine the If-Then rules. Together with these rules, the database (fuzzy sets) and a reasoning mechanism determine a *fuzzy inference system*. At the reasoning part, we have to take into account the inference model [Jyh-Shing Roger 1995].

As shown in figure 5.2, the features extracted go into a pre-processing stage - normalization process for the data set - and they get to the inference model next. We can choose between the Mamdani and the Takagi-Surgeno-Kang (TSK) method [Roussinov 2001]. In Mamdani systems, each rule has a fuzzy set attached, whereas in TSK, each rule has a linear function on the input set of points. While the first approach has as result sets of points, the second one provides one or more real functions. The fuzzy sets resulting from the first method need an additional defuzzification step [Gabrys 2005]. Choosing the inference model is not a problem as we need functions as output so we take the TSK approach. Before defining the rules, a classification of the input data is necessary in order to define the output data. We define the classes that are represented by the points and using the TSK inference method we define a rule-based system for diagnosis. This system is able to provide us, based on the features extracted, the values of the PD. The problem with this system is that it can only detect what it has learned, so if we do not have early cases of PD it will not know to diagnose that level. This is where the prognosis functions come into place, as they evaluate the patients using polynomial functions and following the variation of those functions we can extrapolate for new cases and place them on the PD scale.

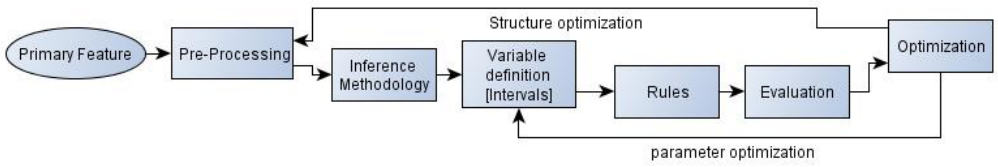

Figure 5.2: Fuzzy Expert System Flowchart

Once the fuzzy inference system is defined, we can apply different learning techniques to link the neural network to the defined system - *neuro-fuzzy modeling*. There are several architectures and learning procedures for adaptive networks. The most popular ones are the *back-propagation neural network (BPNN)* and the *radial basis function network (RBFN)* . The BPNN has the property of learning by propagating the information from the network output to its input. This determines an error rate that permits an adaptive approach on the

learning process. The learning rules can be adapted to the data and use different computation methods (e.g. LSE - least squares estimation or a combination of gradients and LSE). The RBFN method uses Gaussian functions to compute the radial basis functions. This adaptive system represents a hybrid learning method.

A typical ANFIS system possess five layers [Jyh-Shing Roger 1995]:

- Input layer- determines using a function the premise parameters
- The rule strengths
- Normalized firing strengths - weights definition
- Consequent parameters - determined using the weights and the variation functions
- Output - decisional output based on the computed consequence parameters

Following an ANFIS [Bonissone 1997], we can combine the fuzzy control offered by the medical background and statistical analysis with neural networks. The fuzzy features represent the a priori knowledge as a set of constraints - rules. Using Fuzzy Modeling (Fuzzy Inference Systems), we can take a subjective or an objective approach. We have tested the objective approach that uses a clustering algorithm and fuzzy system identification to determine the fuzzy rules. This approach did not perform well on our data. Thus, we determined the intervals for the rules manually for the first learning set. One of the application of ANFIS is presented as a mode to explain past data and predict behavior. In our approach we use as Fuzzy Control (FC) a fuzzy set, which represents a type II typology (type I is a monotonic typology and type III is a linear function of state). For the FC technology we use rule inference where we make the difference between the disease stages. We adapted this approach, but as the neural networks separately did not perform well, we use adaptive interpolation functions.

In our approach, we follow the ANFIS layers, from the input data to the results, adapting the system to our needs. The ground truth is represented by the Hoehn & Yahr (H&Y) grade provided by the medical experts.

5.1.1 Hoehn & Yahr scale

PD severity is most commonly described on a clinical basis using either the Hoehn and Yahr (H&Y) staging system, or the Unified Parkinson's Disease Rating Scales (UPDRS) . One of the standard staging systems used worldwide is the H&Y scale, provided by our neurologists as a basis or a ground truth.

Table 5.1 shows the original Hoehn and Yahr scale, that includes stages 1 through 5, but due to ambiguity at level 2, there are two other stages included on the scale: the 1.5 and 2.5. Stage 1 and Stage 5 are rarely diagnosed; this is the reason why for our database we do not provide values for this stage of the disease. Stage 1 on the scale represents the mild PD cases, the early stage of the disease. The detection for this stage is not possible yet with the cognitive tests. For stage 4 and 5 the patients suffer from tremor so the images, even if they are taken, do not offer valid information. This is the reason why most of the diagnosed

Value	H&Y standard scale	H&Y modified scale (currently employed by SGH)
1	Unilateral involvement only usually with minimal or no functional disability	Unilateral involvement only
1.5		Unilateral and axial involvement
2	Bilateral or midline involvement without impairment of balance	Bilateral involvement without impairment of balance
2.5		Mild bilateral disease with recovery on pull test
3	Bilateral disease: mild to moderate disability with impaired postural reflexes; physically independent	Mild to moderate bilateral disease; some postural instability; physically independent
4	Severely disabling disease; still able to walk or stand unassisted	Severe disability; still able to walk or stand unassisted
5	Confinement to bed or wheelchair unless aided	Wheelchair bound or bedridden unless aided

Table 5.1: H&Y scale differences

patients are stage 2 and 3. We are using the original scale for our system for starters, as differences between stages 1, 1.5 and 2 have not sufficient granularity, but as we base our feature analysis on each hemisphere and the differences between the old scale and the new one is based on this type of analysis we are able to make the system sensitive to these values from the new scale as well.

5.1.2 Prognosis approach

In numerical analysis when talking about interpolation methods we are referring to a method of creating new data points within the range of a discrete set of known data points. The features representing the points will be followed by the function variation. Trying to go through the data points by curve fitting or regression is the approach that we need four our data. There are several manners to follow the data points, but only several interpolation techniques offer the variation required for the needed dispersion. A linear interpolation or a piecewise one would not be able to follow the data, as the features represented are dispersed. We implement a combination of spline and polynomial interpolation techniques. We first study the rule-based fuzzy systems for diagnosis.

Defining the input data and determining a function to normalize these data represents the first stage for an ANFIS system. We perform these steps by determining the features correlated with the diagnosis and then by clustering them.

5.1.3 Feature Clustering

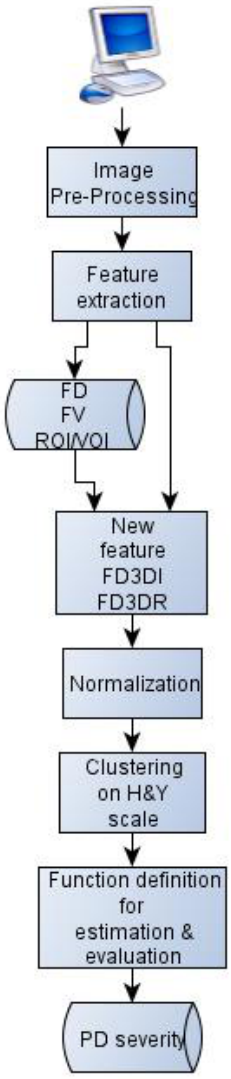

Figure 5.3: Diagnosis based on features -our CAD system

In the clustering process we analyze the features used for this step, their correlation with the clusters and the Statistical Parameter System (SPSS) is used for estimation and pre-evaluation as presented in chapter 6 in table 6.4. Preparing the data for the clustering includes normalization of data and new definition of features for a global view.

$$FD_{3D} = \frac{Nr_F * V}{Vol_{Brain}} \tag{5.1}$$

We define at this point the fiber density at 3D on each side as presented in equation 5.1 where Nr_F represents the number of fibers detected on the hemisphere that we are analyzing; V represents the voxel size and Vol_{Brain} is the brain volume of the patient.

Once we have the features defined, computed and then normalized, the learning stage for the clustering includes intervals of variation on each feature. These intervals are defined using fuzzy classes. We thus have in this case the five severity stages, the control cases class, 0 value, and the -1 value for the undetermined cases. As we have patients for training only for PD stages 2 and 3, the other levels of PD are defined using the variation functions from the prognosis definition. After the interval definition, the rules supporting the intervals on each feature are implemented, including the medical knowledge.

For a characterization of a case using all the features, we introduce new metrics based on the fibers and the hemisphere attendance. In this manner, we evaluate a case globally and also at the local level, including the specificity as well.

For adaptive systems used for this purpose, the learning rules are more complex using together with a basic learning rule, a batch - off-line learning - and a pattern - on-line learning - rules.

When talking about classification methods, the problem of supervised and unsupervised approach is an important aspect. This aspect places the features either into predefined classes, or into unknown ones - the number of classes being unknown. As we want to place the diagnosis onto the same scale used by the medical doctors, we already know the number of classes for our diagnosis so the supervised approach is more appropriate. Among the methods used in the supervised classification, statistical classification is our choice due to the fuzziness of our data and the overlap of the clusters. As table 5.2 shows, we take the normalized data and make intervals depending on the H&Y

Variable	Stage on H&Y scale		
	0	2	3
FD	0.0351 - 0.0353 0.0413 - 0.0417 0.0413 - 0.0417 0.068 - 0.081 0.96 - 0.106 0.180 - 0.187 0.279 - 0.302 0.372 - 0.575	0.0328 - 0.035 0.0353 - 0.0413 0.0417 - 0.048 0.050 - 0.068 0.163 - 0.180 0.187 - 0.272 0.318 - 0.372 0.607 - 0.855	0.081 - 0.096 0.122 - 0.163 0.272 - 0.279 0.302 - 0.318 0.575 - 0.607
$FD_{3D}L$	0.00270 - 0.00272 0.00318 - 0.00371 0.0052 - 0.0062 0.0068 - 0.0072 0.0076 - 0.0081 0.0138 - 0.0144 0.0215 - 0.0233 0.0249 - 0.0353	0.0025 - 0.0027 0.00272 - 0.00318 0.00371 - 0.0052 0.0081 - 0.00941 0.0130 - 0.0138 0.0144 - 0.0210 0.0245 - 0.0249 0.0445 - 0.047	0.0062 - 0.0068 0.0072 - 0.007 0.0094 - 0.0130 0.0210 - 0.0216 0.0233 - 0.0245 0.0353 - 0.0445
$R1_{vol}$	7808 - 8064 8192 - 8448 8832 - 9056 9184 - 9664 10944 - 10976 11040 - 11584 12192 - 13024 13728 - 14112 17312 - 25888	8064 - 8192 8448 - 8832 9120 - 9184 10240 - 10496 10752 - 10944 11584 - 12192 13024 - 13728 14112 - 15808 25888 - 50000	9056 - 9120 9664 - 10240 10496 - 10752 10976 - 11040 15808 - 17312
Vol_{avg}	8432 - 8688 9040 - 9056 9344 - 9504 9536 - 10048 10560 - 10592 11360 - 11456 11872 - 11920 12176 - 12640 13248 - 14448 17536 - 26816	8348 - 8432 8688 - 9050 9056 - 9120 9504 - 9536 10352 - 10560 11248 - 11360 11536 - 11872 11920 - 12176 12640 - 13248 14448 - 16800 26816 - 50000	8244 - 8368 9120 - 9344 10048 - 10352 11456 - 11536 16800 - 17536

Table 5.2: Data Intervals corresponding to the H&Y stages of Parkinson's Disease.[Pataca 2010]

values. We use these intervals for training purpose in the rule-based diagnosis. Each interval determines a fuzzy set that has a rule attached for defining the link between the values and the H&Y level.

5.1.4 Relationship between features and H&Y scale

Using predicates in IF-THEN rules is challenging from the point of view of electing the rules, but at the same time, at this level we can include medical knowledge at the decision point - diagnosis must be based on medical knowledge. There are though two steps in a rule-based system:

- Clustering the features
- Define the input-output relationships

For the first step, using subtractive clustering can bring automatic clustering with fuzzy inference systems. The potential for each data point can be determined by computing the distance between the new points with regard to the other points. The greatest potential value gives the cluster center. The systems characteristic behavior can be estimated by a fuzzy rule after each cluster.

This approach has the advantage of using a priori knowledge and integrating complementary information with the extracted features. It is also used in expert systems and permits interpretation of features. The fuzzy sets at this level although it can include uncertainty and object recognition in a procedural form is better used in labeling. Using neural networks even if it is less restrictive than linear discriminant analysis (LDA), does not perform very well for our data, as it is not so exact and not sensitive enough to small differences on the input data (Fig.5.3).

We decide to use the rule-based approach, as the medical knowledge can be included, it can take into account different features at different stages of analysis and we can refine it. As presented in Chapter 6 at the evaluation stage, there is a clear relation between the fibers parameters on the left hemisphere of the brain and the severity of the disease. There are cases that do not register the fibers due to the image quality or the tracking method, but in those cases we consider the midbrain detected and the right side fibers, if there are fibers detected. This approach is used also when a case can be placed in more than one class - for tangent clusters.

Even if our first approach considered neural networks for clustering, the features do not offer a clear boundary according to the disease. The diagnosis obtained in this manner is not reliable, due to the dispersedly placed values and the overlapping nature of the intervals appertaining to distinctive classes of diseases. We have tested a simple KMeans approach, knowing the number of classes we need. The results were not nearly as good as those obtained with the fuzzy approach.

The definition of the rules for diagnosis includes not only medical knowledge, but overcomes inter-patient variability. It takes into account the hemisphere of the brain, the density of the fibers, the volume of interest where the dopamine flow starts and the 3D density of the

fibers. As presented in equation 5.2, after defining the clusters using the fiber density- HY_{FD}- and based on the midbrain volume- $HY_{VOI_{Vol}}$ - we evaluate the threshold and place a new case depending on these features. When conflicts appear and a decision between clusters is not obvious, another feature is used for diagnosis. If we do not have a positive positioning of the case on the feature axis, than the VOI is not correctly determined due to image quality or insufficient slices on the volume. These conflicts generate the set of rules that we use for the expert system that determines a classification of the cases, depending on the disease severity. The fiber density (FD) values are classified on the H&Y scale in the first row of the table 5.2. These classified FD values from the table are used next for defining the rules in equation 5.2. These rules determine the H&Y value based on the intervals in table 5.2 and considering the correlation between the features in the table and the severity scale. When the left side fiber density does not provide a reliable value for diagnosis, the right side bundle of fibers is taken into account and if the fibers are not determined, the volumes of interest are taken as measures for diagnosis. Testing the rules in equation 5.2 we obtained the variation function of the FD according to the severity of PD represented in figure 5.4.

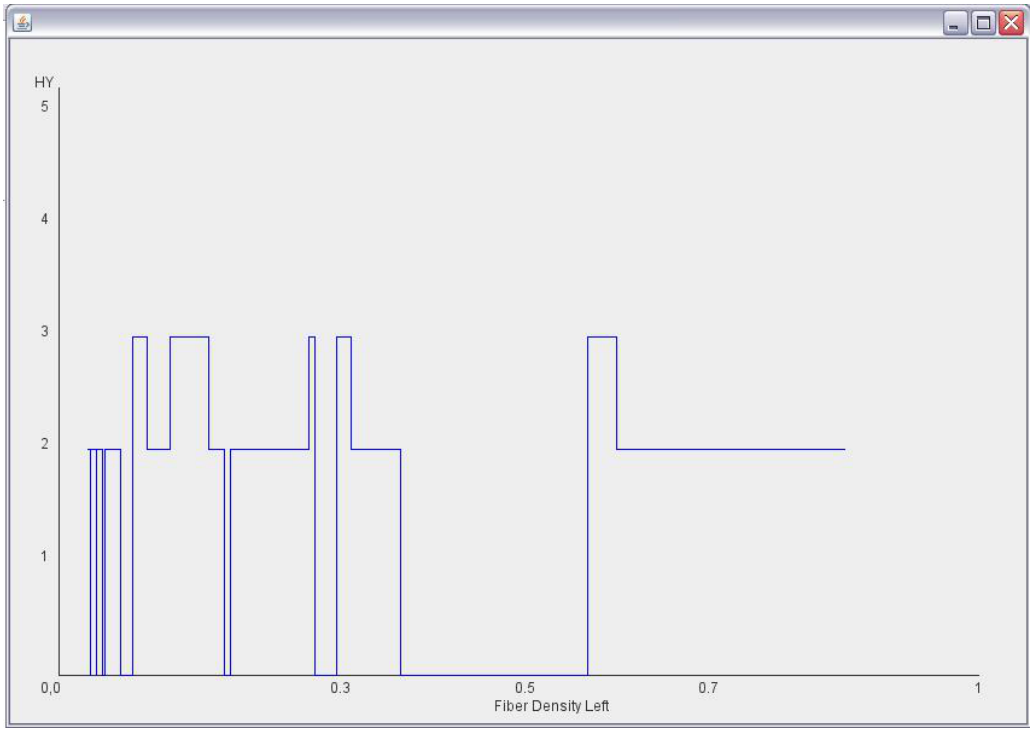

Figure 5.4: Classification with $FiberDensity$ values on the left side [Pataca 2010]

$$
\begin{aligned}
&If(HY_{FD} = HY_{VOI_{Vol}} \wedge HY_{FD} \neq -1)\, then\, HY = HY_{FD}\\
&If(HY_{FD} = -1 \wedge HY_{VOI_{Vol}} \neq -1)\, then\, HY = HY_{VOI_{Vol}}\\
&If(HY_{FD} \neq -1 \wedge HY_{VOI_{Vol}} = -1)\, then\, HY = HY_{FD}\\
&If(HY_{FD} \neq -1 \wedge HY_{VOI_{Vol}} \neq -1) \wedge (HY_{FD} \neq HY_{VOI_{Vol}}))\, then\\
&\quad If(FD_{3D} \neq 0)\, then\, HY = 2\\
&\quad else\, HY = 0\\
&If(HY_{FD} = -1 \wedge HY_{VOI_{Vol}} = -1) then\ The\ image\ is\ invalid!
\end{aligned}
\tag{5.2}
$$

For the moment, at this level, only the difference between the control and the PD cases is possible using this rule-based algorithm. At the PD level, only cases rated stage 2 and 3 can be classified. For new cases, as well as for variation study on the features, we take the clusters and determine their variation.

In an ANFIS architecture the next step is represented by the rule strengths definition. We define a set of rules based on the detected clusters and include the medical knowledge as well.

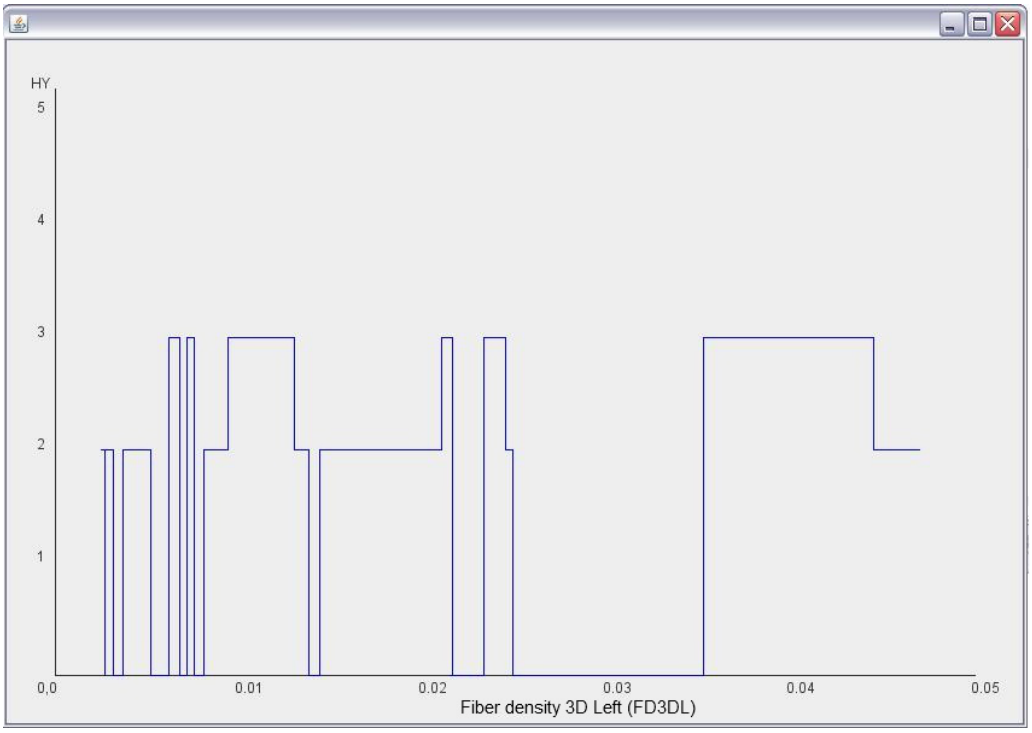

Figure 5.5: Classification based on the FD_{3DL} [Pataca 2010]

Based on the intervals determined in table 5.2, each variable determines a set of data to be part of a rule: the FD variable determines the first rule from equation 5.2 and delivers the HY_{FD} scale value (Fig.5.4), the $FD_{3D}L$ determines the $HY_{3D}L$ from the same equation (Fig.

5.5) and the $HY_{VOI_{Vol}}$ value is determined using values from $R1_{vol}$ row in the same table, the Vol_{avg} row on the same table holds the average values for the volume of the midbrain on the right and the left side. Figure 5.5 is based on the second row of the table 5.2.

5.2 Prognosis method

From diagnosis to prognosis, there is apparently only one step. While the diagnosis based on the rules is matching the patients into the classes that it was trained to recognize, the prognosis can place patients at levels that are not learned by the system. The diagnosis makes a classification of the patient by placing him in one of the disease stages or the control case. The prognosis offers the value of the correlation between the disease and the affected features and by extrapolation is able to find the evolution stage of the features for early cases of the disease.

Prognosis systems learn from the formerly acquired data and by analyzing and studying it, a pattern is revealed and used for new cases. Prediction systems using artificial intelligence can be based on neural networks, on fuzzy logic, on genetic algorithms or on expert systems. The interference among different PD levels at the feature level does not provide a clear boundary for classification using neural networks. We tested the KMeans and KNN approaches and they did not provide satisfactory results on our data. The interference among different feature groups at the class level represents a fuzzy dispersion on the features space. The rule-based expert system, using the fuzzy feature classes identifies the known stages of PD, but it does not have the possibility for prognosis.

At this stage, the learning and classes are already defined and we intend to find a function by using interpolation among the existing points, representing the patient features on the disease severity. The ANFIS architecture at this point has already defined the functions for determining the consequence parameters that provide the final decisional value. In our case we define the interpolation functions for this purpose. The intervals with their limitations can be considered as weights in defining the interpolation functions for the ANFIS approach. Like the RBFN model, in this case the weights represent the medical constraints, encapsulated in the intervals, and the variation functions are in our case the interpolation functions. The function found in this manner should be used for extrapolation onto disease areas that are not detectable at this moment. The function describes the disease variation based on features and for any new patient, a correct placing of the case on the PD scale.

For interpolation method definition there are several steps that must to be taken:

- New data points within the existing range of acquired data
- Meshing the points
- Using the mesh determines the function that approximates the real data variation

The interpolation methods are based on the shape of the mesh function, which can be: linear, polynomial or spline. Analyzing our data set, a linear approach is not possible due to the dispersed points on the plot. A polynomial approach is challenging at the parameter level

and at the degree level as well. The cubic spline interpolation method has weights attached to each flat surface to guide the bending of the variation function, but the challenge at this point is to find the correct variations among the weights.

Looking at the polynomial approach, the Lagrange function that determines the parameters and can be adapted easily is a good choice for our data. This is a good choice also because each time we have a new input, the basis polynomials are recalculated and thus we improve our prediction each step of the way. With the help of weights we can improve the polynomial functions and define the spline as Lagrange functions.

5.2.1 Function definition

We use a combination of functions for estimation purpose. The Lagrange polynomials provide us with the coefficients for the spline functions used for interpolation. These methods are quick and easy, but not very precise. We gain precision by dividing the data set. By defining a Lagrange function on all the test points we obtain a 40-degree function because we have 41 points and we want the function to pass trough all those points.

For a definition of a polynomial using the Lagrange approach we need the coefficients determined using equation 5.3. In this function, the points (x_i,y_j) represent the features extracted in table 5.2 at the image level.

$$L(x) = \sum_{i=0}^{n} y_i * \prod_{j=0, j\neq i}^{n} \frac{x - x_j}{x_i - x_j} \tag{5.3}$$

The 40 degree polynomial that obtains the coefficients using equation 5.3 is hard to handle, as it becomes very complicated and in the case of new points in the data evaluation takes a lot of time and is not accurate. At this point, we divide the feature points in the H&Y space into sets and define a variation function for each set of points. A two point set definition determines a linear function and we already know that the variation is nonlinear; therefore we start from three set points. A five-degree polynomial function becomes too complicated so the highest degree of polynomial representation on an interval is a four-degree polynomial function.

$$\begin{aligned} C_2 &= \tfrac{y_1}{(x_1-x_2)(x_1-x_3)} + \tfrac{y_2}{(x_2-x_1)(x_2-x_3)} + \tfrac{y_3}{(x_3-x_1)(x_3-x_2)} \\ C_1 &= -(y_1 \tfrac{x_2+x_3}{(x_1-x_2)(x_1-x_3)} + y_2 \tfrac{x_1+x_3}{(x_2-x_1)(x_2-x_3)} + y_3 \tfrac{x_1+x_2}{(x_3-x_1)(x_3-x_2)}) \\ C_0 &= y_1 \tfrac{x_2x_3}{(x_1-x_2)(x_1-x_3)} + y_2 \tfrac{x_1x_3}{(x_2-x_1)(x_2-x_3)} + y_3 \tfrac{x_1x_2}{(x_3-x_1)(x_3-x_2)} \end{aligned} \tag{5.4}$$

The prediction function is different on each set of points for the PD stage and we need sub functions defined for each subset of values corresponding to the severity degree. As presented in equation 5.4 we define the parameters for the second degree polynomial function for each set of points.

The polynomial function that gets the parameters defined in equation 5.4 is the second degree Lagrange. Due to the fact that the scale is limited on the upper values at level five, and on the lower boundary at level zero, we apply the same limitations to our functions.

For the forth degree polynomial representation we determine the coefficients as presented in equation 5.5 but for this case, on the last interval, we have points that are far apart for each other. The testing on the whole database will be able to decide if we need the tree-points sets or five-points sets.

$$
\begin{aligned}
C_4 &= \sum_{i=0}^{4} y_i \prod_{j=0, j\neq i}^{4} \frac{1}{x_i - x_j} \\
C_3 &= \sum_{i=0}^{4} y_i \left(\frac{\sum_{j=0, j\neq i}^{4} -x_j}{\prod_{k=0, k\neq i}^{4} (x_i - x_k)} \right) \\
C_2 &= \sum_{i=0}^{4} y_i \left(\frac{\sum_{j=0, j\neq i}^{4} x_i x_j}{\prod_{k=0, k\neq i}^{4} (x_i - x_k)} \right) \\
C_1 &= \sum_{i=0}^{4} y_i \left(- \frac{\sum_{j=0, j\neq i}^{4} x_i \left(\sum_{m=0, m\neq j}^{4} x_m * \sum_{n=m+1}^{4} x_n \right)}{\prod_{k=0, k\neq i}^{4} (x_i - x_k)} \right) \\
C_0 &= \sum_{i=0}^{4} y_i \left(\frac{\prod_{j=0, j\neq i}^{4} x_j}{\prod_{k=1, k\neq i}^{4} (x_i - x_k)} \right)
\end{aligned}
\tag{5.5}
$$

There are intervals where a certain polynomial function works better than another one - constraints determined by the intervals that represent the weights. This is the case with the last points on the forth degree polynomial approach, as the second degree polynomial performs better here. This is the reason why we need to consider not only the interval where the new points are placed when extrapolating the polynomial functions, but also the surrounding intervals and their own functions.

In the four-degree interpolation function, for the last interval, there are not enough points for the interpolation. For this function, a simple linear function follows much better the interpolation points.

5.2.2 Evaluation approach

When we provide a new case for analysis, we extract the fiber features and we try to place it on an interval, determining the left and right closest values. Defining the interval where the new value needs to be placed, we determine the H&Y values corresponding to the interval and the middle value of the same interval. The three H&Y values provide the data for the rule-based diagnosis system. This system provides the final value for the new case. When a new point is to be evaluated and its H&Y value determined, we have several steps to perform. We perform this estimation using the "ideal" set of points. The position of the new point (X)

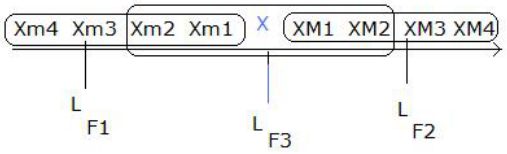

Figure 5.6: Independent Adaptive Polynomial Evaluation (IAPE) data management for introducing a new element

among the others is determined by finding the next point higher (X_M) and lower (X_m) - figure 5.6. For identifying the H&Y value for the new feature X we are using the algorithm from figure 5.7. We estimate the final value using the neighbor values. We start by determining the polynomial function using the next four points smaller than X: L_{F1}, those higher than it: L_{F2} and those that are centered in X: L_{F3}. If at least two of these three functions have as result the same H&Y value for X, then we save this value as HY_1. Otherwise we determine the functions using just the three points - second-degree polynomial functions. We can only arrive at linear functions that ultimately produce the value for HY_1. A second value, HY_2, represents the H&Y value for X determined using the linear function that passes through the points associated with the X_M and X_m values. The final value is given by HY_1 if the difference between this value and HY_2 is not higher than three levels on the scale, otherwise the mean value between the two HY is the final estimated value for the disease severity. This algorithm describes an Independent Adaptive Polynomial Evaluation (IAPE) method as it is applied both on PD and controls determining the most likely polynomial that can be applied on these data. This method is a hybrid ANFIS approach as it uses as back-propagation the difference between polynomials at each stage but it works like the RBF using the Lagrange polynomials. An extension of this approach, adapted for PD cases, is called PD Adaptive polynomial evaluation method (PD-APE). The estimation function is used basically for the PD patients, adding the condition that if HY_1 or HY_2 have as result 0, the other value is taken as result. This condition does not affect the results of the overall performance. The variation function with this condition performs the best on the accuracy level. From the ANFIS point of view this method takes into the second layer the firing strength given by the PD appurtenance.

Determining the control and the PD cases first and then applying the function that provides the best interpolation for the set of points represents a fuzzy adaptive method for prognosis. This variation function uses for the control cases the second-degree polynomial method and for the patient cases the PD adaptive polynomial evaluation method. The variation function using this fuzzy adaptive approach is represented in figure 5.8.

5.3 Conclusion

Diagnosis based on a rule-based system is able to rate the patients but as it does not provide a variation function, we are not able to track new data or extrapolate

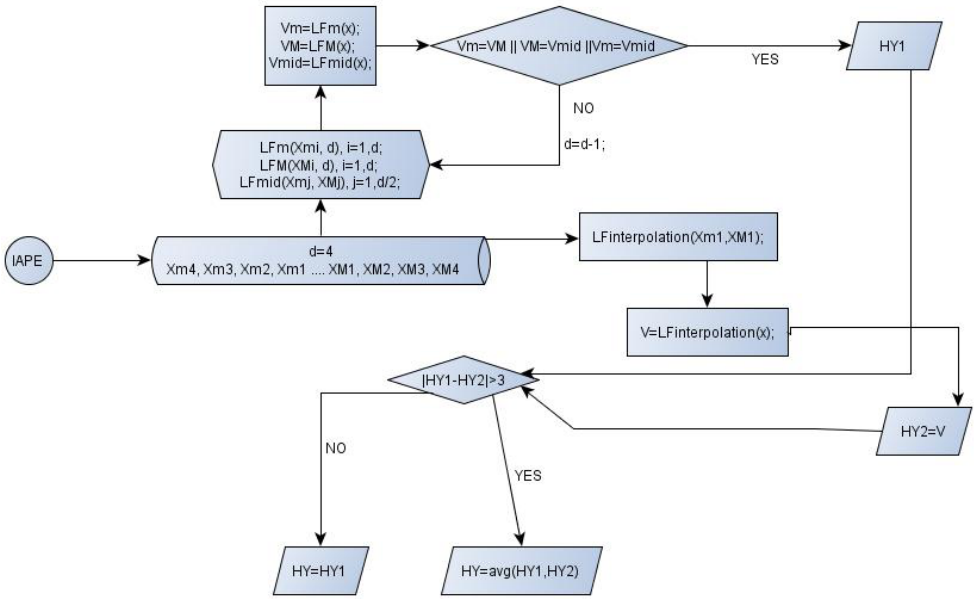

Figure 5.7: Independent Adaptive Polynomial Evaluation (IAPE) data flow specific for this method

for early diagnosis.

The Prognosis approach based on polynomial functions provides not only more accuracy, but it is able to provide a measure of the severity of the disease, even for the early stages. This approach can be also used as extrapolation for the new cases, as well as for new levels of disease. The polynomial degree of the function determines the granularity of the data set and the sensitivity of the function.

For the prognosis method, our approach proposes an ANFIS architecture based on a fuzzy inference system with a rule-based definition and several hybrid approaches at the network level. We define the required polynomials for each set of input data and adapt to the constraints imposed by the medical knowledge when delivering a prognosis value.

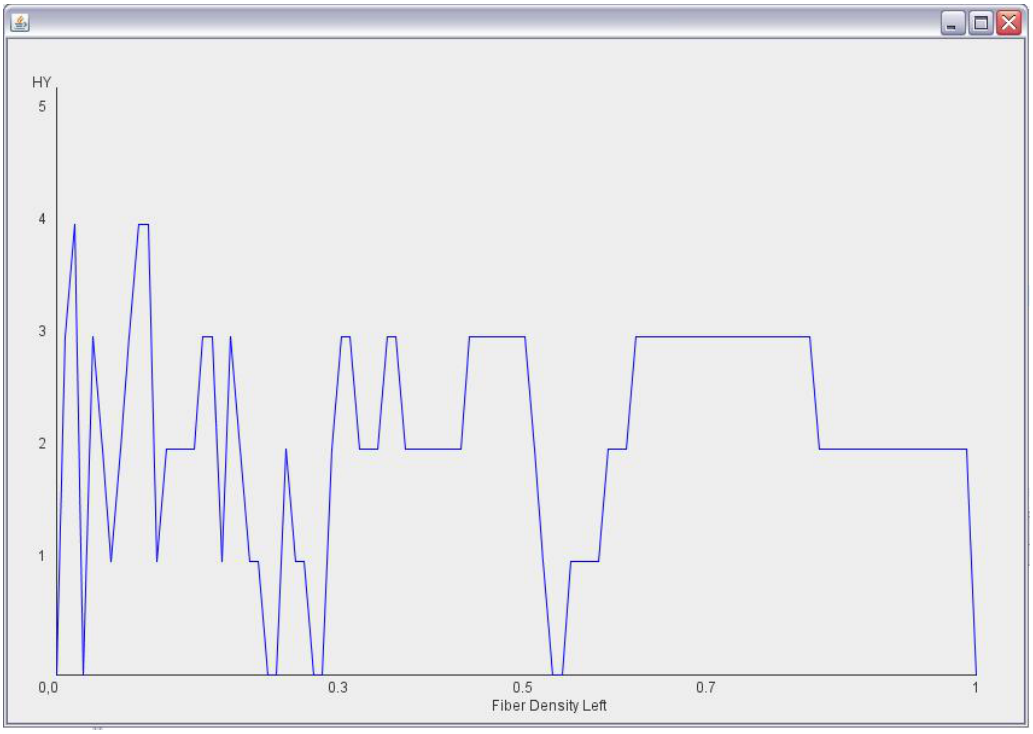

Figure 5.8: The prognosis function variation based on the Fuzzy Adaptive Evaluation (FAE) method

Chapter 6

Evaluation and Results

Contents

EVALUATING AND VALIDATING OUR METHODS are as important as the algorithms themselves. We first determined by manual approach if the anatomical detail needed can be determined in the image. The features extracted at the image level could not be indicative of the disease. This is the reason why the correlation between the features with the disease validates that the image can actually be used as a bio-marker. Another level of testing is represented by the validity of the algorithms. The test are concerned with the validity of the demarche - of they extract what is needed, nothing more and nothing less. The feature evaluation and the performances of the entire system are the final goal of our approach.

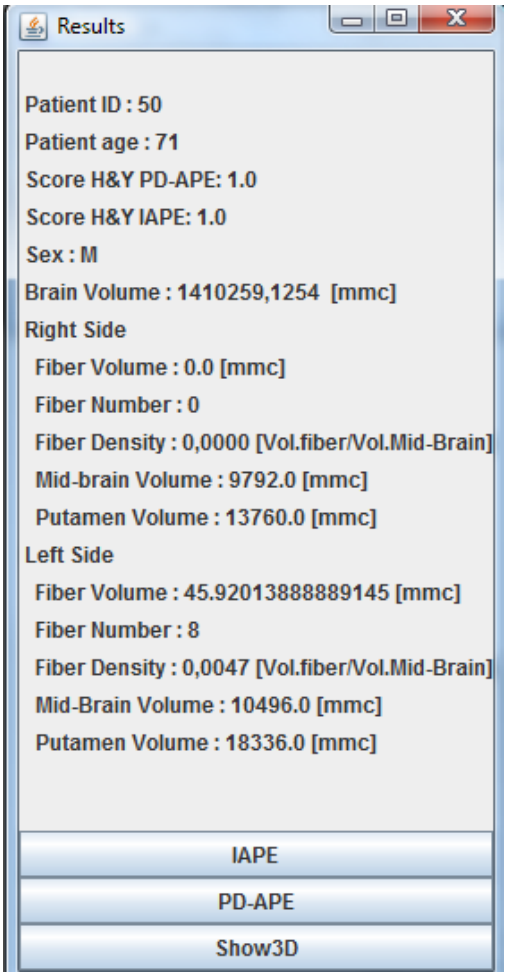

Figure 6.1: The Results Window [Teodorescu 2009c] [Teodorescu 2009a]

This chapter treats the manner in which we evaluate and validate each of the new algorithms, as well as the results obtained for each validated method. The evaluation can be done by comparing our results with the ones obtained with other software/algorithms on the same image database. While the evaluation is performed using a testing batch with PD and control cases, the final test is performed on the entire database. We note that the results and the algorithms presented in this study have been successfully selected (at the methodology level) and presented in radiologic and scientific communications ([Teodorescu 2010] [Teodorescu 2009a] [Teodorescu 2009b].

There are several stages of evaluation of our system. As presented in chapter 4, a first stage of evaluation consists in performing an analysis of the green channel from the FA image on a segmented volume of the midbrain. This study, presented in [Teodorescu 2009a], determines if there are fibers correlated with the PD severity on the AP diffusion direction. The Putamen segmentation is performed then in the direction of diffusion indicated by the fibers staring from the midbrain area. This automatic detection method is then evaluated at the image processing level as well, by comparison with the fibers detected manually. Then the fusion is performed using the VOI detected on the FA stack automatically and registered afterwards on the EPI image. The registration method is a fully automatic geometric registration. This method was visually validated as well, in collaboration with the radiologists. For each stage, we apply an evaluation and a validation of the proposed methods. On the first stage, we take into account the heterogeneity of the subjects from the demographic point of view and we analyze the effects of each element in the testing area, in order to find a test that less sensitive to the inter-patient variability.

For the medical relevance, we use the T-Test for correlation between the obtained values and the cognitive evaluation (ground truth). We validate the volumes obtained by running the results under the supervision of our partner neurologist to verify the placement of the detected

elements on the initial images. The automatic detection is validated also using the manually detected volumes and by performing a logical AND between the two detected images. The result image represents the non-overlapping areas. These areas represent the error rate for the automatic segmentation.

For the fibers, we can only verify that the ones chosen are approximately on the SN area. This is also done by our neurologist, but their number can be checked and provides the performance of our method.

Figure 6.1 represents the features extracted for each patient after the image processing, volume extraction and fiber tracking.

Before evaluating our methods, we define the metrics used for estimating the performance of each method, the significance of the measures and their relevance.

6.1 Evaluate the image algorithms

The performance level of the CAD systems is given by the sensitivity (true-positive rate) of the detection and the false-positive detections - the specificity. When detecting abnormalities in an image, the true and false refer to the decision of the algorithm compared with the clinician decision (Fig. 6.1).

- TP true positive - the algorithm detects correctly the abnormality
- FP false positive - an abnormality is detected while it is not in the image
- TN true negative - no abnormality exists and the algorithm does not detect one either
- FN false negative - the algorithm does not detect an abnormality when it is there

In the segmentation and detection process, these terms are defined having as ground truth, the manual detection. Therefore, when defining the sensitivity and specificity of an algorithm we use:

$$sensitivity = \frac{TP}{TP + FN} \tag{6.1}$$

The sensitivity represents the abnormality rate detected on a set of problematic patients and it is a percentage of success of the algorithm - equation 6.1. The specificity on the other hand represents the normally detected cases and it is a percentage measure as well - equation 6.2.

$$specificity = \frac{TN}{TN + FP} \tag{6.2}$$

The sensitivity reflects the positive cases identified correctly and the specificity represents the negative cases identified as such. Usually, several indices exists for evaluation of computerized methods, like ROC and FROC analysis. This curve represents the space of tradeoffs between the sensitivity and the specificity of an algorithm.

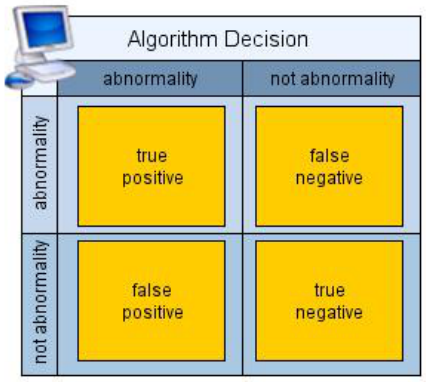

Figure 6.2: True and False positives and negatives [Bankman 2009]

For a view on the entire data set, the accuracy of the system is computed as presented in equation 6.3.

$$accuracy = \frac{TP + TN}{TP + FP + TN + FN} \tag{6.3}$$

In our case, we have two stages where we can evaluate our system: at the image processing level, depending on the fibers detected, and at the analysis level, evaluating the diagnosis. In this way, at the processing level, when evaluating the fibers, we can consider fibers not appertaining to the strationigral tract. Together with the cases that did not provide any valid fibers after the tractography, these cases represent the errors for the first stage. For the second stage, we evaluate the variance of the disease severity: classifying a patient with PD among the controls or classifying a control case among the PD patients. The variance of the disease determines another error rate among the PD patients - considering a patient more or less affected by the disease than it really is the case.

When computing the sensitivity and specificity of the image processing module, we achieve 0.63, respectively 0.87. The same evaluation is momentarily impossible for the diagnosis, as we need confirmation for the FP and FN cases which is achieved by to follow up on the control cases for validation.

Another statistical parameter for defining and estimating the methods proposed is a Receiver Operating Characteristic (ROC) curve representing sensitivity versus specificity. This curve applies to our final methods, at the diagnosis and prognosis level of our approach.

The curve estimates the accuracy of the method and ideally has the shape presented in figure 6.3, where the distributions do not overlap. On the diagonal, all the distributions overlap. The Area Under the Curve (AUC) represents an overall measure of the test performance and allows comparison between different methods. This area is interpreted as a distance between the disease and control test results. Next, we evaluate our algorithms used at each level of the medical image processing. Presenting the evaluation method provides us with the testing batch needed for a proper evaluation.

6.2 Test sets and requirements

Testing procedures must assure that they are sensitive to our parameters, and robust to other exterior factors. Thus, we construct several testing batches by varying parameters that we need our test to be robust to. We apply this procedure for the demographical parameters, as shown in table 6.1.

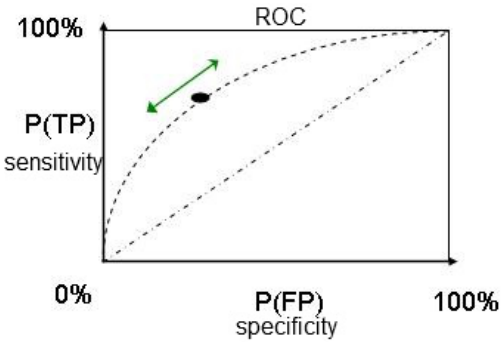

Figure 6.3: Receiver Operating Characteristic (ROC) curve

Test nr	H&Y [avg]	Age		Male/all	
		Patients	Controls	Pat	Control
1	2.312	64.5	59.37	11/16	6/16
2	2.375	63.31	60.93	9/16	9/16
3	2.375	64.06	58.5	8/16	7/16
4	2.467	62.75	61.5	9/16	8/16

Table 6.1: Test batches characteristics [Teodorescu 2009b]

6.2.1 Test parameters and characteristics

In order to evaluate the different stages in image processing, we introduce several testing groups - testing batches - of patients so that we can evaluate the robustness of each stage. The PD diagnosis and prognosis is then evaluated on the whole database, not only on the test batches.

We prepare four test batches from the 42 patients available - 21 PD cases and 21 controls. Age variation can affect the disease by introducing brain atrophy and making the neural fibers harder to detect. This is the reason why we introduce this factor as a parameter in our tests. The patient's gender can affect the detection as the female have smaller skulls. The detection and segmentation of the images is than more difficult. Together with these parameters, the H&Y value represented as the severity degree of the disease could affect the diagnosis and/or prognosis values.

The whole database contains 66 patients and 66 control cases that managed successfully to generate the segmented areas. We dispose of 68 patients and 70 control cases, but due to the image stacks unable to provide the entire volume between the midbrain and the Putamen, 2 patients and 4 controls were eliminated from the test. We use this database to evaluate the methods developed using the test batch.

6.2.2 Choice of test procedure

The test groups are chosen so that one of the demographic parameters varies and the other are correlated among patients and controls. Big differences on the results from one test to another mark the sensitivity of the test on the demographic parameters. A consistent test for all the test batches is not sensitive to the variation parameters (see table 6.1). If the testing procedure has similar results on all the test groups, we can further analyze the results of that particular test, depending on its interpretation and input data. At the image processing level, we have as input data the images and we test the automatic detection against the manual one. At the feature level, we have as input data the extracted values for the neural fibers on the left and the right side, the detected volumes on both sides and/or the new computed parameters: FD, FD_{3D}, FD_{rel}, FV.

For the diagnosis and prognosis, the ground truth is represented by the H&Y value given by the medical doctors using the cognitive tests. The neurologist also performs the validation of the fibers, so that we can be sure of detecting the right bundle of fibers for further study.

6.2.3 Green Channel analysis on the midbrain area

For the green channel study, we have a batch of 42 cases (21 patients and 21 control cases). From this batch, we take out randomly 5 cases from the patients and controls in order to eliminate the subjectivity - the influence of the demographics - from our study (table 6.1). The T-Test is applied on the histogram obtained from the midbrain area by eliminating the noise. This procedure aims at detecting a correlation between the value of the histograms and the H&Y values. The histograms represent the anisotropy value on the AP direction in the midbrain area, which should indicate the motor fibers and in PD could be characteristic for the progression of the disease. Examining this correlation, we vary the age difference between the patients and controls and the number of male subjects in the testing batch, as well as the mean value on the H&Y scale.

The results on the green channel study performed on the patients with the characteristics from Table 6.1 are presented in Table 6.2. This table contains several T-Test methods and their results regarding the correlation between the green channel histogram values and the H&Y values. When we analyze the Independent Sample T-Test, we have a large variation between the values of P, which can be explained only by the variation of demographic characteristics of the patients. In our case, this type of study is affected by demographic characteristics, especially on the left side (e.g 12% - 83 %). We almost have the same range of variation on the Bivariate test, visible on the left side as well. The ANOVA test is the most consistent and has good results, being reliable and adequate for our purpose. An initial approach and the associated results have been presented on the RSNA conference [Teodorescu 2009b] from the clinical point of view. We emphasize here the technical asset. The testing on the green channel was performed on a cropped volume containing the midbrain. The green channel represents the AP direction of diffusion. The information from this image is the anisotropy level on the AP direction. This study confirmed that there is a correlation among the anisotropy on the AP direction and the H&Y severity scale. This correlation was interpreted as fibers staring

Test nr	Independent Sample T-Test		Correlate Bivariate		ANOVA	
	Left	Right	Left	Right	Left	Right
1	24.4	74.0	13	8	0.872	0.937
2	12.2	69.3	7	8	0.906	1
3	75.5	65.3	3	6	0.937	1
4	83.6	71.4	7	7	0.937	0.906

Table 6.2: Study on Green channel on the left and right side [Teodorescu 2009b]

from the midbrain that are correlated with the H&Y scale. The fibers at the midbrain level that are affected according to the PD severity, represented by the H&Y scale, are with no doubt the motor ones. Therefore the motor fibers starting from the midbrain are indicators of the PD severity and have AP directionality. The ANOVA test provided a good correlation, but not applicable for quantization of the disease.

6.2.4 Evaluation of the segmentation algorithms

There are several characteristics when analyzing the result of a region-based segmentation. Comparing an image segmentation result to ground truth segmentation - the manual detected one from the specialist- represents one way of evaluating the automatic segmentation. Another way would be to estimate the overlap between the ground truth image and the segmented one. There can be over-segmentation or under-segmentation when the two images overlap, but one of them is bigger than the other one. When there is a ground truth region that the segmentation does not contain, we are dealing with a missed region. A noise region manifests as a region identified in the segmented image, but not contained in the noise region.

Midbrain automatic detection is preformed on the EPI stack with no diffusion direction. The algorithm providing the segmentation presented in section 4.3 is applied on the test set and the results are studied by our specialist. Validating the algorithm actually means verifying if it managed to segment the whole midbrain and just this part, without taking part of the surrounding tissue or the CSF (see fig. 4.2(a)). This is the criterion followed by the neurologist in validating the algorithm.

For the **Putamen detection** the evaluation is performed by comparing the manually segmented images with the automatically detected ones. Performing a logical AND operation at the image level between the two Putamen slices at the pixel level. We are using the imageJ Image Calculator on the segmented volumes. We compute the number of the non-black pixels at the same position on both images. The difference area gives the error rate of our segmentation algorithm. As shown in table 6.3, the area difference between the two methods determines the values found in column two and three of the table and determines the results in column four and five of the table.

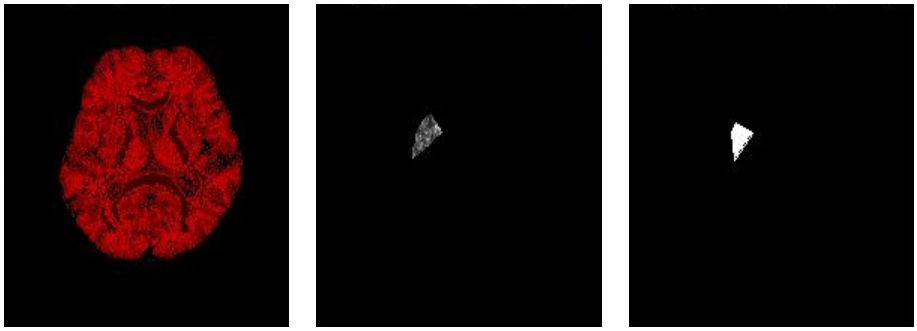

(a) FA image clustered

(b) FA extracted Putamen manually extracted on left side

(c) FA extracted Putamen automatically detected on left side

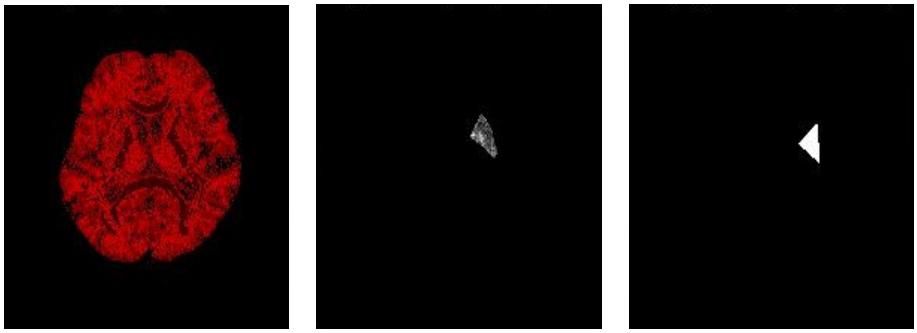

(d) FA image clustered

(e) FA extracted Putamen manually extracted on right hemisphere

(f) FA extracted Putamen automatically detected for the right hemisphere

Figure 6.4: Putamen segmentation

Also a validation done by our neurologist is necessary for this step. For the registration performed on the detected volume, we use medical knowledge for validation and visual evaluation.

The results show a smaller error rate for the left Putamen area, which has more clear boundaries than the right Putamen area. This is consistent with the medical approach as PD patients usually are more affected on the left side of the brain by this disease.

6.2.5 Evaluation of the registration method

The registration has the purpose of aligning two images so that they overlap. We need it for aligning the segmented volume of the Putamen from the FA stack with the one in the EPI stack. As presented in the previous chapters, other algorithms do not deliver satisfactory results from the medical point of view four our images. This is the reason why we propose our own method, specific for the protocol of the images that we are using. For the registration, we tested the

Pat.ID	Left area of Putamen	Right area of Putamen	Relative error for left Putamen detection [%]	Relative error for right Putamen detection [%]
1	77.491	33.005	33.33	26.10
3	24.395	10.045	58.02	77.50
7	61.706	58.836	6.17	30.61
9	64.576	70.316	11.11	57.43
27	50.225	77.491	13.58	73.49
132	66.011	24.395	13.56	45.38
168	66.011	21.525	13.56	51.80
177	54.530	61.706	6.17	38.15

Table 6.3: Preliminary results on Putamen detection [Sabau 2010]

rigid registration automatic method from TurboReg [1] but as it was not developed for head images, it did not perform as expected. The registration is very important, as we have seen also testing the fusion module providing the diffeomorphic demon registration and a manual rigid registration from the Image Fusion module (MedINRIA platform) [Vercaunteren 2008a] [Vercaunteren 2008b] [Modersitzki 2004]. These methods, either changed the target image - the diffeomorphic approach, or are totally dependable on the accuracy of the used in finding the landmarks - the manual approach. Also the fact that our protocol included 12 diffusion directions, instead of 6, like the testing data for the software was offering, slowed down the fiber computation. Due to the registration, we did not find the fibers that we needed for the analysis, as the DTI tracking module offered just the possibility to choose only one region of interest for limitation of the bundle of interest. The 3D Slicer [Ceritoglu 2009] performed good on the manual registration. However, this method was not only time consuming, but also from the resources point of view disappointing as it stopped the machine each time, even before completing the computation.

In our approach, the registration process with the acquired parameters determined in section 4.4 is fully automatic. It uses the EPI stack with no diffusion and the FA one. The results can be visually verified as we are applying the transformation on the Putamen mask and we transpose the image on the EPI. Thus, we verify the correct anatomical position.

6.2.6 Tractography evaluation

The motor tract is automatically detected in our case by growing the fibers between the two volumes of interest: midbrain area and the Putamen. This is consistent with a global tractography method. After computing the FD and FV on each side of the brain, we study the effects of PD in each bundle of interest. For this purpose, we perform the T-Test making the correlation between FD/FV and H&Y scale. As the FD is dependent on the FV, the

[1] TurboReg - http://bigwww.epfl.ch/thevenaz/turboreg/- last accessed on November 2009

two parameters have the same variation. For the medical relevance on correlating the H&Y parameter with the fibers, we test the obtained values using WinSPC (Statistical Process control Software). For the simple correlation purpose, we analyze Pearson's parameter (see Table 6.4 column 2 and 4). We have chosen for testing in this case the ANOVA method: one way ANOVA, General linear model ANOVA (MANOVA) and we test the equal variation on density considering the Lavene parameter.

This evaluation is performed when developing the method and the statistical tests are performed using the test batch with the tests defined in section 6.2. When we perform the global testing taking into account 80% of our data, we obtain p=0.05 for the group homogeneity in the H&Y assigned cases classified using the left fiber results. On the ANOVA test for the same cases, the significance is 83% with an N=35 subjects randomly taken by the software from the 42.

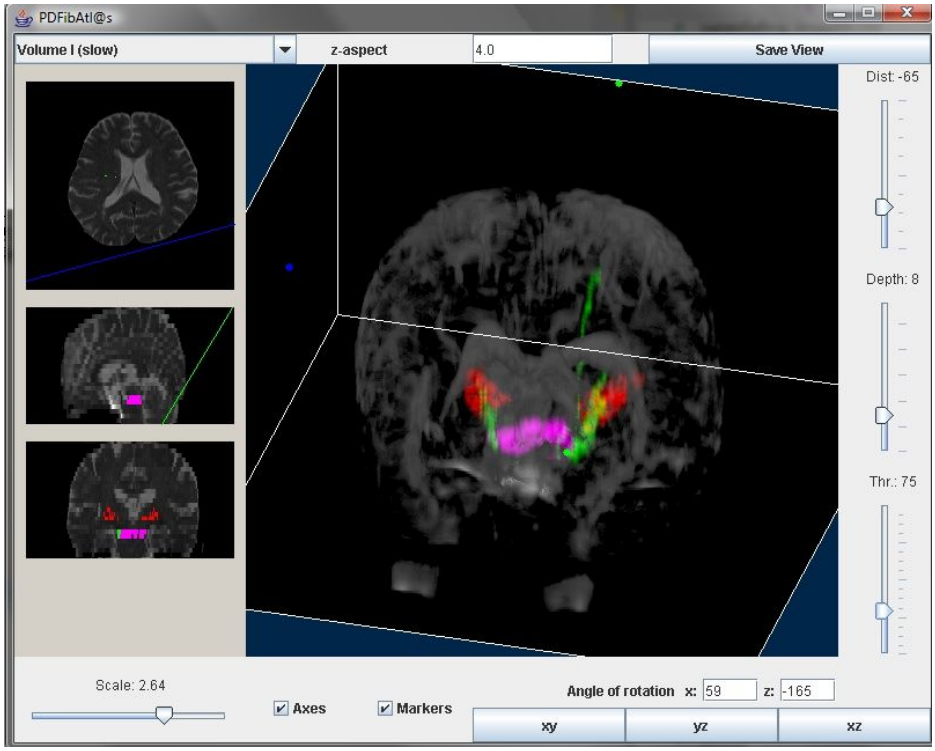

Figure 6.5: 3D View of the grown fibers from PDFibAtl@s

Taking a closer look on the testing batches, we can follow the variation of the relevance degree depending on the demographic elements and with regard to the test taken.

A significant value for correlation is given when the value of Pearson variable is lower than 0.01. In table 6.4 we perform the testing for correlation between the H&Y value and

Test nr	Left Side		Right Side	
	Pearson	P-value	Pearson	P-value
T1	0.041	0.825	-0.096	0.599
T2	0.107	0.555	0.023	0.898
T3	0.010	0.955	-0.037	0.841
T4	0.108	0.555	-0.101	0.581
Total	0.054	0.735	-0.098	0.541

Table 6.4: Simple correlation between the fiber volume (FV) and H&Y values[Teodorescu 2010]

Test nr	One-way ANOVA				MANOVA	
	FV		FD		FD	
	Left	Right	Left	Right	Left	Right
T1	0.00	0.00	0.00	0.00	0.105	0.515
T2	0.00	0.00	0.00	0.00	0.638	0.067
T3	0.00	0.00	0.00	0.00	0.138	0.404
T4	0.00	0.00	0.00	0.00	0.329	0.404
Total	0.00	0.00	0.00	0.00	0.149	0.629

Table 6.5: ANOVA testing [Teodorescu 2010]

the FV. Our conclusion after this test enhances the influence of the testing batch taken into account. For the test batch 3 on the left side, we have both variables indicating a very strong correlation, while the other test vary and appear not to be significant.

For the results presented for the fibers, we perform the same method of testing used for the green channel analysis. This time, we test our batches of patients taking into account the correlation and the regression coefficients. We can distinguish a difference between the two hemispheres of the brain on the results tables. The variations among the testing batches are due to the differences between the subjects. One-way ANOVA test is used to compare three or more unmatched groups and that is the reason we test our results using this test (first 4 columns in table 6.5). MANOVA results are presented in columns 6 and 7 from the same table.

On the ANOVA One-way test, the value considered significant is 0.00. In table 6.5, we can conclude that this test shows a strong significance on all the testing batches, while the MANOVA and the Lavene variable do not show a significance. In some of the cases, the equal variation of density could not be computed due to lack of a certain type of cases (Table 6.6), while the Lavene parameter is significant only for the whole database on the left side. These T-test show the medical relevance of our system, but from the technical point of view, we have to evaluate the robustness of the algorithms and their speed, as well as their accuracy compared with the manual detection and extraction.

Test nr	Test variation of density P-value		Lavene	
	Left	Right	Left	Right
T1	0.499	-	-	-
T2	0.932	0.855	1.33	0.04
T3	0.888	-	-	0.57
T4	0.733	-	-	0.721
Total	0.742	0.542	0.000	0.921

Table 6.6: Variation of density [Teodorescu 2010]

When estimating the entire database after the tractography step, we obtain 2 patients with "NaN" due to the segmentation and 22 with 0 fibers, from the tracing algorithm. From the control cases 14 have as result 0 fibers.

6.3 Method performances

We are presenting next the results obtained at different stages along the way of the processing system and then move towards the extracted features that are first tested with correlation to the disease severity level. After this correlation is established, the whole database is analyzed at the feature level for determining the sensitivity of the system to the image quality and its performance at the diagnosis and prognosis level. All the evaluations are performed using the entire database with our own methods.

We have to consider several parameters like the technical efficacy, the diagnostic accuracy and the error rates for our system. As presented in [Sonka 2009] various computerized methods, the use of different database affects the results. The subtle cases give a lower performance level. The database characteristics influence the training and the objective measures. The way that the database is used affects the performance of a method.

6.3.1 Segmentation results

The results obtained with automatic image segmentation for midbrain and Putamen have a great influence on the fibers detected, especially the Putamen area. The difference in the number of fibers detected with the manually segmented Putamen and the automatic one, for the same patients offer us the error rate for the automatic detection. This error rate is measured by the relative error presented in equation 6.4.

$$Err_{rel} = \frac{x - X}{X} * 100[\%] \tag{6.4}$$

where x represents the measured value and X is the average value of all the measurements - in our case, the difference between the manually detected Putamen area and the automatic

one. When using just the triangular segmentation of the Putamen we detect an error rate of 34.66% on the left side and 35.75% on the right side of the brain. When evaluating the alignment algorithm based on the center of mass the relative error rate is 37.16% on the left side and 39.6% on the right side.

As the Putamen correct placement determines the validation for the strationigral fibers, its placement together with the correct detection of the volume determines the number of fibers and directly affects the analysis results.

6.3.2 Tractography results

For fiber evaluation, the number of fibers identified for each patient represents the measure of a correct or incorrect segmentation. The tracking algorithm does not change, but it is sensitive to the Putamen area. This is the reason why values for the fibers above 20 represent a misplacement of the Putamen area or an incorrect detection - this happens when our algorithm detects more than just the strationigral tract. Based on these elements, we define the metrics for the sensitivity, specificity and accuracy.

- TP - PD patients that have a correct segmentation compared to the manual approach that have less than 20 fibers
- FP - PD patients with a correct segmentation and more than 20 fibers
- TN - Patients that do not have correct identification of the volumes of interest
- FN - Patients with volumes detected that provide no fibers after tracking

With these classes of patients we obtain 89% specificity, 80% sensitivity and 82% accuracy on the PD patients for the combined with triangular approach on the left side detection for the Putamen and the combined triangular and quadrilateral approach algorithm. The same approach on the control subjects offers values of 37% specificity, 82% sensitivity and 75% accuracy. Analyzing the overall performance of the algorithms on the data we have 63% specificity, 81% sensitivity and 78.5% accuracy.

6.3.3 Diagnosis performance

Having the features extracted from the image level, we evaluate the extracted data using the fibers density defined in equation 4.1 and the recalculated values in equation 5.1 from the normalized extracted data at the patient level. We perform pretesting on 26 patients to test the implemented functions. The diagnosis is achieved by using the rule based system on the intervals defined in table 5.2 of the extracted normalized features. We test the system on the intervals of the left fiber density, after training it on the test batch and we retrieve a *61.53%* success rate [Pataca 2010]. The cases that are placed incorrectly are due to the fact that the fiber detection does not identify fibers on the motor tract.

6.3.4 Prognosis results

Using the second and the forth degree polynomial determined in section 5.2 we test the prognosis module on the first 26 patients and obtain on the second degree polynomial function a *19%* error rate on the training set and *34%* with the forth degree polynomial function success rate. This function is determined using the fiber density normalized values on the left side [Pataca 2010].

We first evaluate the Fuzzy Adaptive Evaluation prognosis function on a test batch, representing the manually processed Putamen detection (37 PD patients and 52 control cases that provided valid features after the fiber extraction). Together with the manual Putamen data, in the training function, we include five PD patients from the initial valid 42. With a rate of *32.43%* on the patients and *46.15%* on the control data, the overall system provides a *40.44%* correct rate. When updating the Putamen detection, we perform a reevaluation of

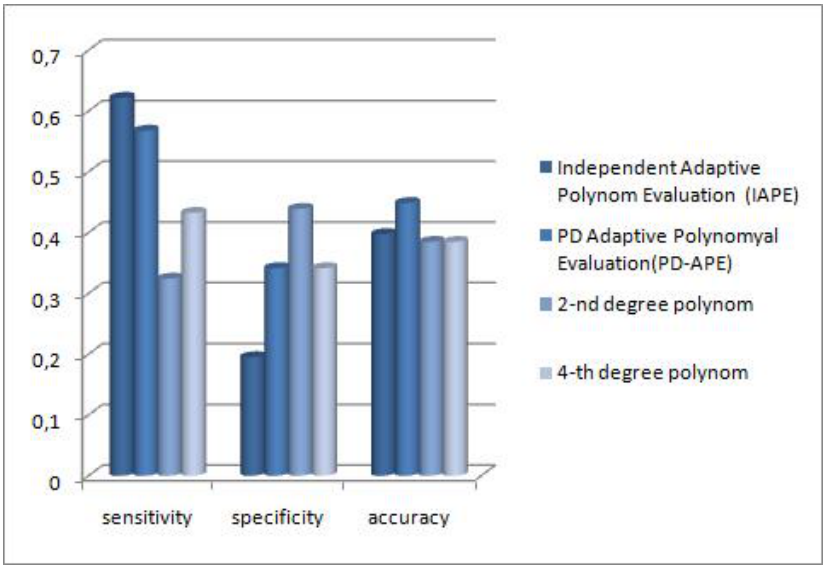

Figure 6.6: The Sensitivity, Specificity and Accuracy of the prognosis methods

the diagnosis and prognosis module on the entire automatic methods applied on the database (68 patients and 66 controls). These results are presented in figure 6.6. For computing the values for the parameters in figure 6.6 using the equations 6.1, 6.2, respectively 6.3, the values for the coefficients represent the following:

TP cases with PD correctly identified

FP control cases identified as PD

TN control cases correctly identified

FN unidentified PD cases

The patients are characterized by the value of the sensitivity - maximum value for the Independent Adaptive Polynomial Evaluation (IAPE) approach with*62.16%*. On the control cases, the specificity represents the evaluation value that characterizes it - maximal value for the second degree polynomial approach is *43.9%*. The accuracy represents the overall performance of the algorithms that performs the best on PD Adaptive Polynomial Evaluation (PD-APE) method offering a *44.87%* value.

The overall performance of the prognosis module is provided by the ROC curve. We compute this metric using the SPSS 17.0 (Statistical Package for the Social Sciences) for the patient estimation, as the prognosis functions are applied for establishing the severity degree of the disease. Evaluating the IAPE method for this case, the area under the curve (AUC) is 0.705, whereas for the PD-APE the value is 0.959 (see figure 6.7). This indicates a much better performance on the patients data for the second method.

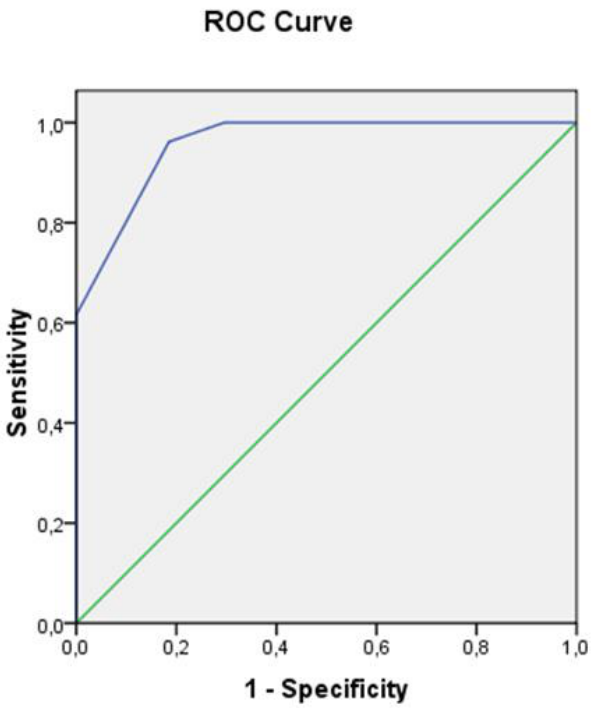

Figure 6.7: ROC curve for PD-APE prognosis method on the patient data. The AUC value for this case is 0.959 on the 68 PD diagnosed patients from the database.

We evaluate the prognosis performances on the control and patient data to estimate the overall capacity of the proposed methods at this level. We compare the ROC curves for different methods and for this purpose we use the MedCalc[2] software. This software provides two approaches for the ROC curve estimation: De Long and Hanley & McNiel. Using the

[2]MedCalc 11.3.3.0 - `www.medcalc.be`

database results on IAPE, the AUC values for these two ROC estimation approaches were the same. We further use the De Long approach when evaluating the ROC, as the error rate provided on the same test is slightly lower compared with the McNiel approach (0.1%). For the PD-APE method of prognosis, we obtain a value of 0.569 for AUC and for IAPE the same metric has a value of 0.745 (see figure 6.8). Comparing the two curves, the difference between the areas is 0.176 - figure 1.9.

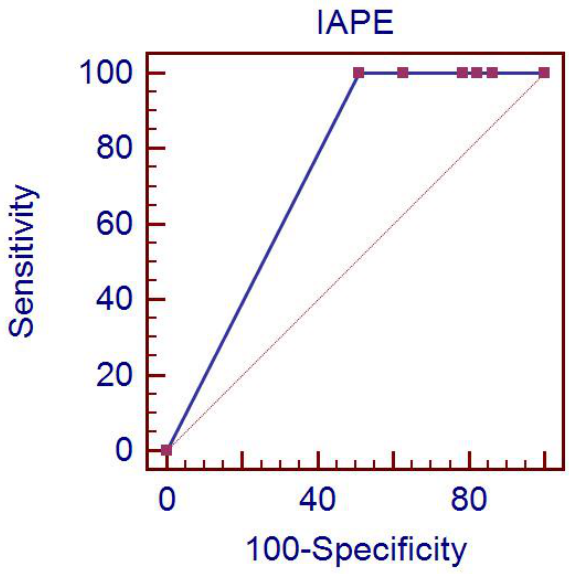

Figure 6.8: The ROC curve representing the IAPE prognosis method applied on the whole database: 68 PD cases and 75 controls. The AUC for this test is 0.745.

6.3.5 Computational speed and requirements

We use Java for all the systems with imageJ toolbox and bio-medical imaging plug-ins [3]. The simple image processing for the preprocessing part is done by enhancing the contrast for the EPI images and removing the noise. For the removal of the skull we use K-Means for making the segmentation based on the pixel intensity. By removing the skull we remove the outside noise surrounding the entire brain, the aura effect induced by the scanner. For the 3D visualization we are using the Volume Viewer from imageJ [4].

The algorithm is tested on Intel core Quad CPU Q660 (2.4GHz; 4.0G RAM) and the average time for each patient is 4.68 min with the automatic detection and the fiber growth algorithm. If with DTI tracker from MedINRIA took us 1-5 min to have the fibers, with our prototype it takes us an average of 2 min. The reason of this computation efficiency is related to the limitation of the area for the fibers performing a global tractography, whereas the

[3] Bio-medical image -http://webscreen.ophth.uiowa.edu/bij/ - last accessed on May 2010
[4] Volume Viewer 3D - http://rsbweb.nih.gov/ij/plugins/volume-viewer.html - last accessed on March 2010

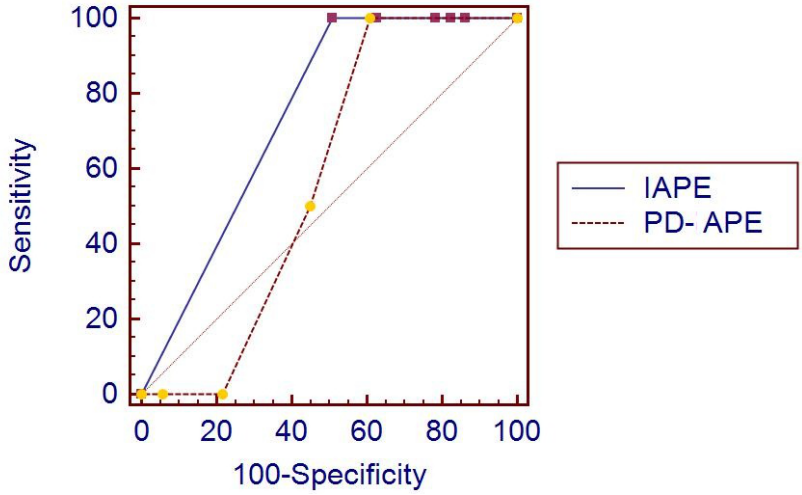

Figure 6.9: The two ROC curves for IAPE and PD-APE methods applied on the database (143 cases: 68 patients and 75 controls). The AUC values for IAPE and PD-APE are 0.745, respectively 0.569. Evaluating the ROC difference between the two tested methods the AUC indicates a difference of 0.176.

method proposed by the DTI tracking module (MedINRIA) takes a local approach without an ending point for the fibers, selecting at the end the fibers passing through a specific volume of interest. The 2 mins represent for our system all the processing time with the automatic volume detection, registration and tractography. A similar time (1.2 min) is provided using a probabilistic global method with the Diffusion Tracking module(TrackVis)for image selection and the tractography, without segmentation and computation for the fiber metrics.

6.4 Conclusion

After determining a correlation between the features and the disease, using the features as a measure for the disease represents a valid option at this point. The modality of using the features representing the technical challenge estimated form several points of view, at each stage and as whole as well.

From the point of view of the evaluation and testing criteria, the contribution revealed in this chapter reside in the testing technique. This technique mixes the cases for revealing the effects of the cognitive parameters and the tests that are not affected by these parameters. The green channel analysis has already been presented in [Teodorescu 2009b] [Teodorescu 2009c] [Teodorescu 2009a]. The original approach on the segmentation of the Putamen was presented in [Sabau 2010]. The fibers and the PDFibAtl@s prototype is presented in [Teodorescu 2010] and as a demo version at [Teodorescu 2009b]. As the diagnosis and prognosis was the final

stage, their preliminary methods using the second and forth degree polynomial approaches were presented in [Pataca 2010].

Another important aspect at this point is finding the appropriate test for the evaluated data. For the green channel study we take into account the one-way ANOVA test as it is not affected by inter-patient variability and detects the correlation between the PD and the fiber directionality. For the fibers density, due to the fact that the nature of the evaluated data has changed, we find a test that reflects more appropriately the correlation and regression values for this type of data: one-way ANOVA, MANOVA, Pearson's variable and the Lavene parameter.

Evaluating the obtained volumes of interest, as well as the techniques implemented, proved to be appropriated for the type of image that we are dealing with, as well as for the resolution of these images. The speed of computation reveals a system that performs in a few minutes the detection of the regions of interest, as well as the computation of the fibers.

We have found a way to evaluate our algorithms separately and the whole approach as well, using the PDFibAtl@s prototype. We need to tune the diagnosis and prognosis functions for a better detection rate. These functions have been created using the manual data with additional five cases from the PD cases.

All the elements in the system affect each other. The Putamen accuracy determines a higher accuracy on the fibers and the fiber accuracy is essential to diagnosis and prognosis module.

Chapter 7

Conclusion and Scientific perspectives

Contents

In the work presented in this thesis, we have several levels where new scientific methods are developed. Proposing a way for estimating the severity of the PD based on the information provided by the image, represents altogether a new demarche. The prognosis represents another scientific act, based on measurable functionality and specific features, to determine at a higher scale the diseases severity, even on early cases. These scientific aims are reached by studying the images and the possibility to extract and use the information specific to the disease from these images. This research corresponds to the learning and understanding part on the image modality study and specific elements. The methods developed for preparing the images and volume-based analysis are created for sustaining the more complex systems corresponding to the volume segmentation algorithms. The tractography method, using the extracted volumes of interest, offers not only a much better time on processing but also the selectivity needed by the diagnosis and prognosis model.

PDFibAtl@s, the prototype system that encapsulates all the new proposed methods and algorithms presented in this thesis, is meant to be an aid for a more complete image on the PD field, offering quantitative unbiased information from the medical image level. In this manner, by using the computerized analysis of the images according to recent studies [Sonka 2009], the performance of the radiologist increases. We eliminate the observer from the image study, by modeling and including at the same time its experience,

therefore we aim at being more accurate at the feature detection and quantification phase.

Our approach is important from the clinical point of view, offering a new method for the neurologists in PD and a mean to verify/confirm their diagnosis and prognosis. From the technical standpoint, the fusion is novel, as it combines the tensor based information and the anatomical details. This system provides data for H&Y estimation and PD prognosis.
Analyzing the results obtained by each new method, we have to take into account the fact that the image quality together with patient variability, influence the algorithms.

The pure geometrical analysis of the specificity of each patient together with the noise elimination represents only the preparation step for the image processing method we developed. The segmentation offers an error rate of 37-40%, that affects the tractography performance. When developing our new segmentation method, the upgrade on this method determined better results on the tractography as well, resulting on an increase of 19%. This aspect reveals the importance of the Putamen in the tractography as well as the robustness of the segmentation method with the direct implication at the feature extraction level.

The performances of the tractography with a level of 78.5% accuracy provide a feature database that can be further used for the diagnosis and prognosis purpose. The metrics introduced for the fibers evaluation provide viable data for the prognosis functions so that a value of 45% accuracy can be obtained. The importance of the segmentation is given also by the fact that unlike the manual segmentation, the automatic approach is much faster and is not influenced by the specialist skills and his capacity to distinguish between close levels of entropy on the image voxels. The computational speed is superior also on the tractography, due to the use of less memory as we are taking into account only the fibers starting from the midbrain and we are validating only those reaching the Putamen volume.

The main breakthrough initiated by this study is represented by the method able to predict PD by offering a view on the early cases as well, not only on those starting from the second stage of the disease. This evaluation method based on the image attributes, on the anatomical and neurological aspects of the patient offers a measurable value of the severity of the disease. As the H&Y test is based on the cognitive facet, our method is complementary to the test, but is placed on the same scale.

PDFibAtl@s is a new system, able to automatically detect the volumes of interest for PD diagnosis using the DTI images and a geometrical approach. The algorithms included in this platform are original and are based not only on the brain geometry, but also including medical knowledge by taking into account the position of different anatomical structures at the brain level, hence the atlas dimension. Concerning the fusion contribution of our work, it brings together the FA clarity at the Putamen level with the tensors matrix for the fiber tracking algorithms. Our algorithm automatically detects the elements that until now were obtained by user interaction: detection of the slice of interest, detection of volumes of interest, automatic detection of the registration parameters. Introducing parameters for fiber evaluation and eliminating the demographic factors at the atlas level, as well as at the volume level represents another important contribution of this thesis.

7.1 Scientific Contribution

The scientific aspect refers to the originality and the impact of the method, as well as its necessity on the area where this method is employed. Both technical and medical areas have to gain from new methods in the medical image processing domain. Combining medical knowledge with new technical approaches, we are able to offer new information that can be exploited for a new overview on the PD. At this point, we are analyzing the originality of the methods, the challenges overcome and the difference with other proposed approaches.

The thesis proposes using the medical images, particularly the DTIs, as a bio-marker for PD prognosis. This represents the main scientific contribution as the diagnosis is based exclusively on the cognitive testing and the visual information is not exploited. Using this information provides as well the quantitative measure of the severity of the disease for the prognosis values as well.

The theoretical hypothesis that the neural fibers constituting the motor tract can be used as indicator for PD is tested in our work and we validated it by finding a correlation with the severity of the disease. At the same time, it represents also the informational potential gained from the medical image level and further used for the prognosis.

Taking the theoretical elements to the practical level, we develop methods able to automatically perform not only the image processing, but also the analysis of the extracted data for prognosis.

At the technical level, our scientific contribution starts at the **pre-processing level** where we develop methods to overcome the noise specific for head DTI images, with even higher interference in the low resolution images. According to our preliminary study, the skull influences the overall results at the anisotropy level. The method removing the skull performs the noise removal as well, so its utility is doubled. The contributions at this level are:

- Finding and defining an automatic algorithm for detecting the slice of interest at the volume level
- Finding and defining specific algorithms that detect at the axial level the placement of each region of interest: the midbrain and the putamen tissue on each side
- Developing an algorithm that determines the axial limitation between the two hemispheres

For the *volumetric measures*, used further at the volume segmentation level, additional study and more complex methods are developed. The success of the segmentation approach together with the registration is linked to these determinations. This gives the importance of the method for determining the geometric parameters. The fact that these parameters are independent on the patient's demographics offers inter-patient independence as well and overcomes this barrier making possible the automation of the other methods. The inter-hemisphere axis used for the volume segmentation and for the registration method, overcomes the intra-patient variability as well. This axis provides information on the image orientation and the position

of the patient in the image. The algorithms, together with the slice detection method, are totally independent on the patient data and the image type.

The *slice detection* method procures the automatic placement of the segmentation image for the volume segmentation algorithm and takes into account the volumetric and anatomical aspects of the brain. This method considers the position of the patient in the image - patients having smaller or bigger skulls or slices starting higher or lower on the patients skull (e.g. at the ear level or under the level of the nose). Using this algorithm, we overcome these differences between patients and we provide a robust placement for the volume segmentation.

In this manner, the sex difference transposed as volume difference is overcome, together with the race difference resulting also in volume difference. The fact that we take into account these variables from the demographic of the population constitutes a contribution by itself. This variability is transposed into parameters at the geometric level providing the elements an automatic approach on the segmentation and the registration methods.

The specificity of each patient is given also by the shape and the placement of the volumes of interest inside each image - some patients have one hemisphere more developed than the other and the anatomical regions are thus differently developed. The volumes can be placed at different levels on the axial plane as well. This variability is surmounted by the methods that establish the starting points for the active volume detection. These algorithms are based on the anatomical map of the brain and the relative placement of the volumes of interest inside the brain. Depending on the volume of interest the algorithm that detects the relative placement in the axial image is different. The midbrain volume is placed on the inter-hemisphere axis and the Putamen is placed on the superior part of the brain, next to the anatomical area named Globus Pallidus. This relative placement is based on the anatomy of the brain, like an atlas. The atlas mapping of the brain offers just the relative position, the actual positioning is given by the intensities of the pixels. This method for identifying the area where to apply the segmentation represents a new approach and overcomes the inter-patients variability given by the different positioning and size of the anatomical structure in each individuals brain. The difference from an atlas approach is given by the segmentation method. Using the anatomical relative positioning inside the brain like an atlas or a map, but not segmenting these areas by using the actual atlas and applying it is as a mask, represents a new method for the segmentation at this level. This method had just the placement of the anatomical region and determines for each case the ROI/VOI including the specificity of the patient.

The segmentation process is based on automatic detection of the region based on the voxel intensity. This approach determines the volume of interest independent on the size of the anatomical region and its angulation or positioning inside the brain. Our method is automatic but also adaptive to each patient. The **volumes of interest are specific** for the disease - the substantia nigra and the Putamen - and the manner in which they are detected, by combining the image specific processing methods, together with the geometrical elements and by integrating the anatomy elements. The method is applicable to any patient as it does not take into account the provenance of the case, for shape variability, or the volume of the brain, that vary according to the sex of the subject. For these reasons, this method is a complex one, integrating concepts from the medical knowledge for technical purpose.

At this level our contribution resides in developing not only

an accurate algorithm for the midbrain and the putamen detection, but one that is independent of the inter-patient variability and is used at the volume level.

For the **midbrain** area, we are using the clustered EPI image that is able to determine the midbrain even if one hemisphere is more developed than the other side.

At the **Putamen** level, the algorithms are different on the left and the right side of the brain, as we take into account the differences between the two hemispheres. Also, the shape is taken into account at different levels of the volume by applying the triangular or quadrilateral approach. This versatility makes the difference between our approach and the classical atlas based approach. On the manual segmentation directly on the FA image, the anisotropy with the piercing fibers on the image determines "holes" on the volumes due to the difference between the voxels. Our approach using the clustered image with the geometrical segmentation does not have this problem and eventual fibers passing through the Putamen are validated, which is not the case for the eventual fibers passing through "holes" on the manual determined volume.

The registration method combines the manual method and the geometrical approach, but it is automatic, as it detects the geometrical elements at the pre-processing level. The robustness of the geometrical approach, combined with the fact that this method eliminates the inter-image variability as well, represents upgrades to the manual approach, which does not beneficiate of the accuracy and objectivity of an automatic approach, this being our contribution at this point. This method actually fuses the information extracted by segmentation form the FA image to the EPI volume.

The most important aspect of the originality of the approach is the combination between the automatic volume detection integrated on the global tractography. The metrics used for estimating the fibers are specific to this approach and are meant not only to evaluate the fibers, but also to overcome demographic variation.

The tractography methodology that uses the volumes of interest is faster than the original one by the fact that it uses only a small volume of the brain for the fiber growth: the midbrain, it researches 2-4 slices and validates only the fibers reaching the Putamen. The originality is given not only by the computational time, but also by the ability to automatically separate the fibers we need from all those residing on the midbrain. **Using the fibers** to evaluate the PD evolution is highly reliable, as in previous studies only our first volume of interest has provided enough data to reach this purpose. Our method adds the 3D aspect in the evaluation, by including the fibers.

The anatomy of the brain incorporates the medical knowledge to the approach, supports the technical elements and is able to link the processing algorithms by offering decisional rules for the detection steps of our system.

It is very valuable to be able to take the images from the files directly and by an automatic approach, without considering the identity/demographic information from the patient, to deliver comprehensive information to the clinician regarding the disease. At the ROI/VOI and registration level not only the actual registration is automatic, but also the determination of the parameters for this purpose. Having an original take on the DTI image processing and

the detection of PD specific volumes adds up to the overall value of the methods. The fiber algorithm has a new perspective by limiting the fibers to the bundle of interest.

From the **analysis and interpretation** perspective, using just the fuzzy rules from an ANFIS architecture for diagnosis proved to be a good approach, but this approach is limited by what the system knows, by what it has learned. This is the reason why a variation function on the features is more suitable for diagnosis and extrapolation. The contribution at this level is given by the function performance and its rate of transfer of knowledge from the feature level to the semantic level. The prognosis evaluation using the ANFIS architecture represents a first approach with the additional Lagrange polynomial functions. This approach defines not only the functions but also a hybrid adaptation using our new features- IAPE method- and for PD- PD-APE method. Our method that combines the knowledge form the fuzzy systems with the mathematical evaluation of the features from the neural networks offers exactitude.

7.2 Clinical Impact and Prognosis potential

Being able to confirm the cognitive test performed to place the patient on a severity scale is helpful for the medical doctor and offers the possibility to augment the degree of trust on the diagnosis. Having a test based entirely on the image is a robust and reliable way to evaluate the patient and his current estate.

Another important aspect is represented by the fact that the diagnosis is directly liked to the severity of the disease, as it can be cognitively detected and placed only after it passes the second level on the H&Y scale. Based on a technical measurable system, with a high granularity, our approach offers the possibility to apply it on any patient at any level of severity of the disease.

The lightness of these algorithms is contained in the versatility, as these volume algorithms can be applied on other types of medical images. For the fibers, we need the tensors, but these algorithms can be perfected by including a tensor analysis based on the green-channel study presented in chapter 6.2.3. We can extend this approach to other similar diseases like Alzheimer by determining in the same manner the specific bundles of interest. We can envision an automatic intuitive atlas of the brain by using the detection of all the anatomical structures. The advantage in this case would be that mapping is not involved and therefore, the demographic aspect is not a problem anymore.

The diagnosis and the prognosis are highly dependable as the early diagnosis is unreachable without having the prognosis step defined. This step is reached by evaluating the patients from our database and placing them on an evolutive function. By extending this function and extrapolating towards the low values of the scale, the early stages of the disease evolution is reached. Having the values for this level of the disease offers the information necessary for placing new patients at this level and making diagnosis for these patients as well. In this manner we use the prognoses for establishing new diagnosis support. The medical doctors can study the detected early cases provided by the prognosis functions and define tests at the

cognitive level for diagnosis.

With the first results from the feature extraction module, we are able to estimate the severity of the disease, using standard polynomial functions (section 5.2). Modifying these standard functions by adding medical knowledge as well as cases for the stages that were not present in our database, will certainly improve this part of PDFibAtl@s.

7.3 Scientific Perspectives

The scientific contributions offer new perspectives and can be further improved as well. The thesis represents a study at the image level with new methods that provide measurable values of the PD severity. As these types of images have not been used in this manner, our approach opens new perspectives for other methodologies and represents a comparison element for future approaches.

From the technical perspective we have a robust system, PDFibAtl@s that encapsulates all the necessary image treatment starting from the scanned images to the motor fibers and their density. Automatic detection of the volumes of interest contours an atlas-based method entirely independent on the subject. Even if this approach is specific for the disease, the proposed detection methods can be used for other diseases, once the specific VOIs related to the specific disease have been identified (with the support of neuro-radiologists). Our contributions can be further used for other medical images, as well as for other diseases. The methods developed to include the image at the prognosis level represent themselves initial steps and can be further developed and adapted, but also important starting points for other methods as well. The main upgrades that we have as perspective at this moment are:

- At the preprocessing level
  - Adding and extracting more geometrical elements to gain accuracy at the other levels
  - Determining other axes for a better volume handling
  - Using more accurate images can augment the performances of the overall system as well
- For the segmentation
  - With more geometrical elements, the region of interest can be limited with more accuracy
  - A putamen detection that bends more on the shape of the tissue could bring more accuracy for the volume
- For the tractography we envision trying the probabilistic approach
- At the prognosis level

  - A dedicated function developed for the nature of the data that we are working with
  - Functions that follow better the variation of the data and can include additional knowledge for the expended H&Y scale

Additionally the perspective of using the new algorithms developed here for other images, diseases and/or purposes altogether is possible as well.

- The idea of using the geometrical landmarks for excluding the inter-patient variability and automatizing the image treatment for the patients can be applied for different head-related projects
- The contour detection with the inter-hemisphere axis is important and can be used in brain stroke and/or tumors
- The automatic segmentation
  - Can be extended to other brain anatomical volumes (structures) and further used for other diseases and/or images
  - If all the anatomical structures are determined, we envision an automatic atlas, without sensitivity to the demographic parameters and/or to the unequal developments in the two hemispheres
  - A follow-up on the same structures can provide additional information on the volume of the specific anatomical regions and théier degree of sensitivity to the disease
- A follow-up on the same patients provides a study of the variation on the extracted parameters and can be further used in the prognosis process providing the variation function for a heathy patient, as well as for the PD ones

Having the main perspectives stated, we can envision specific use of the other aspects of our study as well. The **pre-processing methods** used for eliminating the noise and the skull, independent on the shape of the head and its volume, can be applied on any type of head medical image. The fact that our approach provides good results on low-resolution images like EPIs, means that on high resolution images the result can be improved. The geometrical feature detection is a useful tool on any type of image, independent on the anatomical region. Also the inter-hemisphere axis determination has multiple applicability, offering not just a limitation for the segmentation algorithm, but also directionality on the positioning of the patient in the image, useful in registration methods, warping or fusion. This particular element has its utility in other diagnosis methods that need a comparison between the two hemispheres (e.g. brain stroke or tumors).

At the **segmentation** level, our method can be applied for any anatomical volume of the brain, as long as its relative position inside the brain volume and its position at the axial level are known. The fact that the active tracking algorithms are either based uniquely on the voxel entropy, or on the geometrical limitations, provides a wide range of applicability. In case

of an anatomical region well defined, the method developed for the midbrain segmentation can be useful, together with the algorithm for determination of the initialzation point (e.g. the caudate nucleus positioned on the inter-hemisphere axis and having well defined contour). The algorithm developed for the Putamen can be applied for structures that are not positioned on the hemispherical axis (e.g. the fornix formations).

We can even envision an *automatic specific atlas* that combines our segmentation methods and uses geometrical adapting algorithms for the anatomical elements that provide this information, together with the malleability of the free-form intensity based algorithm developed for the midbrain area. In the case of such an atlas, the anatomical regions that do not consist of a specific form and/or clear limitation can be detected using the surrounding structures as limitations. This type of atlas differs from the classical one, by the fact that it uses only the relative positioning contained in a classical approach, but it is entirely molded on the specific structures of each patient. In this way, a much more correct evaluation of the structures can be achieved.

A follow-up study using our method of segmentation on the volume of specific anatomical regions of the brain can be used to determine the geriatric effects on a normal brain on the control cases, by comparison with those affected by the disease. Similarities among control patients at the volume level define a "normal" aging brain. Volumetric elements that are similar among PD cases but differ from the controls, represent specific metrics for the disease and its severity and can be used for a PD model definition.

The registration method, fully automatic, based on the geometric elements can be further developed for determining skewness elements. Also starting form our method, other type of DTIs can be fused at the information level, even if they have different size and orientation. This purpose can be reached as we already have the volumetric elements and relative positioning of the patient in the image, therefore the ration between two different images as size and skewness should be straightforward. Not only fusion can be achieved in this manner, but also other similar processes like warping and alignment. The automatic method for determining the corresponding structures for the registration algorithm can be applied for other registration approaches that use parameters, as these elements are not affected by changes at the structural level of the brain (e.g. tumors and/or brain stroke). An iconic registration, using the geometrical parameters determined with our method and computing the affine elements as presented like we did could be upgraded and automatized as well.

Another very important aspect of our approach is **the tractography** algorithm based on the anatomical elements: the deterministic approach for the the fibers - the WM importance and the way the motor tract is placed inside the human brain used for the global methodology. The method itself can be improved and the angulations limitation eliminated as only fibers having certain directionality will reach the second volume of interest. Also the information at the voxel level providing the directionality of the fibers can be further used to verify if the same fiber passes more than once trough the same slice, eliminating in this way a source of error. This approach is only feasible when having a limited amount of fibers, just like our case, otherwise the computational effort would be much too heavy on the memory capabilities. Another application of this approach using a limited amount of fibers can be detected in annotating the fibers and by performing comparison between patients to measure the difference

on the severity of the disease between the left and right side. Performing the same study at different time lines on the same patient can provide information on the way that those fibers are affected, the most affected ones and/or the anisotropy levels that are critical for the most affected fibers.

Actually, the automatic detection of the volumes is based on the anatomy of the brain and the relative placement of the detected structures in the brain geometry. The limits imposed for the fiber tracts are not only for imposing a certain granularity for choosing the bundle of interest, but also to validate the obtained bundle from the anatomical point of view, by the neurologist - validation based on the placement of the fibers in the volumes of interest. These volumetric elements can determine also other bundles of interest, depending on the volumes that these fibers pass trough.

Refining the fiber detection method and making it specific to the gray matter can augment the degree of trust for the diagnosis and add reliability to the system. It can also offer a higher correlation factor between the diagnosis success rate and the detected fibers. These fibers offer the possibility to study not just the effects of this particular disease, but also the dopamine flow changes and the degeneration of the fibers depending on the severity of the disease. Applying the global tractography approach for PD on the same patient and providing a follow-up in time, the fibers value reveals the disease progression. Our metrics at the fiber level can be further used as well, as they are based on the relation of these fibers with regard to the volume of the brain. This metrics would not be affected by an atrophy that is unavoidable in geriatrics.

The tractography provides the fiber metrics independent on the two hemisphere and this method can provide the information to make the distinction at the 1.5 and 2.5 H&Y severity levels. Also the fact that the disease affects more the left side, can be verified using the fibers obtained, as well as the degree in which the left side is more affected than the right one. This information included in the diagnosis and prognosis method makes the difference between the old H&Y scale and the new one. This information is able to refine the results from the prognosis method and to update the diagnosis set of rules.

Using a newer tractography method can provide more accurate results and augment the prognosis rate. A probabilistic approach can be used as well because we need just a bundle of fibers and thus the computation time would not be too long, like in the Diffusion Tracking module from TrackVis, but in this case, the noise must be eliminated.

The diagnosis and prognosis are linked together by the variation function of the fibers parameters on the H&Y scale. This function has to be determined on a heterogenous database and should be sensitive only to the fibers metrics, not to the demographic aspects. By introducing the fuzzy expert system in the analysis module, we acknowledge the dispersion of the fiber values - the fuzzy adaptive evaluation method. This approach provides the system with a reliable and flexible way to include an evaluation based on medical knowledge, but also the possibility to change the set of rules by adding new ones that can provide a better clustering. A combination of expert systems and neural networks can provide also better granularity on the diagnosis step.

The prognosis provides values for new cases, even for the early cases of the disease. Our own method for prognosis based on Lagrange polynomial functions can be upgraded by using

functions that have a higher sensitivity to the metrics that we are using. As the detection of the polynomial degree that better determines the severity of the disease has proved to be a good step on the right direction. Introducing the new cases correctly detected among the initial points can augment the rate of prognosis. A mathematical analysis of the variation function can provide a better evaluation at this point. Different metrics provided for the prognosis step can result in different values for this function, but our approach can be still used. Using the anisotropy level from the Substantia Nigra, or a combined value between this value and the fiber density, can be used with the same prognosis method. This prognosis method can be applied in other systems or for other diseases as well because it is entirely independent.

Using the medical image as bio-marker for the PD is not only a new approach, but it shows potential for other neurodegenerative disease as well. It offers a measurable value for the disease, based entirely on the value of the source of the disease, the dopamine level represented on the image. We have developed a manner not only to validate the medical theories at the image level as well, but also a working system independent on the patient that performs the prognosis.

Chapitre 1

Pronostic de la Maladie de Parkinson, basé sur la fusion des caractéristiques d'Images par Résonance Magnétique de Diffusion

Contents

Les algorithmes qui font l'objet de cette étude représentent un systéme de détection,

de diagnostic et de pronostic de la maladie de Parkinson en utilisant les images de type DTI. Notre système propose une alternative à la détéction basée sur des tests cognitifs. On utilise un système capable de détecter automatiquement des volumes d'intérêt utilisés pour le diagnostic de la maladie de Parkinson. Le système utilise ces volumes via un algorithme de détection des fibres neuronales responsables du mouvement - le nerf neuromoteur. Une méthode d'évaluation basée sur les valeurs de ces fibres permet une analyse quantitative de l'évolution de la maladie du patient, en effectuant un diagnostic précoce - pronostic de cette maladie.

Selon des récents résultats de nos collaborateurs radiologues [Chan 2007], la dopamine, un des neurotransmetteurs responsable du flux d'information dans les fibres du tract neuromoteur, réside dans une composante mésencéphale qui s'appelle Substantia Nigra. On considére que le manque de mobilité cumulé avec le tremblement constaté chez les patients de Parkinson est le résultat de la perte de ce neurotransmetteur. Selon une étude récente [Today 2009], la maladie de Parkinson est détectée seulement quand la perte de dopamine arrive a 80-90%. Cette détéction intervient trop tard pour engendrer un traitement réellement éfficaces. La détection utilisant les tests cognitifs est réalisée quand la maladie est au deuxiéme niveau sur cinque sur l'échelle de la gravité - en occurrence, l'échelle Hoehn & Yahr (H&Y) (voire annexe C).

Au lieu de focaliser directement sur le tissu de SN, nous effectuons la segmentation de la région mésencéphale, vu que cette région anatomique contient le SN. Pour déterminer seulement les fibres du tract neuromoteur, on utilise une autre région traversée de maniére certaine par ces fibres. Cette région est le Putamen, qu'on segmente dans les deux hemisphéres pour obtenir séparément le tract pour chaque coté. L'analyse des fibres de chaque coté est basée sur le fait que selon les études médicales [Today 2009], la maladie affecte plutôt la partie gauche du cerveau.

Vue que les valeurs extraites des fibres ne présentent pas une règle de dispersion ou une uniformité, la logique flue nous permet de définir des ensembles de données comme des ensembles flous. Ces ensembles nous permettent de définir les règles pour déterminer le diagnostic basé sur l'apprentissage apriori. Un système d'inférence floue ou un modèle flou permet l'apprentissage tout en permettant l'adaptabilité pour prendre en compte l'imprécision et l'incertitude dans les données. Le lien entre les contrôleur flou et les réseaux neuronaux qui déterminent la classification des données est représenté par les systèmes Adaptive Basées sur Des Réseaux d'Inférence Flous (Adaptive Network-Based Fuzzy Inference Systems (ANFIS)). On utilise cette architecture ANFIS pour le diagnostic et la prédiction. En utilisant les règles floues pour le diagnostic, on est capable de faire la différence entre les cas correspondant aux patients malades et á ceux qui sont sains (contrôle). Pour déterminer l'inférence, on défini des fonctions polynomiales et en utilisant le modèle de Takagi-Surgeno-Kang (TSK) on évalue la possibilité de prédiction des cas précoces.

Aprés la présentation des principaux objectifs de notre approche, comme dans le chapitre 1 de la thése, dans ce résumée, on présente une vue d'ensemble des nouvelles méthodes développées au niveau du traitement des images (voir chapitre 4) avec la partie prétraitement (en 4.2.1) et segmentation des volumes d'intérêt (section 4.3). Dans la partie dédiée á l'analyse des fibres, on propose l'utilisation des algorithmes d'intelligence artificielle (voir chapitre 5).

Á la fin du résumé, nous présentons brièvement les résultats obtenus (voir chapitre 6), ainsi que l'importance de cette étude, ainsi que les futurs développements des algorithmes et les perspectives de recherche ouvertes (voir chapitre 7).

1.1 Presentation des objectifs de la thèse

La thèse vise des objectifs médicaux et des objectifs techniques, traduisant des solutions innovantes pour les problèmes médicaux. *Détecter la maladie de Parkinson* est le but principal du système. Pour arriver á cet objectif, le défi est de *trouver les fibres cérébrales*, permettant d'effectuer un diagnostic de lévolution de la maladie. Comme présenté dans la figure 1.1, notre démarche fait la transition entre le *domaine des caractéristiques des images*, qui son extraites et interprétées, vers le domaine des *caractéristiques spécifiques des images et de l'anatomie cérébrale* mais aussi de la connaissance médicale. Ces caractéristiques représentent les valeurs qui sont analysées et qui sont traduites dans *le domaine des connaissances* au niveau sémantique pour permettre une interprétation de la gravité de la maladie. Nous avons á ce point **le défi technique** : *générer des fibres* qui appartiennent seulement au tract moteur et *les analyser* afin de trouver la corrélation avec la maladie. Pour arriver aux fibres et les séparer des autres, on doit *trouver les volumes d'intérêt* : la Substantia Nigra et le Putamen.

Pour trouver ces volumes automatiquement, il faut *trouver dans le volume du cerveau, la position de notre volume d'intérêt* automatiquement - cela peut être plus haut ou plus bas, selon le cas, peut-être plus grand ou plus petit, vers le milieu ou vers les deux cotés - *la variation démographique* imposée par la différence de sexe, race et âge. La différence de sexe détermine des volumes plus petits pour les femmes - la boite crânienne est plus petite ; la différence de race détermine des différences entre la forme de la tête pour les asiatiques, les européens et les africains ; l'âge détermine l'atrophie cérébrale pour les personnes plus âgées et les formations anatomiques peuvent être comprimées ou/et déplacées. Ces problèmes doivent être pris en compte pour avoir un systéme automatique capable de fonctionner sur n'importe quel cas.

Pour déterminer les volumes anatomiques d'intérêt dans chaque image, on doit savoir leur position et faire la différence entre le volume recherché et les tissues qui l'entoure. Vu qu'on fait une évaluation sur chaque coté, on doit savoir *la limite entre les hémisphères* et déterminer la position des volumes par rapport á cet hémisphère. Pour valider les volumes, on définit *des seuils minimum et maximum pour le volume*, la distance par rapport aux hémisphères et par rapport aux limites extérieures, ainsi que la position des volumes par rapport á la position du cerveau dans l'image.

Une fois les volumes déterminés, on applique l'algorithme de génération des fibres de [Le Bihan 2001], mais pour les valider, elle doivent passer au même temps par les deux volumes d'intérêt de chaque hémisphère. On a des seuils pour la longeur des fibres et leur angulation.

Dans la partie détection et traitement des images, on *défini des métriques* spécifiques pour éliminer les facteurs démographiques et suivre la variation de la corrélation entre la maladie et ces fibres motrices. Les métriques déterminent les données pour *la partie analyse* du système qui génère la valeur de la fonction de pronostic. Cette partie doit trouver la fonction de

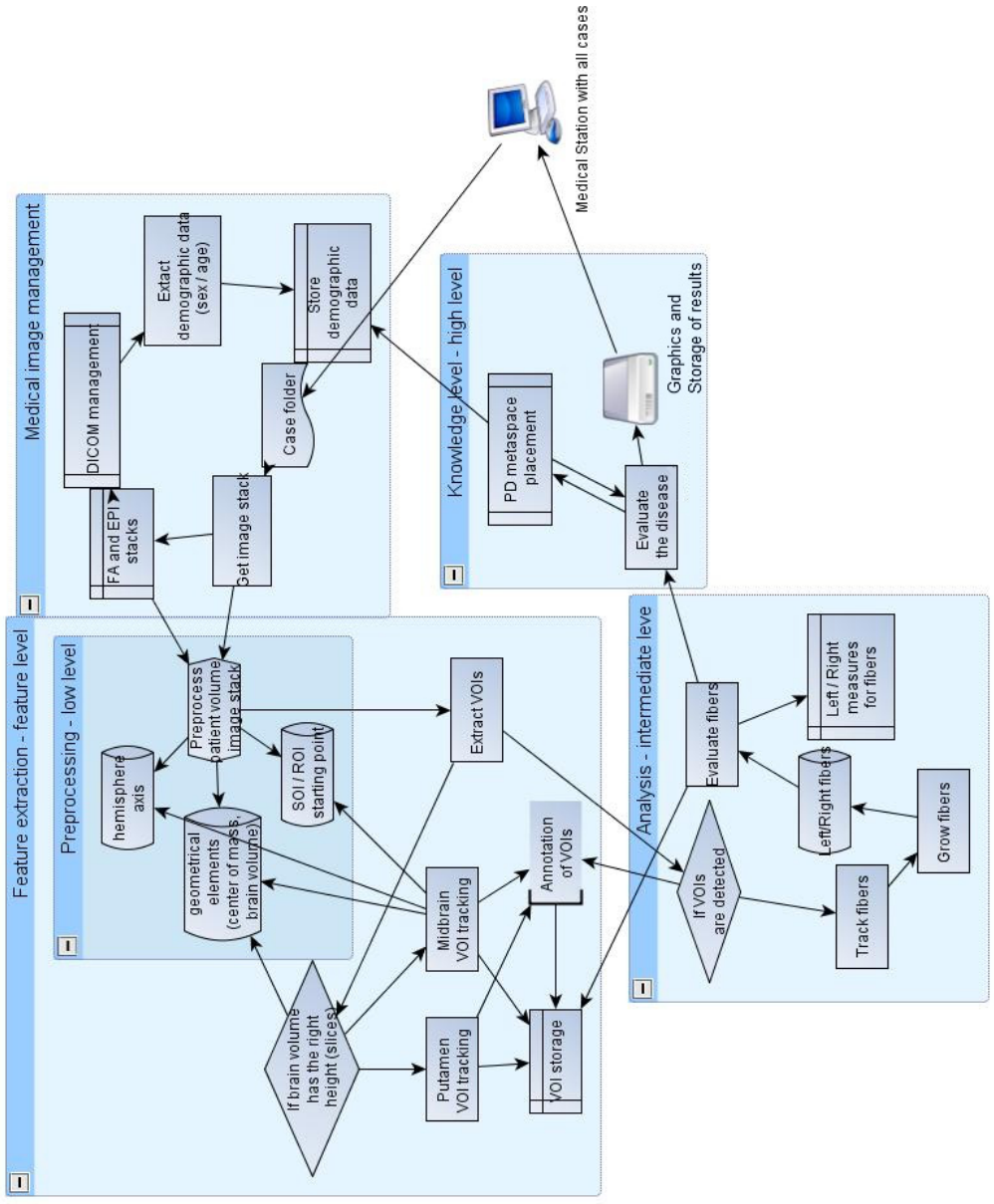

FIGURE 1.1 – PDFibAtl@s processus

variation des fibres correspondant aux différents niveaux de la maladie. Á ce point, nous nous retrouvons devant deux défis : fair *la différence entre les cas malades et les cas sains* et *trouver la gravité de la maladie* pour les cas atteints de la maladie de Parkinson.
Les résultats sont déterminés par la qualité des images et de leurs caractéristiques, ce qui constituent l'objet de la partie traitement et extraction des volumes d'intérêt.

1.2 Caractéristiques et utilisation des images DTI

Notre base de données contient, pour chaque patient, des volumes d'images basées sur l'IRM (Imagerie de Résonance Magnétique) , des images de diffusion(DTI), spécifiques pour l'étude de ce type de maladie. Nous disposons de 68 patients qui ont été identifiés et diagnostiqués par notre neurologue avec la maladie de Parkinson, et de 75 cas de contrôle. Ces patients ont donné leur accord pour participer a cette étude et ont été examinés pour prélever des images de type DTI (TR/TE 4300/90 ; 12 directions ; 4 moyennes ; 4/0 mm sections ; 1.2 x 1.2 mm résolution en-plane), des T_1, des T_2 et des images écoplanaires (EPI).

Nous n'utilisons pas les T_1 ou T_2, vu que ce genre d'images, même si possèdant une trés bonne résolution, ne contiennent pas les tenseurs pour déterminer les fibres neuronales. Cette propriété est spécifique seulement aux images EPI, qui contiennent les 12 directions de diffusion. Nous disposons de 351 images pour chaque cas, avec les directions de diffusion et les images sans diffusion, des images de 4 mm - tranches axiales (slices). Nous avons 27 tranches pour chaque patient, pour obtenir un volume sur une seule direction de diffusion. Les tranches axiale sont prélevées en Commissure Antérieure/ Commissure Postérieure (plain AC/PC).

Nos images sont acquises en utilisant un scanner Siemens Avanto 1.5T (B=800). Les images sont prélevées en format DICOM, chaque fichier contient une image et un fichier header attaché, qui contient le protocole d'acquisition et des donnés du patient. Avant d'utiliser les images et de préparer les volumes, on extrait les donnés sur le patient et sur chaque image - le niveau dans le volume, la direction de diffusion et le type de DTI.

Nous utilisons les images *EPI* parce qu'elles contiennent les tenseurs et nous offrent la possibilité de reconstruire les fibres neuronales. Avant l'utilisation directe de ces images, on a besoin d'éliminer le bruit et d'augmenter la clarté des détails anatomiques.

Dans ce sens, nous effectuons une augmentation du contraste de 0.5%, en utilisant le filtre de imageJ[1] et on élimine le crâne pour une meilleure segmentation du tissu cérébral. Les images d'*d'anisotropie fractionnaire (FA)* obtenues directement du scanner, contiennent l'information du niveau de la diffusion et de la dopamine. Ce type d'image permet une segmentation précise grâce á la diffusion pour le Putamen, meilleure que celle des images T_1 ou T_2, dont la résolution est par contre supérieure.

[1]imageJ : `http://rsbweb.nih.gov/ij/` -accède en May 2010

1.3 Nouveaux Algorithmes pour la préparation des images

Pour manipuler les images on a différents niveaux de définition des algorithmes dans le traitement des images : au niveau de la préparation des images, pour la segmentation et pour l'élimination les artefacts. Pour préparer les images, on doit éliminer les bruits, le crâne et déterminer des éléments géométriques marqueurs. On considère toutes les opérations éffectuées sur les images avant la segmentation comme des algorithmes de préparation de l'image.

Nous avons testé des systèmes concurrents sur les images de notre base de données, afin d'avoir une quantification des capabilities de nôtre méthodes, en comparaison avec les autres (voir chapitre 2.5.1). On évalue la possibilité de segmentation des tissus en matière blanche, grise et liquide intracrânien avec SPM[2] et le VBM[3]). Le SPM est un système dédié aux images DTI, intégré a Matlab - VBM. Ce système accomplit la tâche de segmentation des tissus cérébraux alignés entre les tranches axiales. Ceci étant, le système n'est pas automatique et il est sensible aux éléements d'influence démographique. La segmentation est grossière et basée sur l'atlas Talirarchi [Guillaume 2008] [Gaser 2008] qui propose des versions spécifiques pour chaque race - on a utilise celle pour l'Asie de l'Est (origine de la base d'images utilisée).

Pour voir la qualité des images et la possibilité de segmentation des regions d'intérét nous testons d'abord le 3D Slicer[4] et le DTI tracker de MedINRIA[5]. Les deux systèmes offrent la possibilité de délimiter la région d'intérêt dans les tissus pour la segmentation et l'alignement automatique avec des techniques de recalage. Le 3D Slicer n'est pas capable d'accomplir le recalage ou la segmentation en utilisant des moyens de calculs ordinaires. Avec la méthode automatique de recalage, "diffeomorphic demons" du module Image Fusion (MedINRIA), les contours anatomiques ne sont pas exacts. On teste avec le même module, la méthode automatique : "automatic affine registration". Cet module de MedINRIA permet d'effectuer le recalage, mais seulement une méthode manuelle offre un résultat acceptable. Par ailleurs, la segmentation offre comme résultat, des fichiers spécifiques á ce système, mais il ne permet pas limiter les fibres en utilisant deux volumes d'intérêt (tractographie globale).

Pour la tractographie, on peut aborder une méthode déterministe ou probabiliste. La première méthode utilise la géométrie des donnes de la diffusion et l'autre est basée sur les statistiques des mêmes donnes. La méthode locale de tractographie utilise une source pour les fibres, pendant que celle globale prend en considération la source et la destination des fibres. Le module DTI tracker (MedINRIA) utilise une méthode locale déterministe, mais dans ce cas, on n'est pas capables de séléctionner uniquement les fibres motrices. Une méthode probabiliste globale intégrée dans le module Diffusion Toolkit (TrackVis[6]) offre le résultat le plus proche de nos besoins.

A ce point, après avoir testé ces systèmes existants, nous sommes en mesure d'identifier les problèmes majeurs que notre système doit être capable de surmonter.

---

[2]Statistical Parameter Mapping (SPM) `http://www.fil.ion.ucl.ac.uk/spm/` -accède en May 2010

[3]Voxel Based Morphometry (VBM) `http://en.wikipedia.org/wiki/Voxel-based_morphometry` - accède May 2010

[4]Slicer - `http://www.slicer.org/`- accède en May 2010

[5]MedINRIA - `http://www-sop.inria.fr/asclepios/software/MedINRIA/`- accède en May 2010

[6]TrackVis - `http://www.trackvis.org/`- accède en Juillet 2010

- Initialisation des images
  - éliminer les bruits
  - éliminer la calotte crânienne
  - détéction des hémispheres
  - récupérer les éléments volumétriques
- Identification des volumes d'intérêt
  - identification de la tranche d'intérêt
  - détection de la région anatomique
- Segmentation automatique
- Recalage géométrique intra-patient
- Tractographie déterministe globale
- Diagnostic et Pronostic

Les deux premiers problèmes sont résolus en utilisant la classification de l'intensité des voxels avec KMeans[7]. De cette manière, nous sommes capables de déterminer le tissue crânien et d'éliminer ce tissu avec tous les artefacts en dehors du périmètre de la tête. On élimine ainsi tous les éléments de l'image autour de la tête, c'est á dire, les bruits entourant l'image.

Pour la détection des hemisphères, on utilise l'image sans la calotte crânienne. Afin d'identifier le contour du cerveau, on détermine le point de séparation entre les deux hémisphères. En utilisant ce point et le centre de gravité, on est capables de définir l'axe central entre les hémisphères (voir la figure 1.2). On fait les mesures des éléments volumétriques en utilisant ImageJ (object counter[8]). Le centre de masse de l'image avec le point d'inflexion, détérmine la limite entre les deux hémisphères ; le centre de gravité du cerveau est utilisé par la suite pour déterminer la tranche d'intérêt dans la segmentation des volumes d'intérêt.

1.4 Algorithmes de segmentation des images DTI

Pour la segmentation des volumes, á cause de la variabilité inter-patient, nous devons définir des algorithmes spécifiques pour chaque region anatomique et pour les deux hemispheres. On détecte les volumes d'intérêt en choisissant chaque fois dans le volume de cerveau, la tranche d'intérét. Dans cette image, on détermine la position du volume d'intérét pour la détection intuitive automatique. La segmentation commence une fois que la tranche axiale où les algorithmes de détection des volumes doivent s'appliquer a été détectée.

1.4.1 Position de la tranche d'intérêt

[7] KMeans en ImageJ : `http://ij-plugins.sourceforge.net/plugins/clustering/index.html` accède en Juin 2010

[8] ImageJ plug-in Object Counter : `http://rsbweb.nih.gov/ij/plugins/track/objects.html` -accède en Juin 2010

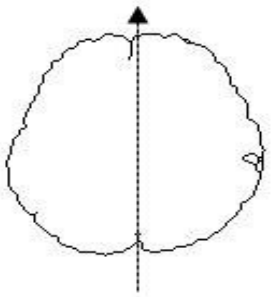

FIGURE 1.2 – Contour du cerveau induisant la variabilité et le positionnement du sinus occipital

La position du mésencéphale dans le volume du cerveau relatif au centre de masse est approximativement 4-8 mm plus haut, c'est à dire 1-2 tranches au dessus de la tranche contenant le centre de masse. Pour déterminer cette position, nous prenons en compte le volume du cerveau pour chaque patient. Le fait qu'on ait des volumes qui contiennent 80-90% du cerveau d'un patient ou 50-60% pour un autre, fait partie de la variabilité inter-patients que nous devons dépasser. Le rapport entre l'aire de la première tranche et celle en contenant le centre de masse, nous permet d'évaluer le volume du cerveau pour chaque patient (équation 1.1). En prenant en compte ce rapport, on divise en quatre categories les patients, selon le volume contenu dans les tranches prélevées (voir 4.2.1).

$$P_{slice} = \frac{Vol_{Zslice}}{Vol_{Fslice}} * \frac{100}{ST} \tag{1.1}$$

ou Vol_{Zslice} et Vol_{Fslice} représente les volumes de cerveau contenu dans la tranche avec le centre de masse et respectivement la première de l'ensemble utile correspondant au patient ; ST représente l'épaisseur de la tranche (4 mm). La valeur calculée nous offre une des quatre catégories de la position de la tranche d'intérét relative au centre de masse.

- tranche $+0$ si $P_{slice}<60$
- tranche $+1$ si $60<P_{slice}<70$
- tranche $+2$ si $70<P_{slice}<85$
- tranche $+3$ si $85<P_{slice}<100$

Les valeurs choisies pour classifier le pourcentage du volume du cerveau sont établîtes en utilisant les études statistiques regardant la position relative du mésencéphale par rapport au centre de masse. La position du Putamen est avec 8 mm plus haute que celle du volume du mésencéphale.

1.4.2 Detection automatique du mésencéphale

Cette région anatomique est située au milieu du cerveau et l'axe qui limite les hémisphères doit passer et diviser cette région. C'est pour cette raison qu'on détermine le centre de gravité de la tranche d'intérét et en suivant la direction de l'axe de symétrie une fois le tissue différèrent de celui du Corpus Callosum trouvée dans cette direction, on a trouvée le mésencéphale. L'axe sépare la partie gauche et droite du mésencéphale (figure 1.3).

On prend les images des tranches d'EPI B0 qu'on classifie en utilisant les cartes des tissues obtenu avec KMeans[9]. Cet classificateur est utilisée pour déterminer quatre types de

[9]KMeans in imageJ : `http://ij-plugins.sourceforge.net/plugins/clustering/index.html`- accède en Juin 2010

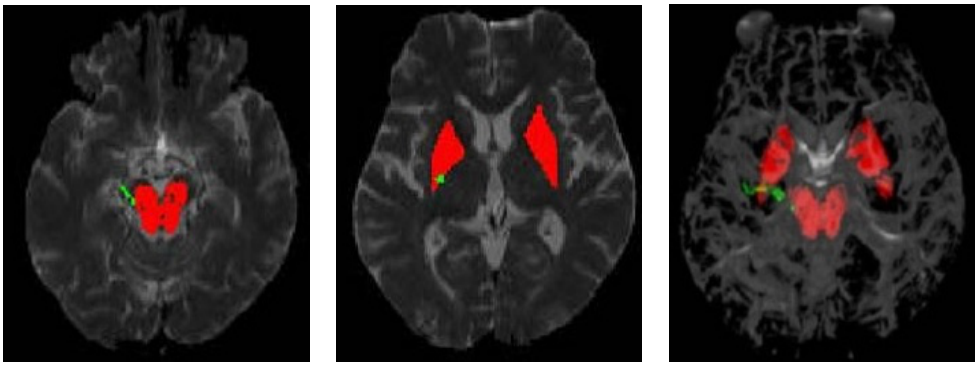

(a) EPI avec le mésencéphale détectée et les fibres

(b) EPI avec le Putamen détectée et les fibres

(c) Image 3D des fibers détectées en passant par les VOIs

FIGURE 1.3 – EPI avec les volumes d'intérét (VOIs) détectées dans 1.3(a), 1.3(b) et 1.3(c) avec les fibres 3D sur un example

tissus dans les images EPI : matière blanche, matière grise, liquide intracrânien et bruit. Sur ces images, on identifie la région du mésencéphale- matière grise- et le repérage des voxels appartenant a cette région. Tous les voxels qui appartiennent á la méme classe du tissue comme celle de la région sur l'axe de symétrie, á coté du centre de gravité, sont considérés partie du mésencéphale (voir chapitre 4 de la thèse).

On élimine les bruits dans la détection du mésencéphale en utilisant des seuils. Les voxels valides comme volume d'intérêt sur les deux tranches qui constituent le mésencéphale sont transformés dans une image masque. Ce masque est utilisé pour sélectionner le volume d'intérêt dans le processus de génération des fibres. La détection de cette région est réalisée sur les images EPI, mais pour le Putamen, les marges ne sont pas claires, méme dans les images de haute résolution. On peut donc utiliser seulement les FA pour ce but, puisque ce type d'image est la seule qui contient le flux de dopamine qui entoure le Putamen et rend visible le contour.

1.4.3 Detection automatique de Putamen

Les images FA sont traitées comme les images EPI, en appliquant le classificateur de KMeans sur quatre catégories de tissus. Cette fois, dans les images FA, on ne traite pas le tissu, mais le flux de dopamine. Pour ce type d'image, les quatre classes représentent les couleurs (RGB), qui codifient les directions de diffusion, et le bruit.

Sur la carte des classes de l'image FA, on considère de nouveau la limite entre les deux hémisphères. Le centre de masse du cerveau et la limite supérieure du cerveau représentent les limitations imposées a cette détection. On classifie les images selon la position du cerveau, en trois catégories : centrée, en haut et en bas de l'image. Dans cet objectif, on utilise la position du centre de masse dans l'image. En fonction de ces repères on obtient des algorithmes qui, en passant par deux régions (classes des voxels) différentes, arrivent á la troisième dans l'image de la carte.

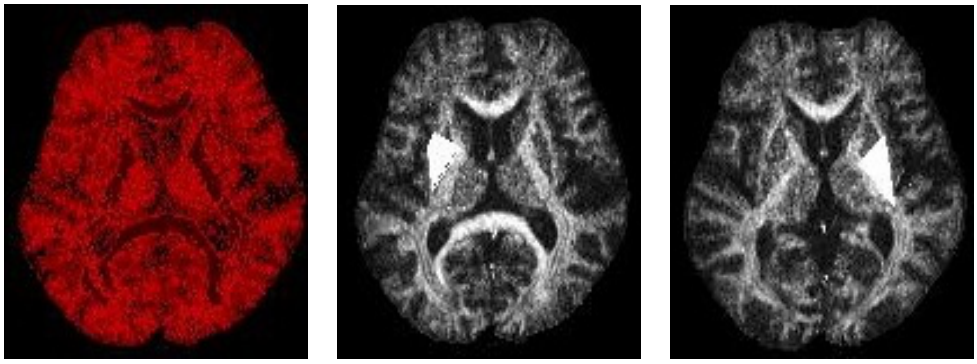

(a) Classification du tissue sur une image de FA (b) Putamen détecté sur la partie gauche (c) Putamen détecté sur la partie droite

FIGURE 1.4 – Detection de Putamen supposé sur des images FA [Sabau 2010]

Le fait que cette région anatomique ait la forme géométrique comparable avec un triangle, nous permet d'utiliser un algorithme intuitif, initialisé comme trois points mobiles sur une surface compacte. On translate ces points jusqu'á ce que le limites de cette surface sont atteintes. Dans les tranches plus hautes, le Putamen a la forme d'un quadrilatère et on initialise l'algorithme avec quatre points mobiles. Les voxels valides sont ceux qui ont la même intensité que ceux initialisées. La condition d'arrêt est obtenue quand une région plus grande qu'un nombre minime de voxels différents, n'appartenant pas á la même classe que notre région, sont détectées - pour pas prendre en compte les bruits (des " trous ") - figure 1.4. Les masques de ces volumes des deux cotés du cerveau doivent étre appliqués sur les images EPI, et pas sur celles oú ils ont été détectés. Pour cette raison, on a besoin d'un recalage entre les images EPI et les images FA.

1.4.4 Recalage

Pour un alignement correct entre la pile d'images EPI et FA, les méthodes basées sur l'intensité des voxels ne donnent pas un bon résultat à cause de la dispersion de la masse cérébrale. Notre approche utilise des éléments géométriques automatiquement détectés :

- le centre de masse
- les limites extérieures du cerveau
- l'axe de limitation entre les hémisphères

Ces éléments détectés déterminent les coefficients pour la translation, la rotation et les obliques. La différence entre le centre de masse dans les deux piles d'images, nous donne les valeurs pour la translation : d_x, d_y et d_z, ainsi que l'angulation entre l'axe de limitation des hémisphères et les axes de l'image. On détermine la direction de cet axe pour pivoter les

images en plan vertical ou horizontal.

$$\begin{bmatrix} x^{'} & y^{'} & z^{'} & 1 \end{bmatrix} = \begin{bmatrix} cos\theta_x & sin\theta_x & 0 & d_x \\ -sin\theta_y & cos\theta_y & 0 & d_y \\ 0 & 0 & 1 & d_z \\ 0 & 0 & 0 & 1 \end{bmatrix} \begin{bmatrix} x \\ y \\ z \\ 1 \end{bmatrix} \tag{1.2}$$

Les transformations effectuées sont contenues dans la matrice 1.1. Ces transformations sont appliquées sur la pile contenant le Putamen, extraite de l'image FA. Nous obtenons la valeur de θ_x qui représente l'angle entre l'axe des hémisphères et l'axe O_x de l'image ; le θ_y est l'angle entre le même axe et O_y dans l'image. La différence entre ces angles déterminées sur

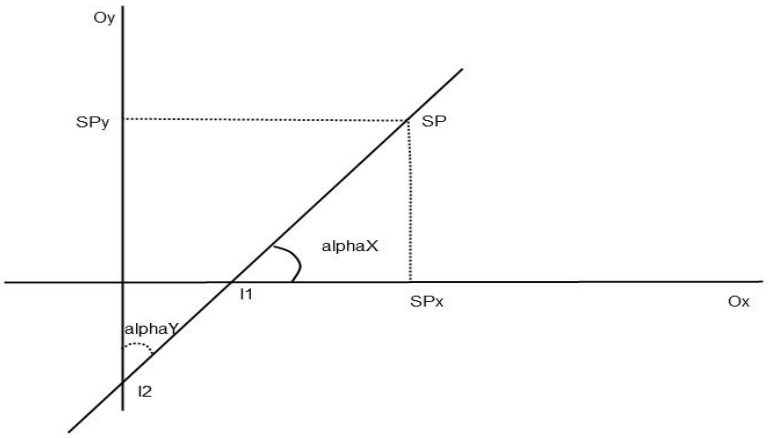

FIGURE 1.5 – Determination géométrique des coefficients du recalage

l'image FA et l'image EPI nous donne l'angulation pour la transformation de la pile avec la masque du Putamen. Cet angulation est déterminée en utilisant les équations 1.3 et 1.4 avec les projections sur les axes de l'image du point situé á la base de la partie occipitale de la boite crânienne, qui correspond au sinus occipital. Ce point est déterminé sur le contour du cerveau par un point d'extremum qui délimite les deux hémisphères. Les angulations pour les images FA et EPI sont nomées respectivement α et β. Leur différence nous donne la valeur pour θ.

$$sin\alpha_x = \frac{SP_y}{I_1SP} \tag{1.3}$$

$$sin\alpha_y = \frac{SP_x}{I_2SP} \tag{1.4}$$

Comme on extrait l'information sur le Putamen de l'image FA, qui représente le niveau de l'anisotropie dans le tissu, et cette information est utilisée dans l'image EPI pour générer les fibres, on obtient ainsi une fusion de caractéristiques provenant de modalités différentes.

1.4.5 Détection des fibres

Les caractéristiques des images d'EPI contiennent les tenseurs, qui représentent la direction de diffusion dans l'angulation au niveau de chaque voxel. La valeur de l'angulation est contenue dans les tenseurs et c'est par cette information que nous pilotons la direction de génération des fibres. On utilise les algorithmes de Bihan [Le Bihan 2001] et Basser [Basser 2000] comme méthode de détection et on impose les limitations utilisées en général pour ce type d'algorithmes : *l'angulation* des fibres doit étre plus grande que 60 degrés et la valeur de *l'anisotropie* doit étre plus grande que 0.1. Cette approche est une méthode déterministe, qui commence la croissance des fibres seulement du mésencéphale. On valide seulement les fibres qui passent/arrivent dans la région détectée du volume du Putamen. La source des fibres est le le volume du mésencéphale et leur destination est représentée par le volume du Putamen. Cette façon de détecter les fibres est spécifique, étant liée á l'approche globale de détection.

La diffusion est calculée dans toutes les directions des gradients. Les tenseurs contiennent les trois directions qui génèrent les vecteurs propres et les valeurs propres [Rorden 2008] [Curran 2005]. L'anisotropie se calcule en utilisant les tenseurs augmentent les valeurs du le flux neuronal passant par les axones. Le degré d'anisotropie pour chaque voxel est calculé en utilisant la diffusivité des tenseurs fournissant la direction de diffusion. La trace des fibres est déterminée en calculant la direction principale de la diffusivité avec la méthode de Gear [Basser 2000] qui représente la diffusion comme des ellipses en 3D [Le Bihan 2001].

Les fibres détectées en utilisant cette technique sont évaluées en utilisant notre propre métrique. Pour éliminer la variation du volume cérébral entre les patients, due a l'atrophie cérébrale ou a la différence de sexe, on utilise un rapport entre le nombre de fibres et le volume du cerveau ou celui du mésencéphale.

$$FD = \frac{F_{Nr}}{Vol_{Brain}};\ FD_{rel} = \frac{F_{Nr}}{Vol_{VOI}} \tag{1.5}$$

ou la valeur de FD représente la densité des fibres calculée en utilisant le numéro des fibres - F_{Nr} - détectées dans le volume de cerveau - Vol_{Brain} et la valeur de FD_{rel} représentant la densité des fibres relative au volume d'intérêt - Vol_{VOI}.

Le volume des fibres computée est présenté dans l'équation 1.6.

$$FV = F_{Nr} * V_{height} * V_{width} * V_{depth} * F_{leng} \tag{1.6}$$

ou la valeur de FV représente le volume des fibres calculé comme un produit entre le nombre de fibres (F_{Nr}), leur longeur (F_{leng}) et les dimensions des voxels $V_{width}, V_{height}, V_{depth}$.

Ces valeur extraites au niveau des fibres sont analysées dans le module de diagnostic et de pronostic médical.

1.5 Analyse des caractéristiques des images. Diagnostic et Prognostic médicale

Á ce point, dans notre système, on prend les valeurs des fibres et en utilisant des algorithmes d'intelligence artificielle, on trouve une corrélation entre la maladie et les valeurs obtenues avec

nos métriques pour les fibres. Deux requétes sont utilis'ees pour l'analyse de ces données : la diagnostic et le prognostic. Pour le diagnostic, on doit faire la différence entre les cas sains et les cas affectées par la maladie. Le prognostic évalue la gravite de la maladie en utilisant les valeurs des fibres. Le modèle architectural utilisé pour le diagnostic et le pronostic comporte cinq étapes :

- Donnes d'entrée - les valeurs extraites des fibres
- Les règles floues et leur poids
- Définition des poids
- Le calcul des paramètres de conséquence - déterminés en utilisant les poids et les fonctions de variation
- La sortie - la décision qui donne la valeur finale

Les deux premières étapes nous fournissent les valeurs pour le diagnostic. Dans notre cas, les poids représentent le degré des polynômes de Lagrange définis dans la quatrième étape. Cette définition des polynômes et les modalités de décision finale représentent une approche hybride correspondant á un système de type ANFIS.

Le diagnostic dans notre système est déterminé en utilisant une approche bassée sur des règles. On défini des classes de valeurs en considérant un groupe de test et basée sur ces classes, on défini les règles dans 1.7. Ces règles prennent en compte la densité des fibres - HY_{FD}- et le volume de mésencéphale - $HY_{VOI_{Vol}}$. En évaluant le seuil avec ces règles, on peut placer le cas dans une des catégories sain (HY=0) ou malade (HY=2 ou HY=3).

$$
\begin{aligned}
&If(HY_{FD} = HY_{VOI_{Vol}} \wedge HY_{FD} \neq -1)\, then\, HY = HY_{FD}\\
&If(HY_{FD} = -1 \wedge HY_{VOI_{Vol}} \neq -1)\, then\, HY = HY_{VOI_{Vol}}\\
&If(HY_{FD} \neq -1 \wedge HY_{VOI_{Vol}} = -1)\, then\, HY = HY_{FD}\\
&If(HY_{FD} \neq -1 \wedge HY_{VOI_{Vol}} \neq -1) \wedge (HY_{FD} \neq HY_{VOI_{Vol}}))\, then\\
&\quad If(FD_{3D} \neq 0)\, then\, HY = 2\\
&\quad else\, HY = 0\\
&If(HY_{FD} = -1 \wedge HY_{VOI_{Vol}} = -1) then\ The\ image\ is\ invalid!
\end{aligned}
\tag{1.7}
$$

On a encore besoin de la fonction dévaluation de la maladie, puisque dans les cas oú on dispose de malades de deuxième et troisième dégré sur l'échelle H&Y. Ceci est le résultat du fait que la diagnostic courant n'est pas encore capable d'effectuer le diagnostic pour les patients de premier dégré. Pour le quatrième et le cinquième dégré, c'est difficile de prélever des images valides.

La fonction de **pronostic** utilise les valeurs de la densité des fibres dans la partie gauche, comme la dégénération est plus prononcée de cet coté. On place ces valeurs dans l'espace de l'échelle H&Y et en utilisant l'interpolation entre ces points, on détermine une fonction de variation (méthode d'inférence TSK). Vu que les points sont très dispersés, on essaye de construire des fonctions pour les intervalles des valeurs. Ces intervalles prennent en compte sois trois, sois cinq points (dans un objectif d'utilisation clinique courante de cette méthode,

nous avons préféré nous limiter á cinq points, pour des raisons de simplicité d'utilisation. Par ailleurs, un grade supérieur nous éloigne trop de la variation réelle de la diffusion.

$$L(x) = \sum_{i=0}^{n} y_i * \prod_{j=0, j\neq i}^{n} \frac{x - x_j}{x_i - x_j} \tag{1.8}$$

Pour cette estimation, nous considérons des fonctions polynomiales composées de polynômes de Lagrange (équation 1.8). Les coefficients pour le cas ou on considère un polynôme de deuxième degré (trois points), sont donnés par : 1.9.

$$\begin{aligned} C_2 &= \tfrac{y_1}{(x_1-x_2)(x_1-x_3)} + \tfrac{y_2}{(x_2-x_1)(x_2-x_3)} + \tfrac{y_3}{(x_3-x_1)(x_3-x_2)} \\ C_1 &= -(y_1 \tfrac{x_2+x_3}{(x_1-x_2)(x_1-x_3)} + y_2 \tfrac{x_1+x_3}{(x_2-x_1)(x_2-x_3)} + y_3 \tfrac{x_1+x_2}{(x_3-x_1)(x_3-x_2)}) \\ C_0 &= y_1 \tfrac{x_2 x_3}{(x_1-x_2)(x_1-x_3)} + y_2 \tfrac{x_1 x_3}{(x_2-x_1)(x_2-x_3)} + y_3 \tfrac{x_1 x_2}{(x_3-x_1)(x_3-x_2)} \end{aligned} \tag{1.9}$$

Pour le cas d'un polynôme de quatrième degré (cinq points), on obtient les coefficients suivants :

$$\begin{aligned} C_4 &= \sum_{i=0}^{4} y_i \prod_{j=0, j\neq i}^{4} \tfrac{1}{x_i - x_j} \\ C_3 &= \sum_{i=0}^{4} y_i \left(\frac{\sum_{j=0, j\neq i}^{4} -x_j}{\prod_{k=0, k\neq i}^{4} (x_i - x_k)}\right) \\ C_2 &= \sum_{i=0}^{4} y_i \left(\frac{\sum_{j=0, j\neq i}^{4} x_i x_j}{\prod_{k=0, k\neq i}^{4} (x_i - x_k)}\right) \\ C_1 &= \sum_{i=0}^{4} y_i \left(-\frac{\sum_{j=0, j\neq i}^{4} x_i \left(\sum_{m=0, m\neq j}^{4} x_m * \sum_{n=m+1}^{4} x_n\right)}{\prod_{k=0, k\neq i}^{4} (x_i - x_k)}\right) \\ C_0 &= \sum_{i=0}^{4} y_i \left(\frac{\prod_{j=0, j\neq i}^{4} x_j}{\prod_{k=1, k\neq i}^{4} (x_i - x_k)}\right) \end{aligned} \tag{1.10}$$

Une méthode d'évaluer des nouveaux patients et de leur associer un pronostic est celle appelée Independent Adaptive Polynomial Evaluation (IAPE). Cette méthode évalue un nouveau cas en utilisant des polynômes de différèrent dégré pour arriver á un résultat plus exact. On place dans l'espace H&Y une nouvelle valeur(X) de la densité des fibres et on trouve les deux plus proches valeurs entourant la nouvelle valeur(X_m et X_M) - figure 1.6. Si la valeur de la fonction obtenue en prenant en compte les densités plus basses pour le nouveau point (L_{F1}) est égale avec celle obtenue pour les points plus grands (L_{F2}) ou avec la fonction centrée sur la nouvelle densité(L_{F3}), cela détermine le niveau H&Y pour la nouvelle densité (HY1). Le

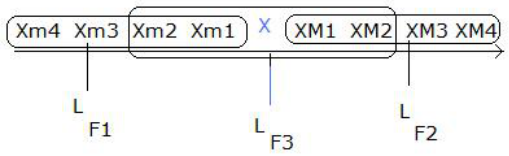

FIGURE 1.6 – Independent Adaptive Polynomial Evaluation (IAPE)

nombre de points voisins pris en compte, donne le dégrée polynomial des fonctions utilisées pour le calcul. On prend en compte au début quatre points et on obtient les polynômes Lagrange de troisième dégré. Si aucune fonction ne donne une valeur égale avec une des autres deux fonctions, on passe au calcul des valeurs des polynômes de deuxième dégré. Á la limite, les fonctions linéaires donnent des valeurs égales. Une autre estimation est calculée avec la fonction obtenue en prenant les deux points voisins : X_m et X_M. Cette fonction estimée pour la nouvelle densité, donne la valeur de HY2. Les deux estimations obtenues, HY1 et HY2 sont comparées par la suite. Si la différence est plus grande que trois niveaux sur l'échelle H&Y, on fait la moyenne pour obtenir la valeur finale de H&Y pour le nouveau cas. Cette manière d'utiliser les polynômes de Lagrange fait partie des fonctions adaptives d'interpolation (Figure 1.7). Comme le modèle a des similitudes avec les réseaux de propagation arrière (back propagation) correspondant á la prise en compte de l'erreur pour améliorer l'inférence. Les polynômes de Lagrange ont la même utilité dans notre système que les fonctions Gaussiennes dans les réseaux RBF (Radial Basis Function). Une variation de cette technique prend en compte seulement les cas de la maladie et élimine les contrôles (PD Adaptive Polynomial Evaluation(PD-APE)). De cette façon, on introduit dans la seconde étape de l'architecture ANFIS, la condition supplémentaire donnée par l'appartenance du cas.

1.6 Analyse des résultats

Au niveau technique, les résultats concernent la détection des volumes d'intérêt en termes de précision comparée avec la détection manuelle ; la sensibilité pour les tissus entourant les zones d'intérêt et de la spécificité. Le niveau technique du module d'analyse nous procure la précision pur la diagnostic et le pourcentage de prédiction. On dispose de 68 patients diagnostiqués avec la maladie de Parkinson et 75 cas de contrôle.

La detection de mésencéphale du au fait que cette région anatomique est très bien délimitée, est plus facile. Pour la détection du Putamen, on effectue la comparaison entre la détection manuelle et celle automatique de notre système. On évalue le ratio d'erreur, en faisant la différence entre les deux détections. Le ratio d'erreur pour la détection basée sur la méthode de triangulation, est de 35% pour la partie gauche et de 45% pour la partie droite. Dans le cas de la détection basée sur la méthode du quadrilatère, on obtient une erreur relative de 46% sur la partie gauche et la même sur la partie droite.

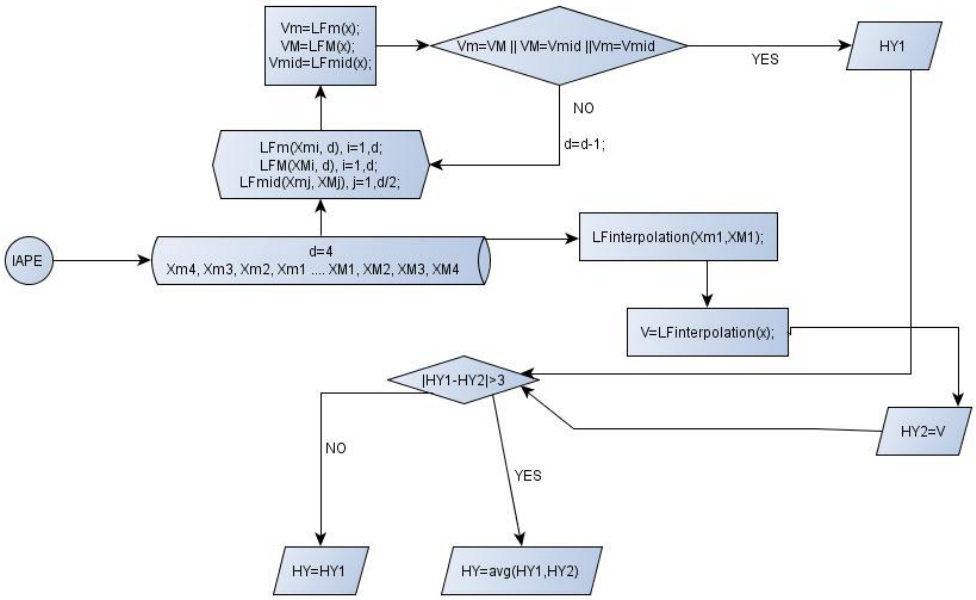

FIGURE 1.7 – La diagramme pour la méthode Independent Adaptive Polynomial Evaluation (IAPE)

En ce qui concerne la détection *des fibres*, pour toutes les cas de notre base de données, les valeurs pour la spécificité sont de 63% et pour la sensibilité de 81%. Pour le niveau de précision, on obtient un 75.5%. On utilise 41 patients (21 contrôles et 20 patients avec la maladie de Parkinson) et on crée les polynômes de Lagrange utilisés pour le diagnostic et le pronostic. On considère ces données comme idéales, du au fait que la segmentation manuelle du Putamen nous offre probablement les meilleurs résultats. On utilise le diagnostic de Dr. Chan comme réalité de terrain pour l'apprentissage. Pour ce groupe de patients, le diagnostic basé sur les règles donne une valeur de précision de 61%, les fonctions d'interpolation de deuxième dégré une précision de 34% et celle de quatrième dégré, de 43%. On introduit dans l'ensemble des patients d'apprentissage, 9 nouveau patients des premiers tests et la précision des algorithmes augmente de 19.2% pour le polynôme de deuxième dégré et de 6% pour l'autre polynôme.

Les fonctions de prédiction nous offrent un ratio de succès de 62.26% pour la méthode IAPE appliquée sur les patients (68 cas de la base de données). Pour le cas de contrôle, on obtient 43.9% pour le polynôme de deuxième dégré. La sensibilité des fonctions est donnée par les patients ayant la maladie (max. 62%) et la spécificité est donnée par les valeurs des cas de contrôle (max. 43.9%). Pour les patients et les contrôles, la méthode PD-APE, qui fait la distinction entre les cas de la maladie et les contrôles, donne une précision de 44.87%.

En utilisant les statistiques, on calcule la courbe ROC du pronostic. Le logiciel de SPSS 17.0 (Statistical Package for the Social Sciences) utilisé pour l'estimation de la méthode

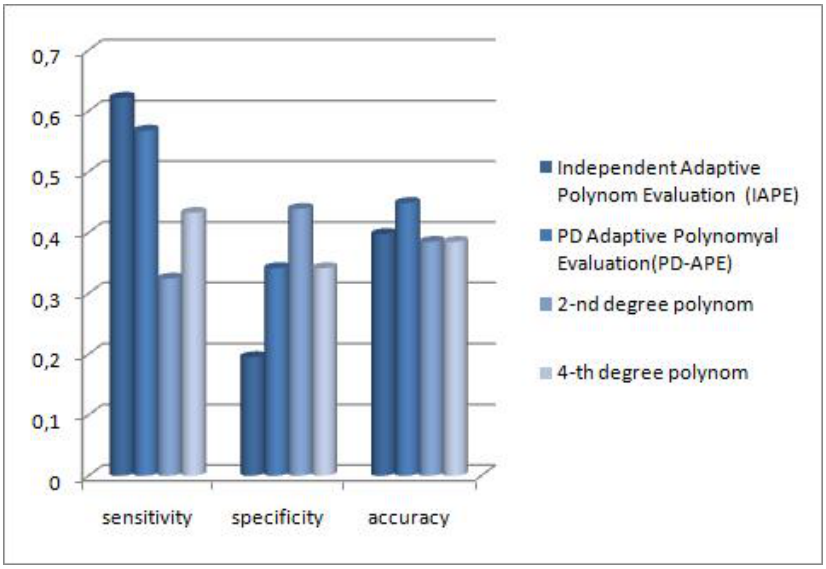

FIGURE 1.8 – Sensibilité et spécificité de polynômes de prediction

IAPE sur les patients, nous donne une valeur de 0.705 pour l'aire située en dessous de la courbe (AUC). Pour la méthode PD-APE, la valeur pour la même aire est de 0.959. Les performances des fonctions de pronostic recommandent la méthode IAPE come la même pour les cas de contrôle et de maladie, avec une valeur pour l'AUC de 0.745 (testées avec le logiciel MedCalc[10]). La variation dans la détection du Putamen affecte les résultats des fibres et le ratio d'erreur est propagé dans le système d'analyse. On peut améliorer le résultat en utilisant un meilleur algorithme de détection des points d'initialisation pour le Putamen.

1.7 Conclusions et perspectives de recherche

En utilisant deux types d'images de DTI, on est capable d'identifier les volumes d'intérêt utilisés pour déterminer les fibres du tract moteur. On effectue toutes ces détéctions automatiquement et les fibres détectées sont analysées par notre module de diagnostic et pronostic qui nous offre la possibilité d'estimer la sévérité de la maladie en générant une valeur sur l'échelle H&Y.

Note prototype qui inclue les méthodes présentées dans ce résumé prend les images en format DICOM et fournit les valeurs pour les fibres et la valeur du pronostic. Cet prototype, PDFibAtl@s, contient des nouveau algorithmes de détéction automatique de la tranche d'intérêt et des éléments géométriques pour le processus d'alignement volumique et pour le recalage. La segmentation du mésencéphale et celle du Putamen représentent une approche globale de

[10]MedCalc 11.3.3.0 - `www.medcalc.be`

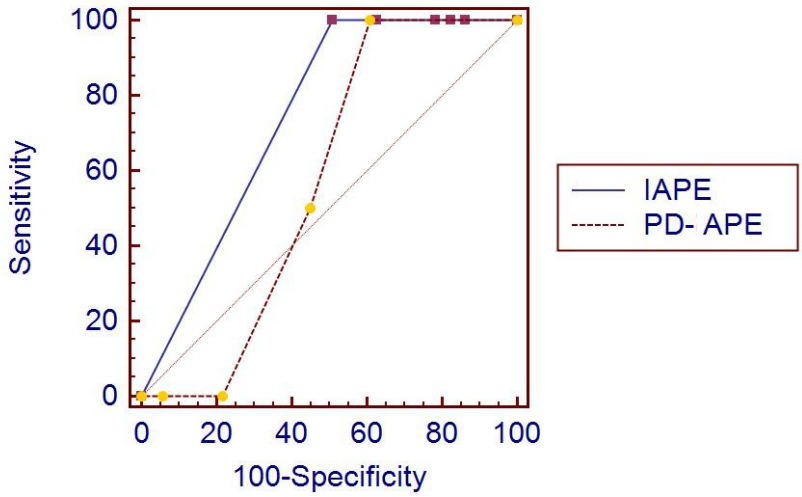

FIGURE 1.9 – Les courbes ROC sur les méthodes IAPE et PD-APE appliquées sur la base de données (143 cas : 68 patients avec PD et 75 contrôles). La difference des performances pour les deux approches est de 0.178 pour l'AUC entre la valeur de 0.745 pour la méthode IAPE et 0.569 pour PD-APE.

génération des fibres. La diffusion est calculée en utilisant une approche déterministe. On introduit des nouvelles mesures pour les fibres afin d'éliminer le facteur démographique de la détéction. Ensemble avec la partie analyse implémentée en utilisant la logique floue et les fonctions polynomiales dans une architecture ANFIS, nous proposons un système complètement automatique basé entièrement sur les informations extraites des images, pour le diagnostic. Le fait que l'information provienne de plusieurs types de DTI constitue la partie de fusion des images au niveau informationnel.

Les résultats peuvent être améliorés au niveau de la détéection du Putamen, menant á une meilleure détection des fibres utilisées pour le diagnostic. Notre système offre une alternative à la détection basée sur les tests cognitifs utilisés par les neurologues pour cette maladie. Notre système offre aussi la possibilité de visualiser les fibres du strationigral et de les évaluer, en utilisant notre mesure quantitative.

On peut améliorer les résultats au niveau de la détéection du Putamen qui va déterminer une meilleure détection des fibres utilisées pour la diagnose. Notre système offre une alternative à la détection basée sur les testes cognitives utilisés par les neurologistes pour cette maladie. Notre système offre aussi la possibilité de visualiser les fibres du strationigral et de les évaluer en utilisant notre mesure quantitative.

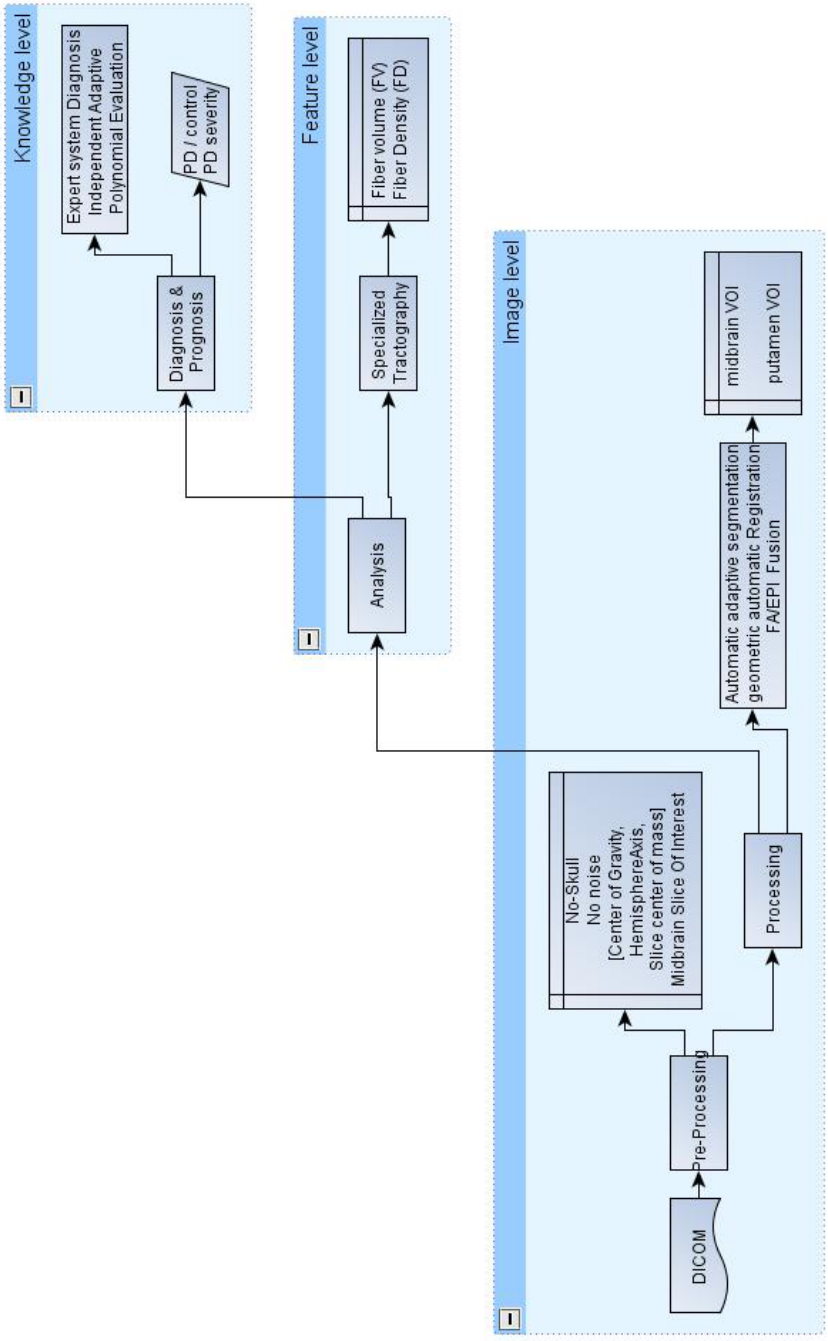

FIGURE 1.10 – PDFibAtl@s : système integrant nos méthodes

Capitolul 2

Prognoza maladiei Parkinson bazat$\breve{a}$ pe fuziunea caracteristicilor extrase din imagini RMN de difuzie

Contents

Introducerea imaginii ca bio-marker în cadrul detecției și al predicției maladiei Parkinson reprezint$\breve{a}$ scopul lucr$\breve{a}$rii de fa$\c{t}\breve{a}$. Demersul complet în acest sens presupune atât studiul metodelor curente de diagnoz$\breve{a}$, al teoremelor privitoare la caracteristici anatomo-fiziologice care sunt legate de maladie, cât și a determin$\breve{a}$rii unei modalități de a utiliza imaginea pentru extragerea caracteristicilor, împreun$\breve{a}$ cu proiectarea și dezvoltarea algoritmilor. Aceast$\breve{a}$

parte presupune proiectarea și dezvoltatea de tehnici capabile să extragă automat caracteristicile specifice de la nivelul imaginii medicale, alături de tehnici de analiză și interpretare a rezultatelor extrase pentru prognoză.

Soluțiile tehnice dezvoltate sunt parte integrantă a unui sistem de diagnoză și prognoză bazat pe imaginile RMN (Rezonanța Magnetică) de difuzie. Utilizând acest tip de imagini oferim o alternativă detecției exclusiv bazate pe teste cognitive, cu ajutorul cărora sunt momentan detectate cazurile de Parkinson și clasificate de către neurologi. Abordarea prezentată în această lucrare se bazează pe analiza și prelucrarea automată a imaginilor medicale, care oferă informații complementare celor cognitive. Metodele propuse se referă la un algoritm complet automat de detecție și segmentare pentru volumele de interes, care după o recalare geometrică oferă posibilitatea de detectie a fibrelor tractului neuromotor. În functie de starea și numărul fibrelor, realizăm un sistem automat de diagnoză evaluând codiția bonavilor dată de prognoză, oferim o valoare estimativa a severitații maladiei.

Dr. Chan [Chan 2007] a realizat un studiu conform căruia cazurile de Parkinson sunt corelate cu diferențe sesizabile în zona din mezencefal numita Substantia Nigra (SN). Această zonă este responsabilă cu producerea dopaminei, unul dintre principalii neurotransmițători. Studii recente au constat că o pierdere a nivelului de dopamină în cazurile de Parkinson. Maladia este detectată doar când dopamina este pierdută în proporție de 80-90% [Today 2009]. Aceasta reprezintă motivația pentru o detecție precoce, bazată nu doar pe elemente cognitive, ci completând aceste elemente cu elemente măsurabile introduse de la nivelul imaginior medicale. Corelând evaluarea maladiei bazată pe imagistică prin plasarea pe scala Hoehn & Yahr (H&Y), aceeași ca și cea folosită în testele cognitive, putem valida și verifica rezultatele. Deoarece Substantia Nigra (SN) nu este usor detectabilă ca zonă de interes, segmentam mezencefalul, deoarece SN este conținuta în acest volum. Cum foarte multe tracturi neuronale pornesc din mezencefal, avem nevoie de un al doilea volum de interes, ca să putem face distincția între fibrele neuromotorii și celelalte care pornind din mezencefal nu fac parte din cel neuromotor. Știind că tractul neuromotor parcurge Putamenul- regiune anatomică cerebrală situată superior în volumul cranian - utilizăm această regiune în procesul de tractografie. Identificând aceasta zonă și limitând fibrele validate la cele care parcurg cele doua volume de interes, determinăm doar fibrele de care avem nevoie.

Deoarece valorile care caracterizează fibrele extrase nu urmează o regulă de dispersie și nu prezintă uniformitate, logica fuzzy este cea care ne permite sa definim seturi de date sub formă de seturi fuzzy. Aceste seturi permit atașarea regulilor pentru diagnoză. Un sistem de inferență fuzzy sau model fuzzy permite o învatare adaptata setului de date, luând în considerare imprecizia sau incertitudinea de la nivelul acestora. Legătura dintre contolerele fuzzy și rețelele neuronale determină un sistem de clasificare Adaptiv Bazat pe Rețele de Inferență Fuzzy (Adaptive Network-Based Fuzzy Inference Systems (ANFIS)). Utilizăm această arhitectură ANFIS pentru diagnoză și prognoză. Utilizând setul de reguli fuzzy suntem capabili să clasificăm fibrele extrase și să le plasăm în seturi, potrivit nivelului de severitate al maladiei pe scala H&Y, așa cum sistemul a fost învățat. Diagnoza face diferența dintre cazurile sănătoase și cele afectate de maladie, pentru nivelele cunoscute și detectabile. Prognoza determină nivelul la care maladia afecteaza cazul analizat, chiar și pentru cazurile precoce. Pentru prognoză, realizăm un sistem de inferență bazat pe modelul Takagi-Surgeno-Kang (TSK). Acest sistem

realizează pre-clasificarea datelor și utilizând polinoame Lagrange realizăm prognoza.

Baza de date utilizată în demersul nostru este pusă la dispoziție de către Singapore General Hospital (SGH) prin intermediul colaboratoarei noastre, Dr. (MD) Ling-Ling CHAN. Același specialist ne-a furnizat pentru baza de date și valorile corespunzătoare severității maladiei pentru fiecare caz pe scala H&Y. Această informație este utilizată ca "ground truth"(valoare de adevăr) în testare si validare.

Rezumatul de față urmărește structura tezei cuprinzând o prezentare generală a metodelor și obiectivele tezei. Structura tezei pe capitole cuprinde în cadrul capitolului 1 al tezei alături de obiective, o prezentare generală a prototipului PDFibAtl@s, care conține noii algoritmi proiectați și dezvoltați. Urmatorul capitol include o prezentare a standardului medical care înglobează imaginile utilizate de sistemul nostru, cu o secțiune pentru imaginile de RMN și specificații ale imaginilor RMN de difuzie. Capitolul 3 din teză conține o prezentare a protocolului specific utilizat pentru achiziția imaginilor din baza noastră de date. De asemenea, în același capitol avem o prezentare a procedurii de preprocecsare a imaginilor pentru eliminarea artefactleor și detecția elementelor geometrice utilizate în continuare. Capitolul 4 conține noile metode care sunt parte a prototipului PDFibAtl@s, sistem care preia imaginile în standard medical DICOM și utlizând implementarea metodelor noastre, este capabil să realizeze prelucrarea imaginilor medicale cu extragerea caracteristicilor. Același sistem conține și modulul de diagnoză și prognoză ale cărui pasi sunt prezentati în capitolul 5. Evaluarea acestor metode și rezultatele obținute sunt prezentate în capitolul 6, iar concluziile și perspectivele științifice, împreună cu impactul metodelor, sunt prezentate în capitolul 7 din teză. Acest rezumat urmează aceeași structură, cu o mai mare detaliere la nivelul metodelor tehnice și nu la nivelul teoretic al demersului științific.

2.1 Prezentarea obiectivelor tezei

Integrarea imaginii ca element definitor pentru a determina severitatea maladiei Parkinson reprezintă scopul principal al lucrării noastre. Pe lângă un studiu al imagisticii medicale, in scopul de a determina în ce măsură premizele teoretice ale utilității acesteia sunt atinse, este nevoie de proiectarea unui sistem care să realizeze practic premizele teoretice. Acest sistem utilizează elemente existente din cadrul procesării imaginlor medicale, dar noi propunem un model unitar și în același timp automat pentru prognoză. Deși obiectivul principal este medical, demersul în sine se bazeaza în totalitate pe imaginile medicale, iar soluțiile dezvoltate reprezintă obiective tehnico-științifice. În acest caz, obiectivele medicale determină dezvoltarea metodelor tehnico-științifice. Este cazul detecției de fibre neuronale, care deși e un obiectiv medical, este atins doar prin procesul de tractografie, pe baza imaginilor de difuzie. Așa cum e prezentat în figura 2.1 metodele din cadrul PDFibAtl@s fac transferul informațional din domeniul imagistic în cadrul celui bazat pe cunoștințe medicale, trecând prin cel al caracteristicilor. Caracteristicile analizate ne oferă posibilitatea de a determina severitatea maladiei. Provocările tehnico-științifice se conturează pe baza celor medicale și sunt plasate pe fiecare nivel informațional al fluxului de date: *creșterea fibrelor* care aparțin în exclusivitate tractului neuromotor și *analiza* lor pentru corelarea fibrelor cu severitatea maladiei. Pentru selecția trac-

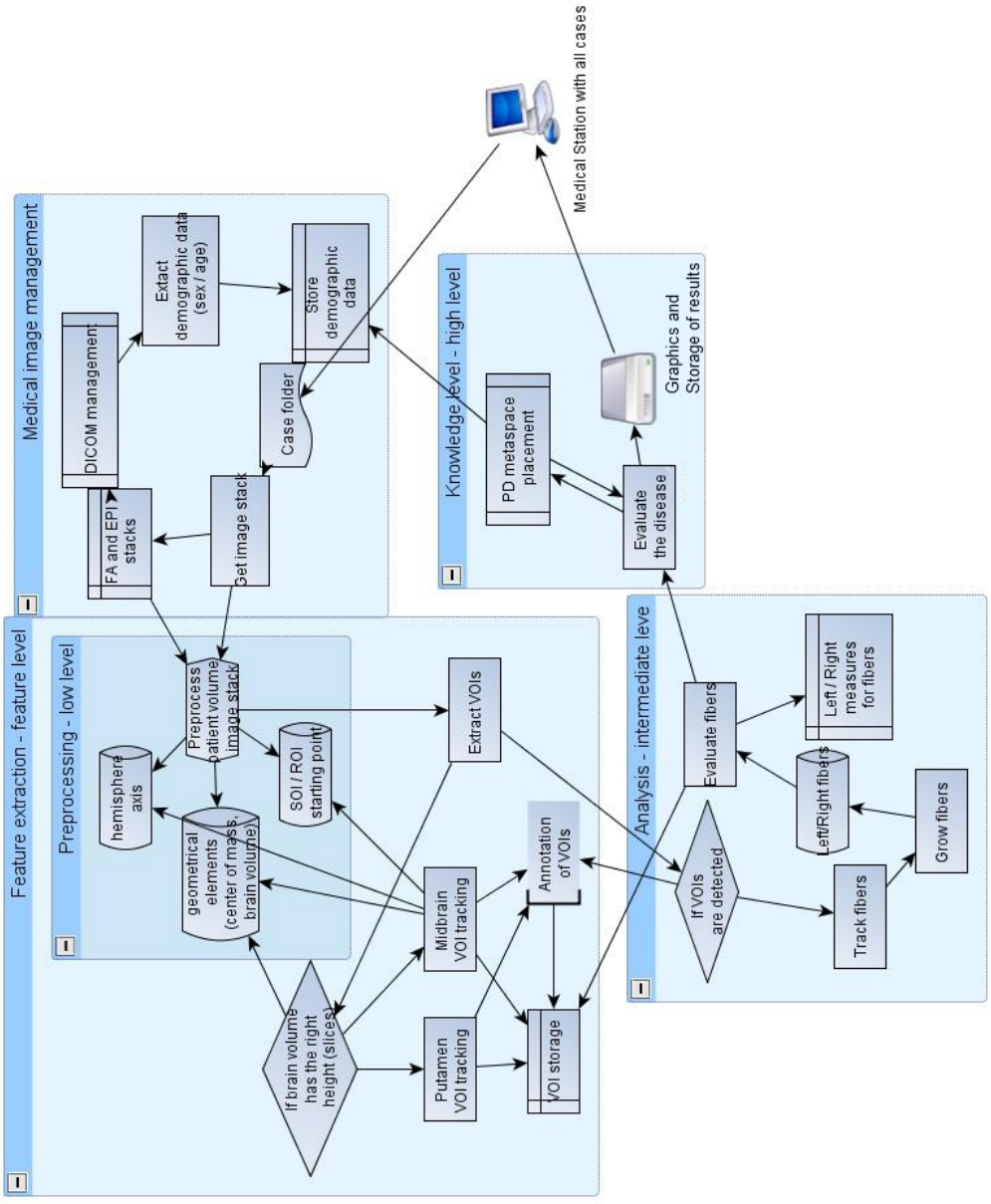

Figura 2.1: Fluxul de date la nivel de PDFibAtl@s

tului neuromotor avem nevoie de două *volume de interes*: Substantia Nigra (SN) si Putamen.

Principala provocare la nivel logistic este realizarea un sistem complet automat care să realizeze nu doar *segmentarea volumelor de interes*, dar și *determinarea plasării algoritmilor* de segmentare în interiorul volumului cerebral. Această *poziționare a volumelor de interes* relativ la volumul cerebral depinde de subiect: volumul căutat poate fi poziționat pe o tranșă (slice) axială superior sau inferior celei care conține centrul gravitațional al masei cerebrale. în aceeași măsură volumul de interes poate fi poziționat în tranșa axială mai aproape sau la distanța mai mare față de axa dintre emisfere. Pentru acest scop avem nevoie de *centrul de greutate al masei cerebrale*, precum și de *axa dintre emisfere*. Variațiile de poziționare se datorează *diferențelor demografice* : diferențe de vârstă, sex și rasă (e.g. volum mai mic pentru populația asiatica; formă diferită a craniului pentru populația africană). Diferențele de vârstă se concretizează în atrofie cerebrală pentru populația în etate, care determină modificari în volumul cerebral și deplasări ale poziției volumelor anatomice. Diferențele de sex determină diferențe ale volumului cutiei craniene, care la rândul lor, determină diferențe ale volumului cerebral. Astfel, pentru o abordare complet automată, aceste diferențe trebuiesc luate în considerare, iar *reperele geometrice* asemeni centrului de greutate și a axei interemisferiale reprezintă una dintre soluțiile propuse de noi. Repere în interiorul imaginii pentru determinarea și plasarea algoritmului de segmentare sunt necesare pentru a nu depăși regiunea de interes. Elemente geometrice care sunt independente de factorii demografici și includ specificitatea cazurilor: determinarea punctului de inflexiune corespunzător limitei occipitale a sinusurilor, limitele superioare și limitele interioare ale volumelor de interes.

După definirea și detecția volumelor de interes, algoritmul determinist de creștere al fibrelor neuronale, care preia abordarea clasică Bihan [Le Bihan 2001] și Basser [Basser 2000] și adaugând volumele de interes oferă o tractografie globală.

După detectarea și extargerea fibrelor *definim metrici* necesare corelării fibrelor cu severitatea maladiei. Aceste valori sunt cele care introduse în modulul de analiză generează datele de intrare pentru modulul de diagnoză și prognoză. Acest modul are doua scopuri: diferențierea între cazurile de control și cele afectate de maladie, pe de o parte, iar pe de altă parte determinarea gradului de severiate al bolii în cazul pacientilor afectați de maladie.

2.2 Caracteristicile și utilitatea imaginilor de difuzie

Baza de date pe care o utilizăm e recoltată în Sigapore, oferind variabilitate demografică și conține pentru fiecare caz medical diferite volume de imagini de difuzie RMN. Dispunem de 68 de pacienți care au fost identificați și diagnosticați de către specialistul neurolog cu maladia Parkinson, alături de 75 de cazuri de control. Toți pacienții și-au dat acordul scris pentru utilizarea imaginilor în cadrul studiului. Imaginile de difuzie (DTI) (TR/TE 4300/90; 12 direcții de difuzie; 4 medii; secțiuni de 4/0 mm ;rezoluție în plan de 1.2 x 1.2 mm), cuprinzând imagini de tip T_1, T_2 și imagini ecoplanare (EPI).

Imaginile de tip T_1 si T_2 nu le utilizăm deoarece, deși au o rezoluție bună comparativ cu celelalte imagini de difuzie, nu conțin tensori pentru determinarea fibrelor neuronale. Acest tip de informație se găseste la nivelul imaginilor de tip EPI, cele care conțin cele 12 direcții

de difuzie. Astfel dispunem de 351 de fisiere DICOM de tip EPI pentru fiecare pacient. Cum avem 12 direcţii de difuzie, obtinem 27 de tranşe axiale în fiecare volum cranian pentru fiecare direcţie de difuzie. Tranşele axiale sunt prelevate în plan AC/PC- Comisura Anterioară/ Comisura Posterioară.

Imaginile bazei de date sunt prelevate utilizând un sistem Siemens Avanto 1.5T (B=800). Acestea sunt achiziţionate în format DICOM, fiecare fişier conţinând alături de imaginea propriu-zisă şi un fişier "header" atasat care oferă informaţii referitoare la protocolul de achiziţie, precum şi date referitoare la pacient. Utilizând fişierul header putem extrage informaţii referitoare la pacient - identificatorul pacientului (PatId), vârstă şi sex - care le utilizăm ulterior pentru fiecare caz.

Utilizăm imagini de tip *EPI* datorită tensorilor şi al posibilităţii de reconstruire pentru fibrele neuronale. Efectuăm o amplificare a contrastului cu 0.5% utilizând filtrul imageJ[1] şi efectuăm o eliminare a craniului pentru a utiliza doar ţesut cerebral în analiza ulterioară în scopul segmentării.

Imaginile de *anizotropie fracţionara (FA)* obţinute direct, în urma scanării, conţin informaţii legate de nivelul de difuzie şi de valorile de dopamină. Acest tip specific de imagine permite o segmentare competitivă a Putamenului datorită difuziei care pune în evidenţă această zonă anatomică. Aceast tip de informaţie nu este prezentă în imaginile cu rezoluţie superioară, cum sunt cele de tip T_1 sau T_2, iar acurateţea anatomică a acestor imagini nu permite o conturare a Putamenului.

2.3 Noi algoritmi de procesare şi analiză a imaginilor medicale

Pentru manipularea imagnilor la diferite nivele informaţionale avem nevoie de metode suplimentare pentru tratarea acestora: la nivelul pregătirii imaginilor, segmentarea lor şi eliminarea artefactelor. Pentru partea de pregătire a imaginilor trebuiesc eliminate artefactele şi zgomotele. Determinarea elementelor geometrice este necesară în partea de segmentare. Algoritmii aplicaţi pentru pregătirea imaginilor înainte de metoda de segmentare sunt metode de preprocesare.

Am testat cateva metode implementate în cadrul unor sisteme existente ca să determinam comportamentul imaginilor pe care le avem pe de o parte, iar pe de altă parte, să avem în vedere punctele slabe ale acestor sisteme ca să încercam să le îmbunătăţim (Capitolul 2.5.1). Evaluăm diferite metode de segmentare la nivelul imaginilor medicale. Metoda globală de segmentare în cazul imaginilor cerebrale se referă la extragerea diferitelor tipuri de ţesut cerebral: materie alba (WM), materie cenuşie (GM) şi lichid intracranian (CBF). Această metoda este adoptată în implementarea Matlab SPM[2] şi VBM[3]. SPM este un sistem dedicat imaginilor de fMRI (RMN functional), cu aplicabilitate şi pentru DTI (Imagini RMN de difuzie),

[1] imageJ : `http://rsbweb.nih.gov/ij/` -accesat în May 2010

[2] Statistical Parameter Mapping (SPM) -`http://www.fil.ion.ucl.ac.uk/spm/` -accesat în Mai 2010

[3] Voxel Based Morphometry (VBM) -`http://en.wikipedia.org/wiki/Voxel-based_morphometry` -accesat în Mai 2010

având ca modul VBM. Acest sistem îndeplinește atât segmentarea, cât și alinierea la nivelul tranșelor axiale. Problema acestei abordări în cazul imaginilor noastre este faptul că nefiind o abordare automată, este sensibilă la parametrii demografici. O segmentare a regiunilor anatomo-cerebrale se poate realiza cu ajutorul acestui sistem, doar că fiind bazată pe atlasul Talairarchi [Guillaume 2008], este asemeni unei matriţe, nu se calează la nivelul fiecărui pacient în funcţie de factorii demografici [Gaser 2008]. Imaginile rezultate sunt "împăturate" nefiind utilizabile în continuare nici măcar pentru a valida sau compara elementele extrase.

Pentru segmentarea regiunilor de interes specifice, pe lângă metoda bazată pe atlas, abordarea manuală este eficientă. Această metodă oferă acurateţea dorită de sistemul nostru și am testat-o pe imaginile DTI utilizând un sistem nou dezvoltat pentru aceste imagini: 3D Slicer[4]. Asemeni lui, modulul DTI track din cadrul sistemului MedINRIA[5], oferă funcţii dedicate segmentării volumelor anatomice, dar și tractografiei. Ambele sisteme oferă posibilitatea segmentării în regiuni de interes atât în funcţie de tipul ţesutului, cât și în funcţie de regiunea anatomică, dar și recalarea automată. 3D Slicer nu este capabil de a realiza recalarea sau segmentarea lucrând pe capacitatea de memorie oferită de noi. MedINRIA poate realiza recalarea, dar doar metoda manuală oferă acurateţea dorită pentru o segmentare ulterioară în regiuni de interes. Faptul că la final acest sistem generează fișiere specifice care nu pot fi utilizate de alte sisteme, nu este un punct bun. De asemenea în tractografie nu putem utiliza mai mult de un volum de interes in DTI tracker, iar meroda de tractografie globală nu poate fi realizată, ci doar o tractografie locală. Faţă de abordarea deterministă implementată în cadrul sistemului nostru, am testat și o abordare probabilistă globală cu Diffusion Toolkit de la TrackVis[6]. Această metodă tractografică oferă rezultate bune, dar cuprinde zgomote în detecţie.

Testând astfel baza de date putem identifica punctele problematice în metodele testate. Definim în aceste condiţii barierele de surmontat la fiecare nivel al modulului:

- Preprocesarea imaginilor
  - eliminarea zgomotelor
  - eliminarea calotei craniene
  - detecţia și limitarea emiserelor cerebrale
  - recuperearea parametrilor volumetrici specifici
- Detecţia tranșei de interes
- Detecţia zonei anatomice de interes în plan axial
- Segmentarea volumelor de interes
  - segmentarea mezencefalului
  - segmentarea Putamenului (emisfera stângă și dreaptă)

[4]Slicer - http://www.slicer.org/- accesat în Mai 2010
[5]MedINRIA - http://www-sop.inria.fr/asclepios/software/MedINRIA/- accesat în Mai 2010
[6]TrackVis - http://www.trackvis.org/ - accesat în Iulie 2010

- Recalarea imaginilor FA în funcţie de cele de EPI
- Tractografierea deterministă globală
- Diagnoza şi prognoza

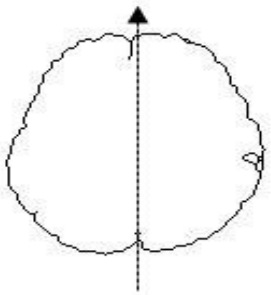

Figura 2.2: Conturul cerebral determinat pe imaginea EPI cu B0

Primele două probleme sunt depăşite prin utilizarea clasificării KMeans[7] în clase de voxeli corespunzând tipurilor de ţesut intra-cranian: materie albă (white matter - WM), materie cenuşie (grey matter - GM), lichid intracranian (cerebro-spinal fluid - CSF) şi ţesut osos provenind de la cutia craniană. Eliminând ultimul strat aparţinând ţesutului osos şi elementele care se află în exteriorul acestuia, eliminăm şi artefactele care înconjoară cutia craniană.

În continuare pentru toţi algoritmii de procesare utilizăm imaginile fără calota craniană. Trasând conturul cerebral şi determinând punctul de inflexiune interemisferiala, corespunzător anatomic sinusului occipital de la baza cutiei craniene din zona occipitala, alături de centrul de masă, determină axa limita dintre emisferele cerebrale (figura 2.2). Realizăm măsurătorile volumetrice utilizând ImageJ (object counter[8]). Centrul gravitaţional este utilizat în continuare ca reper pentru metodele de determinare ale tranşei de interes şi plasarea algoritmilor de deecţie pentru volumele de interes.

2.3.1 Poziţionarea în cadrul volumului de interes

Variabilitatea inter-pacienţi atrage cu sine parametrii pentru abordarea automată a segmentării pentru eliminarea specificităţii. De asemenea cele două emisfere cerebrale pot fi dezvoltate diferit din punct de vedere anatomic, motiv pentru care metodele pentru segmentarea volumelor de interes la nivelul celor două emisfere sunt diferite - *variabilitate intra-pacienăi*. Pentru detecţia volumelor de interes detectăm întâi tranşa cu imaginea axiala care conţine volumul respectiv. În această tranşă detectăm poziţia relativă a volumului de interes în raport cu centrul de greutate al creierului şi de axa care separă emisferele.

Poziţionarea mezencefalului în cadrul volumului cerebral relativ la centrul gravitational este 4-8 mm superior, ceea ce corespunde la 1-2 tranşe axiale deasupra celei care conţine centrul gravitaţional. Pentru o mai bună detecţie a tranşei de interes luăm în considerare poziţionarea pacientului în cadrul volumului. Acesta poate fi poziţionat mai sus sau mai jos în plan axial al imaginii, iar datorită diferenţelor demografice, volumul extras poate conţine

[7]KMeans în ImageJ: `http://ij-plugins.sourceforge.net/plugins/clustering/index.html` accesat în Iunie 2010

[8]ImageJ plug-in Object Counter : `http://rsbweb.nih.gov/ij/plugins/track/objects.html` -accesat în Iunie 2010

mai multe informații anatomice în cazul unei cutii craniene mai mici. Faptul că 80-90% din volumul cerebral e conținut în volumul prelevat sau un volum de 50-60%, reprezintă un neajuns care trebuie depășit. Raportul între volumul conținut în prima tranșă și cel din tranșa cu centrul de masă ne permite sa aproximăm volumul achiziționat, exprimat în ecuația 2.1.

$$P_{slice} = \frac{Vol_{Zslice}}{Vol_{Fslice}} * \frac{100}{ST} \tag{2.1}$$

unde Vol_{Zslice} și Vol_{Fslice} reprezintă volumul cerebral conținut în tranșa cu centrul de masă, respectiv tranșa inițială pentru fiecare pacient; ST reprezintă grosimea tranșei (4 mm). Valoarea calculată oferă posibilitatea poziționării volumului în una dintre cele patru categorii, relativ la centrul de greutate conținut în tranșa notată cu 0:

- tranșa $+0$ si $P_{slice}<60$
- tranșa $+1$ si $60<P_{slice}<70$
- tranșa $+2$ si $70<P_{slice}<85$
- tranșa $+3$ si $85<P_{slice}<100$

Valorile cosiderate pentru clasificarea procentajului volumului cerebral sunt stabilite prin analiză statistică. Poziția Putamenului este cu două tranșe mai sus în volum decât cea a mezencefalului - aproximativ 8 mm.

2.3.2 Detecția automată a mezencefalului

Metoda de detecție lucrează în plan axial doar în interiorul tranșei de interes. Regiunea anatomică mezencefaliană este situată în mijlocul masei cerebrale, iar axa care limitează cele două emisfere trece cu siguranță prin interiorul acestui volum. Centrul de masă al volumului din tranșa de interes împreună cu punctul de inflexiune din zona occipitală determină axa de simetrie. Tipurile de țesut care se regăsesc alături de centrul de masă pe axa de limitare a emisferelor aparțin unor regiuni anatomice diferite. Utilizăm o clasificare KMeans[9] pentru a determina mai ușor tipul de țesut căruia aparțin pixelii și în acest fel a distinge pe cei care aparțn regiunii de interes, știind tipul de țesut căruia îi aparține. Mezencefalul se află pe axa dintre emisfere și este regiune de materie cenușie, spre deosebire de corpus callosum sau lichidul intracranian. Pornind de la centrul gravitațional în direcția axei dintre emisfere cand atingem o zonă care e materie cenușie știm ca am atins mezencefalul (figura 2.3). Pentru detecția mezencefalului considerăm imaginile EPI B0 pe care aplicăm KMeans. Voxelii care fac parte dintr-un volum de interes, detectat pe cele două tranșe axiale ale mezencefalului, sunt transformați în mască. Aceasta mască este utilizată în selecția mezencefalului în procesul de tractografie. Pentru mezencefal această detecție se poate realiza direct pe imaginile de EPI, dar pentru Putamen acest lucru nu este posbili datorită rezoluției și diferenței de contrast. Deși pentru mezencefal detecția se poate realiza și pe aceste imagini, pentru Putamen le utilizăm pe cele de FA.

[9] KMeans in imageJ: `http://ij-plugins.sourceforge.net/plugins/clustering/index.html`- accesat în Iunie 2010

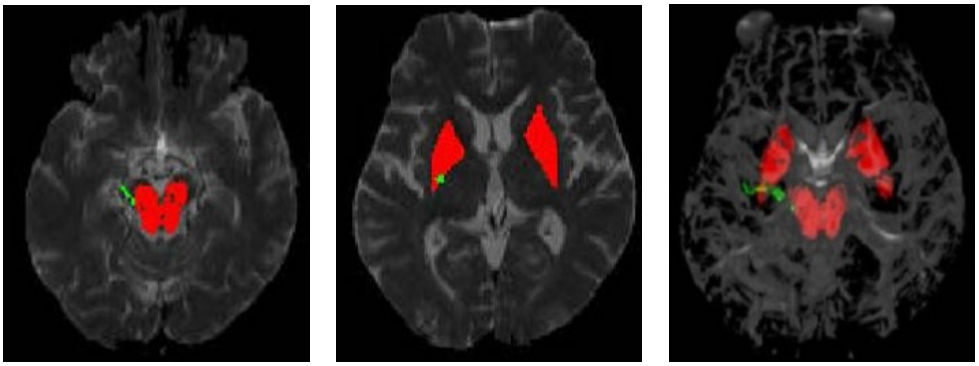

(a) EPI cu mezencefalul detectat și proiecția fibrelor (b) EPI cu Putamenul detectat și proiecșia fibrelor (c) Imagine 3D cu fibrele care trec prin VOI

Figura 2.3: EPI și volume de interes (VOIs) detectate în imaginile 2.3(a), 2.3(b) si 2.3(c) cu fibre 3D pe un exemplu

2.3.3 Detecţia automată a Putamenului

Pe imaginile de FA se aplică, la fel ca și pe cele de EPI, clasificatorul KMeans identificând patru clase de voxeli. Cum utilizăm imaginile de FA, nu vorbim de clase de țesut, ci de direcţii de difuzie reprezentate ca intensităţi ale voxelilor. Considerând aceste direcţii și zgomotul la nivelul imaginii, avem patru clase identificate în KMeans: antero-posterior, sus-jos, stânga-dreapta și artefacte.

Imaginea obţinută din clusterii clasificatorului este cea pe care o utilizăm în segmentare. Pe această imagine, cu centrul de masă și axa dintre emisfere identificate pe tranșa de interes, avem nevoie de poziția Putamenului pentru fiecare emisferă. Clasificăm pacienţii în funcţie de poziţionarea pe verticală a craniului în imagine: central, superior, inferior. Poziția este determinată în funcţie de centrul de masă al volumului din tranșa axială. Aceste repere geometrice care iau în considerare variabilitatea interpacienţi sunt parte a metodei de detecţie a poziţiei Putamenului în imaginea axiala. Impreună cu axa centrală și limitele exterioare ale regiunii cerebrale permit poziţionarea algoritmului de detecţie.

Forma geomertică aproximativă a acestei regiuni anatomice este triunghiulară în cazul tranșelor inferioare și cuadrilaterală în tranșele superioare. Acesta e motivul pentru care metoda de detecţie intuitiva pornește de la aceasta formă și în loc de a realiza pixel cu pixel verificarea și validarea apartenenţei la regiunea de interes, modifică poziția vârfurilor formei geometrice care reprezintă Putamenul. În cazul în care acești voxeli aparţin aceluiași țesut ca și cei inițiali, modificăm poziția vârfurilor triunghului. La fel se întamplă și în cazul algoritmului cu inițializare cuadrilaterala. Punctele inițiale sunt deplasate doar în direcţiile specificate. Tipul de inițializare diferă în funcţie de emisfera și de poziția tranșei axiale în volumul cerebral. Aceasta este aleasă în urma testelor statistice (testele în lucrarea [Sabau 2010]). Limitarea regiunii minime si maxime detectate elimină erorile de detecţie. Detecția se realizează pe

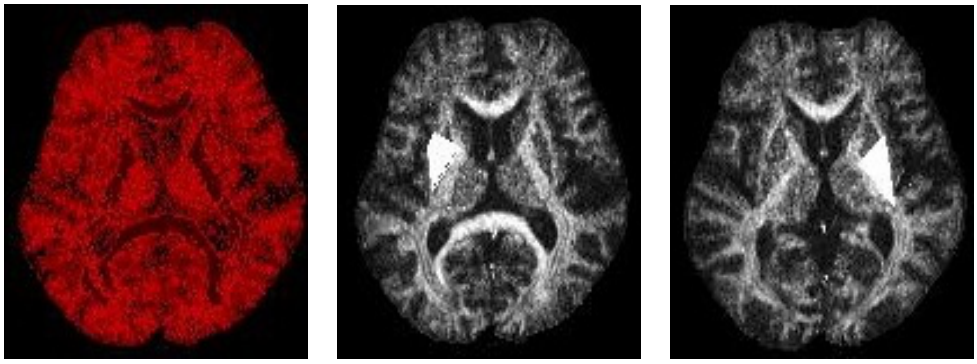

(a) Classificarea țesutului pe o imagine de FA

(b) Putamen detectat pe emisfera stangă

(c) Putamen detectat pe emisfera dreaptă

Figura 2.4: Detecția de Putamen suprapusă pe imagini de FA [Sabau 2010]

trei tranșe consecutive. Aliniem volumele detectate în funcție de centrul lor de masă și transformăm în mască volumul cu tranșele detectate - figura 2.4. Masca determinată, deși detectată pe imagini de FA o vom aplica pe imaginea EPI, dar pentru acest scop cele două imagini trebuiesc să se suprapună. Acesta e scopul algoritmului de recalare și apoi de fuziune informațională prin aplicarea acestei măști pe imaginile EPI.

2.3.4 Recalarea și fuziunea caracteristicilor

Pentru recalarea corectă a volumelor cerebrale FA cu EPI metodele bazate pe intensitatea voxelilor nu oferă rezultate satisfăcătoare. SPM generează în urma alinierii imagini "împaturate", cu MedINRIA modulul de fuziune funcționeaza bine în varianta manuală a alegerii reprerelor. Chiar și în aceste condiții, reperele manuale nu au însă acuratețe și depind de persoana care realizează marcarea punctelor de corespondență din cele două imagini. Datorită faptului că dispunem de doua tipuri diferite de imagini aparținând aceluiași pacient, vom reliza o recalare intrapacient. Metoda propusă de noi este geometrică rigidă, în totalitate automată și se bazează pe elementele detectate la nivel de volum cerebral în ambele stive de imagini:

- Centrul gravitațional cerebral
- Limitele exterioare cerebrale
- Axa dintre emisfere

Utilizând parametrii geometrici detectăm coeficienții pentru translație, rotație și orientarea planelor. Diferența dintre centrul gravitațional detectat în stiva de imagini FA și EPI determină valorile pentru translație: d_x, d_y et d_z. Valoarea unghiului dintre axa emisferială și sistemul de coordonate ale imaginii determină orientarea în spațiu a stivei. Diferența dintre unghiul determinat pe stiva FA și EPI ne oferă valorile pentru rotație. Orientarea axei dintre emisfere

în sistemul de coordonate determină o răsturnare (90 de grade) a volumului.

$$\begin{bmatrix} x^{'} & y^{'} & z^{'} & 1 \end{bmatrix} = \begin{bmatrix} cos\theta_x & sin\theta_x & 0 & d_x \\ -sin\theta_y & cos\theta_y & 0 & d_y \\ 0 & 0 & 1 & d_z \\ 0 & 0 & 0 & 1 \end{bmatrix} \begin{bmatrix} x \\ y \\ z \\ 1 \end{bmatrix} \tag{2.2}$$

Procesul de transformare al imaginii utilizând matricea din ecuația 2.1 presupune aplicarea acestor coeficienți la nivel de voxel în imaginea care este tranformată. În cazul nostru imaginea modificată este cea care conține masca de Putamen extrasă din FA. Valoarea θ_x reprezintă unghiul dintre axa dintre emisfere și axa O_x din imagine; θ_y unghiul dintre aceeași axa și axa O_y din image. Diferența dintre unghiul determinat pe imaginea EPI și cel determinat pe

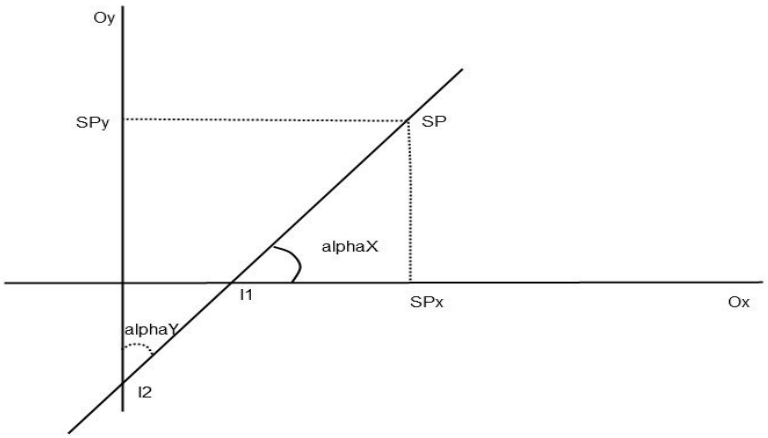

Figura 2.5: Determinarea geometrică a coeficienților de recalare

FA ne oferă valoarea unghiului de rotație utilizat în transformarea stivei care conține masca Putamenului. Această diferență determină valoarea unghiurilor din ecuațiile 2.3 și 2.4 în punctul de inflexiune. Unghiurile pentru imaginile FA sunt notate cu α și pentru EPI cu β. Diferența dintre aceste unghiuri o notăm cu θ.

$$sin\alpha_x = \frac{SP_y}{I_1SP} \tag{2.3}$$

$$sin\alpha_y = \frac{SP_x}{I_2SP} \tag{2.4}$$

Volumul Putamenului este extras din imaginea de FA, unde informația reprezentată este difuzivitatea, pe când în EPI, unde utilizăm masca, informația reprezentată este anatomică și tensorială. Astfel transferul de cunoștințe dinspre FA spre EPI beneficiază de ceea ce e mai bun în ambele tipuri de imagini.

2.3.5 Tractografia: extragerea fibrelor neuronale

Avantajul imaginilor EPI este faptul că acestea conțin pe fiecare direcție de difuzie valorile care determină tensorii pentru a calcula difuzivitatea. Algoritmul utilizat pentru tractografie este varianta clasică propusă în [Le Bihan 2001] și [Basser 2000].

Difuzia se bazează pe faptul că moleculele de apă sunt atenuate în difuzie de materia cenusie. La nivel cerebral materia cenușie este constituită din axonii neuronilor, iar dendritele constituie materia alba. Acesta este motivul pentru care trasmiterea impulsului neuronal și direcția de transmitere poate fi determinată prin intermediul difuziei de-a lungul fibrelor neuronale [Rorden 2008] [Curran 2005].

Difuzivitatea se calculează utilizând tensorii care conțin direcțiile utilizate în prelevarea imaginilor. Utilizând valorile proprii și vectorii proprii, calculati pe baza tensorilor, putem determina anisotropia. Această metrică este specifică difuzivității. Trasarea fibrelor în funcție de direcția principală de difuzie și de valorile tensorilor este limitată de algoritmul nostru prin utilizarea volumelor de interes. Pentru eliminarea zgomotelor în detecție introducem valori limită pentru angulație și anisotropie. Utilizăm valori recomandate de cei care au propus algoritmul în acest scop.

Trasăm doar fibrele care pornesc din volumul mezencefalului și numai cele care trec prin Putamen sunt validate și considerate ca și rezultate. Această abordare este specifică tractografiei globale care se bazează pe o zonă sursa - la noi mezencefalul- și pe o zonă destinație - la noi Putamenul.

Pentru a evalua fibrele determinăm densitatea lor introducând metrici proprii ca să eliminăm atrofia cerebrală și diferența de volum prin raportarea acestora la volumul regiunilor de interes sau la volumul cerebral.

$$FD = \frac{F_{Nr}}{Vol_{Brain}};\ FD_{rel} = \frac{F_{Nr}}{Vol_{VOI}} \tag{2.5}$$

unde valoarea pentru FD reprezintă densitatea fibrelor calculată utilizând numărul de fibre determinate - F_{Nr} - în cadrul volumului cerebral - Vol_{Brain}, iar valoarea FD_{rel} reprezintă densitatea fibrelor relativ la volumul de interes- Vol_{VOI}. Volumul de fibre calculat în urma tractografiei este prezentat în ecuația 2.6.

$$FV = F_{Nr} * V_{height} * V_{width} * V_{depth} * F_{leng} \tag{2.6}$$

unde valoarea reprezentată de FV este volumul calculat al fibrelor ca și produs între numarul de fibre (F_{Nr}), lungimea lor (F_{leng}) și dimensiunile voxelilor $V_{width}, V_{height}, V_{depth}$. Utilizând aceste metrici putem evalua în continuare valorile caracteristicilor extrase.

2.4 Analiza caracteristicilor. Diagnoza și prognoza medicală

La acest nivel informațional în fluxul de date valorile detectate prin tractografie sunt evaluate. Corelarea dintre valorile evaluate și severitatea maladiei determină o prognoza a acestei boli. Avem doua cerințe pentru acest modul: diagnoza și prognoza. În diagnoză trebuie facută

diferența dintre cazurile de control și cele afectate de maladie. Prognoza evalueaza severitatea maladiei pentru cazurile afectate. Modelul arhitectural utilizat pentru diagnoză și prognoză conține cinci pași:

- Date de intrare - valorile extrase de la nivelul fibrelor
- Reguli fuzzy și greutatea lor
- Definirea nivelelor de importanță (weights)
- Calculul parametrilor de consecință- determinați utilizând nivelele de importanța și funcțiile de interpolare
- Ieșirea - decizia care generează valoarea finală

Primele două etape furnizează valorile pentru diagnoză. În cazul nostru nivelele de importanță sunt reprezentate de gradul polinoamelor Lagrange, definite in etapa a patra. Această definire a polinoamelor ca unelte decizionale reprezintă o abordare hibridă a unui sistem bazat pe arhitectura ANFIS.

Diagnoza în cadrul sitemului nostru este realizată utilizând un sistem bazat pe logica fuzzy care utlizează valorile metricilor de la nivelul fibrelor. Aceste valori sunt clasificate în funcție de valoarea pe scala H&Y determinată pe baza testului cognitiv pentru pacienții pe care realizăm antrenarea părții de clasificare. În funcție de aceste clase realizăm un sistem de reguli pe care le utilizăm pentru determinarea valorii diagnozei (regulile din ecuația 2.7). Sistemul de reguli determină valoarea H&Y în funcție de densitatea fibrelor - HY_{FD}- și de volumul mezencefalului - $HY_{VOI_{Vol}}$. Utilizând valorile detectate pentru fibre, în funcție de regulile proprii putem face diferența dintre cazurile de control - HY=0 și cele afectate de maladie, dar deoarece dispunem de pacienți cu HY=2 si HY=3, doar aceste nivele ale maladiei le putem evalua și antrena sistemul.

$$
\begin{aligned}
&If(HY_{FD} = HY_{VOI_{Vol}} \wedge HY_{FD} \neq -1)\, then\, HY = HY_{FD}\\
&If(HY_{FD} = -1 \wedge HY_{VOI_{Vol}} \neq -1)\, then\, HY = HY_{VOI_{Vol}}\\
&If(HY_{FD} \neq -1 \wedge HY_{VOI_{Vol}} = -1)\, then\, HY = HY_{FD}\\
&If(HY_{FD} \neq -1 \wedge HY_{VOI_{Vol}} \neq -1) \wedge (HY_{FD} \neq HY_{VOI_{Vol}}))\, then\\
&\quad If(FD_{3D} \neq 0)\, then\, HY = 2\\
&\quad else\, HY = 0\\
&If(HY_{FD} = -1 \wedge HY_{VOI_{Vol}} = -1) then\ The\ image\ is\ invalid!
\end{aligned}
\tag{2.7}
$$

Acesta este motivul pentru care avem nevoie de funcția de evaluare: determinarea gradului de afectare chiar daca nu dispunem de pacienți în baza de date care să aiba același grad - extrapolare a funcției de evaluare. Astfel prin extrapolare putem determina și cazurile precoce - stadiul incipient al maladiei.

Funcția de **prognoză** utilizează valorile densității fibrelor din emisfera stangă, datorită faptului că degenerarea cauzată de maladie este, confrom studiilor, mai pronunțată pe această parte. Plasând valorile fibrelor în funcție de scala H&Y putem să trasăm o funcție (metoda TSK) pe care sa o utilizăm pentru evaluare. Având în vedere dispersia valorilor determinăm

funcția de evaluare pe intervale. În construirea funcției pe intervale luăm în considerare valorile determinate utilizând Putamenul detectat manual. Intervalele iau în considerare trei sau cinci puncte în construirea funcției polinomiale. Nu luăm mai multe puncte deoarece funcția se complică, iar la mai puține puncte am avea o abordare lineara, neconformă cu amplasarea datelor. Funcția de evaluarea este un polinom Lagrage (prezentat în ecuația 2.8) cu ordinul dat în funcție de numărul de punctele considerate.

$$L(x) = \sum_{i=0}^{n} y_i * \prod_{j=0, j\neq i}^{n} \frac{x - x_j}{x_i - x_j} \tag{2.8}$$

Funcțiile polinomiale construite pentru estimare cu ajutorul polinoamelor Lagrange au coeficienții calculați fie de setul de ecuații 2.9, fie de ecuațiile 2.10.

$$\begin{aligned} C_2 &= \tfrac{y_1}{(x_1-x_2)(x_1-x_3)} + \tfrac{y_2}{(x_2-x_1)(x_2-x_3)} + \tfrac{y_3}{(x_3-x_1)(x_3-x_2)} \\ C_1 &= -(y_1 \tfrac{x_2+x_3}{(x_1-x_2)(x_1-x_3)} + y_2 \tfrac{x_1+x_3}{(x_2-x_1)(x_2-x_3)} + y_3 \tfrac{x_1+x_2}{(x_3-x_1)(x_3-x_2)}) \\ C_0 &= y_1 \tfrac{x_2x_3}{(x_1-x_2)(x_1-x_3)} + y_2 \tfrac{x_1x_3}{(x_2-x_1)(x_2-x_3)} + y_3 \tfrac{x_1x_2}{(x_3-x_1)(x_3-x_2)} \end{aligned} \tag{2.9}$$

Setul de ecuații 2.9 determină polinoame de gradul doi, iar setul bazat pe cinci puncte din ecuația 2.10 determină polinoame de gradul patru.

$$\begin{aligned} C_4 &= \sum_{i=0}^{4} y_i \prod_{j=0, j\neq i}^{4} \tfrac{1}{x_i - x_j} \\ C_3 &= \sum_{i=0}^{4} y_i \left(\frac{\sum_{j=0, j\neq i}^{4} -x_j}{\prod_{k=0, k\neq i}^{4} (x_i - x_k)}\right) \\ C_2 &= \sum_{i=0}^{4} y_i \left(\frac{\sum_{j=0, j\neq i}^{4} x_i x_j}{\prod_{k=0, k\neq i}^{4} (x_i - x_k)}\right) \\ C_1 &= \sum_{i=0}^{4} y_i \left(-\frac{\sum_{j=0, j\neq i}^{4} x_i \left(\sum_{m=0, m\neq j}^{4} x_m * \sum_{n=m+1}^{4} x_n\right)}{\prod_{k=0, k\neq i}^{4} (x_i - x_k)}\right) \\ C_0 &= \sum_{i=0}^{4} y_i \left(\frac{\prod_{j=0, j\neq i}^{4} x_j}{\prod_{k=1, k\neq i}^{4} (x_i - x_k)}\right) \end{aligned} \tag{2.10}$$

Evaluarea unui nou caz presupune diagnoza, apoi prognoza. Evaluăm valorile pentru noul pacient cu ajutorul setului de reguli. În urma testelor polinomul de gradul doi oferă rezultate mai bune în prognoza cazurilor de control. Abordarea intuitiva care pornește de la funcții polinomiale de gradul trei, pana la cele lineare generează rezultate de o acurateţe ridicată pentru diferite nivele ale maladiei. Incercăm să introducem noua valoare determinând valorile cele mai apropiate de această noua valoare (figura 2.6). Împreuna cu valorile învecinate

(valoarea imediat inferioară X_m și cea imediat superioară X_M) determinăm funcțiile polinomiale și evaluăm noua valoare H&Y pentru densitatea fibrelor nou introdusă utilizând aceste funcții. Această evaluare adaptivă utilizând punctele învecinate determină funcțiile polino-

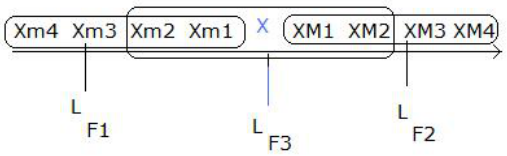

Figura 2.6: Independent Adaptive Polynomial Evaluation (IAPE)

miale cu ajutorul cărora în cazul în care valoarea în punctul nou (X) evaluată pe cel putin doua din funcțiile polinomiale coincide, atunci luăm această valoare ca și rezultat HY : HY1. Pentru cazul în care valorile sunt diferite redeterminăm funcțiile polinomiale utilizând mai puține puncte pentru o funcție polinomială de grad inferior. Un pas suplimentar în determinarea valorii H&Y este valoarea în noul punct (X) dată de funcția liniară care trece prin punctele învecinate (X_{m1} și X_{M1}) celui pe care îl introducem: HY2. In cazul în care diferența dintre HY1 și HY2 depășește trei nivele pe scala H&Y, atunci facem media între cele două valori determinate (Figura 2.7). Această manieră de a utiliza polinoame Lagrange face parte din categoria abordărilor adaptive de interpolare, cu similitudini relativ la retelele cu back-propagation. Această similitudine este la nivelul propagării erorii pentru a ameliora inferența. Polinoamele Lagrange au aceeași utilitate în cadrul sistemului nostru ca și funcțiile Gausiene în cadrul rețelelor RBF (Radial Basis Function). În cazul în care H&Y pe una dintre estimări este nulă, deci pacientul este caz de control, considerăm valoarea care indică valoarea de maladie. Această abordare este adaptivă și se bazează tot pe polinoame Lagrange -PD Adaptive Polynomial Evaluation (PD-APE). Abordarea aceasta include la al doilea nivel al arhitecturii ANFIS o condiție suplimentară dată de diagnoză.

2.5 Evaluare și rezultate

Sunt câteva nivele unde putem evalua noile metode dezvoltate pe baza noastră de date, dar mai întâi trebuie specificate caracteristicile bazei de test. Metricile pentru evaluarea algortmilor se referă la sensibilitate, specificiate si acurateţe, dar la fiecare nivel masurăm alte aspecte. La nivelul segmentării evaluăm diferența dintre abordarea manuală și metoda noastră. Aceleași metrici exprimă pentru modulul de diagnoză și prognoză metoda noastră comparativ cu cea bazată pe testele cognitive.

Detecţia mezencefalului cu ajutorul metodei noastre a fost validată de către specialistul neurolog. În cazul detecției Putamenului rata de eroare a algoritmului nostru este dată de diferența dintre detecția manuală și cea automată. Rata de eroare pentru detecția bazată pe triangulație este de 35% pentru Putamen pe partea stangă și pentru dreapta de 45%. În

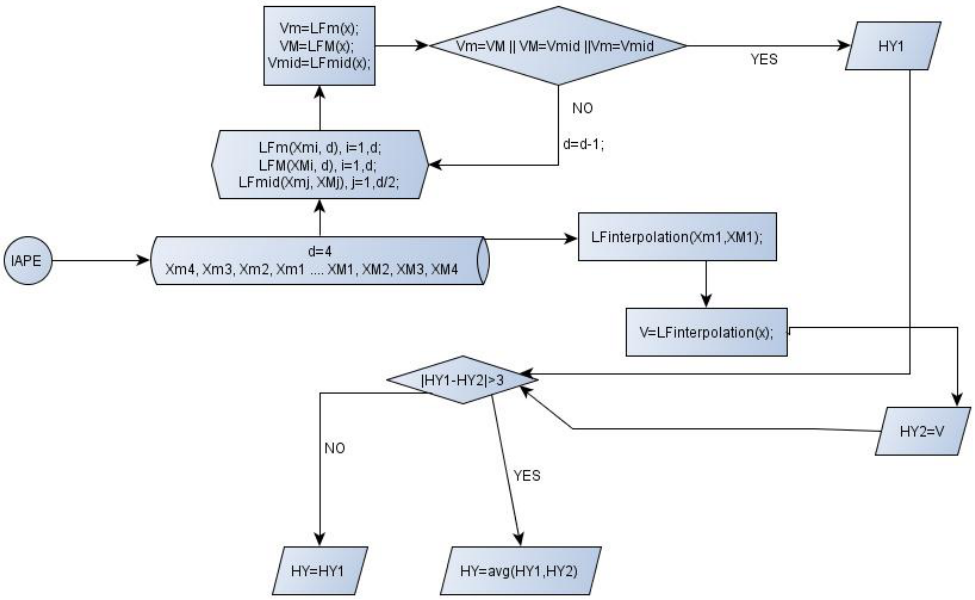

Figura 2.7: Diagrama fluxului de date în metoda Independent Adaptive Polynomial Evaluation (IAPE)

cazul metodei cuadrilaterale obținem o eroare relativă a detecției Putamenului de 46% atât în stânga, cât și în dreapta.

Evaluând valorile pentru detecția fibrelor pe baza de date obținem o valoare a specificității de 63%, sensibilitatea ofera valori de 81%, iar acuratețea este de 75.5% . Considerăm cazurile cu detecția manuală ca fiind cazuri ideale - au mai puține erori în detecție generate de algoritm. Acesta este motivul pentru care utilizăm valorile acestui set de date pentru setarea parametrilor și pretestare. Astfel dispunem de 41 de cazuri (21 control și 20 pacienți detectați cu maladia Parkinson) pe care facem setările pentru funcțiile polinomiale Lagrange utilizate în diagnoză și prognoză. Utilizăm întreaga bază de diagnoză oferită de Dr. Chan ca valoare de adevăr în evaluarea și antrenarea sistemului. Pentru acest grup de pretest diagnoza bazată pe reguli are o valoare de 61%, iar funcțiile de interpolare de gradul doi au valori de 34% și cele de gradul patru au 43%. Introducând în setul de antrenare al bazei de date 9 noi cazuri automate din primele teste, avaând toate metodele noastre integrate, acuratețea algoritmilor crește cu 19.2% pentru polinomul de gradul doi și cu 6% pentru cel de gradul patru.

După setarea parametrilor și evaluarea funcțiilor testăm metodele pe întreaga bază de date. Rata de succes dată de funcțiile de predicție este de 62.16% pentru pacienți utilizând abordarea intuitivă polinomială - metoda IAPE. Cazurile de control generează o valoare de 43.9% în cazul acurateții pentru polinomul de gradul doi. Sensibilitatea funcțiilor este caracteristică pacienților care au maladia (max. 62%) iar specificitatea este influențată de valorile cazurilor de control (max. 43.9%). In cazul pacienților, cât și al cazurilor de control, metoda intuitivă

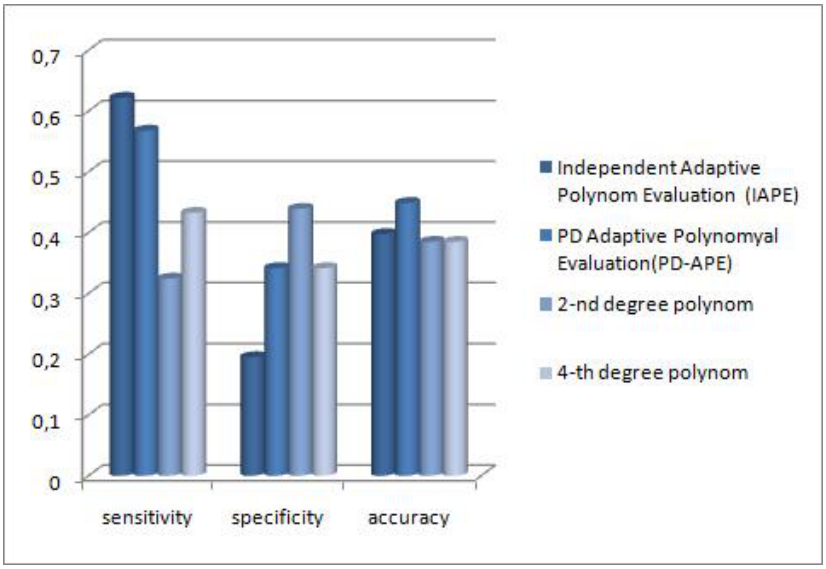

Figura 2.8: Sensibilitatea și specificitatea pentru polinoamele de predicție

generează o valoare a acurateții de 44.87%.

Utilizând curbele ROC obținem o evaluare statistică pentru metodele de prognoză. Cu ajutorul programului SPSS 17.0 (Statistical Package for the Social Sciences) obținem o evaluare a metodelor de prognoză. Pentru metoda IAPE obținem o valoare de 0.705 pentru aria de sub curba ROC (AUC). În cazul metodei PD-APE valoarea pentru această arie este de 0.959. Performanțele funcțiilor de prognoză recomandă metoda IAPE pentru evaluarea întregii baze de date, pacienți si control, cu o valoare AUC de 0.745 - testarea comparativă efectuată cu sistemul MedCalc[10](figura 2.9). Performanțele algoritmilor de segmentare afectează performanțele metodelor de analiză. Astfel detecția Putamenului care afectează numărul de fibre are efecte asupra caracteristicilor care sunt ulterior analizate în cadrul modulului de diagnoză și prognoză.

2.6 Concluzii. Noi perspective de cercetare

Cele două tipuri de imagini medicale de difuzie conțin informații complementare și oferă posibilitatea de a realiza o segmentare performantă. Informațiile de natură diferită din cele două tipuri de imagini se completează și atât în procesare, cât și la nivelul analizei. Realizăm toate aceste procese automat, atât în partea de procesare, cât și în cea de analiză. Metodele prezentate în cadrul tezei, puse împreună, fac trecerea de la nivelul vizual la nivelul cunoștințelor. Acest transfer este realizat cu ajutorul metodelor de la fiecare nivel informațional în cadrul sistemului nostru - fig. 2.10.

[10]MedCalc 11.3.3.0 - `www.medcalc.be`- accesat în Iulie 2010

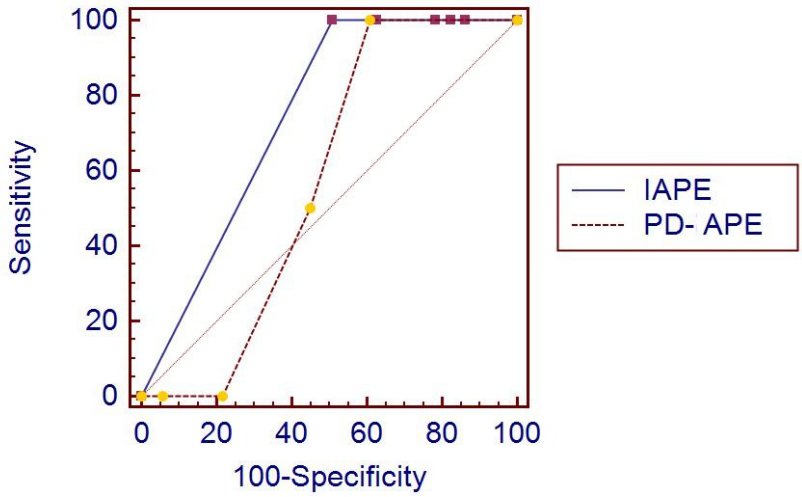

Figura 2.9: Grafic comparativ al curbelor ROC pentru metodele IAPE și PD-APE aplicate pe întreaga bază de date (143 cazuri: 68 pacienți și 75 de cazuri de control). Diferența performanțelor celor două metode este de 0.178 pentru valoarea AUC: 0.745 pentru IAPE față de 0.569 pentru PD-APE

Faptul că detecția volumelor de interes este automată oferă nu doar timp superior în segmentare, dar prin faptul că lucram cu măsti, nu cu elemente detectate manual, oferă o detecție mai bună a fibrelor datorita faptului ca nu avem "găuri" cauzate de "zgomote". De asemenea abordarea automata nu este afectată de acuratețea persoanei care realizează segmentarea, iar obiectivitatea este un element evident în cazul abordarii automate.

Abordarea geometrică în cazul recalării elimină o parte din variabilitatea interpacienți, dar prin determinarea parametrilor geometrici ca repere, abordarea propusa de noi are o nouă utilitate. Această recalare oferă de asemenea nu doar utilitatea pentru detecția fibrelor, ci și o fuziune la nivel informațional datorită complementarității conținutului imaginilor.

În tractografie metoda deterministă elimină o parte din erori în detecție, iar abordarea generalizată prin aplicarea volumelor de interes oferă viteza algoritmului prin faptul ca nu generează toate fibrele. De asemenea, metoda aceasta oferă posibilitatea selecției fascicolului de interes.

La nivel de diagnoză și prognoză metodele propuse de noi iau în considerare atât cunoștințe medicale, dar oferă și o alternativă la abordarea bazată pe testele cognitive. Cum abordarea bazată pe imagini nu a mai fost utilizată, prototipul nostru este complet nou. Partea de logică fuzzy ia în considerare dispersia și suprapunerea intervalelor caracteristicilor, integrată într-un sistem ANFIS permite și prognoza. Funcțiile de evaluare sunt o prima încercare în analiza de acest fel a caracteristicilor fibrelor neuronale, motiv pentru care abordări specifice setului de date pot îmbunătăți sensibil rata de succes a acestor algoritmi.

Importanţa abordării noastre poate fi privită atât la nivel de sistem funcţional, care este capabil să realizeze diagnoza pe baza imaginilor, cât şi ca element preliminar pentru prognoza cazurilor precoce. De asemenea această abordare oferă complementaritate testelor cognitive şi un nou mod de a privi diagnoza şi prognoza la nivelul maladiilor neurodegenerative. Metodele luate separat sunt toate automate, ceea ce oferă robusteţe abordării în sine în cadrul prototipului PDFibAtl@s.

Partea de preprocesare cu metoda de detecţie a limitei interemisferiale poate fi aplicată pentru analiza atacului cerebral sau a detecţiei tumorale. Elementele geometrice permit o recalare interpacienţi şi elimină variabilitatea de la acest nivel, aspect important în toate abordările bazate pe imagini cerebrale. Segmentarea automată oferă alternativa la abordarea bazată pe atlas eliminând astfel aspectul demografic legat de rasă - pentru fiecare rasă este utilizată momentan o alta masca. Abordarea bazată pe atlas nu ia în considerare modificări datorate atrofiei cerebrale şi variaţii în poziţia anumitor structuri anatomice, specifice fiecărui caz în parte, fapt care nu este integrat în metoda propusă de noi.

La nivel de tractografie, o abordare probabilistică nouă poate ridica nivelul rezultatelor, modificând şi valoarea de diagnoză şi prognoză. Acealşi lucru poate fi realizat prin aplicarea unei funcţii dedicate în locul polinoamelor Lagrange în partea de prognoză.

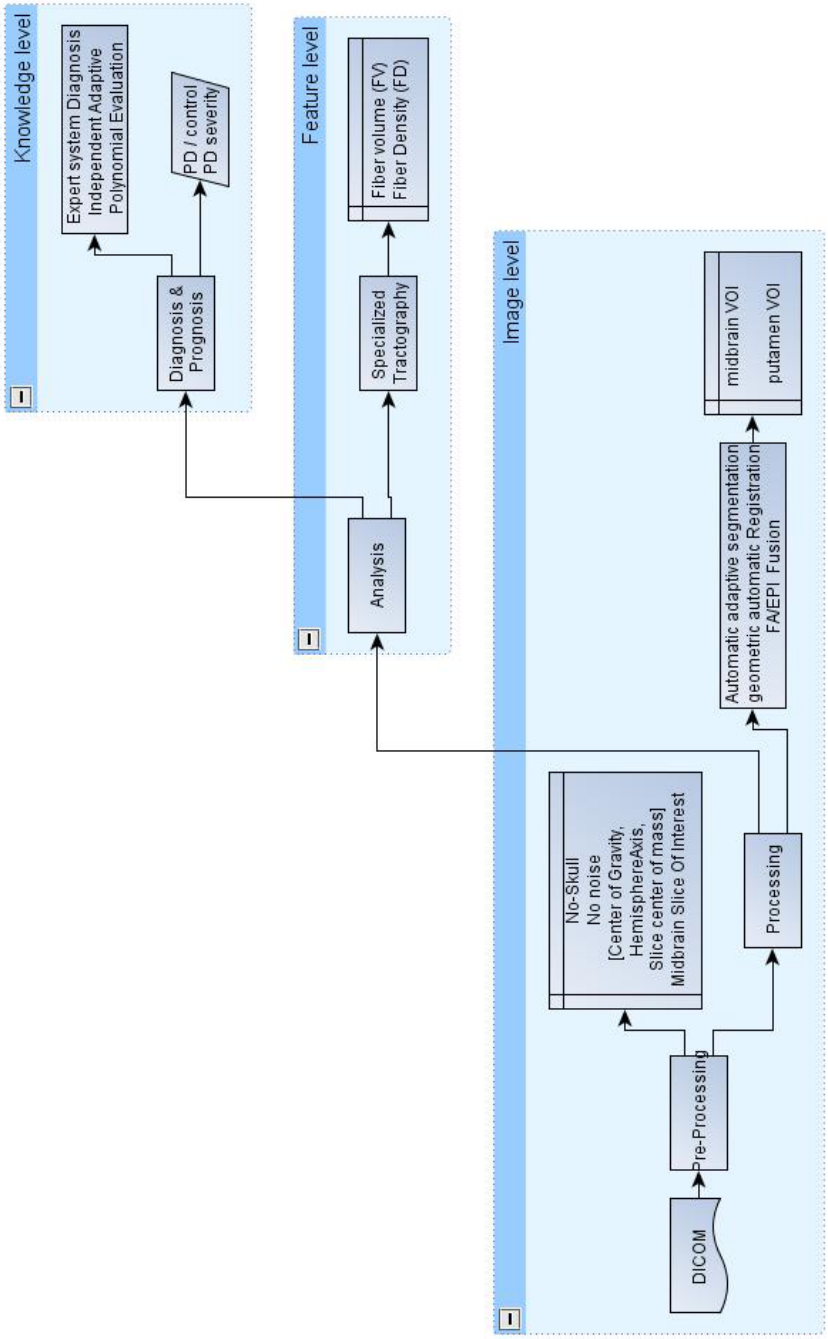

Figura 2.10: PDFibAtl@s: prototipul care include toate metodele propuse

Index

Appendices

Appendix A

Dissemination

A.1 Journals

Teodorescu, R.; Racoceanu, D.; Leow, W.-K. & Cretu, V. *Prospective study for semantic Inter-Media Fusion in Content-Based Medical Image Retrieval* Medical Imaging Technology, 2008, 26, 48-58

Anda Sabau, **Roxana Oana Teodorescu** and Vadimir Ioan Cretu. *A New Cerebral Anatomical-Based Automated Active Segmentation Method* - to appear, Scientific Bulletin of the Politehnica University of Timisoara, Transactions on Automatic Control and Computer Science, ISSN 1224-600X, 2010.

A.2 Book Chapters

Roxana Oana Teodorescu, Vladimir Ioan Cretu and Daniel Racoceanu *Medical Image Processing and Analysis for Parkinson's Disease Diagnosis and Prognosis* - under publication, working title "Biomedical Engineering, Trends, Researches and Technologies", ISBN 978-953-7619-X-X, published by INTECH, 2010.

Lacoste, C.; Chevallet, J.-P.; Lim, J.-H.; Hoang, D. L. T.; Wei, X.; Racoceanu, D.; **Teodorescu, R.** & Vuillenemot, N. *Inter-media concept-based medical image indexing and retrieval with umls at IPAL* Lecture Notes in Computer Science, Evaluation of Multilingual and Multi-modal Information Retrieval, 2007, 4730, 694-701.

Racoceanu, D.; Lacoste, C.; **Teodorescu, R.** & Vuillemenot, *N. A semantic fusion approach between medical images and reports using umls Lecture Notes in Computer Science*, (Eds.): Asian Information Retrieval Symposium, 2006, 4182, 460-475.

A.3 Conferences & Workshops

Anda Sabau, **Roxana Oana Teodorescu** and Vadimir Ioan Cretu. *Automatic Putamen Detection on DTI Images. Application to Parkinson's Disease.* ICCC-CONTI, vol. 1, pages 1-6, may 2010.

Teodorescu, R.; Racoceanu, D.; Smit, N.; Cretu, V. I.; Tan, E. K. & Chan, L.-L. *Parkinson's disease prediction using diffusion based atlas - poster session* SPIE - Computer Aided Diagnosis [7624-78] PS2, 13-18 Febr., San Diego CA, USA 2010.

Teodorescu, R.; Racoceanu, D.; Chan, L.; Lovblad, K. & Muller, H. *Parkinson's disease detection using 3D Brain MRI FA map histograms correlated with tract directions - oral presentation Neuroradiology (Brain: Movement and Degenerative Disorders SSC13 - 09)* RSNA,95th Radiological Society of North America Scientific Conference and Annual Meeting, November 29 to 4 December, McCormick Place, Chicago IL, USA, 2009.

Teodorescu, R. O. & Racoceanu, D. *Prognosis of Parkinson's Disease - poster session*, A*STAR Scientific Conference, 28-29 Oct., Biopolis, Singapore 2009.

Teodorescu, R. O.; Racoceanu, D. & Chan, L.-L. *H&Y compliant for PD detection using EPI and FA analysis - poster session*, NIH Workshop Inter-Institute Workshop on Optical Diagnostic and Biophotonic Methods from Bench to Bedside, 1-2 Oct, Washington DC, USA 2009.

Teodorescu, R.; Cernazanu-Glavan, C.; Cretu, V. & Racoceanu, D. *The use of the medical ontology for a semnatic-based fusion system in Biomedical Informatics - Application to Alzheimer disease* ICCP Proceedings, 2008, 1, 265-268.

Teodorescu, R.; Cretu, V. & Racoceanu, D. *The use of medical ontology in a semantic-based fusion system* CONTI, 2008, 1, 48-52.

R. Teodorescu and D. Racoceanu. Semantic Inter-Media Fusion Design for a Content-Based Medical Image Retrieval System. Japanese Society of Medical Imaging Technology - JAMIT-ONCO-MEDIA workshop, vol. Tsukuba, Japan, pages 43-47, 21 - 22 july 2007.

A.4 Technical reports

Roxana Teodorescu. *H&Y Compilant for PD Diagnosis and Prognosis using EPI and FA images.* Phd report no. 2, Politehnica University of Timisoara, February 2010.

Roxana Oana Teodorescu. *Feature extraction and Ontology use for Brain medical images - PhD Report No 1.* Rapport technique 1, UPT and UFC, January 2009.

A.5 Research stages

February-April 2009 Research stage in Singapore at IPAL(Image & Pervasive Access Lab)- the Singaporean-French Image & Pervasive Access Lab under the supervision of Prof. Daniel RACOCEANU

April -October 2009 Research stage in Singapore at Image & Pervasive Access Lab under the supervision of Prof. Daniel RACOCEANU from French National Research Center.

18-20 February 2009 Participation at the French-Singaporean symposium at NUS and IPAL Singapore.

July -October 2008 - Image Processing Stage in Geneva at Université de Geneve with the MedGIFT laboratory - Collaborator Dr. Henning Müller

March-June 2007 - ONCO-MEDIA project at IPAL (Image Perception Acess and Language) Laboratory, joint research laboratory in Singapore - CNRS (French National Research Center), A* Singapore - Institute for Infocomm Research, NUS (National University of Singapore) and UJF (Joseph Fourrier University) France - Supervisor Dr. Daniel RACOCEANU(UFC), collaborator Dr. Wee Kheng LEOW (NUS)

March - September 2006 - IPAL (Image Perception Acess and Language) Laboratory, joint research laboratory in Singapore - CNRS (French National Research Center), A* Singapore - Institute for Infocomm Research, NUS (National University of Singapore) and UJF (Joseph Fourrier University) France - 21 Heng Mui Keng Terrace, Singapore - Supervisor Dr. Daniel RACOCEANU

A.6 Scholarship

June 2007-December 2009 Young Doctors Scholarship TD (Tineri Doctoranzi) 46/2008 from the Romanian Research and Learning Ministry.

Appendix B

DICOM Header Example file

This Appendix contains an example of several tags used in our system from the DICOM header files. These files are more complex and contain more tags, but we extract just the ones presented here.

Title: 21599424
Width: 201.25 mm (448)
Height: 230.00 mm (512)
Resolution: 2.226 pixels per mm
ID: -2
Coordinate origin: 0,0
Bits per pixel: 16 (unsigned)
Display range: 0 - 754
No Threshold

code	Information
0002,0003	Media Storage SOP Inst UID: 1.3.12.2.1107.5.99.2.2716.30000008042402440731200014325
0008,1030	Study Description: headŜGH Brain
0008,103E	Series Description: t2_tse_DTI_overlay_highRes
...	...
0010,0010	Patient's Name: 001
0010,0020	Patient ID: 001
0010,0030	Patient's Birth Date: 19411122
0010,0040	Patient's Sex: M
0010,1010	Patient's Age: 064Y
...	...
0018,0023	MR Acquisition Type: 2D
0018,0024	Sequence Name: *tse2d1_13
0018,0025	Angio Flag: N
0018,0050	Slice Thickness: 4
0018,0080	Repetition Time: 5700
0018,0081	Echo Time: 89
0018,0083	Number of Averages: 3
0018,0084	Imaging Frequency: 63.673778
0018,0085	Imaged Nucleus: 1H
0018,0086	Echo Numbers(s): 0
0018,0087	Magnetic Field Strength: 1.4939999580383
0018,0088	Spacing Between Slices: 4
...	...
0020,0013	Image Number: 10
0020,0032	Image Position (Patient): -121.20970194079 -122.75359890362 -9.4565671015186
0020,0037	Image Orientation (Patient): 0.99817062741895 -0.0175064983057 0.05786986327205 0.02265170415277 0.99573051228909 -0.0894854580112

Table B.1: Example of DICOM header tags

Appendix C

Hoehn & Yahr classification

Stage	Symptoms
HY-I	1. Signs and symptoms on one side only
	2. Symptoms mild
	3. Symptoms inconvenient but not disabling
	4. Usually presents with tremor of one limb
	5. Friends have noticed changes in posture, locomotion and facial expression
HY-II	1. Symptoms are bilateral
	2. Minimal disability
	3. Posture and gait affected
HY-III	1. Significant slowing of body movements
	2. Early impairment of equilibrium on walking or standing
	3. Generalized dysfunction that is moderately severe
HY-IV	1. Severe symptoms
	2. Can still walk to a limited extent
	3. Rigidity and bradykinesia
	4. No longer able to live alone
	5. Tremor may be less than earlier stages
HY-V	1. Cachectic stage
	2. Invalidism complete
	3. Cannot stand or walk
	4. Requires constant nursing care

Table C.1: Hoehn and Yahr Staging of Parkinson's Disease [Goetz 2004].

Bibliography

[Ashburner 2000] John Ashburner and Karl J. Friston. *Voxel-Based Morphometry - The methods*. Neuroimage, vol. 11, pages 805–821, 2000. The Wellcome Department of Cognitive Neurology, Institute of Neurology. 29

[Atasoy 2004] Husein Atasoy, Nuyan Tugrul, Tunc Oguz and Tugba et al. *T2-weighted MRI in Parkinson's disease; substantia nigra pars compacta hypointensity correlates with the clinical scores*. Neurology India, vol. 52, pages 332–337, 2004. 15

[Bankman 2009] Isaac Bankman, editeur. Handbook of medical image processing and analysis. Academic Press Series in Biomedical Engineering. Academic Press in an imprint of Elsevier, 2 édition, 2009. 32, 36, 69, 80, 99

[Basser 2000] Peter J. Basser, Sinisa Pajevic, Carlo Pierpaoli, Jeffrey Duda and Akram Aldroubi. *In vivo fiber Tractography using DT-MRI data*. Magnetic Resonance in Medicine, vol. 44, pages 625–632, 2000. 75, 76, 137, 149, 157

[Bonissone 1997] Piero P. Bonissone. *Adaptive Neural Fuzzy Inference Systems (ANFIS): Analysis and Applications*. GE CRD Schenectady, NY USA, 1 1997. 83

[Burger 2008] Wilhem Burger and Mark J. Burge. Digital image processing - an algorithmic introduction using java, volume 1 of *1*. Springer, first édition, July 2008. 24

[Cachier 2003] Pascal Cachier and et al. *Iconic feature based non-rigid registration: the PASHA algorithm*. Computer Vision and Image understanding, vol. 89, pages 272–298, 2003. 73

[Ceritoglu 2009] Can Ceritoglu, Kenichi Oishi, Xin Li and et al. *Multi-contrast large deformation diffeomorphic metric mapping for diffusion tensor imaging*. NeuroImage, vol. 47, pages 618–627, 2009. 104

[Chan 2007] L-L Chan, H. Rumperl and K. Yap. *Case Control study of Diffusion tensor imaging in Parkinson's disease*. J. Neurol. Neurosurg. Psychiatry, vol. 78, pages 1383–1386, 2007. 15, 19, 20, 50, 67, 127, 146

[Chetelat 2005] G. Chetelat, B. Landeau, F. Eustache and et al. *Using voxel-based morphometry to map the structural changes with rapid conversion in MCI: A logitudinal MRI study*. NeuroImage, vol. 27, pages 934–946, 2005. 29

[Curran 2005] K.M. Curran and D.M. Alexander. *Comparison of Similarity Measures for Driving Diffusion Tensor Registration*. Proc. Intl. Soc. Mag. Reson. Med., vol. 13, page 226, 2005. 28, 137, 157

[Deisseroth 2009] K. Deisseroth and et al. *Stanford Study improves insight into Parkinson's disease and possible treatments*. Stanford University Medical Centre, vol. 1, page 1, 2009. last accessed on March 2010. 63

[Descoteaux 2007] Maxime Descoteaux, Rachid Deriche and Alfred Anwander. *Deterministic and Probabilistic Q-Ball Tractography: from Diffusion to Sharp Fiber Distorsions*. Rapport de recherche 6273, INRIA Sophia Antipolis, August 2007. Projet Odyssee. 38

[Dictionary 2010] Medical Dictionary. *The Free Dictionary By Farlex*. On-line, april 2010. http://encyclopedia.thefreedictionary.com/. 25

[Facon 2005] David Facon, Augustin Ozanne and Pierre Fillard. *MR Diffusion Tensor Imaging and Fiber Tracking in Spinal Cord Compression*. ANJR, vol. 26, pages 1587–1594, 2005. 30

[Fillard 2002] Pierre Fillard and Guido Gerig. *Analysis Tool for Diffusion Tensor MRI*. MICCAI, vol. 1, no. 1, pages 1–3, sept. 2002. 53

[Fillard 2007] Pierre Fillard, Jean-Christophe Souplet and Nicolas Toussaint. *Meidcal Image Navigation and Research tool by INRIA (MedINIRA)*. Rapport technique, INRIA Sophia Antipolis, 2007. 56

[Fillard 2009] Pierre Fillard, Cyril Poupon and Jean-Francois Mangin. *A novel global tractography algorithm based on an adaptive spin glass model*. MICCAI, vol. 1, pages 1–8, 2009. 38

[Friston 2000] Karl J. Friston. *Experimental Design and Statistical Parameter mapping*. Dept. of Cognitive Neurology, vol. 1, no. 1, page 25, September 2000. SPM Presentation. 43, 51, 53

[Gabrys 2005] Bogdan Gabrys, Kauko Leiviska and Jens Strackeljan. Do smart adaptive system exist?, volume 173 of *Studies in fuzziness and soft computing*. Springer, 2005. ISBN: 978-3-540-24077-8. 82

[Gaser 2008] Christian Gaser. *Structural Brain Mapping Group*. presentation web-page, december 2008. Software presentation and download site. http://dbm.neuro.uni-jena.de/vbm/vbm5-for-spm5/ - last accessed on March 2010. 43, 131, 151

[Gholinpour 2007] Ali Gholinpour, Nasser Khetanarvaz and et al. *Brain Functional Localization: a Survey of Image Registration Techniques*. IEEE Transactions on Medical Imaging, vol. 26, pages 1–20, 2007. 73, 74

[Goetz 2004] Christopher G. Goetz, Werner Poewe, Olivier Rascol, Cristina Sampaio, Glen T. Stebbins and et al. *Movement disorder society task force report on the Hoehn and Yahr staging scale: Status and Recommendations*. Movement Disorders, vol. 19, no. 9, pages 1020–1028, June 2004. 176

[Guillaume 2008] Guillaume. *SPM Documentation*. pdf technical report, October 2008. Trust Center for Neuroimaging. http://www.fil.ion.ucl.ac.uk/spm/doc/ - last accessed on May 2010. 43, 131, 151

[Jain 1988] Anil K. Jain and Richard C. Dubles. Algorithms for clustering data. Prentice Hall Advanced Reference Series. Prentice Hall, 1988. 68

[Jain 1997] A. Jain and D. Zongker. *Feature selection: Evaluation, application and small sample performance*. IEEE Transactions on Pattern Analysis and Machine Intelligence, vol. 19, no. 2, pages 153–158, 1997. 81

[Jones 2008] Craig Jones. *Matlab Scripts*. web presentation, University of Western Ontario, July 2008. http://www.imaging.robarts.ca/ cjones/software/ - last accessed on May 2010. 30

[Jyh-Shing Roger 1995] Jang Jyh-Shing Roger and Sun Chuen-Tsai. *Nuero-Fuzzy Modeling and Control*. The Proceesings of IEEE, vol. 83, pages 387–406, 1995. 82, 83

[Karagulle Kenedi 2007] AT Karagulle Kenedi, S. Lehericy and M. Luciana. *Altered Diffusion in the Frontal Lobe in Parkinson's Disease*. AJNR Am J Neuradiol Brain - Original Research, vol. 29, pages 501–05, 2007. 76

[Kiebel 1999] S.J. Kiebel, J.B. Poline, K.J. Friston, A.P. Holmes and K.J. Worksley. *Robust Smoothness Estimation in Statistical Parametric Maps Using Standardized Residuals from the General Linear Model*. NeuroImage, vol. 10, pages 756–766, 1999. 29

[Kretschmann 2003] Hans-Joachim Kretschmann and Wolfgang Weinrich. Cranial neuromiaging and clinical neuroanatomy - 3rd edition. Thieme Classics, 2003. 69

[Le Bihan 2001] Denis Le Bihan, Jean-Francois Mangin, Cyril Pupon and Chris A. Clark. *Diffusion Tensor Imaging : concepts and application*. Journal of Magnetic Resonance Imaging, vol. 13, pages 534–546, 2001. 75, 76, 128, 137, 149, 157

[Lehericyr 2004] S. Lehericyr, M. Ducros, P.F. Van de Moorele and et al. *Diffusion tensor fiber tracking shows distinct corticostriatal circuis in humans*. ANN Neurol, vol. 55, pages 522–529, 2004. 15, 63

[Maintz 2000] Antoine J.B. Maintz and Max A. Viergever. *A survey of medical image registration*. Medical Image Analysis, vol. 1 and 2, pages 1–32, 2000. 73, 75

[Modersitzki 2004] Jan Modersitzki. Numerical methods for image registration, volume Oxford Science Publications of *Numerical Mathematics and Scientific Computation*. Oxford University Press, hardcover édition, 2004. 104

[NEMA 2008] Suite 1752 NEMA. *DICOM Standard*. electronic, Medical Imaging and Technology Alliance, december 2008. 23, 24

[Parker 2004] G.J.M. Parker. *Analysis of MR diffusion weighted images*. The British Journal of Radiology, vol. 77, pages S176–S185, 2004. 35

[Pataca 2010] Cristina Izabela Pataca. Detection and prognosis of parkinson's disease. Master's thesis, "Politehnica" University of Timisoara, Romania, June 2010. 86, 88, 89, 108, 109, 113

[PD 2009] PD. *Parkinson's disease statistics*. on-line, July 2009. http://parkinsons-disease.emedtv.com/parkinsonease-statistics.html. 14

[Rorden 2008] Rorden. *DTI analysis*. Worshop Report, October 2008. last accessed on May 2010. 28, 137, 157

[Roussinov 2001] Dimitri G. Roussinov and Hsinchun Chen. *Information navigation on the web by clustering and summarizing query resuls*. Information Processing & Management, vol. 37, no. 6, pages 789–816, November 2001. 82

[Sabau 2010] A. Sabau, R.O. Teodorescu and V.I. Cretu. *Automatic putamen Detection on DTI Images. Application to Prakinson's Disease*. ICCC-CONTI, vol. 1, pages 1–6, may 2010. 71, 104, 112, 135, 154, 155

[Sonka 2009] Milan Sonka and J. Michael Fitzpatrick, editeurs. Handbook of medical imaging, volume 2 Medical Image Processing and Analysis of *Diagnostic Imaging - Handbooks*. SPIE Press, P.O. box 10 Bellingham, Washington 98227-0010 USA, 3 édition, 2009. ISBN 0-8194-3621-6. 23, 31, 32, 65, 69, 81, 107, 114

[Starr 2009] Cindy Starr and George Mandybur. *Grant to improve targeting in Parkinson's Surgery*. University of Cincinnati neuroscience institute, January 2009. Mayfield Clinic. 70

[Teodorescu 2009a] R. O. Teodorescu, D. Racoceanu and L.-L. Chan. *H&Y compliant for PD detection using EPI and FA analysis*. Presentation Number: NIH09-NIH01-88, 1-2 October 2009. Natcher Auditorium, National Institutes of Health in Bethesda, MD USA. 97, 112

[Teodorescu 2009b] Roxana Teodorescu, Daniel Racoceanu and L.L. et al. Chan. *Parkinson's disease detection using 3D Brain MRI FA map histograms correlated with tract directions*. RSNA, vol. 8015681, page 1, 2009. Chacago, IL USA. 97, 100, 101, 102, 112

[Teodorescu 2009c] Roxana Oana Teodorescu and Daniel Racoceanu. *Prognosis of Parkinson's Disease*. ASTAR Scientific Conference, 28-29 Oct. 2009. Biopolis, Singapore. 97, 112

[Teodorescu 2010] Roxana Teodorescu, Daniel Racoceanu, Nicolas Smit, Vladimir Ioan Cretu, Eng King Tan and Ling-Ling Chan. Parkinson's disease prediction using diffusion based atlas. SPIE Medical Imaging, Computer Aided Diagnosis, San Diego, California, USA, 13-18 Feb. 2010. 97, 106, 107, 112

[Tharin 2007] Suzanne Tharin and Alexandra Golby. *Functional Brain Mapping and Its Applications to Neurosurgery*. Operative Neurosurgery, vol. 60, pages 185–202, 2007. 34

[Thomopoulos 1994] Stelios C. A. Thomopoulos. *Sensor Selectivity and Intelligent Data Fusion*. Proceedings of the 1994 International Conference on Multisensor fusion and Integration for Intelligent Systems (MFI'94), vol. 2, no. 5, pages 529–537, oct 1994. decision and control systems lab - sensors data fusion. 35, 53

[Today 2009] Medical News Today. *Brain bank Appeal aims to double number of brain donors*. www.medicalnewstoday.com, March 2009. Parkinsons awareness week 2009, 20-26 April. 14, 127, 146

[Tretter 1995] Daniel Tretter, Nasir Memon and Charles A. Bouman. *Multispectral Image Coding*. In Handbook of Image and Video Coding, Academic, pages 539–551, 1995. 33

[University 2008] South Carolina University. *The DICOM standard*. Web presentation, december 2008. Technical Report. http://www.sph.sc.edu/comd/rorden/dicom.html - last accessed on May 2010. 24

[Vaillancourt 2009] D. et al Vaillancourt. *Imaging Technology May trace Development of Parkinson's disease*. University of Illinois at Chicago, Rush University, vol. 1, page 3, 2009. 15, 34, 63

[Vercaunteren 2008a] T. Vercaunteren, X. Penec and et al. *Diffeomorphic Demons: Efficient Non-parametric Image Registration*. NeuroImage, vol. 45, pages 61–72, 2008. 104

[Vercaunteren 2008b] Tom Vercaunteren, Xavier Pennec, Aymeric Perchant and Nicholas Ayache. *Symmetric Log-Domain Diffeomorphic Registration: A Demons - Based Approach*. Lecture Notes in Computer Science - Medical Image Computing and Computer-Assisted Intervention -MICCAI, vol. 5241, pages 754–761, 2008. 104

[Wang 2007] Ruopeng Wang, T. Benner, A.G. Sorensen and V.J. Wedeen. *DiffuionToolkit: A software package for diffusion imaging data processing and tractography*. ISMRM abstract, vol. 15, page 3720, 2007. Martinos Center for Biomedical Imaging, Massachusetts General Hospital. 41

[Westin 2002] C.-F. Westin, S.E. Maier and H. Mamata. *Processing and visualization for diffusion tensor MRI*. Medical Image Analysis, vol. 6, pages 93–108, 2002. 70

[Wirijadi 2001] Oliver Wirijadi. *Survey of 3D Image Segmentation Methods*. Fraunhoffer technical report, vol. 1, page 1, 2001. 75

[Woodward 2009] N. Woodward, D. Zald and Z. et al. Ding. *Cerebral morphology and dopamine D2/D3 receptor distribution in humans: a combined [18F] fallypride and voxel-based morphometry study*. NeuroImage, vol. 46, pages 31–38, 2009. 15, 63

[Yaasa 2004] Michael A. Yaasa. *Voxel - Based Morphometry*. Electronic presentation (ppt), The Johns Hopkins School of Medicine, Division of Psychiatric Neuroimaging, december 2004. 51, 52

[Yendiki 2010] Anastasia Yendiki. *Future duirections: TRActs Constrained by UnderLying Anatomy (TRACULA)*. ppt presentation, February 2010. HMS/MGH/MIT Athinoula A. Martions Center for biomedical imaging. 38, 39

[Yushkenvich 2008] Paul Yushkenvich, Hui Zhang and James Gee. *Tract-Specific Analysis for DTI of Brain White Matter*. presentation- IPAM Summer School, july 2008. PICSL. 53

[Zitova 2003] Barbara Zitova and Jan Flusser. *Image Registration: A Survey*. Image and Vision Computing, vol. 21, pages 977–1000, 2003. 63, 74